ISSN 0973-8916

Current Trends in Biotechnology and Pharmacy

Volume- 16 Issue 4 October 2022

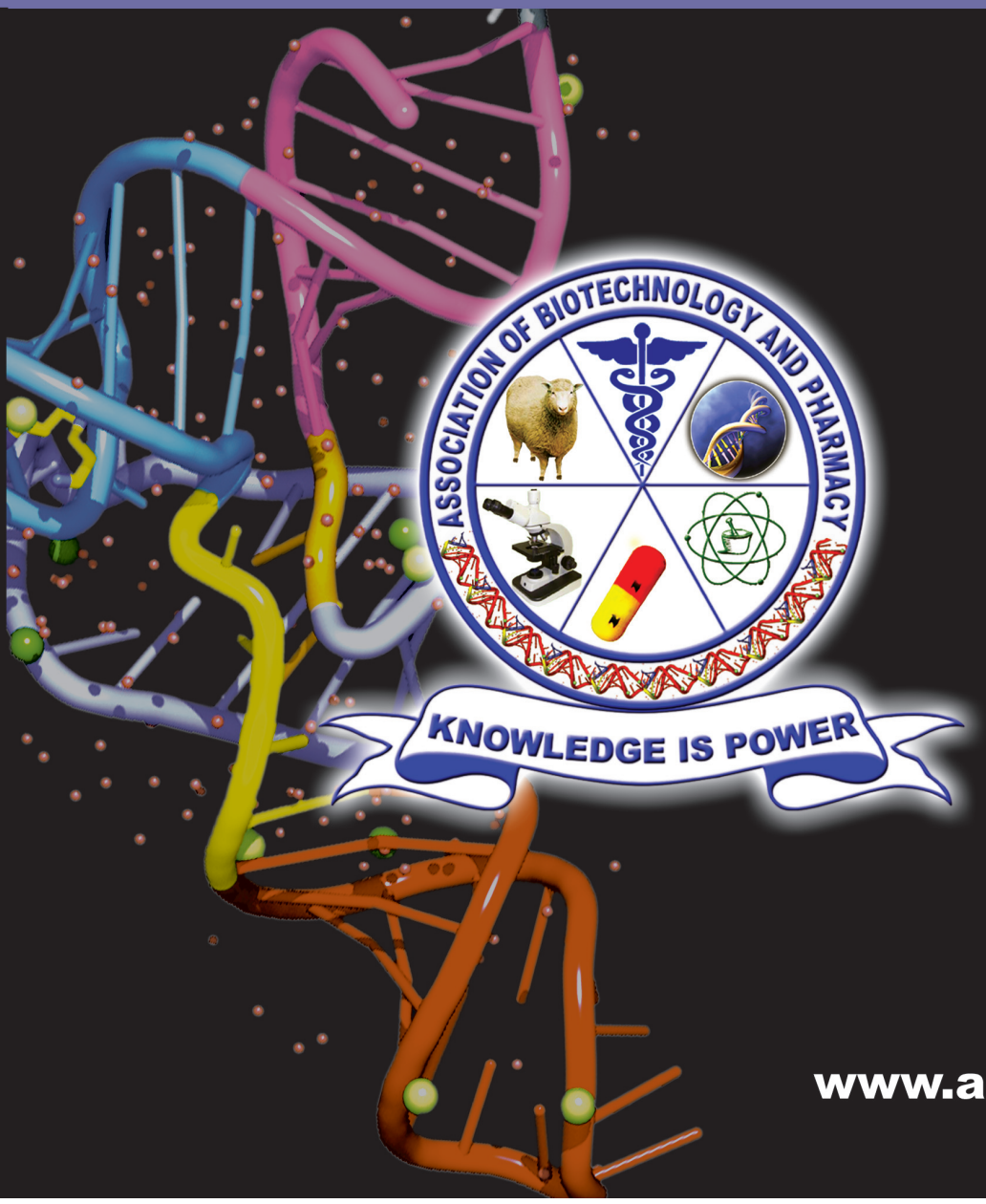

www.abap.co.in

Current Trends in Biotechnology and Pharmacy

ISSN 0973-8916 (Print), 2230-7303 (Online)

www.abap.co.in

ISSN 0973-8916

Current Trends in Biotechnology and Pharmacy

(An International Scientific Journal)

Volume 16 Issue 4 October 2022

www.abap.co.in

Indexed in Chemical Abstracts, EMBASE, ProQuest, Academic SearchTM, DOAJ, CAB Abstracts, Index Copernicus, Ulrich's Periodicals Directory, Open J-Gate Pharmoinfonet.in Indianjournals.com and Indian Science Abstracts.

Association of Biotechnology and Pharmacy
(Regn. No. 28 OF 2007)

The Association of Biotechnology and Pharmacy (ABAP) was established for promoting the science of Biotechnology and Pharmacy. The objective of the Association is to advance and disseminate the knowledge and information in the areas of Biotechnology and Pharmacy by organising annual scientific meetings, seminars and symposia.

Members

The persons involved in research, teaching and work can become members of Association by paying membership fees to Association.

The members of the Association are allowed to write the title MABAP (Member of the Association of Biotechnology and Pharmacy) with their names.

Fellows

Every year, the Association will award Fellowships to the limited number of members of the Association with a distinguished academic and scientific career to be as Fellows of the Association during annual convention. The fellows can write the title FABAP (Fellow of the Association of Biotechnology and Pharmacy) with their names.

Membership details

(Membership and Journal)		India	SAARC	Others
Individuals	– 1 year	`Rs. 600	Rs. 1000	$100
LifeMember		Rs. 4000	Rs. 6000	$500
Institutions	– 1 year	Rs. 1500	Rs. 2000	$200
(Journal only)	Life member	Rs.10000	Rs.12000	$1200

Individuals can pay in two instalments, however the membership certificate will be issued on payment of full amount. All the members and Fellows will receive a copy of the journal free.

Association of Biotechnology and Pharmacy
(Regn. No. 28 OF 2007)
#5-69-64; 6/19, Brodipet
Guntur – 522 002, Andhra Pradesh, India

Current Trends in Biotechnology and Pharmacy
ISSN 0973-8916

Volume 16 (4) **CONTENTS** **October 2022**

A comparative study of lipid profile in oral squamous cell carcinoma (oscc) cases and controls.
Samata Gadde, Sudhakar Poda, Lakshmi Addala
10.5530/ctbp.2022.4.77 429 - 444

Antimelanogenic and Anticancer activity of Isorhamnetin isolated from Acalypha indica Linn. on A375 cell line.
Ms. Kalaivani D Dr. Arun V
10.5530/ctbp.2022.4.78 445 – 455

Host Specificity and Symbiotic association between indigenous Rhizobium strain and Arachis hypogaea plants
Sanjeev Kumar K and Pavan Kumar Pindi
10.5530/ctbp.2022.4.79 456 – 470

Non-Recombinant Mutagenesis of Bacillus mojavensis CUIE1819 for Hyper Production of Lipase and Treatment of Polluted Lakes
J Irene Infancy, Erumalla Venkata Nagaraju,Vaddi Damodara Reddy, Kuppusamy Alagesan Paari
10.5530/ctbp.2022.4.80 471 - 480

Automated Detection Of Breast Cancer Using Machine Learning Algorithms: A Compartive Analysis
Venkata Srinivas Babu Oguri, Sudhakar Poda
10.5530/ctbp.2022.4.81 481 – 489

Formulation, Evaluation and Characterization of Mouth Dissolving Film of Cisapride
Prashant L. Pingale, Dattatray M. Shinkar, Sahebrao S. Boraste, Sunil V. Amrutkar
10.5530/ctbp.2022.4.82 490 – 499

Is olive oil Consumption Suitable for Colorectal Cancer? In Vivo Preliminary Studies on Azoxymethane-Induced Colon Cancer in Rats
Sheba R David, Aida Batrisyia Mohd Taufik, Lim Ya Chee, Ashok Kumar Balaraman, Rajan Rajabalaya
10.5530/ctbp.2022.4.83 500 – 510

India's International Collaboration in Biotechnology
Manohar Pathak Atul Bhatt N K Prasanna
10.5530/ctbp.2022.4.84 511 - 517

Evaluation of invitro anticancer effect of hydroalcoholic extract of *Lepidagathis spinosa* wight Ex Nees.
Sutha Ponnusamy, Sangameswaran Balakrishnan
10.5530/ctbp.2022.4.85 518 - 528

In-Silico Investigation of Plant-Derived Natural Allosteric Compounds Towards Enhanced Drug-Protein Interaction of MOA Protein Complex in Depression Based on Molecular Docking and Molecular Dynamic Simulation Approaches
Abhimanyu, Poornima Srivastava,Chakresh Kumar Jain,
10.5530/ctbp.2022.4.86 529 - 539

Vernonia amygdalina leaf extract protects against carbon tetrachloride-induced hepatotoxicity and nephrotoxicity: possible potential in the management of liver and kidney diseases
Temidayo Ogunmoyole, Yetunde Apanisile,OmowumiJayeola Makun,
Olaitan Daniel Johnson, Yusuff Adewale Akeem
10.5530/ctbp.2022.4.87 540 – 552

Efficacy of entomopathogenic fungi Beauveria bassiana in pest management
Srivani MVK[1], Jalaja N[2]
10.5530/ctbp.2022.4.88 553 - 561

Cardiovascular Toxicity of Oral Antidiabetic Drugs and the Efficacy of Natural Organosulfure Compounds from Aged Garlic Extract (AGE)
Kumkum Sharma, Vibha Rani
10.5530/ctbp.2022.4.89 562 - 576

COVID 19: a new insight into organ failure and complications caused by novel SARS-CoV-2 virus and discussion on the role of nanotechnology in detection, treatment and prevention of the disease
ManneAnupama Ammulu, Kanaka Durga Devi Nelluri, Praveen Kumar Vemuri ,
SomaiahChowdary Mallampati, Sudhakar Poda
10.5530/ctbp.2022.4.90 577 - 602

Information to Authors

The Current Trends in Biotechnology and Pharmacy is an official international journal of Association of Biotechnology and Pharmacy. It is a peer reviewed quarterly journal dedicated to publish high quality original research articles in biotechnology and pharmacy. The journal will accept contributions from all areas of biotechnology and pharmacy including plant, animal, industrial, microbial, medical, pharmaceutical and analytical biotechnologies, immunology, proteomics, genomics, metabolomics, bioinformatics and different areas in pharmacy such as, pharmaceutics, pharmacology, pharmaceutical chemistry, pharma analysis and pharmacognosy. In addition to the original research papers, review articles in the above mentioned fields will also be considered.

Call for papers

The Association is inviting original research or review papers and short comunications in any of the above mentioned research areas for publication in Current Trends in Biotechnology and Pharmacy. The manuscripts should be concise, typed in double space in a general format containing a title page with a short running title and the names and addresses of the authors for correspondence followed by Abstract (350 words), 3 – 5 key words, Introduction, Materials and Methods, Results and Discussion, Conclusion, References, followed by the tables, figures and graphs on separate sheets. For quoting references in the text one has to follow the numbering of references in parentheses and full references with appropriate numbers at the end of the text in the same order. References have to be cited in the format below.

Mahavadi, S., Rao, R.S.S.K. and Murthy, K.S. (2007). Cross-regulation of VAPC2 receptor internalization by m2 receptors via c-Src-mediated phosphorylation of GRK2. Regulatory Peptides, 139: 109-114.

Lehninger, A.L., Nelson, D.L. and Cox, M.M. (2004). Lehninger Principles of Biochemistry, (4th edition), W.H. Freeman & Co., New York, USA, pp. 73-111.

Authors have to submit the figures, graphs and tables of the related research paper/article in Adobe Photoshop of the latest version for good illumination and allignment.

Authors can submit their papers and articles either to the editor or any of the editorial board members for onward transmission to the editorial office. Members of the editorial board are authorized to accept papers and can recommend for publication after the peer reviewing process. The email address of editorial board members are available in website www.abap.in. For submission of the articles directly, the authors are advised to submit by email to krssrao@abap.co.in or krssrao@yahoo.com.

Authors are solely responsible for the data, presentation and conclusions made in their articles/research papers. It is the responsibility of the advertisers for the statements made in the advertisements.

Current Trends in Biotechnology and Pharmacy
Vol. 16 (4) 429 - 444, Oct 2022, ISSN 0973-8916 (Print), 2230-7303 (Online)
10.5530/ctbp.2022.4.77

A Comparative Study of Lipid Profile in Oral Squamous Cell Carcinoma (OSCC) Cases and Controls.

Samata Gadde[1], Sudhakar Poda[2*], Lakshmi Addala[3]

[1] Department of Biotechnology, Acharya Nagarjuna University

[2]Department of Biotechnology, Acharya Nagarjuna University

[3] Department of Genetics, Osmania University

*Corresponding author: sudhakarpodha@gmail.com

Abstract

The purpose of this study is intended to detect and evaluate serum lipid concentrations and establish the interrelationship between the lipid profile variables for both oral and non oral cancer. This case control study included 100 clinically diagnosed and histopathologically confirmed OSCC cases and 100 age and gender matched healthy control subjects who had neither any history of cancer nor suffered from any major illness. Serum lipid concentrations such as total cholesterol, HDL cholesterol and triglycerides were determined by enzymatic colorimetric assays. LDL and VLDL cholesterol concentrations were calculated from the above findings. ANOVA was performed to compare mean, standard deviation and P- values of the parameters using SPSS 15.0 version for windows. The results have shown significantly decreased levels of serum lipid concentrations in OSCC cases when compared to normal control subjects, showing an inverse relation between serum lipid levels and Oral Squamous cell carcinomas. The detected lower concentrations of serum lipid components in the head and neck cancer cases might be due to the utilization of lipids by the cancer cells to maintain cell integrity. Plasma lipid status may be a useful bio-marker indicator for initial changes occurring in neoplastic cells.

Key words: Lipids, Cholesterol, Triglycerides, Oral Squamous cell carcinoma ,head and neck cancers, HDL, LDL, VLDL, areca nut, alcohol, tobacco, smoking, HNSCC, carcinogenesis, oral cancer.

Lipids are chief cell membrane components crucial for various biological functions including cell growth and division of normal and malignant tissues, maintenance of the structural and functional integrity of all biological membranes, activity of membrane-bound enzymes and stabilization of the DNA helix. Total cholesterol (TC), triglycerides (TG), high density lipoproteins cholesterol (HDLC), low density lipoproteins cholesterol (LDLC), and very low density lipoproteins cholesterol (VLDLC) constitute the lipid profile. Lipoproteins transport free cholesterol in the circulation, LDLC help in the transportation of cholesterol from liver to the other cells, HDLC in the transportation of cholesterol from other cells to the liver, VLDLC packs and transports the triglycerides, which are taken up and degraded by cells to perform cellular functions. Cholesterol, an amphipathic lipid is vital for cellular uptake and is distributed systematically in the domains of membranes and exists either as free cholesterol or connected with a long chain fatty acid, as cholesteryl ester. Cholesterol is synthesized in many tissues from acetyl-Co-A,

and is eliminated from the body in the bile as cholesterol or bile salts. Specialized membranes called 'lipid rafts' are maintained enriched with sphingolipids and cholesterol, which act as the platform for signal transduction. Head and Neck Squamous Cell Carcinoma (HNSCC) advances from the mucosal epithelial cells that underlines the oral cavity, larynx, pharynx, sinonasal tract and the use of tobacco products is associated with inflammation in the exposed tissues (1). Tobacco smoke has been reported to kindle H_2O_2 and hydroxyl radicals in addition to direct carcinogenic effects on the epithelial cells of the oral mucous membrane. Extensive use of areca nut and tobacco carcinogens induce the production of free radicals and reactive oxygen species (ROS), which has been implicated in pathogenesis of several diseases including cancer. Oxidative stress is the chief leading causes of toxicity attributed to the interactions of ROS and reactive nitrogen species (RNS) with cellular macromolecules like DNA, lipid, and proteins, which hamper the signal transduction pathways such as protein kinases, phosphatases, and transduction mechanisms (2). ROS enhances the rate of oxidation and per-oxidation of polyunsaturated fatty acids, thus disturbing essential constituents of cell membrane and apparently involving carcinogenesis. Animal studies have shown that nicotine, a tobacco carcinogen, affects the activity of enzymes responsible for lipid metabolism (3). Lipid metabolism in rapidly proliferating cancerous cells is based on redirecting the carbon from energy production into membrane biosynthesis. During signal transduction cascades, lipids are broken down into bioactive lipid mediators, which regulate an array of carcinogenic processes like cell growth, cell migration and metastasis formation (4).

Cancer is a leading cause of morbidity globally and a growing public health concern, with the increasing annual number of new cancer cases it is projected to amplify to 13.1 million deaths in 2030 (5). In 2015 caused over 8.7 million deaths globally, being the second leading cause of death behind cardiovascular diseases (6). The most common histological type of oral cavity cancer is Squamous cell carcinoma, which accounts for more than 90% of cases (7), with more than 450,000 new cases and 350,000 deaths annually (8-11). The distressing rates of mortality reported in HNSCC are usually owing to high incidence of loco-regional recurrence and metastatic disease (12). The incidence of HNSCC continues to mount and is estimated to enhance by 30% (1.08 million new cases annually) by 2030 (13-14), and critical needs for novel therapies to improve overall survival is indispensable (15) .Despite some modest improvements in the treatment ,the overall 5-year survival rate remained just about 40–50% chiefly due to poor accessibility of effective therapeutic options for HNSCC cases with recurrent disease (16) whereas the recurrence rates remain high (17). Cancers of the lip and oral cavity are vastly common in South Central Asia (India, Sri Lanka, and Pakistan) (18) as well as Melanesia (Papua New Guinea, with the highest incidence rate worldwide in both sexes), reflecting the popularity of betel nut chewing (19). Incidence rates are also high in Eastern and Western Europe and in Australia/ New Zealand and have been linked to alcohol consumption, tobacco smoking, HPV infection for cancers of the oropharyngeal region, and to ultraviolet radiation from sunlight exposure for lip cancer (19-22). OSCC develops in the oral cavity and oropharynx and can occur due to many etiological factors, but smoking and alcohol remain the most common risk factors especially in the Western world (23). Though treatment is complex for cases with head and neck cancers[24], its early detection can improve the prognosis significantly (25). Oral cancer is a preventable disease, where smoking and alcohol, considered major risk factors are present in 90% of cases (26), and having them both derives a synergic effect (27). There is

now sufficient understanding of the causes, and adequate information to facilitate early detection and well-timed treatment of another third of cases (28) which remains to be the key to improving survival (29).

Materials and Methods

A total of 200 individuals were included in our case control study. Out of them 100 were histopathologically confirmed and untreated OSCC cases from MNJ cancer hospital, Hyderabad and the remaining 100 were normal healthy subjects who had never suffered any major illness that alters serum lipid concentrations. Fasting blood samples were collected from the cases and controls by obtaining a written informed consent from each of them. Serum was separated and stored in small aliquots at -20º C. Total cholesterol, HDL cholesterol and triglyceride concentrations in serum were determined in mg/dl by using standard commercially available kits manufactured by Transasia Bio-Medicals Ltd, Daman (India) in collaboration with ERBA Diagnostics Mannheim GmbH, Germany.

Serum Total cholesterol concentrations in mg/dl were determined by CHOD-PAP enzymatic method, a modified Roeschlau's method in which 20 µl of serum was mixed with 1 ml of working enzyme reagent containing cholesterol esterase, cholesterol oxidase, peroxidase, sodium phenolate, 4-aminoantipyrine, phosphate buffer (pH: 6.5) and lipid clearing agent. Then the mixture was incubated at 37º C for 10 minutes and the absorbance was measured at 505 nm.

Serum HDL cholesterol concentrations in mg/dl were determined by phosphotungstic acid method in which 250 µl of serum was mixed with 500 µl of precipitating reagent that precipitates LDL and VLDL fractions of lipid cholesterol. The mixture was then allowed to incubate at room temperature for 10 minutes and then centrifuged at 4000 rpm for 10 minutes. The clear supernatant obtained was then assayed as per the serum total cholesterol estimation.

Serum triglyceride concentrations in mg/dl were determined by GPO-Trinder Method, an enzymatic method in which 10 µl of serum was mixed with 1 ml of working enzyme reagent containing lipoprotein lipase, glycerol kinase, glycerol phosphate oxidase, di-hydroxy-acetone phosphate, adenosine triphosphate, 4-aminoantipyrine, 3,5-dichloro-2-hydroxybenzene sulfonate, peroxidase and buffer (pH:7.0). The mixture was incubated at 37º C for 10 minutes and then the absorbance was measured at 505 nm. The serum VLDL and LDL cholesterol concentrations in mg/dl were calculated as per the following formula:

Serum VLDL cholesterol = Serum Triglycerides ÷ 5

Serum LDL cholesterol = Serum Total cholesterol – (HDL cholesterol + VLDL cholesterol)

Statistical analysis: Results of the study were tabulated for OSCC and control groups. All the parameters in the study were statistically analyzed for mean values, standard deviation, range and *P*- values. ANOVA was performed to compare mean, standard deviation and *P*-values of the parameters using SPSS version 15 (SPSS, Chicago, IL) for windows.

Results and **Discussion:**

Age range for OSCC cases was 9-87 years in males and 27-75 years in females, and in controls 21-80 years in males and 22-87 years in females. However, many of the ages mentioned in case sheets are given by cases were subjective, while exact age of 100 OSCC cases (Males 45 and Females 55) and 100 controls (Males 55 and Females 45) was available, hence analysis was carried out with those, mean age at which OSCC identified was 9-87/ 49.30±15.55 in male and 27-75/84.20±11.26 in female years .To comprehend the role of

gene mutations/ polymorphisms in onset of the disease, the cases and controls were divided into 4 categories, <25 years (1% cases and 3% controls), 26 to 45 years (27% cases and 19% controls), 46 to 65 years (60% cases and 70% controls), and above 66years (12% cases and 8% controls). Highest percentage of OSCC cases was identified between 46-65 years in both case and control group. Regarding the primary tumor site, there was a neat predominance on the BM adding up 35 cases (35.0%), followed by tongue adding up 23 cases (23.0%), then Mandible, oral cavity and RMT adding up 12, 10, & 8 cases (12%, 10% and 8%) (Table 1). In the present study Stage III showed the highest frequency (39%) when compared to Stage IV (34 %) and Stage II (21%), and further types of tumor grade like Stage I (6%) showed very low frequency when compared to other stages (table 1). Histopathologically OSCC were graded as: well differentiated Squamous cell carcinoma (WD SCC), moderately differentiated, (MD SCC) and poorly differentiated (PD SCC) based on the degree of differentiation. In the present study, the serum lipid levels in OSCC cases were found to be slightly elevated in WD SCC and MD SCC compared to PD SCC. The levels showed significant correlation with serum TC, LDL, VLDL, HDL and triglycerides among the degrees of differentiation (Table2). The gender wise levels of the various parameters of lipid profiles were found significantly lower in OSCC cases as compared with controls (table 3). ANOVA and P-values were calculated (Table 3). The P-values were found significant for serum total cholesterol, VLDL, LDL, HDL and for serum triglycerides, revealing an inverse relationship between serum lipid profile in OSCC and controls. The mean serum levels of total cholesterol was significantly (p= 0.0001) lowered in OSCC cases (148.1±22.8) compared to controls (181.45±23.67). In OSCC cases both the HDL (45.52±11.1) and LDL (84.69±17.4) were also lowered when compared to levels of HDL (47.92±10.60) and LDL (98.86±17.58) in controls. However the decreased HDL levels were not found significant (p=0.13) when compared to controls. There was significant (0.0001) decrease in the levels of VLDL (18.0±6.0) when compared to controls (29.05±8.19) and triglycerides were found to be little higher in controls (145.53±40.73) than compared to cases (89.7±30.4) respectively.

Among one hundred OSCC cases, the number of cases who had only Chewing habit showed a high frequency of 31%, than only smokers 6% while we did not find, only alcohol habituates in cases. Analysis pattern of the cases with two habits revealed that chewing and alcohol habituate cases were more prevailing (26%) than Alcohol and Smoking (14%) and Smoking and chewing (2%), and cases who were having all the three risk factors: alcohol, smoking and chewing habits were found to be 10%. In the present study 11% were found without any habitual risk factors.

95% C.I and t stat values were observed and p values were calculated correlating the risk factors with the lipid components in OSCC cases and control subjects and marked for significance (table 5).

- We observed that only alcohol risk factor habituates were not present in our study.
- The smoking risk factor was significant in TC, VLDL and TG values (<0.0001), and insignificant in HDL (>=0.014) and LDL values (=0.001).
- Chewing risk factor was significant in all the cholesterol components TC, HDL, LDL, VLDL and TG (<0.0001).
- Smoking and alcohol combination risk factor also was relatively significant in this case study (<0.0001).
- In alcohol and chewing combination risk factor, only TG was insignificant (<0.0003).
- With the other risk factor combinations:

chewing and smoking (<0.0001), chewing, smoking and alcohol (<0.0001), all showed a statistical significance in TC, HDL, LDL, VLDL and TG values.

- No habits group also showed a statistical significance (<0.0001), in our case control study.

Majority of the cases in our study were in the age group of 46-65 years (60%), which is in accordance, and observed a similar range of 41-60 years (40%) (30). Interesting finding observed was that low serum cholesterol concentration (i.e. <5.16 mmol/L) magnifies the overall mortality from cancer and enhances prostate, colon and lung cancer among men over 60 years of age (31).

Male predominance was observed in studies (32-33) which is similar with our findings. While numerous studies suggest that low cholesterol levels are linked with various cancers, it was recorded that high total cholesterol level (≥240 mg/dL) and was positively associated with breast cancer in women and prostate, colon cancers in men, but negatively associated with risk of liver, stomach cancer in both men and women, and lung cancer in men (34).

Cases with tumors in advanced stages might have lower lipid levels due to malnutrition caused by an inadequate food intake. In accordance to our study well and moderate groups were higher than poorly differentiated (35-36), and no correlation between the T stage and lipid levels was also observed excluding the possible link between tumor stages, malnutrition and low lipid levels in cases (37). While the correlation between histological grading and serum lipid profile in Oral Cancer and pre-cancer was not noted (38), studies have established the linkage with tobacco abuse and histological grading (39).

Carcinogenesis leads to reduced level of cholesterol in proliferating tissues and blood (40), probably due to the augmented tumor cells. The new membrane biogenesis occurs due to degradations of lipoprotein fractions (41), like HDL, VLDL and LDL of cholesterol in the blood compartments (42). A significant decrease was noticed in mean serum cholesterol levels of lipoproteins in oral carcinoma and leukoplakia groups of cases (43) while both total cholesterol (TC) levels and triglyceride levels were considerably reduced in oral Squamous cell carcinoma cases as compared to the healthy controls (44). TC, LDL and TG were lowered and a significant decrease in all the lipid fractions correlates to oral malignancy (45-46) is in accordance with our study. The lower serum lipid level status may be an important indicator for initial changes occurring in neoplastic cells which might be due to utilization of cholesterol for membrane biogenesis. Hypolipidemia may occur due to the direct lipid lowering effect of tumor cells or the malfunction of the lipid metabolism (47), while cancer mortality risk with low plasma cholesterol was attributed to the effect of existing cancer disease (31). However, earlier studies observed that higher mortality due to cancer was observed in cases with high total cholesterol levels (38) although total cholesterol (mg/dL) was significantly lower in cases who were deceased (48). The crucial role of lipid classes and molecular species in supporting tumor growth and metastatic dissemination (49), and the dependence of cancer cells on aberrant lipid and cholesterol metabolism might point to these pathways as prominent targets to treat cancer as well as to sensitize them to anticancer therapies(50). Total lipids, cholesterol and HDL cholesterol levels are inversely associated with incidence of cancer whereas triglycerides levels were significantly elevated in cancer cases (51).

Lipids are major cell membrane components which are vital for various biological functions involving cell division and growth of normal and malignant cells (52) and cholesterol,

an integral part of lipid rafts plays a vital role in pathways governing carcinogenesis, drug resistance and metastasis (53). Oxidative stress increases with the increase of lipid peroxidation, causing inflammation and tissue damage in OSCC cases with compromised antioxidant defence (54). Tumor promotion is associated with perioxidant status as ROS participates in carcinogenesis (55). Carcinogens from tobacco cause liberation of free radicals and reactive oxygen radicals which cause high rate of peroxidation of unsaturated fatty acids causing increased utilization of lipids like TG, TC, lipoproteins for membrane biogenesis of cancer cells. The present study could be a preliminary study where such a correlation of lipid profile with risk factors was done.

Smoking alone:

Approximately 90% of people with oral cancer are tobacco users. A reduction in the total cholesterol, TG, LDL and HDL in all forms of tobacco users with OPC and OSCC cases was observed[56] in accordance with our study, but the HDL values were slightly increased in our study. A decreasing serum lipid status in the chronic smokers, especially the LDL can be used as an early indicator for changes in the neoplastic cells. Using tobacco is an important etiologic factor which aids in the development of oral precancerous lesions /conditions and head and neck cancer (30). HDL values were significantly lowered in the tobacco habituates when compared to the healthy controls (57), and passive smoking was reported to be a significant risk factor for decreased HDL(58). Contrarily our study suggests that smoking was an insignificant risk factor for HDL& LDL, so future study considering a larger sample could yield some better difference if at all it exists.

Areca nut chewing alone:

Chewing correlated with lipid profile was significant in our case control study. We found that all the lipid component values were significant ($p< 0.0001$) which is in accordance with the study, which reported a dose-dependent relationship between areca nut use and triglyceride(59). Contrarily current and former areca nut chewers had an elevated triglyceride level, more than normal values (1.7 mM) while a significantly lower level of HDL was observed in current areca nut chewers (60). A rise in the levels of TG, LDL and VLDL with a decrease in the HDL level was observed when the lipid profile of tobacco chewers was analyzed (61). The chief alkaloid in areca nut arecoline undergoes nitrosation and gives rise to N-Nitrosamine, which may have cytotoxic effect on the cells. These carcinogens induce generation of free radicals and reactive oxygen species, which are accountable for high rate of oxidation ⁄ peroxidation of polyunsaturated fatty acids releasing peroxide radicals. In the course of areca nut chewing, ROS produced, attacks salivary proteins; alters the structure of oral mucosa, activating an inflammatory response (62). Cross-sectional studies have shown that smokeless tobacco use seems to have an adverse effect on lipid profiles, wherein smokeless tobacco users had 2.5 times the adjusted risk of hypercholesterolemia compared to nonusers (63).

Smoking and alcohol:

Studies indicate a multiplicative effect of tobacco consumption and alcohol containing more than 300 carcinogenic chemicals including polycyclic aromatic hydrocarbons with respect to frequency and duration of OSCC (64). We understand from our study that all the lipid component values were significant ($p<0.0001$) when correlated with smoking and alcohol risk factor. This can be explained with the consideration that tobacco smoke increases the ethanol acetaldehyde in the mouth (65) and alcohol consumption promotes carcinogenic effects of tobacco smoke and they confer a synergistic risk for oral cancer (66).

Alcohol and chewing:

In our study, it was observed that the lipid components TC, HDL and LDL showed significance (< 0.0001) when correlated with risk factors alcohol and chewing, but TG and VLDL did not show any significance. The effect of alcohol along with tobacco has deleterious effects on the epithelium thereby enhancing carcinogenesis (66).

Chewing and smoking:

Tobacco chewing, a significant risk factor of oral cancer in India is due to consumption of betel quid (67), and the carcinogens present in tobacco and areca nut enhance breakage of cellular structural blocks such as lipids due to lipid per oxidation (68). In our study the lipid components TC, HDL, LDL, VLDL & TG were found to be significantly reduced in alcohol and chewing cases compared to controls, and statistically significant when correlated with the risk factors, which is partly in accordance with a study (69).

Smoking, chewing and alcohol:

Well-known risk factors for OSCC are areca nut chewing, sniffing of tobacco and alcohol consumption in various forms, which results in increased free radicals formation causing lipid peroxidation, affecting diverse cellular vital activities like growth, differentiation and gene expression (70). Our study recorded that all the lipid components (TC, HDLC, LDLC, VLDLC and TG) were statistically significant in correlation to combination of all the three risk factors - smoking, chewing and alcohol. In India, where the habits of chewing tobacco with betel nut, reverse smoking and alcohol usage are extensive, there is a striking incidence of oral cancer which accounts for as many as 30% of all cancers (71).

No Habits:

In our study, a statistical significance in correlation to lipid profile was observed in cases and controls without any habits of alcohol, chewing or smoking. Contrarily, no significance was reported in studies which considered the no habits group (33, 44).

Summary and conclusions:

Newly forming and rapidly proliferating malignant cells necessitate various crucial components such as lipids, well above the normal physiological limits leading to reduced lipid stores (72). Hence, increased de novo synthesis of fatty acids occurs due to intensive tumor growth (49) may perhaps signify overutilization of lipids during transformation from oral precancer to cancer (38). Intracellular and comprehensive cholesterol concentrations are tightly regulated by the balance between *de novo* biosynthesis, uptake, efflux, and storage, and metabolic alterations in lipid pathways supporting hypotheses that the lower cholesterol values, even before the manifestation or detection of cancer; maybe the result of carcinogenesis. Secondly, lower cholesterol values may head the development of cancer, and serve as biomarkers and might be a promising approach for cancer detection and therapeutics. Cancer cells harness lipid metabolism to generate components for biological membranes, and signaling molecules required for proliferation, survival, invasion and metastasis. Dysregulation in lipid metabolism is among the main important metabolic alterations in cancer. Taking into consideration the above facts, the importance of serum lipid levels as a diagnostic marker of oral cancer, should be noted. This study was designed to evaluate the changes in serum lipid levels in OSCC cases and healthy volunteers, in correlation to risk factors which might give an insight into the significant prognostic indicators in diagnosis of oral cancer. Changes to lipid organization that result in cancer initiation and progression contribute to the understanding of carcinogenesis and identification of potential therapeutic targets.

Table 1 Clinical Characteristics of the OSCC Cases & Healthy controls

Clinical Characteristics	n = 100 (Cases)	n = 100 (Controls)
Gender Males Females Mean age & Range Males Mean age & Range Females	 45(45%) 55 (55%) 50.53/9-87 55.27/30-75	 55(55%) 45 (55%)
Age Distribution 26-45 46-65 66 and above	 28 (28%) 60 (60%) 12 (12%)	 22(22%) 70(70%) 8 (8%)
Habitual Risk Alcoholics Smokers Tobacco chewing Alcohol + Smoking Alcohol + Tobacco chewing Smoking + Tobacco chewing Alcohol + Smoking + Tobacco chewing No Habits	 - 6(6%) 31(31%) 14 (14%) 26 (26%) 2 (2%) 10(10%) 11(11%)	 3 (3%) 13 (13%) 30 (30%) 6 (6%) 13(13%) 4 (4%) 6 (6%) 25 (25%)
Site of Diagnosis Tongue Buccal mucosa (BM) Mandible Oral Cavity Retromolartrigone Floor of mouth Lip Base of tongue Maxilla Palate	 23(23%) 35 (35%) 12 (12%) 10 (9%) 8(8%) 4(4%) 3(3%) 2 (2%) 2 (2%) 1 (1%)	
Staging Stage 1 Stage 2 Stage 3 Stage 4	 6 (6%) 21 (21%) 39 (39%) 34(34%)	

Table 2 Lipid profiles according to gender wise distribution

S.No	MEAN ±SD (Patients)			F Statistics	P-value	MEAN ±SD (Control subjects)			F Statistics	P-value
	Males (N=45)	Females (N=55)	Total (N=100)			Males (N=55)	Females (N=45)	Total (100)		
TC	146.2±20.5	149.6±24.6	148.1±22.8	.560	0.0001	178.29±22.04	185.31±25.23	181.45±23.67	1.3	0.34
HDL	42.5±10.1	47.9±11.3	45.52±11.1	6.181	0.0001	47.83±10.66	48.02±10.64	47.92±10.60	1.0	0.9
VLDL	17.5±6.2	18.3±6.0	18±6.0	.478	0.0001	28.41±7.58	29.82±8.9	29.05±8.19	1.37	0.2
LDL	86.1±18.1	83.4±16.9	84.69±17.4	.592	0.0001	96.69±16.57	101±18.58	98.86±17.58	1.2	0.4
TG	87.6±30.7	91.3±30.3	89.7±30.4	.371	0.0001	142.21±37.53	149.57±44.4	145.53±40.73	1.39	0.23

SD= Standard deviation; n=number of cases; F-statistics=ANOVAs.

Table 3 Lipid profiles according to tumor degree of differentiation.

S.No	WD SCC (N=64)	MD SCC (N=31)	PD SCC (N=5)	F-Statistics	P-value (Paired Samples Test)
TC	148.1±21.6	148.5±25.17	137.0±24.8	0.621	0.0001
HDL	45.5±10.8	44.9±10.5	46.8±19.0	0.089	0.0001
VLDL	18±6.1	17.9±6.1	15.8±4.9	0.353	0.0001
LDL	84.69±17.0	85.7±18.8	74.4±13.3	0.93	0.0001
TG	89.7±31.0	89.6±30.3	78.6±25.1	0.357	0.0001

WD= Well differentiated; MD= Moderately differentiated; PD= Poorly differentiated

Table 4: Correlation of risk factors of OSCC with Lipid Profile

Habits in cases	**TC MEAN ±SD**	**HDL MEAN ±SD**	**VLDL MEAN ±SD**	**LDL MEAN ±SD**	**TG MEAN ±SD**
Smoking	150.33 ± 20.50	46.00 ± 10.88	19.33 ± 6.44	85.00 ± 22.32	97.00 ± 31.46
Alcohol	No cases	No cases	No cases	No cases	No cases
Chewing	140.66 ± 16.67	40.19 ± 10.40	17.44 ± 6.09	83.03 ± 10.80	87.38 ± 30.49
Smok + Alch	140.43 ± 18.05	39.71 ± 7.64	17.29 ± 5.78	85.57 ± 12.16	86.29 ± 29.01
Alch + Chew	145.15 ± 26.31	45.38 ± 13.12	17.93 ± 7.53	82.88 ± 22.76	89.54 ± 37.53
Chew + Smok	133.5 ± 54.45	41.5 ± 28.99	14.5 ± 2.12	77.5 ± 27.58	72.5 ± 12.02
All three habits	137.0 ± 20.57	43.7 ± 7.53	17.4 ± 4.25	75.9 ± 14.04	86.7 ± 20.91
No habits	148.2 ± 27.30	43.5 ± 11.87	18.8 ± 6.43	85.9 ± 20.75	94.4 ± 31.31
Habits in control	**TC MEAN ±SD**	**HDL MEAN ±SD**	**VLDL MEAN ±SD**	**LDL MEAN ±SD**	**TG MEAN ±SD**
Smoking	172.38 ± 19.31	43.85 ± 11.22	32.15 ± 8.64	93.23 ± 11.60	161 ± 43.41
Alcohol	165.67 ± 23.80	39 ± 10.58	35.67 ± 4.16	91 ± 18.36	178.67 ± 20.53
Chewing	181 ± 24.20	51 ± 10.92	36 ± 9.57	94 ± 16.65	180 ± 47.44
Smok + Alch	227 ± 19.50	71 ± 9.38	33 ± 2.66	96 ± 12.90	166 ± 13.30
Alch + Chew	210 ± 20.79	59 ± 9.92	22 ± 6.63	109 ± 15.85	108 ± 32.98
Chew + Smok	210 ± 21.51	54 ± 6.61	29 ± 2.65	127 ± 22.02	143 ± 12.37
All three habits	195 ± 23.45	53 ± 8.26	28 ± 5.25	114 ± 20.49	140 ± 26.04
No habits	130 ± 26.59	36 ± 10.69	25 ± 9.00	69 ± 20.31	124 ± 44.70

Table 5: Statistical correlation for significance of risk factors with lipid profile:

LIPIDS		Smoking	Alcohol	Chewing	Smok + Alch	Alch + Chew	Chew + Smok	Chew+smok+alch	No habits
		MEAN ±SD	MEAN ±SD	MEAN ±SD	MEAN ±SD	MEAN ±SD	MEAN ±SD	MEAN ±SD	MEAN ±SD
TC	Case	150.33 ± 20.50	No cases	140.66 ± 16.67	140.43 ± 18.05	145.15 ± 26.31	133.5 ± 54.45	137.0 ± 20.57	148.2 ± 27.30
	Control	172.38 ± 19.31	165.67 ± 23.80	181 ± 24.20	227 ± 19.50	210 ± 20.79	210 ± 21.51	195 ± 23.45	130 ± 26.59
	95% CI	16.49-27.60		34.54-46.13	62.73-110.40	58.23-71.46	64.95-88.04	51.84-64.15	-25.71—10.68
	t-Stat	7.83		13.72	7.16	19.33	13.06	18.59	-4.77
	p-value	<0.0001		<0.0001	<0.0001	<0.0001	<0.0001	<0.0001	<0.0001
HDL	Case	46.00 ± 10.88	No cases	40.19 ± 10.40	39.71 ± 7.64	45.38 ± 13.12	41.5 ± 28.99	43.7 ± 7.53	43.5 ± 11.87
	Control	43.85 ± 11.22	39 ± 10.58	51 ± 10.92	71 ± 9.38	59 ± 9.92	54 ± 6.61	53 ± 8.26	36 ± 10.69
	95% CI	0.76-6.93		7.83-13.78	28.90-33.67	10.37-16.86	6.63-18.36	7.09-11.50	-10.65—4.34
	t-Stat	2.46		7.16	25.86	8.28	4.2	8.3	-4.69
	p-value	>=0.014		<0.0001	<0.0001	<0.0001	<0.0001	<0.0001	<0.0001
VLDL	Case	19.33 ± 6.44	No cases	17.44 ± 6.09	17.29 ± 5.78	17.93 ± 7.53	14.5 ± 2.12	17.4 ± 4.25	18.8 ± 6.43
	Control	32.15 ± 8.64	35.67 ± 4.16	36 ± 9.57	33 ± 2.66	22 ± 6.63	29 ± 2.65	28 ± 5.25	25 ± 9.00
	95% CI	10.69-14.94		16.32-20.79	14.45-16.96	2.09-6.04	13.83-15.16	9.26-11.93	4.01-8.38
	t-Stat	11.87		16.36	24.69	4.05	42.72	15.69	5.6
	p-value	<0.0001		<0.0001	<0.0001	0.0001	<0.0001	<0.0001	<0.0001
LDL	Case	85.00 ± 22.32	No cases	83.03 ± 10.80	85.57 ± 12.16	82.88 ± 22.76	77.5 ± 27.58	75.9 ± 14.04	85.9 ± 20.75
	Control	93.23 ± 11.60	91 ± 18.36	94 ± 16.65	96 ± 12.90	109 ± 15.85	127 ± 22.02	114 ± 20.49	69 ± 20.31
	95% CI	3.26-13.19		7.05-14.88	6.93-13.92	20.65-31.58	42.54-56.45	33.20-42.99	-22.62—11.17
	t-Stat	3.27		5.52	5.88	9.41	14.02	15.33	-5.8
	p-value	0.001		<0.0001	<0.0001	<0.0001	<0.0001	<0.0001	<0.0001
TG	Case	97.00 ± 31.46	No cases	87.38 ± 30.49	86.29 ± 29.01	89.54 ± 37.53	72.5 ± 12.02	86.7 ± 20.91	94.4 ± 31.31
	Control	161 ± 43.41	178.67 ± 20.53	180 ± 47.44	166 ± 13.30	108 ± 32.98	143 ± 12.37	140 ± 26.04	124 ± 44.70
	95% CI	53.42-74.57		81.49-103.74	73.41-86	8.6-28.31	67.09-73.90	46.71-59.88	18.83-40.36
	t-Stat	11.93		16.42	24.97	3.69	40.87	15.96	5.42
	p-value	<0.0001		<0.0001	<0.0001	0.0003	<0.0001	<0.0001	<0.0001

Conflicts of interest:

All authors declare no conflict of interest.

References:

1. Johnson DE, Burtness B, Leemans CR, Lui VW, Bauman JE, Grandis JR, Head and neck squamous cell carcinoma. *Nature Reviews Disease Primers*, 6 (2020) 1.

2. Aggarwal V, Tuli H, Varol A, Thakral F, Yerer M, Sak K, , Varol M , Jain A, Khan MA & Sethi G, Role of reactive oxygen species in cancer progression: Molecular mechanisms and recent advancements. *Biomolecules*, 9(2019)735.

3. Ashakumary L & Vijayammal PL, Effect of nicotine on lipoprotein metabolism in rats. *Lipids*, 32 (1997) 311.

4. Kunkel GT, Maceyka M, Milstien S & Spiegel S, Targeting the sphingosine-1-phosphate axis in cancer, inflammation and beyond. *Nature Reviews Drug Discovery*, 12 (2013) 688.

5. Wong MCS, Fung FDH, Leung C, Cheung WWL, Goggins WB & Ng CF, The global epidemiology of bladder cancer: a joinpoint regression analysis of its incidence and mortality trends and projection. *Sci Rep* ,8 (2018) 1129.

6. GBD 2015 Mortality and Causes of Death Collaborators. Global, regional, and national life expectancy, all-cause mortality, and cause-specific mortality for 249 causes of death, 1980-2015: a systematic analysis for the Global Burden of Disease Study 2015. *Lancet,* 388(2016)1459

7. Thompson LDR, World Health Organization classification of tumours: Pathology and genetics of head and neck tumours. *Ear, Nose & Throat Journal*, 85 (2006) 74.

8. de Abreu PM, Có ACG, Azevedo PL, do Valle IB, de Oliveira KG, Gouvea SA, Cordeiro-Silva MF, Louro ID, de Podestá JRV, Lenzi J, Sena A, Mendonça EF& von Zeidler SLV, Frequency of HPV in oral cavity squamous cell carcinoma. *Cancer*, 18(2018)324.

9. Noone, A. M., Cronin, K. A., Altekruse, S. F., Howlader N, Lewis D R, Petkov V I & Penberthy L, Cancer Incidence and Survival Trends by Subtype Using Data from the Surveillance Epidemiology and End Results Program, 1992-2013. *Cancer epidemiology, biomarkers & prevention: a publication of the American Association for Cancer Research, cosponsored by the American Society of Preventive Oncology* , 26(2017)632.

10. Jemal A, Simard EP, Dorell C, Noone AM, Markowitz LE, Kohler B, Eheman C, Saraiya M, Bandi P, Saslow D, Cronin KA, Watson M, Schiffman M, Henley SJ, Schymura MJ, Anderson RN, Yankey D &Edwards BK, Annual Report to the Nation on the Status of Cancer, 1975-2009, featuring the burden and trends in human papillomavirus(HPV)-associated cancers and HPV vaccination coverage levels. *J Natl Cancer Inst,* 105(2013)175.

11. Brouwer AF, Eisenberg MC & Meza R, Age effects and temporal trends in HPV-related and HPV-unrelated oral cancer in the United States: A multistage carcinogenesis modeling analysis. *PLOS ONE*, 11 (2016) e0151098.

12. Braakhuis BJM, Brakenhoff RH & René Leemans C, Treatment choice for locally advanced head and neck cancers on the basis of risk factors: Biological risk factors. *Annals of Oncology*, 23 (2012) 173.

13. Ferlay J, Colombet M, Soerjomataram I, Mathers C, Parkin DM, Piñeros M, Znaor A & Bray F, Estimating the global cancer incidence and mortality in 2018: Globocan sources and methods. Int J Cancer, 144(2019) 1941.

14. Bray F, Ferlay J, Soerjomataram I, Siegel RL, Torre LA & Jemal A, Global cancer

statistics 2018: Globocan estimates of incidence and mortality worldwide for 36 cancers in 185 countries. *CA: A Cancer Journal for Clinicians*, 68 (2018) 394.

15. Muzaffar J, Bari S, Kirtane K & Chung C.H, Recent Advances and Future Directions in Clinical Management of Head and Neck Squamous Cell Carcinoma. *Cancers*, 13 (2021) 338.

16. Canning Madison, Guo Gang, Yu Miao, Myint Calvin, Groves Michael W, Byrd James Kenneth & Cui Yan, Heterogeneity of the Head and Neck Squamous Cell Carcinoma Immune Landscape and Its Impact on Immunotherapy. *Frontiers in Cell and Developmental Biology*, 7 (2019) 52.

17. Mehanna H, Kong A & Ahmed SK, Recurrent head and neck cancer: United Kingdom National Multidisciplinary Guidelines. *The Journal of Laryngology & Otology*, 130 (2016)181.

18. Ferlay J, Ervik M, Lam F, Colombet M, Mery L & Piñeros M, Global Cancer Observatory: Cancer Tomorrow. Lyon, France:International Agency for Research on Cancer, 2020.

19. Gupta S, Gupta R, Sinha DN & Mehrotra R, Relationship between type of Smokeless Tobacco & Risk of cancer: A systematic review. *Indian Journal of Medical Research*, 148 (2018) 56.

20. Bagnardi V, Rota M, Botteri E, Tramacere I, Islami F, Fedirko V, Scotti L , Jenab M, Turati F, Pasquali E, Pelucchi C, Galeone C , Bellocco R , Negri E, Corrao G, Boffetta P, & La Vecchia C, Alcohol consumption and site-specific cancer risk: A comprehensive dose–response meta-analysis. *British Journal of Cancer*, 112(2014)580.

21. Han AY, Kuan EC, Mallen-St Clair J, Alonso JE, Arshi A & St John MA, Epidemiology of squamous cell carcinoma of the lip in the United States. *JAMA Otolaryngology–Head & Neck Surgery*, 142 (2016) 1216.

22. Rigel DS, Cutaneous ultraviolet exposure and its relationship to the development of skin cancer. *Journal of the American Academy of Dermatology*, 58 (2008)129.

23. Tandon P, Dadhich A, Saluja H, Bawane S & Sachdeva S, The prevalence of squamous cell carcinoma in different sites of oral cavity at our rural health care centre in Loni, Maharashtra – A retrospective 10-year study. *Współczesna Onkologia*, 2 (2017) 178.

24. Adelstein D, Gillison ML, Pfister DG, Spencer S, Adkins D, Brizel DM, Burtness B, Busse PM, Caudell JJ, Cmelak AJ, Colevas AD, Eisele DW, Fenton M, Foote RL, Gilbert J, Haddad RI, Hicks WL, Hitchcock YJ, Jimeno A, Leizman D, Lydiatt WM, Maghami E, Mell LK, Mittal BB, Pinto HA, Ridge JA, Rocco J, Rodriguez CP, Shah JP, Weber RS, Witek M, Worden F, Yom SS, Zhen W, Burns JL, Darlow SD, NCCN guidelines insights: Head and neck cancers. *J Natl Compr Canc Netw*, 15(2017)761.

25. Sujir N, Ahmed J, Pai K, Denny C & Shenoy N, Challenges in early diagnosis of oral cancer: Cases series. *Acta Stomatologica Croatica*, 53 (2019) 174.

26. Dissanayaka WL, Pitiyage G, Kumarasiri PV, Liyanage RL, Dias KD & Tilakaratne WM, Clinical and histopathologic parameters in survival of oral squamous cell carcinoma. *Oral Surgery, Oral Medicine, Oral Pathology and Oral Radiology*, 113(2012) 518.

27. Koontongkaew S, The tumor microenvironment contribution to development, growth, invasion and metastasis of head

and neck squamous cell carcinomas. *Journal of Cancer*, 4 (2013) 66.

28. Petersen PE, Oral cancer prevention and control – the approach of the World Health Organization. *Oral Oncology*, 45 (2009) 454.

29. Mehrotra R & Gupta DK, Exciting new advances in oral cancer diagnosis: Avenues to early detection. *Head & Neck Oncology*, 3 (2011)1.

30. Poorey VK & Thakur P, Alteration of lipid profile in patients with head and neck malignancy. *Indian Journal of Otolaryngology and Head & Neck Surgery*, 68 (2015) 135.

31. Eichholzer M, Stähelin HB, Gutzwiller F, Lüdin E & Bernasconi F, Association of low plasma cholesterol with mortality for cancer at various sites in men: 17-y follow-up of the prospective basel study. *The American Journal of Clinical Nutrition*, 71 (2000) 569.

32. Mehrotra R, Pandya S, Chaudhary A K, Singh H P, Jaiswal R K, Singh M, Gupta S C, & Singh M, Lipid profile in oral submucous fibrosis. *Lipids in Health and Disease*, 8 (2009) 29.

33. Singh S, Ramesh V, Premalatha B, Prashad KV & Ramadoss K, Alterations in serum lipid profile patterns in oral cancer. *Journal of Natural Science, Biology and Medicine*, 4 (2013) 374.

34. Kitahara CM, Berrington de González A, Freedman ND, Huxley R, Mok Y, Jee SH & Samet J. M, Total cholesterol and cancer risk in a large prospective study in Korea. *Journal of Clinical Oncology*. 29 (2011) 1592.

35. Chawda JG, Jain SS, Patel HR, Chaduvula N & Patel K, The relationship between serum lipid levels and the risk of oral cancer. *Indian Journal of Medical and Paediatric Oncology*, 32 (2011) 34.

36. Samata Gadde, Sudhakar Poda, Suryanarayana Veeravilli & Lakshmi Addala, Lack of the brafv600e mutation in oral squamous cell carcinoma. *Journal of Medical Science And Clinical Research*, 04 (2016) 14912.

37. Wilms T, Boldrup L, Gu X, Coates PJ, Sgaramella N & Nylander K, High levels of low-density lipoproteins correlate with improved survival in patients with squamous cell carcinoma of the head and neck. *Biomedicines*, 9 (2021) 506.

38. Lohe VK, Degwekar SS, Bhowate RR, Kadu RP & Dangore SB, Evaluation of correlation of serum lipid profile in patients with oral cancer and precancer and its association with tobacco abuse. *Journal of Oral Pathology & Medicine*, 39 (2010) 141.

39. Kumar P, Augustine J, Urs AB, Arora S, Gupta S & Mohanty VR, Serum lipid profile in oral cancer and leukoplakia: Correlation with tobacco abuse and histological grading. *Journal of Cancer Research and Therapeutics*, 8 (2012) 384.

40. Nydegger Urse & Bütler Rene, Quantitative lipoprotein and Lipid determinations in patients with various malignancies. *Protides of the Biological Fluids*, (1972) 311.

41. Patel PS, Shah MH, Jha FP, Raval GN, Rawal RM, Patel MM, Patel JB & Patel DD, Alterations in plasma lipid profile patterns in head and neck cancer and oral precancerous conditions. *Indian J Cancer*, 41 (2004) 25.

42. Mehta R, Gurudath S, Dayansoor S, Pai A & Ganapathy K S, Serum lipid profile in patients with oral cancer and oral precancerous conditions. *Dental research journal*, 11 (2014) 345.

43. Sachdev R, Garg K, Singh G & Mehro-

tra V, A comparative study to assess the independency of lipid profile and blood sugar levels as a diagnostic marker in oral cancer and precancerous disorders. *Indian Journal of Dental Sciences*, 12 (2020) 187.

44. Ghosh G, Jayaram KM, Patil RV & Malik S, Alterations in serum lipid profile patterns in oral squamous cell carcinoma patients. *The Journal of Contemporary Dental Practice*, 12 (2011) 451.

45. Ray G & Husain SA, Role of lipids, lipoproteins and vitamins in women with breast cancer. *Clinical Biochemistry*, 34 (2001) 71.

46. Sherubin EJ, Kannan KS, Kumar DN & Joseph I, Estimation of plasma lipids and its significance on histopathological grades in oral cancer: Prognostic significance an original research. *Journal of Oral and Maxillofacial Pathology*, 17 (2013) 4.

47. Rajendran R & Sivapada Sundaram B; Benign and malignant tumors of the oral cavity. *Shafer's Textbook of Oral Pathology*, (Elsevier New Delhi), 2009, 101.

48. Hohneck AL, Rosenkaimer S, Hofheinz R-D, Akin I, Borggrefe M & Gerhards S, Blood cholesterol and outcome of patients with cancer under regular cardiological surveillance. *Current Oncology*, 28 (2021) 863.

49. Guo C-bin, Cui L-hui, Yu G-yan, Liu D-xin, Meng S-cong & Song Q, Endogenous fatty acid synthesis in squamous cell carcinomas of the oral cavity. *British Journal of Oral and Maxillofacial Surgery*, 38 (2000) 506.

50. Germain N, Dhayer M, Boileau M, Fovez Q, Kluza J & Marchetti P, Lipid metabolism and resistance to anticancer treatment. *Biology*, 9 (2020) 474.

51. Naik PP, Ghadge MS & Raste AS, Lipid profile in leukemia and hodgkin's disease. *Indian Journal of Clinical Biochemistry*, 21 (2006) 100.

52. Jahanshahi G & Sabaghian M, Comparative immunohistochemical analysis of angiogenesis and mast cell density in oral normal mucosa and squamous cell carcinoma. *Dental Research Journal*, 9 (2012) 8.

53. Sharma B & Agnihotri N, Role of cholesterol homeostasis and its efflux pathways in cancer progression. *The Journal of Steroid Biochemistry and Molecular Biology*, 191 (2019) 105377.

54. Beevi SS, Rasheed AM & Geetha A, Evaluation of oxidative stress and nitric oxide levels in patients with oral cavity cancer. *Japanese Journal of Clinical Oncology*, 34 (2004) 379.

55. Cerutti PA, Prooxidant states and tumor promotion. *Science*, 227 (1985) 375.

56. Singh M, Singh AB, Singh A & Agarwal SP, Correlation of plasma lipid levels and histopathological grading in patients with oral squamous cell carcinoma and its pre-cancerous lesions. *International Journal of Otorhinolaryngology and Head & Neck Surgery*, 4 (2018) 1436.

57. Kritchevsky SB, Wilcosky TC, Morris DL, Truong KN & Tyroler HA, Changes in plasma lipid and lipoprotein cholesterol and weight prior to the diagnosis of cancer. *Cancer Research*, 51 (1991) 3198.

58. Neufeld EJ, Mietus-Snyder M, Beiser AS, Baker AL & Newburger JW, Passive cigarette smoking and reduced HDL cholesterol levels in children with high-risk lipid profiles. *Circulation*, 96 (1997) 1403.

59. Guh J-Y, Chuang L-Y & Chen H-C, Betel-quid use is associated with the risk of the metabolic syndrome in adults. *The American Journal of Clinical Nutrition*, 83

(2006) 1313.

60. Lee B-J, Chan M-Y, Hsiao H-Y, Chang C-H, Hsu L-P & Lin P-T, Relationship of oxidative stress, inflammation, and the risk of metabolic syndrome in patients with oral cancer. *Oxidative Medicine and Cellular Longevity*, (2018).

61. Rao S & Subash EY, The effect of Chronic Tobacco Smoking and Chewing on the Lipid Profile. *J Clin Diagn Res*, 7 (2013) 31.

62. Jeng JH, Ho YS, Chan CP, Wang YJ, Hahn LJ, Lei D, Hsu CC &Chang MC, Areca nut extract up-regulates prostaglandin production, cyclooxygenase-2 mrna and protein expression of human oral keratinocytes. *Carcinogenesis*, 21 (2000) 1365.

63. Tucker LA, Use of smokeless tobacco, cigarette smoking, and hypercholesterolemia. *American Journal of Public Health*, 79 (1989) 1048.

64. Parkin DM, Bray F, Ferlay J & Pisani P. Global cancer statistics, 2002. *CA: A Cancer Journal for Clinicians*, 55 (2005) 74.

65. Salaspuro V & Salaspuro M, Synergistic effect of alcohol drinking and smoking onin vivo acetaldehyde concentration in saliva. *International Journal of Cancer*, 111 (2004) 480.

66. Castellsagué X, Quintana MJ, Martínez MC, Nieto A, Sánchez MJ, Juan A, Monner A, Carrera M, Agudo A, Quer M, Muñoz N, Herrero R, Franceschi S & Bosch FX, The role of type of tobacco and type of alcoholic beverage in oral carcinogenesis. *International Journal of Cancer*, 108 (2004) 741.

67. Proia NK, Smoking and smokeless tobacco-associated human buccal cell mutations and their association with Oral Cancer--A Review. *Cancer Epidemiology Biomarkers & Prevention*, 15 (2006) 1061.

68. Subbulakshmi AC, Mohan N, Thiruneervannan R & Naveen S, Comparative evaluation of serum lipid profile in patients with oral submucous fibrosis and oral squamous cell carcinoma with that of control subjects: A case control study. *Journal of Pharmacy and Bioallied Sciences*, 9 (2017) 191

69. Thabusum D, Reddy R, Ramesh T & Rajesh N, Lipid profile as a marker of prestage cancer and oral cancer in tobacco users. *International Blood Research & Reviews*, 3 (2014) 26.

70. Gurudath S, Ganapathy KS, D. S, Pai A, Ballal S & Asha ML, Estimation of superoxide dismutase and glutathione peroxidase in oral submucous fibrosis, oral leukoplakia and oral cancer - A comparative study. *Asian Pacific Journal of Cancer Prevention*, 13 (2012) 4409.

71. Patil PB, Bathi R & Chaudhari S, Prevalence of oral mucosal lesions in dental patients with tobacco smoking, chewing, and mixed habits: A cross-sectional study in South India. *J Family Community Med*, 20 (2013) 130.

72. Neerupakam M, Sathish S, Polisetty N, Alaparthi RK, Katta SA & Damera S, Alterations in plasma lipid profile patterns in oral cancer. *Journal of Indian Academy of Oral Medicine and Radiology*, 26 (2014) 274.

Current Trends in Biotechnology and Pharmacy
Vol. 16 (4) 445 - 455, Oct 2022, ISSN 0973-8916 (Print), 2230-7303 (Online)
10.5530/ctbp.2022.4.78

Antimelanogenic and Anticancer Activity of Isorhamnetin isolated from *Acalypha indica Linn.* on A375 cell line.

Kalaivani D[1] Arun V[2]

[1] Department of Biotechnology
Sri Ramachandra Institute of Higher Education and Research Porur, Chennai
[2] Department of Biotechnology Sri Ramachandra Institute of Higher Education and Research Porur, Chennai
*Corresponding author: arun.v@sriramachandra.edu.in

Abstract:

Hyperpigmentation refers to the skin darkening which is mainly due to the increased production of melanin. Many synthetic drugs are available in the market to cure hyperpigmentation but produce various side effects. Medicinal plants are the way forward to curing hyperpigmentation with less side effects and beneficial to the consumers. *Acalypha indica* is one of the traditional medicinal plants that is used for treating various skin disorders but has not been explored for hyperpigmentation and other aesthetic treatments. Therefore, the present study is aimed at isolation of active compounds from *Acalypha indica* for antimelanogenic and anticancer activity on human melanoma cell line A375. The ethyl acetate fraction of *A. indica* was chosen from the sequential fraction since it has flavonoids and polyphenols in high quantity when compared with other fractions. The compound was isolated using column chromatography technique and further characterized by various analytical techniques including mass spectra, FT-IR spectra, and ^{13}C-NMR and ^{1}H-NMR. Cytotoxicity study on A375 melanoma cell line was studied using MTT assay and the IC_{50} value was calculated. The mode of cell death was studied by acridine orange and ethidium bromide staining. Melanin and Tyrosinase activity was studied using the cell line. Western blotting was performed using various pro-apoptotic and apoptotic genes. Results revealed that the compound isolated was Isorhamnetin and the compound showed significant antiproliferative activity with the IC_{50} value of 8.26 µg/ml. The cell cycle analysis revealed that the compound arrested the cells at sub G0/G1 phase with the depletion of cells in S and G2-M phase. The anti-apoptotic genes such as Caspase 3, Caspase 9 and BCL-2 were down regulated and Bax protein was upregulated.

Keywords: A375 cell line, Isorhamnetin, Cell cycle arrest, Docking, Bax Protein

Introduction

In humans, skin pigmentation diverges among various populations based on the level of UV penetration. Population near the poles and located far from the tropical region receives very low intensity of UVB radiation. Contrastingly, the populations near the equator region are exposed to high amounts of UVB radiation. Exposure to UVB radiation induces the process named as melanogenesis by the organelle called melanosomes (1). Dysregulation of melanisation may lead to hyperpigmentation or hypopigmentation. Among the different dermatological disorders, variation in pigmentation is the third common disorder which causes high psychosocial impairment (2). Various skin disorders including skin melanoma, freckles, nevus,

and age spots are mainly due to hyperpigmentation due to increased production of melanin pigment (3). Therefore, hyperpigmentation can be treated by the regulation of melanisation process (4).

The age-old drug for treating this hyperpigmentation is hydroquinone which is a hydroxyl phenolic compound. Because of the adverse effects of this drug like contact dermatitis, skin irritation etc., hydroquinone has been removed from the cosmetic industry in various countries including the European Union (5). Another drug used in the cosmetic industry as a skin bleaching agent is tretinoin. These drugs are the synthetic agent involved in the inhibition of the tyrosinase activity. Due to the various side effects of these synthetic compounds, identification of compounds from natural sources with little or no side effects are the need of the hour (6). In the present study, the plant *Acalypha indica* was chosen because of its traditional use in skin disease including skin eruptions (7). Preliminary studies in our laboratory showed that the ethyl acetate extract had potent anti-melanogenic activity on zebrafish embryos and significant cytotoxicity on A375 melanoma cell line. Therefore the present study is focused on isolating an anti-melanogenic compound from the ethyl acetate fraction of the *Acalypha indica* and identifying the mechanism of action.

Materials and Methods

Maintenance of cell line

A375 melanoma cell line was obtained from National Centre for Cell Science, Pune, India (NCSS). The cells were maintained in Minimal Essential Media supplemented with 10% FBS, penicillin (100 U/ml) and streptomycin (100µg/ml) in a 5% CO_2 at 37° C.

Isolation of active compound

The ethyl acetate extract was dissolved in methanol and adsorbed on silica gel 60 – 120. After evaporation of the solvent it was loaded into a silica gel column (100 – 200 mesh size), prepared in hexane. The column was eluted with hexane followed by gradually increasing polarity with Hexane: ethyl acetate (90:10; 80:20; 70:30; 60:40; 50:50; 40:60; 30:70; 20:80) and finally with 100% Ethyl acetate. The column was further eluted with Ethyl acetate: Chloroform (90:10; 80:20; 70:30; 60:40; 50:50; 40:60; 30:70; 20:80) and finally with 100% Chloroform. The column was further eluted with Chloroform: Methanol (98:2; 94:2; 92:8; 90:10; 85:15; 80:20). A total of 124 fractions were collected and monitored under TLC. The fractions 43 to 56 showed similar bands and these fractions were combined and the solvent was evaporated under reduced pressure. The resulting crude materials were purified by using activated charcoal in hot ethanol and the fractions are kept for crystallization. The obtained crystals were analyzed further for mass spectra, FT-IR spectra, and ^{13}C-NMR and ^{1}H-NMR (8).

MTT assay using isolated compound

The anticancer activity of the isolated compound was studied in the A375 cell line. $5*10^3$ cells were seeded in the 96 well plate and incubated at 37 °C for 24 hours. Once the cell reaches 80% of confluency, media was removed. The cells were treated with different concentrations of the isolated compound and incubated again for 24 hours. After the incubation period, the test drug was removed and 100 µl of the MTT prepared in PBS was added and further incubated for 4 hours. After the incubation period was complete, the formazan crystal formed was dissolved using DMSO and the absorbance was measured at 570 nm (9).

Estimation of melanin content in cell line

The melanin content was estimated by a slightly modified method (10). A375 cells were cultured at a density of 10^5 cells per well in 96 well microtiter plates at 37 °C overnight. The test sample (3.125, 6.25, 12.5, 25, 50 and 100 µg/ml) was added to well, and incubated for 24 hr. Then, the supernatant was removed and wells

were rinsed with phosphate buffer saline (PBS) twice. The detached cells were transferred to 1.5 ml micro-tubes and centrifuged at 1100 rpm for 7 min. 100 µl of 2 M NaOH was added to cells, incubated at 100 °C for 30 min and optical density was measured using a microtiter plate reader at 405 nm.

Estimation of tyrosinase activity

A375 melanoma cells were cultured in 96 well microtiter plates. The cells were mixed with different concentrations (3.125, 6.25, 12.5, 25, 50 and 100 µg) of the extract and incubated for 24 hr. The supernatant was removed and the cells were washed with PBS twice. The detached cells were transferred to 1.5 ml micro-tubes and centrifuged at 1100 rpm for 7 min. To the pellet, 100 µl of lysis buffer containing 100 mM Na_3PO_4 (pH=6.8) was added to the cells and incubated for 30 min in ice cold condition. After centrifugation at 10000 rpm at 4 °C for 20 min, 100 µl of 5 mM L-dopa was added to 100 µl of supernatant (each containing 100 µg of the protein) at 37 °C for 2 hr. Tyrosinase inhibition was calculated by measuring the absorbance of each well and comparing it with the control group (without plant extract) at 475 nm (10).

Acridine orange and ethidium bromide staining:

To visualize the apoptotic body formation and nuclear changes after the drug treatment, the cells were stained with AO/EtBr. Briefly $5x10^4$ cells were seeded in the six well plate and incubated at 37 °C for 24 hours for reaching the confluence. Once the cells reached the 80% confluency, the cells were treated with different concentrations of the isolated compound for 48 hours. After the incubation period, the media was removed and the cells were fixed with methanol: glacial acetic acid (3:1). After fixing the cells, the plate was washed with PBS and stained with a 1:1 ratio of AO/EtBr. Once the cells were stained, it was observed under fluorescence microscopy with a magnification of 40X (9) .

DNA fragmentation

The A375 melanoma cell line was seeded in the 6 well plate at the density of $5x10^3$ cells. After treatment, the cells were harvested by pipetting and rinsed with ice-cold buffer. The cell pellets were resuspended in 200 µl of lysis buffer consisting of 0.2% Triton X-100, 10 mM Tris, and 1 mM EDTA (pH 8.0). After incubation for 10 minutes, the samples were centrifuged at 5000g for 5 min. The DNA in the supernatant was extracted using a 25:24:1 (v/v/v) equal volume of phenol: chloroform: isoamyl alcohol. The DNA was precipitated with ethanol, air dried and dissolved in the TE buffer (pH 8.0). The samples were analyzed electrophoretically on 1% agarose gel containing 0.1 µg/ml ethidium bromide. The entire procedure was repeated for the control Vero cell line (11).

Western blotting

The cultured A375 cells were treated with different concentrations of drugs for 48 h. After 48 hours of treatment, the media was removed and washed with PBS. The cells were washed with a lysis buffer (50 mM Tris-HCl, 150 mM NaCl, 0.1% SDS, 100 μg/ml PMSF, 1 μg/ml Aprorinin, 1% NP-40). After lysis, the cells were centrifuged and the supernatant was taken in a separate tube. The proteins were separated using 10% SDS-Polyacrylamide Gel and the gel was transferred to the PVDF membrane. The membrane was incubated with the primary antibody for the different proteins including p53, Bax, BCl2, Caspase 3 and Caspase 9 (12).

Cell cycle analysis by fluorescence-activated cell sorting (FACS)

To check the inhibitory effect on cell cycle, FACS was performed. After treatment, control and treated cells were washed with ice-cold phosphate-buffer saline (PBS). The cells were scraped using rubber policeman and centrifuged at 2000 rpm for 10 min. Then, cells were mixed with 500 µl of hypotonic solution (1% sodium citrate, 0.04% RNAse, 0.05% Propidium

Iodide (PI), and 3%Triton X-100) and the distribution of cells in different phase was determined by C6 Accuri (BD) flow cytometer (9).

Docking

The 3D structure of the 5M8M.pdb was downloaded from the protein data bank. Molecular docking was performed using the Autodock4.2 software. The 3D structure of molecules was optimized using chemdraw 13.0 using MMFF 94 (Maximum number of interaction: 5000, minimum RMS gradient: 0.100). All avoidable water and ligand were removed from the enzyme and the default docking parameters were fixed and docking was performed.

Results and Discussion

Structural elucidation of compound

The molecular weight of the isolated compound was determined by high-resolution mass spectrometry and the molecular ion peak appeared at m/z 317.09 (M-1). The ^{1}H NMR spectrum of compound revealed several resonances in the aromatic region 7.67 – 7.69 (1H, d, Ar-H); 7.75 (1H, s, Ar-H); and 6.19 (1H, s, Ar-H); 6.47 (1H, s, Ar-H); 6.94 – 6.93 (1H, d, Ar-H). The doublet peaks with the magnitude of the coupling constants were observed indicating meta coupling. Three typical broad hydroxyl signals were 9.44 (1H, s, -OH); 9.74 (1H, s, -OH); 10.76 (1H, s, -OH); and a sharp signal appeared at 12.46 (1H, s, -OH) indicating an alcoholic proton chelated by a ketone. Peak at δ 55.73.74, indicated the presence of methoxy moiety which was correlated with 1H-NMR signal at 3.84. The proton signals appeared at δ 6.19 – 7.75 were correlating with carbons at δ 175 – 102.99 respectively.

The ^{13}C-NMR spectrum showed signals at δC 175, 148.78, and 135.79 ppm typical of C-4, C-2 and C-3, respectively, which confirms the flavanone structure. The chemical shifts at δC 175, 163, 160, 135 ppm were corresponding to three aromatic carbons connected to hydroxyl groups at C-5, C-7 and C-3, C-4' respectively. The flavonoid ring junctions appearing at δC 98.16 and 155 ppm correspond for carbons C-9 and C-10 respectively. The carbonyl suggested by the 1H-NMR spectrum was confirmed by the ^{13}C-NMR resonance observed at δC 175.84.

The FTIR spectra showed the peaks at 3289 cm^{-1} - 3402.78 (-OH group), 3138 (=CH stretch), 3101 (–CH3 asymmetric stretch). The carbonyl group C=O stretching band was located at 2360 and aromatic double bond 2340 cm-1. In the fingerprint region, the –CH bending vibration peaks were observed at 1505 and 1162 cm^{-1}.

This pattern of the spectrum was identical with that of compound Isorhamnetin [1]. The structure of compound-1 as shown in Fig-1.

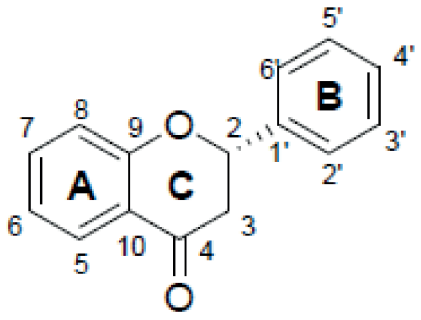

Fig 1: Flavonoid ring system

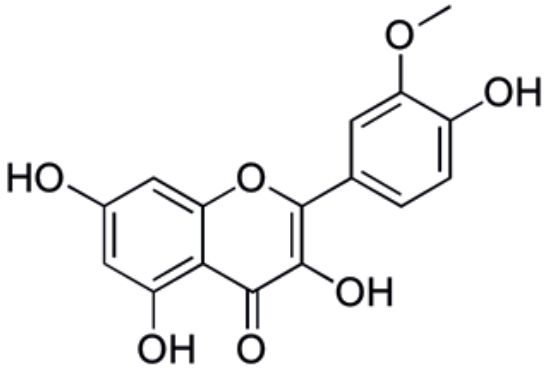

Fig 2. Isorhamnetin

The cytotoxicity analysis of the isolated compound was studied using MTT assay on A375 melanoma cell line. The dose dependent decrease in the cell viability was observed after 24 hours of incubation. The IC_{50} value for the isolated compound was found to be 8.26 µg.

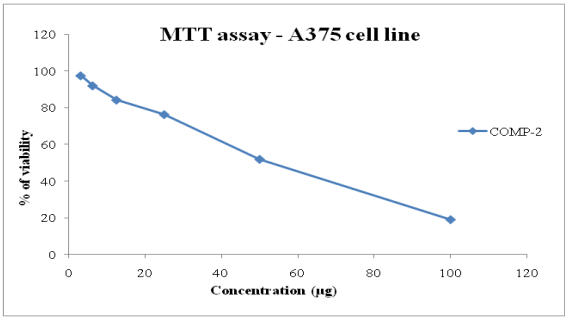

Graph 1: Cytotoxic effects of isolated compound against A375 melanoma cells. Cell viability was calculated and dose dependent decrease in cell viability was observed in A375 cells. The mechanism of cell death was evaluated through apoptosis or necrosis.

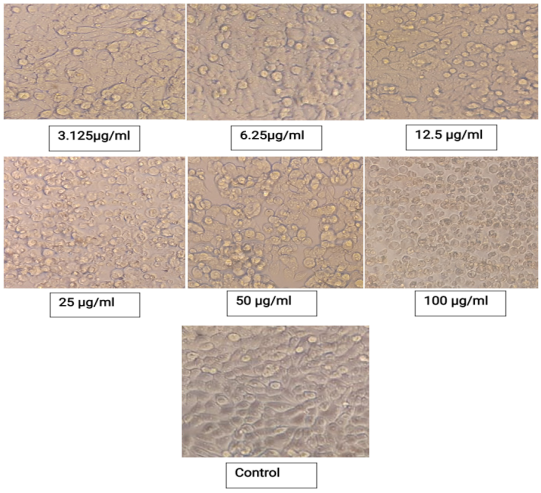

Fig 3: Morphological changes observed in A375 cell line. Phase contrast images revealed the distorted morphology in the treated cell line.

The cells were stained with AO/EtBr and observed under fluorescent microscopy. In the control group, the intact cells with green fluorescence were observed. In the compound treated cells, early apoptotic, late apoptotic, necrotic cells were observed (Fig 4).

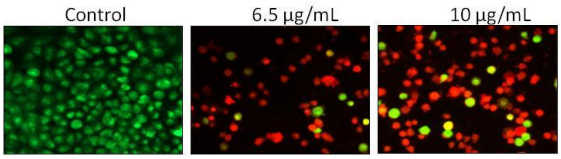

Fig 4: Control cells showed live cells whereas treated cells showed apoptotic and necrotic population dose dependently.

DNA fragmentation

DNA fragmentation reveals DNA damage in the A375 melanoma cells treated with Isorhamnetin. In the control Vero cells, intact DNA was observed. Cells treated with the compound at concentration of 6.5 µg/ml and 10 µg/ml showed fragmented DNA which initiates the apoptotic mechanism in the cells (Fig 5).

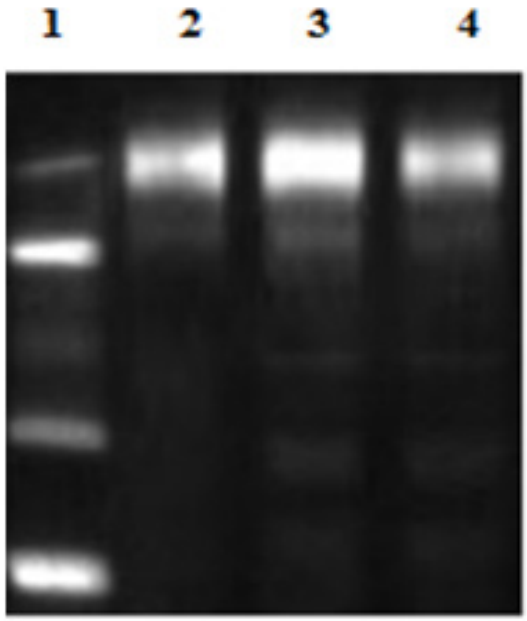

Fig 5: Control cells showed intact DNA whereas treated cells showed fragmented DNA in treated cells. Lane 1) Marker (1000 kb); 2) Control; 3) Cells treated 6.5 µg/ml of Isorhamnetin; 4) Cells treated 10 µg/ml of Isorhamnetin.

Cell cycle analysis

Distribution of cells in various phases of cell cycle was examined using flow cytometry. Results showed accumulation of cells in sub G0/G1 phase in dose dependent manner when compared to control (Fig 6). The depletion of cells in S and G2-M phase was also observed in the treated cells.

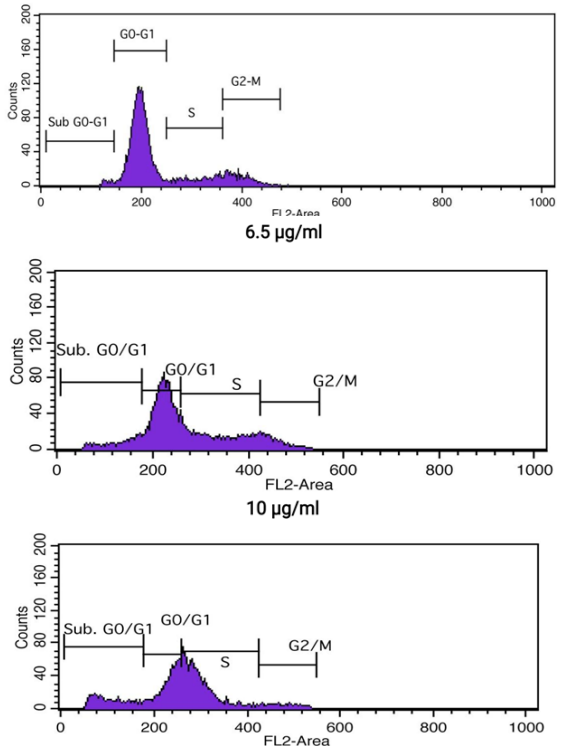

Fig 6: Cell cycle analysis by flow cytometry

Estimation of melanin content

To study the effect of the isolated compound against hyperpigmentation, melanin content in the A375 melanoma cell line was estimated. At 100 µg/ml concentration of the compound, the inhibition of melanin content was found to be 80%. The IC_{50} value for the melanin inhibition assay was found to be 26.63 µg/ml.

Estimation of tyrosinase activity

The inhibition of hyperpigmentation activity was further confirmed by the cellular tyrosinase activity. Percentage of tyrosinase inhibition was calculated and inhibition of the enzyme increased in dose dependent manner.

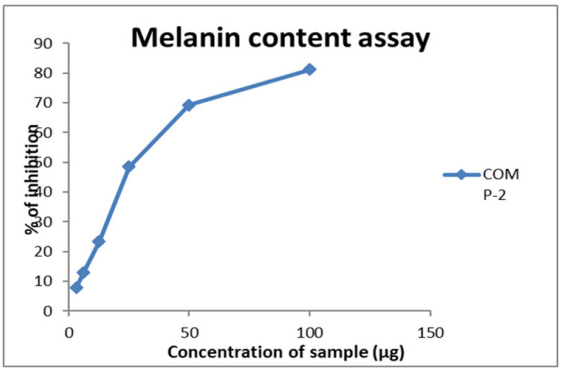

Graph 2: Inhibition of Melanin content of the isolated compound in A375 cells.

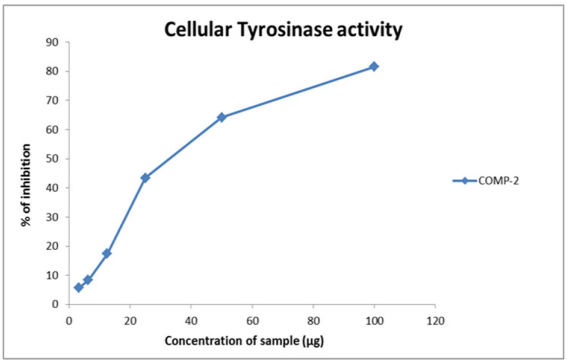

Graph 3: Inhibition of tyrosinase activity of the isolated compound in A375 cells.

Isorhamnetin upregulates the BAX protein

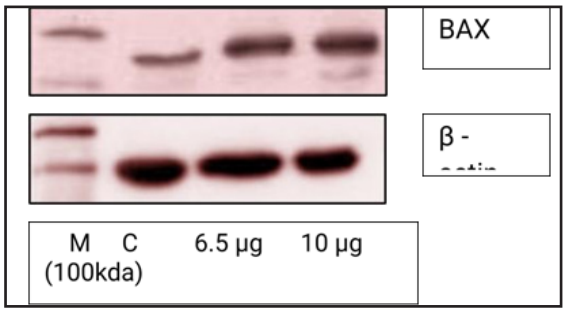

Fig:7 Western blot image of Bax protein. Bax was upregulated in Isorhamnetin treated cells while it was downregulated in control cells.

Anticancer activity of Isorhamnetin was further confirmed by the analysis of expression of various proapoptotic and apoptotic markers like BAX. Results showed increased expression of BAX in the compound treated groups when compared to control.

Role of Isorhamnetin in inhibition of BCL-2 protein

BCL-2 plays a vital role in apoptotic processes therefore the role of Isorhamnetin in inhibition of BCL-2 was studied. BCL-2 expression was upregulated in the control cells whereas in the treated cells there was marked reduction (Fig 8).

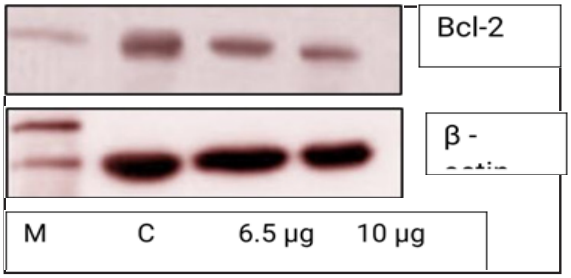

Fig:8 Western blot image of BCL2 protein. BCL2 was upregulated in the control cells with concomitant decrease in the Isorhamnetin treated cells.

Expression of caspase 3 and caspase 9 in A375 cell line:

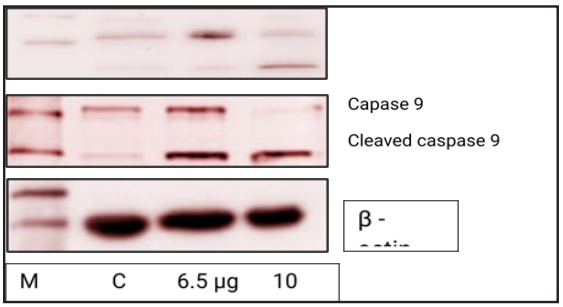

Fig:9 Western blot image of caspase protein. Caspase 3 and 9 was upregulated in the control cells with concomitant decrease in the Isorhamnetin treated cells. Cleaved caspase 3 and caspase 9 was down regulated in the control cells whereas increased expression was observed in Isorhamnetin treated cells.

Role of Isorhamnetin in the expression of caspase 3 and caspase 9 was studied using western blot. Both the caspases 3 and 9 and its cleaved form was expressed in the Isorhamnetin treated cell line when compared with the control. Caspase 3 and 9 expression was inhibited by the Isorhamnetin in the A375 cell line (Fig 9).

Upregulation of P53 expression in Isorhamnetin treated cell line

Western blot analysis of p53 expression reveals 10 µg Isorhamnetin upregulates the expression of p53 when compared with the control (Fig 10).

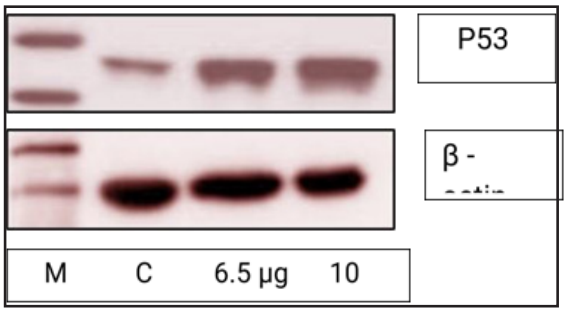

Fig 10: Western blot image of p53. p53 was downregulated in the control cells and the expression of p53 in the Isorhamnetin treated cells was upregulated.

Molecular docking of 5M8M with Isorhamnetin

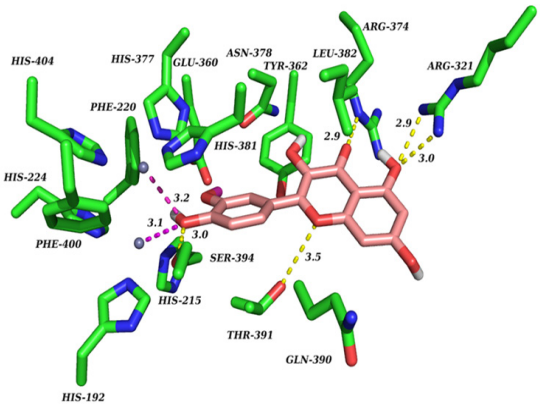

Fig 11: Interaction of Isorhamnetin with Human Tyrosinase (5M8M)

Table 1: Interaction of ligands Isorhamnetin (3,5,7-trihydroxy-2-(4-hydroxy-3-methoxyphenyl) chromen-4-one) with 5M8M.pdb

Compound ID	Binding Energy (Kcal/mol)	Inhibition constant (μM)	Interacted aminoacid	Bonding Distance Å	Bonding Types	Binding site of protein (5M8M)	Binding site of Ligand
Isorhamnetin	-5.64	73.07	SER394	3.0	Conventional hydrogen bonding	Oxygen of SER394	Oxygen of 4-hydroxy of phenyl
			ARG321	2.9	Conventional hydrogen bonding	Nitrogen of ARG321	Oxygen of 5-hydroxy of chromenone
				3.0		Nitrogen of ARG321	Oxygen of chromen-4-one
			ARG374	2.9	Conventional hydrogen bonding	Nitrogen of ARG374	Oxygen of chromen-4-one
			THR391	3.5	Conventional hydrogen bonding	Oxygen of THR391	Oxygen of 4-hydroxy of phenyl
			CU2+	3.2	Conventional hydrogen bonding		Oxygen of 3 methoxy phenyl
			CU2+	3.1	Ionic interactions		
					Ionic interactions		

Isorhamnetin showed high binding capacity with the 5M8M protein with the binding energy of -5.64 Kcal/mol. The compound effectively binds with the following amino acids *viz* SER394, ARG321, ARG374, THR391 with the bonding distance of 3.0 Å, 2.9 Å, 2.9 Å and 3.5 Å respectively (Table 1).

In the present study, Isorhamnetin; the compound isolated from *Acalypha indica, was* examined for anticancer activity in A375 melanoma cell lines. A375 is the human malignant melanoma cell line that has the characteristic feature of cutaneous melanoma with the mutation of B-RAF and CDKN2 (13).

Cell viability of A375 cells were examined using MTT assay which showed decreased cell viability dose dependently with an IC_{50} value of 58.26 μg/ml for the isolated compound, Isorhamnetin from *A.indica* ethyl acetate fraction. The isolated compound did not show any cell death in the Vero cell line up to 100 μg/ml. Since the compound did not show any cytotoxicity in the normal cell line; further studies were carried out to investigate the anticancer activity of Isorhamnetin. Once the cytotoxicity is observed, the cells will undergo apoptosis or necrosis (14). In order to check the rate of cells undergoing apoptosis or necrosis, the cells were stained with AO/EtBr. The compound induced

both apoptosis and necrosis in a dose dependent manner. To further investigate the role of Isorhamnetin exhibiting anticancer properties, the mechanism of apoptosis should be studied. Apoptosis can be initiated and the result can be evaluated by morphological changes, elevation of biochemical markers, chromatin condensation and fragmentation in the nucleus and DNA damage (15). DNA damage in the cell line was observed using DNA fragmentation assay and the result showed dose dependent fragmentation of DNA in Isorhamnetin treated cells when compared to control.

Cell cycle is the common pathway occurring in the cell; which comprises various checkpoints for cell division. Escaping from the cell cycle is one of the common strategies for the cancer cells to undergo rapid divisions (16). Duration of cell cycle in both the normal and tumor cell will be the same but the proportion of cell division is high in cancer cells when compared to normal cells (17). In the present study, the cell cycle inhibition was observed at G0/G1 phase and depletion of cells in the subsequent phases. In previous studies, Isorhamnetin treated in A549 lung cancer cell line showed G2/M phase arrest (16). To further confirm the anticancer activity, the level of protein BCLl-2, Bax and p53 was estimated using western blot technique. BCL2 and BAX are the important proteins in apoptosis where the former protein is involved in inhibition of apoptosis, while the latter is involved in promoting the apoptotic mechanism. p53 is a tumor suppressor protein that has an important role in cell cycle progression and induces apoptosis (18). In this study, expression of BAX and p53 in the control group was reduced but it was increased dose-dependently in the Isorhamnetin treated groups. Once the apoptotic signal is received, the initiator caspase 9 will get activated and caspase 3 will be involved in the execution of apoptosis (19). In this study, the caspase 3 and caspase 9 were upregulated in the Isorhamnetin treated groups when compared to the control. Molecular Docking results revealed high binding efficacy of Isorhamnetin with 5M8M Human tyrosinase protein (Fig 11). The type of interaction and the affinity of the compound to bind between the target protein and the ligand can be analyzed by the hydrogen bond formation and binding energy. Stable and stronger bonds are indicated by the lower binding energy since the affinity of the ligand to bind the target protein is higher. In this study, the melanogenesis enzyme target protein tyrosinase-related protein 1 (TRP 1) (PDB ID: 5M8M) was chosen to study the inhibitory activity of the compound to melanogenesis enzyme. The lower binding energy value between the compound and the TRP1 indicates stronger interaction between the compound and melanogenesis enzyme, hence isorhamnetin has the potential to inhibit melanogenesis enzyme and depigmentation. The binding energy of Isorhamnetin was found to be -5.64 Kcal/mol; which is lower, therefore, stronger and stable bonds with higher affinity are produced between the ligand and the target protein. The bond distance value of less than or equal to 3 Å indicates that the method is valid and the compound can be further be taken for docking analysis (20). The compound isorhamnetin was found to be equal to 3 Å which showed a good and valid root mean square distance value. This showed that the compound Isorhamnetin has a potential to exhibit anti melanogenic and depigmentation activity to tyrosinase-related protein 1 (TRP 1) (PDB ID: 5M8M).

Conclusion

The present study showed the anticancer and anti melanogenesis activity of Isorhamnetin isolated from *A.indica* ethyl acetate fraction on A375 cell line. The compound inhibited the melanin content and tyrosinase activity. Similarly the compound showed anticancer activity by downregulating the anti-apoptotic genes and upregulating the proapoptotic genes.

Reference

1. Nouveau S, Agrawal D, Kohli M, Bernerd F, Misra N, Nayak CS.(2016) Skin

hyperpigmentation in Indian population: Insights and best practice. Indian J Dermatol;61:487-95.

2. Halder, R. M., &Nootheti, P. K. (2003). Ethnic skin disorders overview. Journal of the American Academy of Dermatology, 48(6), S143-S148.

3. Akaberi, M., Emami, S. A., Vatani, M., &Tayarani-Najaran, Z. (2018). Evaluation of Antioxidant and Anti-Melanogenic Activity of Different Extracts of Aerial Parts of N. Sintenisii in Murine Melanoma B16F10 Cells. Iranian journal of pharmaceutical research :IJPR, 17(1), 225–235.

4. Ghosh A, Das A, Sarkar R. Diffuse hyperpigmentation: A comprehensive approach. Pigment Int 2018;5:4-13.

5. Clark, A. K., &Sivamani, R. K. (2016). Phytochemicals in the treatment of hyperpigmentation. *Botanics: Targets and Therapy*, *6*, 89-96.

6. Lee, R., Ko, H. J., Kim, K., Sohn, Y., Min, S. Y., Kim, J. A., ... & Yeon, J. H. (2020). Anti-melanogenic effects of extracellular vesicles derived from plant leaves and stems in mouse melanoma cells and human healthy skin. *Journal of extracellular vesicles*, *9*(1), 1703480.

7. Nag, A., Anoop, M., Sharma, K., & Verma, K. (2018). Acalypha Indica L. an Important Medicinal Plant with Antimicrobial agents: a Review. International Journal of Research and Analytical Reviews, 5(4); i304-i309.

8. Zhang, J., Jia, F. U., &Shuqing, J. I. A. O. (2009). Extraction of flavonoids from cherry leaves with supercritical CO2. Heilongjiang Medicine And Pharmacy, 32(2), 10N11.

9. Kalaivani, M. K., Arockiasamy, S., John, C., Vasanthi, H. R., &Soundararajan, P. (2018). Therapeutic potential of Boerhaviadiffusa L. against cyclosporine A-Induced mitochondrial dysfunction and apoptosis in madin–Darby canine kidney cells. *Pharmacognosy Magazine*, *14*(55), 132.

10. Rahimi, V. B., Askari, V. R., Emami, S. A., &Tayarani-Najaran, Z. (2017). Anti-melanogenic activity of Viola odorata different extracts on B16F10 murine melanoma cells. Iranian journal of basic medical sciences, 20(3), 242.

11. Sambrook, J., & Russell, D. W. (2006). Purification of nucleic acids by extraction with phenol: chloroform. Cold Spring Harbor Protocols, (1), pdb-prot4455.

12. Senthilkumar K, Elumalai P, Arunkumar R, Banudevi S, Gunadharini ND, Sharmila G, Selvakumar K, Arunakaran J.(2010). Quercetin regulates insulin like growth factor signaling and induces intrinsic and extrinsic pathway mediated apoptosis in androgen independent prostate cancer cells (PC-3). Mol Cell Biochem. Nov;344(1-2):173-84. doi: 10.1007/s11010-010-0540-4. Epub 2010 Jul 25. PMID: 20658310.

13. Avram, S., Coricovac, D. E., Pavel, I. Z., Pinzaru, I., Ghiulai, R., Baderca, F., Soica, C., Muntean, D., Branisteanu, D. E., Spandidos, D. A., Tsatsakis, A. M., &Dehelean, C. A. (2017). Standardization of A375 human melanoma models on chicken embryo chorioallantoic membrane and Balb/c nude mice. Oncology reports, 38(1), 89–99. https://doi.org/10.3892/or.2017.5658.

14. Ndlovu, B., De Kock, M., Klaasen, J., &Rahiman, F. (2021). In Vitro Comparison of the Anti-Proliferative Effects of Galeniaafricana on Human Skin Cell Lines. *Scientia Pharmaceutica*, *89*(1), 12.

15. Li WY, Ng YF, Zhang H, Guo ZD, Guo DJ, Kwan YW, Leung GP, Lee SM, Yu

PH, Chan SW. Emodin elicits cytotoxicity in human lung adenocarcinoma A549 cells through inducing apoptosis. Inflammopharmacology. (2014) Apr;22(2):127-34. doi: 10.1007/s10787-013-0186-4. Epub 2013 Aug 22. PMID: 23975033.

16. Zhang, B. Y., Wang, Y. M., Gong, H., Zhao, H., Lv, X. Y., Yuan, G. H., & Han, S. R. (2015). Isorhamnetin flavonoid synergistically enhances the anticancer activity and apoptosis induction by cis-platin and carboplatin in non-small cell lung carcinoma (NSCLC). *International journal of clinical and experimental pathology*, *8*(1), 25.

17. Hu, X., Yang, Z., Liu, W., Pan, Z., Zhang, X., Li, M., ... & Li, D. (2020). The anti-tumor effects of p-coumaric acid on melanoma A375 and B16 cells. *Frontiers in Oncology*, *10*.

18. Venkatachalam, P., &Nadumane, V. K. (2021). Modulation of Bax and Bcl-2 genes by secondary metabolites produced by Penicillium rubens JGIPR9 causes the apoptosis of cancer cell lines. *Mycology*, *12*(2), 69-81.

19. Jelínek, M., Balušíková, K., Schmiedlová, M., Němcová-Fürstová, V., Šrámek, J., Stančíková, J., ... &Kovář, J. (2015). The role of individual caspases in cell death induction by taxanes in breast cancer cells. *Cancer cell international*, *15*(1), 1-16.

20. Jain A. J and Nicholls A. 2008. Recommendations for evaluational methods. *Comput. Aided Mol*, 22: 133-139.

Current Trends in Biotechnology and Pharmacy
Vol. 16 (4) 456 - 470, Oct 2022, ISSN 0973-8916 (Print), 2230-7303 (Online)
10.5530/ctbp.2022.4.79

Host Specificity and Symbiotic Association Between InDigenous *Rhizobium* Strain and *Arachis hypogaea* Plants

Sanjeev Kumar K and Pavan Kumar Pindi*

Department of Microbiology, Palamuru University, Mahabubnagar, Telangana, India. 509001

*Corresponding author: pavankumarpindi@gmail.com

Abstract

Legume nodules are a major source of accessible nitrogen in the biosphere. A symbiotic interaction between soil bacteria termed rhizobia and other legume plants results in the formation of nitrogen-fixing nodules. The goal of this research was to use bio-inoculants in conjunction with specific legume plant diversity to improve nodulation and plant growth. The method entails the organic selection of 36 rhizobial isolates, of which 6 strains were isolated to determine the efficacy of relative host-specific inoculation on nodulation and development in *Arachis hypogaea* legumes. The six isolates are identified as *Bradyrhizobium yumangenesis* sps. AB5 (NCBI Accession no.: ON724398), *B. japonicum* BD5 (ON724369), *B. elkanii* KT5 (ON729445), *B. arachidis* ET5 (ON729963), *B. liaongense* JN5 (ON734019), and *B. elkanii* NP5 (ON734425). All promising combinations of preferred rhizobial strains were examined in sterile circumstances for improved nodulation and to screen for the best isolate with enhanced features by inoculation in diverse soils. The nitrogen concentration of *Arachis hypogaea* ranged from 1.2 to 2.9 percent. The strains from Amrabad were shown to be highly host specific for *Arachis hypogaea* plants, and when inoculated, they boosted nodulation and plant growth. Because of the useful traits in AB5, more research was done, using this *Bradyrhizobium yumangenesis* sps. AB5 (NCBI: ON724398). This rhizobium species AB5 was studied for its ability to unravel and improve crop production in barren, polluted, and agricultural soils, with improved *Arachis hypogaea* plant features. This method may be employed across the globe of same climatic conditions for the retrieval of plants from soils where agriculture has failed.

Key words: *Arachis hypogaea*,Host specificity, nodulation,*Bradyrhizobium* sp. strain.

Introduction

Nitrogen fixation is regarded as a significant step in the evolution process because vital molecules like proteins and nucleic acids cannot be synthesized by photosynthesis products or by other means. Lightning and combustion are examples of natural processes that can fix nitrogen (N_2) oxidatively, accounting for 10% of total nitrogen fixed. The reductive process is known as the Haber-Bosch process; it is used in the production of industrial ammonia in which H_2 gas reacts with N_2 gas over an iron-based catalyst at high temperature and pressure. This method accounts for 30 percent of total nitrogen fixation. Biological nitrogen fixation (BNF), which is also known to be a reductive process that produces ammonium (NH_4^+), is responsible for the remaining significant N_2-fixation. It does, however, occur at ambient temperature and pressure and

does not require the usage of H_2. BNF is the major support system for life on earth due to its substantial delivery of fixed nitrogen to the biosphere (1).

Biological nitrogen fixation (BNF) was reported by Beijerinck and is carried out by a specialized group of prokaryotes (2). Aquatic organisms like cyanobacteria, free-living soil bacteria like *Azotobacter*, bacteria that create associative relationships with plants like *Azospirillum*, and bacteria that form symbiotic relationships with legumes and other plants like *Rhizobium* and *Bradyrhizobium* are among these prokaryotes (3).

Between rhizobia, the degree of host specificity varies. Some strains have a very narrow host range, whereas others have a very broad range. The establishment of a symbiotic interaction between legume species and rhizobia is a difficult task. Biofertilizer technology is a new age in biological input technology that has resulted in a large increase in annual agricultural production in recent decades (4). *Rhizobium* sp. is well recognized for its symbiotic nitrogen fixing ability through nodulation in legumes, which is critical for soil nitrogen richness and cultivated land management. The importance of microbial nitrogen fixation, particularly symbiotic fixation, to agricultural productivity has fascinated scientists for over a century (5). The inability of an inoculant strain to nodulate under field conditions is caused by a variety of living and nonliving factors. Nitrogen-fixing bacteria (NFB) in the mycorrhizosphere, as well as the exploitation of these bacterial partnerships as a technique to boost plant growth, are two hot topics in biotechnology right now. One of the two major groups of eurosids is the Fabidae, which includes the majority of species capable of endosymbiotic nitrogen fixation (6). For increased nodulation specificity, these types of investigations also require molecular identification of microorganisms, and molecular microbial identification may offer an advantage over culture approaches (7,8). Previous research has shown that gene discovery and characterization can help legumes and non-legume plants with nodulation and productivity. Rhizobia, in addition to nitrogen fixing action with legumes, can boost plant phosphorus nutrition by mobilizing inorganic and organic phosphorus.

PGPR bacteria are found near the rhizosphere (9). Even in the face of a variety of stressors, such as drought, the bacteria promote plant growth (10). Plant growth promoting rhizobacteria (PGPR) are root colonization bacteria (rhizobacteria) that have a beneficial influence on plant growth via direct or indirect methods (11). Plant growth-promoting rhizobacteria is now well-known for its ability to promote growth. Kloepper and Schroth (12) described plant growth boosting rhizobacteria as soil bacteria that colonize the roots of plants following seed inoculation and enhance plant growth. The difficulty of PGPR to colonize plant roots has been attributed for its ineffectiveness (13, 14). The synergistic relationships of these pathogens collectively caused more yield, loss to this key pulse crop than the sum of their individual losses (15, 16). Furthermore, increasing bacterial populations in a plant's rhizosphere during its life cycle can improve microbial behaviour (17-19). In a pair-wise inoculation experiment, the seven most efficient nitrogen-fixing strains can be tested for their competitiveness against less effective strains, and nodule occupancy for the most efficient strain can be identified (20). Greenhouse and field studies with PGPR strains have demonstrated enhanced nodulation and nitrogen fixation in soybean, lentil, pea, chickpea and common bean (21, 22). Plant growth-promoting rhizobacteria (PGPR) are helpful native soil bacteria that colonize plant roots and boost plant development (23), plant growth regulator production (24), and plant water and nutrient intake (25). Antifungal action of PGPR can also inhibit soil-borne plant diseases (26). Because it is nodulated by rhizobia capable of nodulating a wide set of legumes and a vast group of unrelated rhizobia, peanut is regarded

as a promising promiscuous species (27). Peanut-rhizobia symbiosis has been shown to contribute 40.9 kg per hectare of biological nitrogen fixation (BNF) (28). The local or indigenous strains isolated from a geographical location have been proven to be more particular to the crop in that same geography (29) which is the primary motivation for conducting this research.

Materials and Methods

Selection of rhizosphere soils

Undisturbed rhizosphere soils along with relative six legume species [*Arachis hypogaea* (Ground nut), *Glycine max* (Soya bean), *Cicer arietinum* (Chickpea), *Phaseolus vulgaris* (Common bean),*Vigna radiata* (Mung bean), *Cajanus cajan* (pigeon pea)]in triplets were collected from six forest soils of Jannaram (JN)- Adilabad, Eturunagaram (ET)-Warangal, Narsapur (NP)-Medak, Bhadrachalam (BD)-Khammam, Amrabad (AB)-Mahabubnagar and Kataram (KT)-Karimnagar areas. The soil samples are brought to the laboratory in sterile zip-lock covers/bags.

Physico-chemical analysis of soil

There was no past history of chemical fertilizer use in these rhizosphere soils, therefore there was no risk of chemical fertilizer-induced growth inhibition of natural bioinoculants. The alkaline potassium permanganate approach was used to estimate available nitrogen in the soil (30), while the Bray and Kurtz (31) method was used to evaluate available phosphorous. Potassium is determined by flame photometrically (32).

Screening of host-specific rhizobial strains by cultivable method

Soil sample preparation

The soil samples collected from various locations were brought to the laboratory and then followed by the removal of foreign materials such as roots, gravels, stones, and pebbles. Later, using the quartering technique, the bulk amount of soil is reduced to the desired quantity (33, 34). These soil samples were used as a source sample for the isolation of host-specific rhizobium, and for seed germination.

Sowing of arachis hypogaea seed

The seeds of *Arachis hypogaea* were taken from a single lot. For sowing, undamaged and healthy seeds of the proper shape and size were chosen. Ethrel was used to break seed dormancy of the peanut seeds (35). The seeds were first surface sterilized with 0.1 percent $HgCl_2$ solution (36), and then washed 5 times with sterile distilled water to remove any remaining $HgCl_2$ traces. Then the pots are filled with respective soil samples and used to implant seeds in each pot. The seeding was done at an average 2.5 cm depth, using 10 seeds per pot. After germination, the thinning was done, staying three plants per pot. The pots were irrigated on a regular basis. Hoagland's solution course was given from time to time. Three duplicates were maintained.

Root nodule study

The nodules serve as a home for the bacteria, which obtain energy from the host plant and fix free N_2 before converting it to combined nitrogen (37). In exchange, the plant receives fixed nitrogen from nodules and produces food and forage protein (38). The fascinating thing is that nodules that fix higher amounts of N_2 are also awarded more resources, whereas nodules that fix lower amounts are penalized by the host in terms of C allocation (39-41). The most productive symbioses feature nodules with high sink strength that also distribute large amounts of organic N to the host, resulting in a strong, positive feedback on plant development under N-limiting situations (42, 43). This explains why nodule biomass is proportional to the rhizobia's N_2-fixing capacity in many symbioses (43, 44).

Because white nodules are undeveloped or may have formed as a result of the wrong bacterium, they are not included in the study. N_2

fixation is active and effective in pink or rusty nodules. Effective nodules can turn green and then revert to black, signaling that they are dead, under unfavorable conditions such as nutritional deficit, illness, or water stress (45). Peanut plants have smaller nodules, but since they are densely packed with rhizobium-infected cells, they have stronger nitrogen-fixing activity (46), implying a unique link between peanut nodule size and nitrogen-fixing activity.

Physical parameters such as number, size, fresh and dry weight of the nodules were assessed after selecting relatively large, pink, and efficient root nodules and detaching them from the plants. Leg-hemoglobin estimation is performed.

Isolation of rhizobia from nodules

A healthy plant with intact soil around the roots was uprooted. Following that, the roots were thoroughly cleansed with a jet of water. Rhizobium was isolated from nodules that are pink multi-lobed and located on the top of the root. The nodule is gently detached from the root so that a section of root on the nodule's side remains attached and the nodule is not damaged. The nodules were rinsed well under running tap water before being placed in a tube with a nylon mesh on one end. For roughly five minutes, the other end of the tube was linked to tap.

Thoroughly washed nodules were transferred to a sterile test tube and treated with 0.1% $HgCl_2$ and 70% ethyl alcohol, for 3 min and one min respectively. The test tube is shaken periodically in order to remove the adhering air bubbles and the fresh sterilant gets in touch with the nodules. After three minutes, $HgCl_2$ solution is decanted off and nodule was immersed in alcohol for 1 minute. After the nodule surface gets sterilized it was washed with sterile water for at least ten times so as to remove the sterilants completely. Nodules were crushed with a sterile glass rod with flat end. Care was taken so that test tube may not break during crushing. Suspension obtained after crushing of nodule was used for isolation of *Rhizobium*. Serial dilution of the same was done and 10^{-6} dilution was selected for isolation.

Yeast extract mannitol agar (YEMA) was used as a selective medium for isolation of *Rhizobium* sp. 100µl of 10^{-6} dilution was inoculated on sterile YEMA media plates by spread plate technique and incubated at 28°C 3 to 8 days. Based on the color of the colony and other characteristics, *Rhizobium* was isolated and various other confirmatory tests were performed.

Confirmatory Tests

Confirmatory tests are designed as discussed by Somasegaran and Hoben, 2012 (47).

Congo red test

Congo red can aid the identification of rhizobia from other kinds of bacteria. In broad the Rhizobia absorb the stain weakly while several of the common soil bacteria take it up strongly.

Growth on alkaline medium

A. radiobacter can be isolated by streaking on Hoffer's alkaline medium (pH 11) in which *Rhizobium* growth is inhibited, while *A. radiobacter* grow. YEMA added with 1 ml/lit of thymol blue (1.6% sol.) is adjusted to pH 11. On slants, the growth of *A. radiobacter* and the change in colour of indicator is observed up to 15 days. If no growth (or) change in colour is observed, it may be *Rhizobium*.

Growth in glucose peptone agar

Glucose peptone agar

(Glucose 10 g, Peptone 20.0g, NaCl 5.0g, Agar - 15.0g, Bromo cresol purple 1.0 ml (1.6% alcoholic sol.) pH 7.1) was used to distinguish rhizobia, which generally show little growth on the medium without changing the

pH, whereas *Agrobacteria* grow well shows enormous growth. Observations were taken after 15 days of incubation for growth and change in pH.

Ketolactose test

Most of the strains of *A. tumifaciens* and *A. radiobacter* have been found to produce 3-Ketolactose in lactose containing medium but not rhizobia. The composition of medium used for this test is same as that of the yeast mannitol agar except mannitol is replaced by lactose (10 g/l). The medium is poured in plates and on solidification the inoculum is streaked on it. After incubation when sufficient growth is observed, the media plates were flooded with Benedict's reagent. Development of yellow colored ring of cuprous oxide (after 30 min to one hr) around the growth of organism is indicative of *Agrobacterium* contamination.

Nodulation tests:

Nodulation tests were conducted by the following methods.

Agar tube method

This method is good to study the nodulation and differentiation of symbiotic effectiveness with plants having small seeds. In this method the plants are wholly enclosed within the glass tube.

Preparation of agar tubes

Sufficient JSA medium (1.0g $CaHPO_4$, 0.2g K_2HPO_4, 0.2g $MgSO_4.7H_2O$, 0.2g NaCl, 0.1g $FeCl_3$, 8-15g Agar, 1litre Distilled water, (1ml/litre trace element solution) is added to the medium (15 ml for deep and 20 ml for slope) was put in the tubes (200 mm x 25 mm). The tubes were closed with cotton plugs with uniform depth (20 mm) and modest compactness. The tubes were autoclaved and set as agar deep tubes or slopes as required.

- ***Nitrogen supplied control***: Nitrogen-controls were provided to a final concentration of approximately 70 ppm N (0.05% KNO_3).
- ***N-deficient control***: Agar tubes without inoculation are planted with seed or pre-germinated seedlings and put as uninoculated N-deficient control.

Microbial Identification by molecular study

Isolation of DNA from the bacterial isolates

The DNA was isolated from the bacterial colony. The obtained DNA sample was analyzed by colony PCR.

DNA was isolated from the Bacterial culture; the DNA was used in PCR to amplify bacterial 16S rDNA PCR Kit (800). Our PCR process uses the rDNA PCR Kit obtained from (TAKARA), Catalog number-RR182A. Using primers from the kit, we amplified a 1500bp amplicon and no amplicon was visible in the negative (no DNA) control and the expected sized amplicon (1500bp) was seen in the positive control. The test amplicon of 1500 bp was purified using magnetic beads and the product sequenced by Sanger's method of DNA sequencing. The sequencing results were assembled and compared with NCBI data base.

PCR analysis

In polymerase chain reaction 16S rRNA Universal primers were used to amplify the small subunit rRNA of each sample's culture DNA. The reaction mixture 50 µl contains 4µl bacterial DNA (nearly 200ng), 1µl Taq-DNA polymerase, 5µl of Taq buffer, 5µl of 2mM dNTP mix, 5 µl of forward primer (10 pM/µl) and 5 µl of reverse primer (10 pM/µl). PCR Amplification was carried out in a Bio-Rad thermo cycler run for 30 cycles. Denaturation was done for 94ºC for 20s, annealing at 48ºC for 20s and extension was done at 72ºC for 40s for each cycle, final extension was carried out for 5min at 72ºC at the end of all 30 cycles. The amplified PCR product of approximately 1542 bp was separated on a 1% agarose gel and purified by Qiagen spin columns (48).

16S rRNA gene Sequencing

The purified 1542bp PCR product was sequenced using universal primers. The complete 16S rRNA gene sequence of the isolate was subjected to BLAST sequence similarity search and Ez Taxon to identify the nearest taxa. The entire related 16S rRNA gene sequence was downloaded from the database (http://www. nbi .nlm.nih-gov) aligned using the celestial – program.

Seed inoculation and plant growth assessment

Sterile soils in triplicates from six forest places were collected and brought to the laboratory. They were taken in pots (Triplicates) and the seeds inoculated with different rhizobial strain of respective species were sown and then the growth parameters of each plant were assessed.

Undamaged and clean seeds of uniform size, selected to a reasonably uniform size were rinsed with 95% ethanol and immersed for 4 minutes in 0.2% $HgCl_2$. Seeds were then washed five times with sterile water. The viable seeds are sown after sterilization and washing, either using two seeds per tube (seedlings later can be thinned to one) or singly, allowing sufficient extra tubes. After 8 weeks of growth, the growth parameters like nodulation efficiency, number of nodules, nodular dry weight, dry weight of the plant and the plant height were assessed.

The presences of nodules, their nature at the time of harvesting that are pink because of leg-hemoglobin were accounted as effective. The rhizobial strains were isolated and tested for host specificity. All probable combination of the selected rhizobial isolates were checked under sterile conditions for improving nodulation to isolate the best host specificity plant.

Estimation of nitrogen in arachis hypogaea

Soil preparation and sowing

Soil is collected, vigorously washed and subjected to sterilization - to remove the nutrients and microorganisms particularly nitrogen fixing microorganisms from the soil to ensure that no external agent acts as source of nitrogen. The seeds of *Arachis hypogaea* from a single batch of the same size were picked and soaked in ethrel solution (5ml in 10 litres of water) for almost 12 hours before being shade dried to break dormancy before being sowed in the pots filled with sterile and nutrient free soil (35). The pots were inoculated with specific bioinoculants (Nitrogen fixing Rhizobia under study) except the controls. Negative control is maintained without any nitrogen source except the nitrogen contained in the seed initially. Positive control is treated with sufficient/unlimited nitrogen source. All the pots are irrigated frequently with Nitrogen-free Hoagsland solution. After 60 days of sowing the plants are extricated for examination of parameters.

Estimation of nitrogen by snell and snell (1949) method

A dried and ground plant sample (0.1 g) is digested completely with H_2SO_4 and heated. Then add H_2O_2 again until it is colorless. The intensity of color developed after treatment with NaOH, sodium silicate, and Nessler's reagent is then measured in the colorimeter at 440nm (blue filter). The obtained OD values are plotted on the standard graph. The nitrogen content is measured using a standard graph (49).

Estimation of leghemoglobin

The amount of nitrogen (N) fixed in the symbiotic association between the rhizobia and the plant is closely correlated with the amount of leghemoglobin (LHb) content of the root nodules of leguminous plants. A rapid, quantitative method for determining LHb in plant tissue would greatly facilitate research into symbiotic N fixation. Wilson and Reisenauer's cyanmethemoglobin method (1962) was used to determine the concentration of leghaemoglobin (50). 50 to 100mg nodules were collected and crushed in 9 volumes of

Drabkin's solution in a microfuge tube with a glass rod before centrifugation at 12,000rpm for 15 minutes. A 0.2m syringe filter was used to filter the supernatant. The filtrate was collected in a micro cuvette, and its absorbance at 540 nm was measured using a spectrophotometer (51).

Collection of soil samples from different problematical sites

Soil samples from different sites such as polluted soils, barren soils and agriculture soils were taken in triplets and inoculated with rhizobial strains in order to check the improvement in nodulation and development of these respective plants during inoculation in field trials.

Results and Discussion

The steps carried out in the present study have been represented in Figure 1. The steps include selection and collection, soil characteristics, isolation, screening and confirmatory tests for rhizobial strains, isolation of pure cultures, selection of the best isolate, Experiments carried out with the best rhizobial strain particular to legume speciesis studied and later tested in the same relative plants grown in various soils. The results of the same are presented in the following sequence as in Figure 1.

Six forest rhizosphere soils along with respective six legume species (*Arachis hypogaea*, *Glycine max*, *Cicer arietinum*, *Phaseolus vulgaris*,*Vigna radiata*, *Cajanus "cajan*) were collected from Jannaram (JN), Eturunagaram (ET), Narsapur (NP), Bhadrachalam (BD) Amrabad (AB) and Kataram (KT) areas. The physico-chemical characteristics of the soil samples were carried out.All the soils under investigation varied slightly in their soil types, the pH of different soils was slightly acidic and varied from pH 6.2 to 8.3 as shown in Table 1.

For carrying out the study six legume

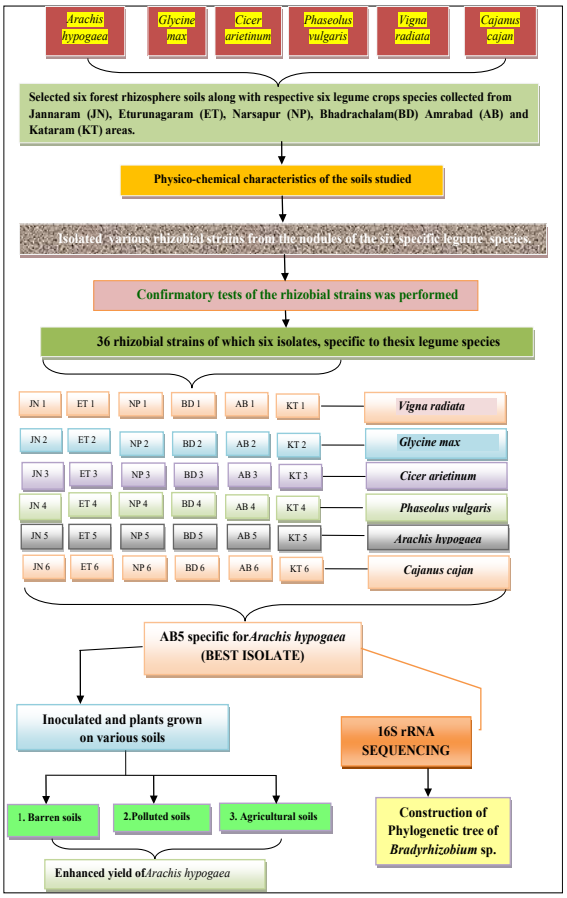

Figure 1: Steps involved in host specificity and effect of nodulation by indigenous *Bradyrhizobium* sp. AB5 in *Arachis hypogaea*

species (*Arachis hypogaea*, *Glycine max*, *Cicer arietinum*, *Phaseolus vulgaris*,*Vigna radiata*, *Cajanus cajan*) were selected and the specific rhizobial strains from the nodules of these six particular legume species were isolated. The confirmatory tests of these isolates were carried out and the pure cultures of these isolates were obtained. Thirty six rhizobial strains, six isolates specific to the six legume species were tested. The strains JN1, ET1, NP1, BD1, AB1, KT1 were specific to *Vigna radiata,*the isolates JN2, ET2, NP2, BD2, AB2, KT2 showed specificity to *Glycine max*strains JN3, ET3, NP3, BD3, AB3, KT3 showed to *Cicer arietinum*, while JN4, ET4, NP4, BD4, AB4, KT4 strain showed

Table 1: Physico-chemical characteristics in 6 forest soils (NPK in kg/hectare)

Sample collected from	Coordinates		Soil type	N	P	K	pH
	Latitude	Longitude					
Jannaram	19.1156 N	78.999 E	Red soil	265.06	105.19	160.65	6.9
Eturnagaram	18.338	80.426	Red soil	223.01	110.21	150.05	6.3
Narsapur	17.738	78.284	Deep black soil	272.73	112.32	160.00	6.2
Bhadrachalam	17.668	80.893	Red soil clay	273.03	118.11	157.02	6.7
Kataram	17.544	80.646	Red soil	272.08	104.03	147.00	6.2
Amrabad	16.383	78.833	Sandy loam	244.70	27.20	451.55	8.3

specific features with *Phaseolus vulgaris***,** JN5, ET5, NP5, BD5, AB5, KT5 isolates showed with *Arachis hypogaea* and JN6, ET6, NP6, BD6, AB6, KT6 strains were specific to *Cajanus cajan.* Among all these rhizobial isolates, JN5, ET5, NP5, BD5, AB5, KT5 were specific to*Arachis hypogaea* plantswere studied in detail**.**

The six isolates obtained from the nodules of *Arachis hypogaea*namely AB5, BD5, ET5, JN5, NP5, and KT5 are identified as *Bradyrhizobium yumangenesis* sps. AB5 (NCBI Accession no.: ON724398), *B. japonicum* BD5 (ON724369), *B. arachidis* ET5 (ON729963), *B. liaongense* JN5 (ON734019), *B. elkanii* KT5 (ON729445), and *B. elkanii* NP5 (ON734425).

Field trial studies exposed that the bacterial inoculation by rhizobia AB5 isolate on *Arachis hypogaea*plantseffects the growth and symbiotic characteristics. *Bradyrhizobium sps.* AB5 strains increased the number of nodules, nodular dry weight, dry weight of the plant and plant height compared with the control. A critical perusal of the Table 2 reveals that all the isolates under investigation induced nodulation with *Arachis hypogaea*species. However, the nodulating efficiency varied with the isolate and the plant. A lot of variation is evident with regard to the number, size and dry weight of the nodules induced by different strains.

In perusal, it was observed that AB5 isolate showed highest number of nodules in comparison with the other strains. An enhanced nodulation size was seen in KT5, AB5 and BD5 rhizobial strains. Dry weight of the nodules with the different isolated strains ranged from 15.2 to 35mg. efficient nodules were produced by AB5 isolate in *Arachis hypogaea*plant and also showed a maximum dry weight of 35 mg as seen in Graph1.

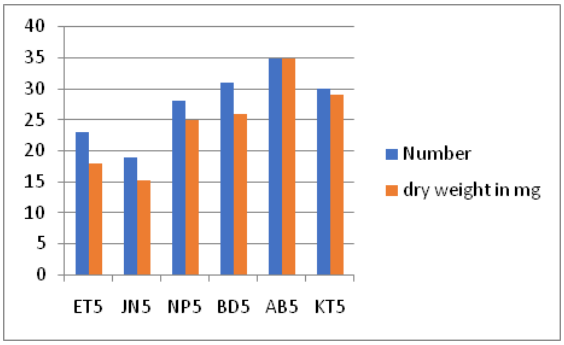

Graph 1: representing the number of nodules and total dry weight of nodules developed by various strains of rhizobium.

Plant height of *Arachis hypogaea*when inoculated with different rhizobium isolates (JN5, ET5, NP5, BD5, AB5, KT5) ranged between 24.6 and 37.8 cm. Maximum height 37.8 cm was induced by the AB5 isolate in*Arachis hypogaea*. The least height of the plant, 24.6cm was recorded with the inoculants ET5 which showed a raise in height with that of control. AB5 strain with comparison to the control showed about 2 times increase in height of *Arachis hypogaea*species.

With respect to the depth of the root AB5 measured 12 cm, which was the highest among other rhizobial strains. There was an increase in

the size of the root by 1.6 times compared to the control as tabulated in Table 2.

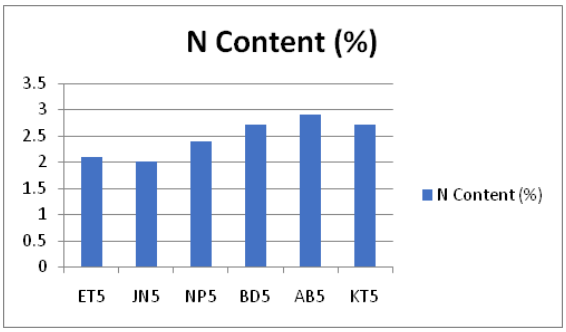

Graph 2: Representing the Nitrogen content in Arachis hypogaea by various rhizobium strains.

Increase in nitrogen content of the plant *Arachis hypogaea*was significant with inoculations of AB5, BD5 and KT5 isolates. Maximum nitrogen content recorded was about 2.9 percent and the least recorded was 2 percent in the plants inoculated with host specific strains as shown in Graph 2. The uninoculated plants showed significantly low efficiency among all the plants (Table 2) which indicates that the isolates were increasing the nitrogen content not only in the plant but also increasing the fertility of the rhizosphere soils. With respect to the effect of dry weight on shoot and root with rhizobial strains on *Arachis hypogaea*, it was observed that the AB5 strain were found to be highly host specific and the dry weight of shoot and root was maximum 1.61g and 0.72g respectively, as recorded in Table 2.

As previously indicated, the amount of nitrogen (N) fixed in the symbiotic relationship between the rhizobia and the plant is closely connected with the amount of leghemoglobin (LHb) content of the root nodules, and there is a difference in LHb concentrations between strains. LHb concentrations ranged from 0.03 to 0.08 µg/ml. The outcomes are depicted in the Graph 3.

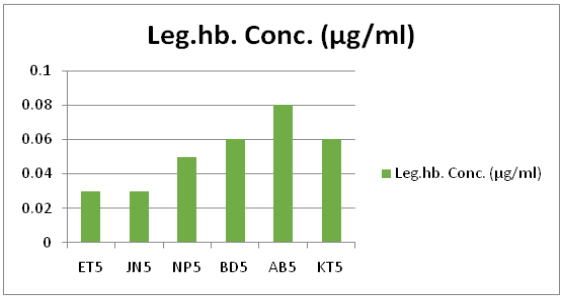

Graph 3: Representing the concentration of leghemoglobin in Arachis hypogaea and various rhizobium strains.

Table 2: Screening and isolation of different indigenous rhizobial strains from host-specific *Arachis hypogaea* species from forest areas of Telangana.

Name of the plant	Rhizobial strain	Nodulation				Plant Height(cm)		Plant dry weight (gm)		N Content (%)
		No.	Size (mm)	Leg.hb. Conc. (µg/ml)	Dry weight (mg)	Shoot	Root	Shoot	Root	
Uninoculated control	-	-	-		-	18.4 ±0.3	7.4 ±0.02	0.28 ±0.02	0.42 ±0.03	0.7 ±0.03
Arachis hypogaea	ET5	23	1.5	0.03	18±0.03	24.6±0.5	8	0.95	0.64	1.2
	JN5	19	2	0.03	15.2±0.03	25 ±0.5	8	0.88	0.57	2
	NP5	28	2	0.05	25±0.03	29 ±0.5	10	0.98	0.58	2.4
	BD5	31	1.5	0.06	26±0.03	35 ±0.5	11	1.02	0.68	2.7
	AB5	35	3	0.08	35±0.05	37.8 ±0.5	12	1.61	0.72	2.9
	KT5	30	2.5	0.06	29±0.03	35 ±0.5	11	1.01	0.67	2.7

Among all these rhizobial isolates,JN5, ET5, NP5, BD5, AB5, KT5, specific to *Arachis hypogaea* plantsstudied in detail, it can be concluded that AB5 isolate was the best isolate. Because of desirable characters of AB5, nucleic acid sequencing was performed and identified as *Bradyhizobium sp*. AB5 (ON724398).

Further studies were carried on with this strain on various soils like agricultural soils, polluted soils and barren soils with *Arachis hypogaea* plants. All the possible combinations of the potential B*radyrhizobium* sp. AB5 was also tested under field conditions for evaluating the improvement of nodulation and growth in these plants through inoculation in field trials for the categorization and amelioration of crop production in barren, polluted and agricultural soils. The nodulation ability of this isolate was confirmed by inoculation tests. The results showed a considerable increase in nodulation, size and nodular dry weight. There was an enhanced growth rate seen in the plant and also an increase in its dry weight. The nitrogen content was high in the plants. It can be concluded that the *Bradyhizobium sp*. AB5 played an essential role in the development of plants by showing significant increase in nodulation properties even in barren and polluted soils as shown in Table 3.

The results indicate that the *Bradyhizobium sp*. AB5 is host-specific to the plant*Arachis hypogaea*collected from different rhizosphere soils. This strain also increased the fertility of the barren soils that in turn increases the yield of the plant which is not possible with the wild type plants in such soils.

In the present study, with *Bradyrhizobium sps.* AB5 strain, there was increase in number of nodules in *Arachis hypogaea* which is similar to the work of Ruben Dario et al (2011) on other leguminous plants. Ruben Dario et al. (2011) observed that the commercial strain *B. japonicum* improved nodulation capacity of Argentinean commercial soybean and contributed to a higher yield (52). A simple increase in the number of nodules is not a sufficient indicator for considering peanut as an efficient nitrogen fixer, but an increase in nodule weight is a good indicator of efficient nitrogen fixation in peanut (53). With respect to the nodule weight, dry weight of the shoot, root and plant height with rhizobial isolate on *Arachis hypogaea* therewas a considerable rise observed which is in accordance with Faridul Alam et al. (2015) which states, soybean plants of all genotypes inoculated with Rhizobium sp. BARIRGm901 produced greater nodule numbers, nodule weight, shoot and root biomass, and plant height than non-inoculated plants (54). This study also revealed an increase in nitrogen content in *Vigna radiata*sp. treated with the rhizobial strain that usually increased

Table 3: Effects of Nodulation in Arachis hypogaea by Bradyrhizobium sps. AB5 isolate in agricultural, barren and polluted soils

Name of the plant	Soil types	No. Nodulation Size (mm)		Leg.hb. Conc. (µg/ml)	Dry weight (mg)	Plant Height(cm) Shoot	Root	Plant dry weight (gm) Shoot	Root	N content (%)
Control		-	-		-	18.30 ±0.5	13.20 ± 0.3	4.97 ±0.3	0.463 ±0.04	0.90 ±0.03
Arachis hypogaea	Agricultural soils	45	3	0.08	44.1	47	15	7.5	2.5	3.1
	Polluted soils	40	3	0.08	34.3	41.5	12	7.1	2.23	2.8
	Barren soils	41	3	0.08	39.77	37.5	12	7.2	2.31	2.5

the fertility of the soil (55). Jones (1998) showed that higher nodulation and biomass yields of inoculated plants could be attributed to high nitrogen fixation incorporated into nitrogen biosynthesis (56). The highest nitrogen contents and uptake were recorded in inoculated soybeans might be attributed to the greater ability of these plants to fix and assimilate nitrogen (57-60). The field trials was carried out with this isolate *Bradyhizobium sp*. AB5 (ON724398) on various soils like barren, polluted and agricultural soils on *Arachis hypogaea*. When grown in various types of soils *Arachis hypogaea* showed enhanced characters of the plant, i.e. number of nodules, size of the nodule, dry weight of root and shoot, plant height. There was an increase in nitrogen content indicating that this strain not only increases the fertility in all soil types but also increases the crop production without the use of chemical fertilizers. Rhizobia often spread from their initial habitats (61); however, the success of their introduction into new environments relies upon their ability to adapt to numerous biotic and abiotic factors (62).With respect to estimation of nitrogen accumulation with rhizobial strain AB5 inoculations, a similar study was carried using rhizobia (63). Plank (1989), reveals that there was 3.5% to 4.5% nitrogen accumulation in groundnut (64); while Oscar Yédéou Didagbé et al. (2014) shows that the nitrogen accumulation was between 1.3% and 3.9% in groundnut (65). Variation in nitrogen accumulation ranged between 2.3% to 3.75% with AB5 strain inoculated plants which are in accord to the above studies. Sulfab et al. 2011 (66) states that mineral nitrogen acts as a starter dose on the growth and production of *Vigna radiata*, which reveals that AB5 rhizobial strain can be used as a bioinoculant, based on the results.

These studies were aimed for improvement in nodulation and growth of the *Arachis hypogaea* plants through inoculation in field trials and thereby increase crop production by *Bradyrhizobium* sp. AB5 (ON724398) strain in barren, polluted and agricultural soils. The results indicate that the rhizobial strains AB5 showed host-specific characteristics to the plant *Arachis hypogaea* collected from different rhizosphere soils. The plant growth promoting characteristics of *Bradyrhizobium* sp. AB5 strain increased the quantity of seed per pod and efficiency in plants.

Conclusion

Our present perceptive of the premature events in nodulation is based on recognition and description of symbiotic association of rhizobium species with the host legume plant. Further characterization showed that this strain helped in providing interesting results. Approaches targeting downstream of the early nodulation events helped to provide a more widespread view of the association between nodule growth and a complete parameter of nodulation in legumes. The above method is an easy and cost effective method for the selection of efficient rhizobium bioinoculants like *Bradyrhizobium* sp. AB5 for its application to the legume plants in soils of same geographical region and it can be applied globally. This technique reduces the use of toxic fertilizers which the farmers do, to increase the fertility of the soil. The use of chemical fertilizers can also have a negative impact on human health and on our environment. All these can be avoided by using natural rhizobial isolates like *Bradyrhizobium* sp. AB5 which are non pathogenic but eco-friendly that can increase the fertility of various soil types, provide nutrients to the plants and in turn augment the yield of the plant because of its symbiotic association.

References

1. Smith B.E, Richards R.L and Newton W.E (eds.), (2004) Catalysts for Nitrogen Fixation: Nitrogenases, Relevant Chemical Models, and Commercial Processes, 1-31. © Kluwer Academic Publishers.

2. Beijerinck, M. W. Über oligonitrophile Mikroben. Zbl. Backt. 7, 561-582 (1901)

3. Postgate, J. R. The Fundamentals of Nitrogen Fixation. New York, NY: Cambridge University Press, 1982.

4. Pindi P.K (2012) Liquid Microbial Consortium-A Potential Tool for Sustainable Soil Health. J Biofertil Biopestici, 3:124. doi:10.4172/2155- 6202.1000124

5. Hungria M, Bohrer TRJ (2000) Variability of nodulation and dinitrogen fixation capacity among soybean cultivars. Biology and Fertility of Soils 31(1): 45-52.

6. Wang H et al. (2009) Rosid radiation and the rapid rise of angiosperm-dominated forests. Proc. Natl Acad. Sci. USA 106: 3853–3858.

7. Pavan Kumar Pindi, Hara Kishore K, Reddy GSN, Shivaji S (2009) Description of *Leifsonia kafniensis* sp. nov and Leifsonia antarctica sp. nov. Int. J. Syst. Evol. Microbiol 59: 1348–1352.

8. Pavan Kumar Pindi, Ruth Manorama, Zareena Begum, Shivaji S (2010) *Arthrobacter antarcticus* sp. nov., isolated from sediment from the Antarctic Sea. Int. J. Syst. Evol. Microbiol 60: 2263-2266.

9. Martı´nez-Viveros O, Jorquera MA, Crowley DE, Gajardo G, Mora ML (2010) Mechanisms and practical considerations involved in plant growth promotion by rhizobacteria. J Soil Sci Plant Nutr 10: 293–319

10. Creus CM, Sueldo RJ, Barassi CA (1996) Azospirillum inoculation in pregerminating wheat seeds. Canadian J Microbiol 42: 83–6.

11. Nelson LM (2004) Plant growth promoting rhizobacteria (PGPR): Prospects for new inoculants. Online Crop Management 10.1094/CM2004030105RV.

12. Kloepper JW, Schroth MN (1978) Plant growth promoting rhizobacteria on radishes. In: Proceeding of the 4th International Conference on Plant Pathogenic Bacteria. Vol. 2, (879-882). Station de Pathologie Vegetale et Phytobacteriologie, INRA, Angers, France,

13. Benizri E, Baudoin E, Guckert A (2001) Root colonization by inoculated plant Growth Promoting Rhizobacteria. Bio Sci Tech 11: 557-574.

14. Lugtenberg BJJ, Dekkers Land, Bloemberg GV (2001) Molecular determinants of rhizosphere colonization by Pseudomonas. Annu Rev Phytopathol 39: 461-490.

15. Siddiqui ZA, Husain SI (1992) Interaction of Meloidogyne incognita race 3 Macrophomina phaseolina and Bradyrhizobium sp. in a root rot disease complex of chickpea, Cicer arietinum. Fundam Appl Nematol 15: 491-494.

16. Akhtar MS, Siddiqui ZA (2008a) Biocontrol of a root-rot disease complex of chickpea by Glomus intraradices, Rhizobium sp. And Pseudomonas straita. Crop Protec 23: 410-417.

17. Pooran C, Singh PK, Govardhan M, Chand P (2002) Integrated management in rain fed castor (*Ricinus communis*). Ind Prog Agri 2: 122-124.

18. Bajpai RK, Upadhyay SK, Joshi BS, Tripathi RS (2002) Productivity and economics of rice (*Oryza sativa* L.) wheat (*Triticum aestivum*) cropping system under integrated nutrient supply systems. Ind J Agron 47: 20-25

19. Cheuk W, Lo KV, Branion RMR, Fraser B (2003) Benefits of sustainable waste management in the vegetable greenhouse industry. J Environ Sci Health 38: 855-863.

20. Hafeez FS, Hameed T, Ahmad K, Malik (2001) Competition between effective and less effective strains of *Bradyrhizobium* spp. for nodulation on Vigna radiate. Biology and Fertility of Soils Vol 33 (5): 382-386

21. Chanway CP, Hynes RK, Nelson LM (1989) Plant growth promoting rhizobacteria: effects on growth and nitrogen fixation of lentil (Lens esculenta Moench) and pea (*Pisum sativum* L.).Soil Biol Biochem 21: 511–517.

22. Dileep KB, Berggren I, Mårtensson AM (2001) Potential for improving pea production by co-inoculation with fluorescent Pseudomonas and Rhizobium. Plant Soil 229: 25-34.

23. Glick BR (1995). The enhancement of plant growth by free living bacteria. Can J Microbiol 41: 109-114.

24. De Freitas JR (2000) Yield, N assimilation of winter wheat (*Triticum aestivum* L., var. Norstar) inoculated with rhizobacteria. Pedobiol 44: 97-104.

25. Okon Y, Labandera-Gonzalez CA (1994) Agronomic applications of Azospirillum: an evaluation of 20 years worldwide field inoculation. Soil Biol Biochem 26: 1591-1601.

26. Lifshitz R, Kloepper JW, Kozlowski M (1987) Growth promotion of canola (rapeseed) seedlings by a strain of Pseudomonas putida under gnobiotics conditions. Can. J. Microbiol 33: 390-395.

27. Alwi, N., Wynne, J. C., Rawlings, J. O., Schneeweis, T. J., & Elkan, G. H. (1989). Symbiotic relationship between Bradyrhizobium strains and peanut. Crop science, 29(1), 50-54.

28. Okito, A., Alves, B. J. R., Urquiaga, S., & Boddey, R. M. (2004). Nitrogen fixation by groundnut and velvet bean and residual benefit to a subsequent maize crop. Pesquisa Agropecuária Brasileira, 39, 1183-1190.

29. Pindi P.K, Satyanarayana SDV, Kumar KS (2020) Rhizobium-Legume Symbiosis: Molecular Determinants and Geospecificity. J Pure Appl Microbiol. 14 (2):1-8.

30. Subbiah BV, Asija GL (1956) A rapid procedure for the estimation of available nitrogen in soils. Curr. Sci. 25: 259-260.

31. Bray RH, Kurtz LT (1945) Determination of total, organic, and available forms of phosphorus in soils. Soil Science 59: 39-45.

32. Jackson ML (1973) Soil Chemical Analysis. Prentice Hall of India Pvt. Ltd., New Delhi, India

33. Schumacher, B. A., Shines, K. C., Burton, J. V., & Papp, M. L. (1990). Comparison of three methods for soil homogenization. Soil Science Society of America Journal, 54(4), 1187-1190

34. Campos-M, M., & Campos-C, R. (2017). Applications of quartering method in soils and foods. International Journal of Engineering Research and Application, 7(1), 35-39

35. Rajan, D., Kumar, R., Devyani, K., & Ramya, M. J. (2020). Role of Ethrel and Storage in Dormancy Breaking in Groundnut (Arachis hypogaea L.). Int. J. Curr. Microbiol. App. Sci, 9(2), 2550-2564.

36. Ramakrishna, N., Lacey, J., & Smith, J. E. (1991). Effect of surface sterilization, fumigation and gamma irradiation on the microflora and germination of barley

seeds. *International journal of food microbiology*, *13*(1), 47-54

37. Dénarié, J., Debellé, F., & Rosenberg, C. (1992). Signaling and host range variation in nodulation. Annual review of microbiology, 46(1), 497-531.

38. Cristina Gonçalves Ceolin, A. N. A., Celeste Gonçalves-Vidigal, M. A. R. I. A., Soares Vidigal Filho, P. E. D. R. O., Vinícius Kvitschal, M. A. R. C. U. S., Gonela, A., & Alberto Scapim, C. A. R. L. O. S. (2007). Genetic divergence of the common bean (*Phaseolus vulgaris* L.) group Carioca using morpho-agronomic traits by multivariate analysis. Hereditas, 144(1), 1-9.

39. Simms EL, Taylor DL, Povich J, Shefferson RP, Sachs JL, Urbina M, Tausczik Y. 2006. An empirical test of partner choice mechanisms in a wild legume–rhizobium interaction. Proceedings of the Royal Society B: Biological Sciences 273, 77–81.

40. Regus JU, Gano KA, Hollowell AC, Sofish V, Sachs JL. (2015). Lotus hosts delimit the mutualism–parasitism continuum of Bradyrhizobium. Journal of Evolutionary Biology 28, 447–456

41. Westhoek A, Field E, Rehling F, Mulley G, Webb I, Poole PS, Turnbull LA. 2017. Policing the legume–Rhizobium symbiosis: a critical test of partner choice. Scientific Reports 7, 1419

42. Kaschuk G, Hungria M, Leffelaar PA, Giller KE, Kuyper TW. 2010a. Differences in photosynthetic behaviour and leaf senescence of soybean (Glycine max [L.] Merrill) dependent on N2 fixation or nitrate supply. Plant Biology 12, 60–69.

43. Quides KW, Stomackin GM, Lee HH, Chang JH, Sachs JL. 2017. Lotus japonicus alters in planta fitness of Mesorhizobium loti dependent on symbiotic nitrogen fixation. PLos One 12, e0185568.

44. Pampana S, Masoni A, Mariotti M, Ercoli L, Arduini I. 2016. Nitrogen fixation of grain legumes differs in response to nitrogen fertilisation. Experimental Agriculture 54, 66–82

45. Cumming G et al. (2014) Northern Mungbean -Best Management Practices Training Course, Module 2. Pulse Australia Ltd.

46. Tajima, R., Lee, O. N., Abe, J., Lux, A., & Morita, S. (2007). Nitrogen-fixing activity of root nodules in relation to their size in peanut (Arachis hypogaea L.). Plant Production Science, 10(4), 423-429

47. Somasegaran, P., & Hoben, H. J. (2012). Handbook for rhizobia: methods in legume-Rhizobium technology. Springer Science & Business Media.

48. Barlett, J., & Stirling, D. (2003). PCR Protocols. Methods in molecular biology, 226, 556.

49. Snell PD, Snell GL. (1949) Colorimetric method of analysis. 3rd Edition Volume II. D van Nostrand Co. Inc, New York,

50. Wilson, D. O., & Reisenauer, H. M. (1963). Determination of leghemoglobin in legume nodules. Analytical Biochemistry, 6(1), 27-30.

51. Kannan, V. R., Sithara, S., & Chandru, S. (2015). Proportional analysis of leghaemoglobin concentration in various nodulating plants and intuitive Rhizobium species. European Journal of Experimental Biology, 5(4), 15-23.

52. Rubén Darío S, Monica A, Mariangela H, Pedro Alberto B. (2011) Nodulation

capacity of Argentinean soybean (Glycine max L. Merr) cultivars inoculated with commercial strains of *Bradyrhizobium japonicum*. Am. J. Plant Sci.; 3:130–140.

53. Kremer, R. J., & Peterson, H. L. (1983). Field Evaluation of Selected Rhizobium in an Improved Legume Inoculant 1. Agronomy Journal, 75(1), 139-143.

54. Faridul Alam, M.A.H. Bhuiyan, Sadia Sabrina Alam, Tatoba R. Waghmode, Pil Joo Kim & Yong Bok Lee (2015) Effect of Rhizobium sp. BARIRGm901 inoculation on nodulation, nitrogen fixation and yield of soybean (*Glycine max*) genotypes in gray terrace soil, Bioscience, Biotechnology, and Biochemistry, 79:10, 1660-1668, DOI: 10.1080/09168451.2015.1044931.

55. Kumar, S., & Pindi, P. K. (2021). Data on host specificity and symbiotic association between indigenous Rhizobium BD1 strain and Vigna radiata (green gram). Data in brief, 39, 107520.

56. Jones JBJ (1998) Plant nutrition manual. 1st ed. Boca Raton (FL): CRC Press; p. 149.

57. Mendel RR, Hänsch R. (2002) Molybdoenzymes and molybdenum cofactor in plants. J. Exp. Bot. 53:1689–1698.

58. Pramanik P, Haque MM, Kim PJ. (2013) Effect of nodule formation in roots of hairy vetch (Vicia villosa) on methane and nitrous oxide emissions during succeeding rice cultivation. Agric. Ecosyst. Environ; 178:51–56.

59. Vieira RF, Cardoso EJBN, Vieira C, Cassini STA. (1998) Foliar application of molybdenum in common beans. I. Nitrogenase and reductase activities in a soil of high fertility. J. Plant Nutr; 21:169–180.

60. Raven PH, Evert RF, Eichhorn SE. (1999) Biology of plants. 6th ed. New York, NY: W.H. Freeman and Company; p. 686.

61. Stępkowski T, Hughes CE, Law IJ, Markiewicz Ł, Gurda D, Chlebicka A, Moulin L. Diversification of lupine (2007) Bradyrhizobium strains: evidence from nodulation gene trees. Appl Environ Microbiol.; 73:3254–3264.

62. Trotman AP, Weaver RW. (1995) Tolerance of clover rhizobia to heat and desiccation stresses in soil. Soil Sci Soc Am J. 59:466–470.

63. Howieson J.G and Dilworth M.J. (Eds.) Working with rhizobia (2016) ISBN 978 1 925436 18 1 (PDF) Pg.No: 78-81

64. Plank, C. O., (1989). Plant analysis handbook for Georgia. Georgia Cooperative Extension Service, university of Georgia, Athens, GA.

65. Oscar Yédéou Didagbé, Pascal Houngnandan, Haziz Sina, Charlotte Carmelle Zoundji, Félix Alladassi Kouelo, Janvier Lakou, Fatiou Toukourou, Lamine Baba- Moussa. (2014) Response of groundnut (*Arachis hypogaea*) to exogenous Bradyrhizobium sp strains inoculation and phosphorus supply in two agro-ecological zones of Benin, West Africa. Journal of Experimental Biology and Agricultural Sciences, Vol: 2(6): 623-633.

66. Sulfab. H. A, Mukhtar. N. O, Hamad .M. E and Adam. A. I (2011) Effect of Bio-Organic and mineral nitrogen starter dose on growth and production of groundnuts (Arachis hypogaea L.) in Malakal Area. Journal of Science and Technology 12 (02): 13-22.

Current Trends in Biotechnology and Pharmacy
Vol. 16 (4) 471 - 480, Oct 2022, ISSN 0973-8916 (Print), 2230-7303 (Online)
10.5530/ctbp.2022.4.80

Non-Recombinant Mutagenesis of *Bacillus mojavensis CUIE1819* for Hyper Production of Lipase and Treatment of Polluted Lakes

Irene Infancy J[1], Erumalla Venkata Nagaraju[*] Vaddi Damodara Reddy, Kuppusamy Alagesan Paari

[1]Department of Life Sciences, CHRIST (Deemed to be University), Bengaluru-560029.

[2]DR Biosciences, Research and Development Unit, Bettahalasur, Bangalore-562157.
[3]Department of Biotechnology, REVA University, Yelahanka, Bangalore-560064.
*Corresponding author: venkatanagarajue@gmail.com

Abstract

Microorganisms that degrade oil contribute significantly to the bioremediation of polluted lakes. Many microorganisms synthesize lipases, which are commercially significant. In the present study microorganisms producing extracellular lipase were isolated from various polluted lakes in Bangalore by using tributyrin agar. A lipase assay was done to determine the most efficient lipase-producing organism, which was then named *Bacillus mojavensis* CUIE1819 based on 16srRNA sequencing. After UV irradiation, the selected immobilized organisms were used to treat the lake water samples.

Keywords: Microbial Lipase, screening, production, Lipase assay, oil degradability, mutagenesis

Introduction

Microorganisms, because of their great plasticity and physiological flexibility, are ubiquitous. They have developed the ability to adapt and to survive in different environmental conditions, even in the most inhospitable conditions making them almost invincible and the underlying reason being the efficient enzyme system. Their ability to produce extracellular enzymes is of great significance for their survival adaptability in any niche. Many microorganisms, with the help of their diverse extracellular enzyme mechanisms, have found ways to degrade toxic chemicals and compounds into safe, tolerable, and useful products, and thus play a major role in bioprospecting.

A study, titled 'Wetlands: Treasures of Bangalore (Abused, Polluted, Encroached and Vanishing)', conducted and led by Professor Ramachandra T V from the Energy and Wetlands Research Group, Centre for Ecological Sciences, IISc, Bangalore, surveyed 105 lakes in the city and found that only four lakes seemed to be in a good condition while 25 lakes were in a very bad state fully covered with macrophytes or dumped with solid or liquid wastes and with little or no water. Sustainedflow of untreated sewage, the release of untreated industrial effluents, and the dumping of solid waste and building debris were found to be the main causes of lake pollution. (1)

Microorganisms that are living in such lakes may have developed the ability to sustain themselves in such an environment by releasing certain proteins or enzymes that help to degrade the substances that inhibit their growth. By isolating such organisms, we may be able to find ways to obtain such enzymes/ proteins or couture a mixture of organisms to degrade the harmful substances and revive the lake back to its ecological health. (2)

The effluents rich in oils released into

the lakes can also be degraded by enzymes such as lipases that are extracellularly released by microorganisms to prevent the decrease in the dissolved oxygen content and maintain a sustainable environment.

Isolation of extracellular lipase producing organism has always gained a lot of importance due to its various biotechnological importance and application in production such as detergents, textile, and dairy industries; oil processing; production of surfactants; synthesis of chiral pharmaceuticals. There is an interest to find new lipases that could create novel applications as each industrial application may require specific properties of the enzyme (3).

Bacterial lipases are mostly inducible enzymes, requiring some form of oil, fatty acids, fatty acid alcohol, or fatty acid ester for induction. Triacyl glycerols, the main substrates of lipases, are uncharged lipids. The triacylglycerols with long-chain fatty acids are esterified with glycerol and are insoluble in water, although those with short-chain fatty acids are sparingly soluble in water. Biosynthesis of lipase by microorganisms was found to be enhanced by the optimization of culture condition factors such as temperature, pH, aeration, medium composition, etc. (4-11)

Mutation of a producer strain and selection of a hyper producing phenotype has proved successful for strain improvement and yield of enzymes and primary and secondary metabolites (12). Although product yield may be improved by optimizing the culture conditions, productivity is ultimately controlled by the genome. Thus, to improve productivity, the organism's genome must be modified and this may be achieved in two ways viz. mutation or recombination. Recent advances in molecular biology have increased the number of methods by which genetic variation can be generated, the mutation is still the most important means of quickly and efficiently creating genetic variation in a population. Mutation represents an invaluable tool for biotechnological innovations and plays an important role in strain improvement of microorganisms used in the industry. Increased yield of fermentative lipase through mutagenesis followed by the subsequent selection of high yielding strain is found to be reported as a significant technique in the fermentation process. (13-16).

Immobilization of enzymes is a process of physical localization of enzymes in a defined surface to improve the enzymatic properties and enhance their operational performance without altering their catalytic activity(17). Many techniques are available to immobilize enzymes using natural and synthetic materials like adsorption, ionic bonding, entrapment, and covalent bonding. The use of immobilized enzymes at the industrial level is extensive as they show potential advantages over their counterparts like maintaining stability (even under harsh environmental conditions of temperature, pH, and organic solvents), reusability, and easy recovery of enzyme and thus lowering production cost. (18-22)

However, it is also important to look into the aspect of the bioremediation process of polluted water sources. With the ability of the lipase enzyme to break down lipids and glycerides, it can be used to treat lake water sources that are polluted by various industrial effluents that are rich in oil wastes. In this paper, we isolate and screen the extracellular lipase producing microorganisms from four different lake water sources (Bellandur, Varthur, Agara, and Madivala lakes) by obtaining water and soil samples and characterized by using lipase assay to obtain the best lipase-producing microorganism and identifying using 16srRNA sequencing. The identified organism was made to undergo non-recombinant UV- Mutagenesis for hyper production of the extracellular lipase and the best lipase microorganism is immobilized and used for the treatment of the polluted lake water.

Materials and Methods

Experimental chemicals

The chemicals and reagents used in this research were purchased from sigma USA and Hi media. The experiments were conducted in triplicates and the mean values were considered.

Collection and preparation of sample

Water and soil samples were collected in July from Agara, Bellandur, Madivala, and Varthur Lakes, Bangalore urban district, Bangalore, Karnataka, India. The pH and temperature of both water and soil were noted. The lake water samples were centrifuged and the obtained supernatant was preserved for further analysis. The samples were labeled and preserved at 8^0C.

Primary screening of lipase producing organism by plate assay

The 100µl of the serially diluted samples was placed on tributyrin agar media plates containing 5g of peptone; 3g of yeast extract; 10 ml of tributyrin, and 20 g of agar-agar per liter, followed by incubation for 48 h at 37 °C. After incubation, colonies that had a higher zone of clearance were used for further studies.

Secondary screening of lipase producing organism and optimisation of lipase production media

The four selected colonies were cultured in autoclaved tributyrin broth and incubated at 37^0C for 48 hours. Four different cultivation media were evaluated for the production of lipase. The composition of the different production media is summarized as follows: Medium (A) per 100ml media: 0.3g of yeast extract, 0.1g of peptone, 1ml of olive oil, 0.07g of K_2HPO_4, 0.03g of KH_2PO_4, 0.05g of $MgSO_4$, 0.01g of $MnCl_2$, 0.025g of $(NH_4)_2SO_4$ and 0.01g of $CaCl_2$. Medium (B) per 100ml media: 1ml Tween 80 which replaced olive oil in media (A). Medium (C) per 100ml media: 2g dextrose added to media (A). Medium (D) per 100ml media: 2g dextrose added to media (B). The pH of all the production media was adjusted to 6.5 using 0.5 HCl, before autoclaving at 121°C for 15 min. The enzyme production was carried out in 500 ml Erlenmeyer flasks containing 94 ml of production media that was inoculated with 6 ml of the overnight incubated culture. The flasks containing the different production media were incubated in a shaker incubator at 37^0C with constant agitation at 125rpm for 48 hours. The cells were pelleted out by centrifugation at 10000rpm 4°C for 10 minutes. The supernatant was taken and used to determine the lipase activity. The highest lipase activity expressing organism in the specific media was selected for further analysis.

Assay for lipolytic activity

For the standard, 0.5µg/ml of p-nitrophenol working standard was prepared. 0, 0.1, 0.2, 0.3, 0.4, 0.5, 0.6, 0.7, 0.8, 0.9 and 1.0 ml of working standard was pipetted out into a series of labelled test tubes. It was then made up to 2ml using phosphate buffer of pH 6.5. The same set of test tubes was placed in the water bath at 60^0C for 30 minutes. 0.25ml of 0.1M Na_2CO_3 was added to each of the samples to stop the reaction. Using a UV-Vis spectrophotometer, the optical density of the reaction mixture was determined at 410 nm. The reaction mixture containing 0.2 ml of the enzyme extract, 1.8 ml of 0.05 M phosphate buffer (pH 6.5), and 0.01M p-NPP dissolved isopropanol was kept at 60^0C for 30 minutes in a water bath. To stop the reaction 0.25ml of 0.1M Na_2CO_3 was added. Using a UV-Vis spectrophotometer, the optical density of the reaction mixture was determined at 410 nm. One unit of lipase activity was defined as the amount of enzyme which liberated 1 µmol of p-nitro phenol per min from p-nitro phenyl palmitate. From the lipase assay, the organism that produced a higher amount of lipase was selected for further studies.

Molecular characterisation of the selected extracellular lipase producing microorganism

By sequencing and analysis of the 16SrRNA gene, the molecular identification of the selected strain was carried out. The genomic DNA was extracted with the commercial kit Qiagen and the partial 16S gene was amplified using the pair of primers 16S-F:AGAGTTTGATCCTGGCTCAG and 16S-R:AAGGAGGTGATCCAGCCGCA. The reaction mixture consisted of 50 µl 1× buffer of Taq DNA polymerase, 0.2 mM of each dNTP, 0.5 µMof each primer, 2 mM of magnesium chloride, 1 U of Taq DNA polymerase (Invitrogen), 50 ng of genomic DNA, and the final volume adjusted with ultrapure water. The program used for PCR was 94°C for 240 sec, followed by 35 cycles of 94°C for 30 sec, 50 °C for 30 sec and 72 °C for 30 sec, and finally, extension at 72°C for 360 sec.

The amplified product was cleaned and analyzed on BDT v3.1 cycle sequencer on ABI3730XL, Genetic Analyzer. Consensus sequence of 16SrDNA gene was generated from forward and reverse sequence data using aligner software. The 16S rDNA gene sequence was used to carry out BLAST with the database of NCBI gene bank database. Based on the maximum identity score first ten sequences were selected and aligned using the multiple alignment software program ClustalW. Distance matrix was generated and the phylogenetic tree was constructed using MEGA 7.

Improvement of strain by uv- mutagenesis

The selected organism was then cultured in the tributyrin broth in a rotary shaker incubator at 150rpm 37^{0}C for 48 hours. A stock culture containing 7×10^3 cells/ml was prepared by centrifuging the cultured media at 10000rpm for 10 minutes at 4^{0}C and the pellet was resuspended in 0.9% saline solution. In a sterile 80 mm diameter Petri dish, 20 ml of 7×10^3 cells/ml was pipetted aseptically. UV mutation was carried out in the biosafety cabinet. The exposure time was 10, 20, 30, 40, 50, and 60 minutes. To avoid photo reactivation of the mutants, the UV-exposed suspension was stored in the dark overnight under refrigerated conditions. It was then serially diluted in saline in such a way that by the end of 10^{-5} dilution only 1×10^3 cells were present and were spread-plated on tributyrin agar medium. (4) The plates were incubated for 48 hours at 37^{0}C and the number of colonies in each plate was counted assuming each colony to be formed of a single cell. Mutants for hyperproduction of lipase were detected visually by the intensity of the zone of clearance and were further selected based on the enzyme production in the liquid medium.

Production of lipase using selected mutants

The selected mutants were then cultured in 100 ml of optimized media, composed of 6ml of the inoculum, and incubated in the shaker at 150rpm, 37^{0}C for 48 hours. Lipase assay was carried out using p-NPP (23) for the wild and the other two mutant strains. The mutant that produced relatively higher lipase was selected for further work.

Analysis of the lake water samples

Prior to the treatment of lake water, the total protein, total carbohydrate, and free fatty acid content were measured by using standard protocols (23-24).

Immobilization of the organism

The wild and the mutant strains were cultured separately in the optimized media for 48 hours at 37^{0}C in a rotary shaker incubator at 150rpm. When the culture showed 7×10^3 cells, 2ml of the culture each of the wild and the selected mutant strains were taken and centrifuged at 4^{0}C, 10000 rpm for 10 minutes and the pellet was resuspended in saline solution to halt the growth. 100ml of 4% sodium alginate was prepared and heated to melt the sodium alginate and then cooled to 37^{0}C. Meanwhile, 250ml of 2% $CaCl_2$ was prepared and stored in

ice-cold condition until its use. 20g of dummy sodium alginate beads were prepared by adding it dropwise to ice-cold 2% $CaCl_2$.2ml of the wild strain was added to 100 ml of the 4% freshly melted sodium alginate at 37^0C and mixed well. 20g of this bead was prepared by adding dropwise to ice-cold 2% $CaCl_2$. Similarly, 2ml of the mutant strain was added to 100 ml of the 4% freshly melted sodium alginate at 37^0C and mixed well. 20g of this bead was prepared by adding dropwise to ice-cold 2% $CaCl_2$.

Treatment of lake water using immobilized organisms

To the conical flask containing 100ml of lake water inoculated with 5g of dummy beads. The other conical flasks were inoculated with 5g of the immobilized wild strain followed by the addition of 5g of the immobilized mutant strain and incubated in a rotary shaker incubator at 37^0C for 48 hours. To check if the treatment procedure was carried out successfully, free fatty acid concentration was estimated by the titrimetric method.

Results and Discussion

Screening by plate assay

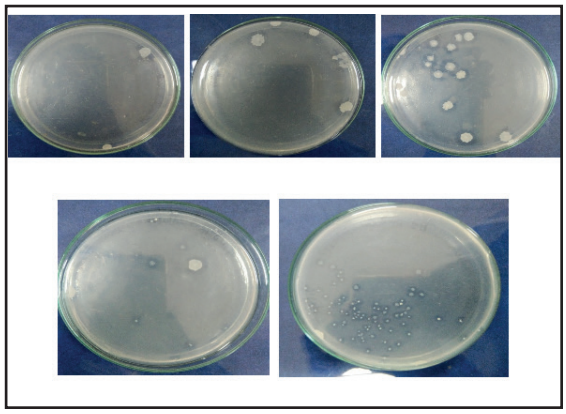

The serially diluted water, soil sample, and direct water samples were placed on tributyrin agar media (TBA). After 48 hours of incubation period zone of clearance was observed (Fig. 1-3). The colonies obtained from the Madivala lake and Bellandur lake samples were used for the production of lipase.

Optimization of lipase production media and lipase assay using p-npp

Media (C) supplemented with dextrose as carbon, and olive oil an inducer of lipase showed the maximum concentration of lipase. Lipase assay using p-NPP as a substrate was conducted by spectrophotometric analysis using a UV-Vis spectrophotometer. In this study, the

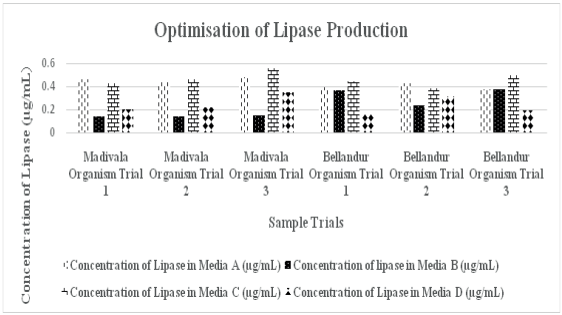

organism isolated from Madivala lake produced the highest average concentration of lipase of 0.493µg/mL and thus was selected for further work. (Fig. 4)

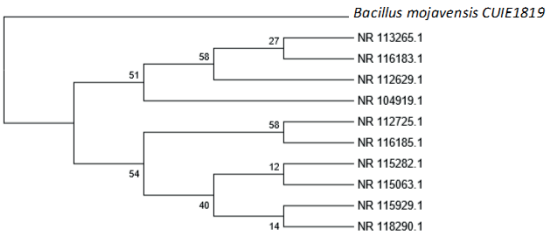

Fig. 5: Phylogenetic analysis

Fig. 4: Optimisation of lipase fermentation media using Madivala and Bellandur microorganism

Molecular characterisation of the selected lipolytic organism

The Madivala organism was cultured in tributyrin broth and pelleted and sent for sequencing and showed high similarity with *Bacillus mojavensis* based on nucleotide homology and phylogenetic analysis. (Fig. 5) The evolutionary history was inferred by using

the Maximum Likelihood method based on the Kimura 2-parameter model. Evolutionary analyses were conducted in MEGA7 using the bootstrap method and the phylogenetic tree was constructed using Neighbor-join and BioNJ to a matrix of pairwise distances that were estimated using the Maximum Composite Likelihood approach (MCL). The sequence was then submitted in NCBI as *Bacillus mojavensis CUIE1819* and the accession number was given as MK49204.

Strain improvement by uv- mutagenesis

The parental strain of *Bacillus mojavensis CUIE1819* was subjected to UV treatment for different time intervals i.e. 1o to 60 minutes. Of all the isolated obtained, 50 minutes and 60 minutes of mutation showed active mutant organism with lesser cell mass with a higher zone of clearance compared to the parent strain. For better analysis of the mutants, the mutants were cultured in the optimized media and after 48 hours of incubation in the rotary shaker incubator at 37^0C at 150rpm. After centrifugation of 2ml of the culture with triplets for both mutants and the parent strain (for comparison) and the pellet was suspended in saline solution and serially diluted from 10^{-1} to 10^{-3}

Strain	Dilution	Number of Colonies	Average Size of Zone of Clearance (mm)
Wild strain trial 1	10^{-1}	360	4
	10^{-2}	172	
	10^{-3}	3	
Wild strain trial 2	10^{-1}	156	6
	10^{-2}	79	
	10^{-3}	2	
50 minutes mutant trial 1	10^{-1}	0	NA
	10^{-2}	0	
	10^{-3}	0	
50 minutes mutant trial 2	10^{-1}	450	6
	10^{-2}	173	
	10^{-3}	60	
50 minutes mutant trial 3	10^{-1}	0	NA
	10^{-2}	1	
	10^{-3}	0	
60 minutes mutant trial 1	10^{-1}	0	NA
	10^{-2}	0	
	10^{-3}	0	
60 minutes mutant trial 2	10^{-1}	136	6
	10^{-2}	25	
	10^{-3}	6	
60 minutes mutant trial 3	10^{-1}	67	7
	10^{-2}	26	
	10^{-3}	2	

Production of lipase by mutant strains

The isolates were inoculated in 100mL of the optimized fermentation medium to check for lipase enzyme production (Fig. 6). The hyper enzyme-producing strains were selected for lake water treatment.

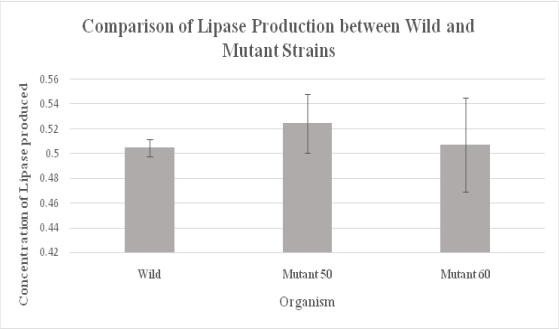

Fig. 6: Comparison of lipase production between wild and mutant strains

Lake water analysis for protein, carbohydrate and free fatty acid

Protein estimation

The amount of protein present in each of the water samples was estimated using Lowry's Method of Protein estimation using 0.01 mg/ml of BSA as the working/standard solution. (Table 2). The highest amount of protein was found to be present in Varthur lake followed by Bellandur and Madivala. Agara lake showed less protein.

Table 2: Amount of protein present in the lake water samples

Lake Sample	Concentration of protein (mg/ml)
Agara	0
Bellandur	0.014
Madivala	0.002
Varthur	0.079

Carbohydrate estimation

The amount of carbohydrate present in each water sample was estimated by the Anthrone method of Carbohydrate Estimation using 100µg/ml of glucose as the working/standard solution. (Table 3). Again, the highest amount of carbohydrate was found to be present in Varthur lake followed by Bellandur, Agara, and Madivala.

Free Fatty Estimation

The amount of free fatty acid present in each of the samples before treatment was estimated titrimetrically against an alkali like 0.01N KOH.

Table 3. Amount of carbohydrates present in the lake water samples

Lake Sample	Concentration of carbohydrate (µg/ml)
Agara	4.179
Bellandur	16.886
Madivala	3.612
Varthur	67.385

Immobilization and treatment of lake water samples

5g each of the immobilized dummy, wild, and mutant strain beads that were prepared using 4% sodium alginate in 2% $CaCl_2$, were added to each of the 100ml of the four different lake water samples (Fig. 7-10) and incubated in a rotary shaker incubator at constant agitation of 150 rpm, at 37^0C for 48 hours. After 48 hours each of the samples was tested for fatty acid content by the titrimetric method using 0.01N KOH. (Fig. 11). From this we can infer that the lipase enzyme that was released by *Bacillus mojavensis CUIE1819* could degrade the lipids that were present in the Agara lake. However, in the case of Bellandur, Madivala, and Varthur lakes, no increase in fatty acid was observed may be due to the inhibitory action of certain compounds that may be present in the other lakes.

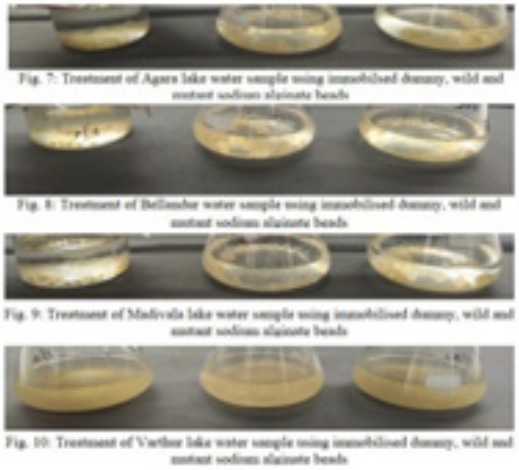

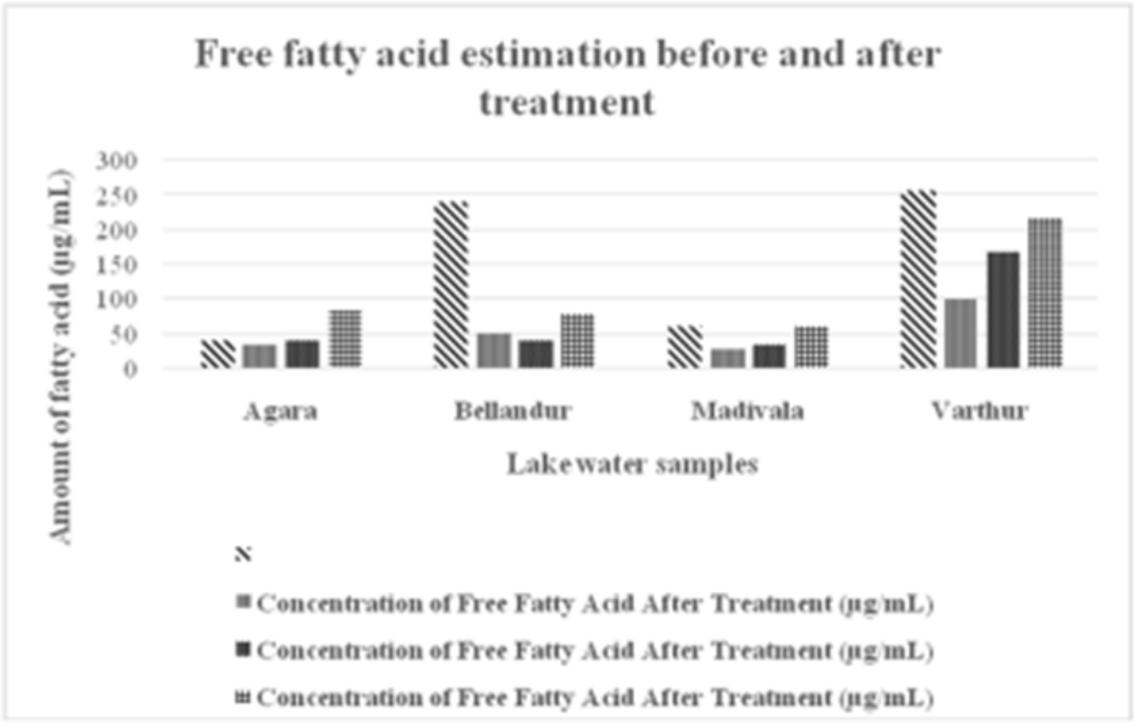

Fig. 11: Estimation of free fatty acid before and after treatment with the immobilized organism

Conclusion

Lipase producing bacteria were isolated from four different lakes: Agara, Bellandur, Madivala, and Varthur. Based on the zone of clearance, two organisms were selected to determine the highest lipase producing organism by using four different media, supplemented with dextrose as the sole carbon source and olive oil as the lipase inducer. The highest lipase producing organism was determined spectrophotometrically by lipase assay using p-NPP as substrate. After 16srRNA sequencing, the organism was found to be *Bacillus mojavensis CUIE1819* (MK49204) and was mutated by UV irradiation to check for hyper lipase production in the optimized media. The mutant that was exposed to UV for 50 minutes was seen to produce a higher amount of lipase compared to the parental/wild strain.

Water analysis of the different lake water samples was done for protein, carbohydrate, and free fatty acid using Lowry, Anthrone, and titrimetric estimation using KOH respectively. Both wild and mutant strains were immobilized in 4% sodium alginate and added to 100 mL of the lake water sample to treat it. After 48 hours of incubation in the rotary shaker incubator at 150rpm, 37^0C, free fatty acid estimation was done to see if there was an increase in the free fatty acid content. Agara lake water sample showed an increase in the free fatty acid level. However, the other lake water samples showed negative results. This could be due to the presence of certain lipase enzyme inhibitors. It is also seen that the Agara lake water sample is much cleaner compared to the other lakes. Therefore, there are chances of the absence of the lipase enzyme inhibitors and so the treatment was successful.

Acknowledgment

The authors would like to thank the HOD, VC, Pro VC, CHRIST University, REVA University and DR Biosciences Research and Develop-

ment Unit for providing the necessary facilities to carry out this work.

Conflicts of Interest

The authors declare no conflict of interest.

References

1. Ramachandra, T., Asulabha, K., Sincy, V., Sudarshan, P. and Bharath, H. (2016). Wetlands: Treasure of Bangalore.

2. Kamath. and Ganesh. (2008). Bioremediation of Lakes: Myths and Realities. 44-49.

3. Kiran, S. (2016). Microbial Lipases: Production and Applications: A Review. J. Biochem. Biotechnol. Biomater. 1(2): 7-20.

4. Ekinci, AP., Incer, BD., Baltas, N. and Adigüzel, A. (2016). Partial purification and characterization of lipase from Geobacillus stearothermophilus AH22. J. Enzyme Inhib. Med. Chem. 31(2): 325-331.

5. Verma, M., Azmi, W. and Kanwar, S. (2008). Microbial lipases: At the interface of aqueous and non-aqueous media. Acta Microbiol. Immunol. Hung. 55(3): 265-294.

6. Singh, P., Srivastava., D. Kumari., D. and Tiwari, S. (2017). Extracellular Lipase Production and Estimation from Staphylococcus and Aspergillus species. International Journal of Innovative Research in Science, Engineering and Technology. 6(5): 7600-7609.

7. Kumar, D., Kumar, L., Nagar, S., Raina, C., Parshad, R. and Gupta, VK. (2012). Screening, isolation and production of lipase/esterase producing Bacillus sp. strain DVL2 and its potential evaluation in esterification and resolution reactions. Arch. Appl. Sci. Res. 4(4): 1763-1770.

8. Pabline, RMB., Tatianne, FO., Mrcio, C. and Manoel, SSJ. (2014). Selection and optimization of extracellular lipase production using agro-industrial waste. African J. Biotechnol. 13(4): 566-573.

9. Cihangir, N. and Sarikaya, E. (2004). Investigation of lipase production by a new isolate of Aspergillus sp. World J. Microbiol. Biotechnol. 20(2): 193-197.

10. Awad, GEA., Mostafa, H., Danial, EN., Abdelwahed, NAM. and Awad, HM. (2015). Enhanced production of thermostable lipase from Bacillus cereus ASSCRC-P1 in waste frying oil based medium using statistical experimental design. J. Appl. Pharm. Sci. 5(9): 007-015.

11. Treichel, H., Oliveira, D., Mazutti, MA., Di Luccio, MD. and Oliveira, JV. (2010). A review on microbial lipases production. Food Bioprocess Technol. 3(2): 182-196.

12. Venetia, A. and Jon R Saunders. (1987). Microbial Strain Improvement and Novel Products. Microbial Genetics Applied to Biotechnology. 265-305.

13. Destain., D. and Thonart, P. (1997). Improvement of lipase production from Yarrowia lipolytica. Biotechnol. Lett. 19(2): 105-107.

14. Sandana Mala., JG. Kamini, NR. and Puvanakrishnan, R. (2005). Strain improvement of Aspergillus niger for enhanced lipase production. J. Gen. Appl. Microbiol. 47(4): 181-186.

15. Bapiraju, KVVSN., Sujatha, P., Ellaiah, P. and Ramana, T. (2004). Mutation induced enhanced biosynthesis of lipase. J. Biotechnol. 3(11): 618-621.

16. Venkatanagraju, E. Chittanranjan, D. (2011). Non-recombinant Mutagenesis of Bacillus subtilis MTCC 2414 for Hyper Pro-

duction of Laccase. Asian j. pharma. Hea, Sci. 6(1): 1396-1400.

17. Immobilization, O., Prakash, S. and Aldrich, A. (2011). Immobilization studies of purified lipase. 9: 93-101.

18. Al-adhami, AJH., Bryjak, J., Greb-markiewicz, B. and Peczyn, W. (2002). Immobilization of wood-rotting fungi laccases on modified. 37: 387-394.

19. Bryjak, J., Szymańska, K. and Jarzebski, AB. (2012). Laccase immobilisation on mesostructured silicas. Chem. Process Eng. Chem. Proces. 33(4): 611-620.

20. Hongshuai Gao, Jianmin Xing, Xiaochao Xiong, Yuguang Li, Wangliang Li, Qingfen Liu, Yong Wu, and Huizhou Liu. (2008). Immobilization of ionic liquid [BMIM][PF6] by spraying suspension dispersion method. Ind. Eng. Chem. Res. 47(13): 4414-4417.

21. Cordeiro, GD., Taniguchi, M., Flechtmann, CHW and Alves-dos-Santos, I. (2010). Phoretic mites (Acari: Chaetodactylidae) associated with the solitary bee Tetrapedia diversipes (Apidae: Tetrapediini). Apidologie. 42(2): 128-139.

22. Lee, WE., Ojovan, MI., Stennett, MC. and Hyatt, NC. (2005). Immobilisation of radioactive waste in glasses, glass composite materials and ceramics. Adv. Appl. Ceram. 105(1): 3-12.

23. Tripathi, R., Singh, J., Bharti, RK. and Thakur, IS. (2014). Isolation, purification and characterization of lipase from microbacterium sp. and its application in biodiesel production. Energy Procedia. 54: 518-529.

24. Lowry. H., Nira J. and Farr, AL. (1994). The folin by oliver. Anal. Biochem. 217(2): 220-230.

Current Trends in Biotechnology and Pharmacy
Vol. 16 (4) 481 - 489, Oct 2022, ISSN 0973-8916 (Print), 2230-7303 (Online)
10.5530/ctbp.2022.4.81

Automated Detection Of Breast Cancer Using Machine Learning Algorithms: A Comparative Analysis

Venkata Srinivas Babu Oguri[1], Sudhakar Poda[2]
[1]Department of Computer Science and Engineering, Mahindra University, Hyderbad, Telangana
[2]Department of Biotechnology, Acharya Nagaarjuna University, Nagarjunanagar, Guntur-522510, India
Corresponding author: Sudhakar Poda@hotmail.com

Abstract

Breast Cancer is one of the most commonly diagnosed cancers in women. There is a 12.6% chance that a women can develop invasive breast cancer in her lifetime. All the clinically performed methods have some limitations. Automated diagnosis became an important area of cancer studies. Development of such systems require machine learning algorithms. Machine Learning has became a popular tool in the field of medical diagnosis. This study aims to provide a comparative analysis of various algorithms that can be used in the classification of Breast Cancer. The dataset used was retrieved from UCI machine learning repository and was created by University of Wisconsin. A total of 9 algorithms were employed to classify Benign and Malignant Tumors. 9 models were created using these algorithms. These models were compared by various metrics such as Accuracy, Precision, Recall Score and F1 Score.

Keywords Breast Cancer, LightGBM, Jupyter notebook, Pearson Correlation, ROC curve, Accuracy, F1 Score

Introduction

Breast Cancer is one of the most commonly diagnosed cancers in women. There is a 12.6% chance that a women can develop invasive breast cancer in her lifetime(1). 95% of Breast Cancers arise from breast epithelial elements and are carcinomas. Two main types of Breast Cancer are invasive carcinomas and *in situ* carcinomas. Breast cancer cases are high in ages upto 50(2). Genetics might play an important factor as 6% of the cases are hereditary(3). Also, women diagnosed with breast Cancer have higher risk factor of developing new cancer in either the second or the treated breast. This risk factor will increase by 1% every year. Much research had been done trying to establish a relationship between specific foods and diagnosis of Breast Cancer. The only reliable relation identified was with alcohol(4). Furthermore, according to Nurses Health Society, postmenopausal women who exercised at least one hour per week are 20% less likely to be diagnosed with Breast Cancer. Clinical diagnosis of this disease is generally done by physical examination, mammography and ultrasound(5). All these methods have some limitations. Ultra sound may not detect cancer at all times. Also, analysis of mammographic image is difficult as it shows little contrast between tumors and normal tissue(6). Early diagnosis helps in delaying of the disease progress and limits treatment expenses. Automated diagnosis became an important area of cancer studies. Development of such systems require machine learning algorithms. Several studies were involved in automated

cancer detection using various algorithms(7)(8). Machine Learning has become a popular tool in the field of medical diagnosis. This study aims to provide a comparative analysis of various algorithms that can be used in the classification of Breast Cancer.

Material and Methods

The dataset was retrieved from UCI machine learning repository. It has a total of 32 attributes and 569 instances. The creators of this dataset were Dr. William H. Wolberg, W. Nick Street and Olvi L. Mangasarian of University of Wisconsin. The attributes were calculated from Digitalised image of FNA of a breast mass. Fig1 shows a section of the dataset. In the diagnosis attribute, B stands for Benign while M stands for malignant. Fig2 and Fig3 depict the relation between Texture Mean, Radius Mean and Area Mean, Concavity Mean. The dataset underwent pre-processing initially. Correlation coefficients were calculated between every attribute. The correlation matrix is shown in Fig4. The correlation Coefficient has values ranging from -1 to 1. Highly correlated attributes will have values closer to 1, while uncorrelated ones will have values closer to 0. Attributes with coefficients greater than 0.9 were removed. Out of 31 features (excluding diagnosis), 10 were removed and new dataset was created. Next, this dataset was split into testing and training data. 20% was set aside for testing and 80% was used to train the model. A total of 9 algorithms were used to create 9 models. Each of these models were fit(trained) with the training data. Various parameters for accessing the performance of each of the model were also calculated. Random Forest, Decision Tree, XGBoost, LightGBM, Naive Bayes, Logistic regression, KNN, SVM and AdaBoost classifiers were the algorithms used in this study.

id	diagnosis	radius_mean	texture_mean	perimeter_mean	area_mean	smoothness_mean	compactness_mean	concavity_mean	concave points_mean	symmetry_mean	fractal_dimension_mean	radius_se	texture_se
842302	M	17.99	10.38	122.8	1001	0.1184	0.2776	0.3001	0.1471	0.2419	0.07871	1.095	0.9053
842517	M	20.57	17.77	132.9	1326	0.08474	0.07864	0.0869	0.07017	0.1812	0.05667	0.5435	0.7339
84300903	M	19.69	21.25	130	1203	0.1096	0.1599	0.1974	0.1279	0.2069	0.05999	0.7456	0.7869
84348301	M	11.42	20.38	77.58	386.1	0.1425	0.2839	0.2414	0.1052	0.2597	0.09744	0.4956	1.156
84358402	M	20.29	14.34	135.1	1297	0.1003	0.1328	0.198	0.1043	0.1809	0.05883	0.7572	0.7813
843786	M	12.45	15.7	82.57	477.1	0.1278	0.17	0.1578	0.08089	0.2087	0.07613	0.3345	0.8902
844359	M	18.25	19.98	119.6	1040	0.09463	0.109	0.1127	0.074	0.1794	0.05742	0.4467	0.7732
84458202	M	13.71	20.83	90.2	577.9	0.1189	0.1645	0.09366	0.05985	0.2196	0.07451	0.5835	1.377
844981	M	13	21.82	87.5	519.8	0.1273	0.1932	0.1859	0.09353	0.235	0.07389	0.3063	1.002
84501001	M	12.46	24.04	83.97	475.9	0.1186	0.2396	0.2273	0.08543	0.203	0.08243	0.2976	1.599
845636	M	16.02	23.24	102.7	797.8	0.08206	0.06669	0.03299	0.03323	0.1528	0.05697	0.3795	1.187
84610002	M	15.78	17.89	103.6	781	0.0971	0.1292	0.09954	0.06606	0.1842	0.06082	0.5058	0.9849
846226	M	19.17	24.8	132.4	1123	0.0974	0.2458	0.2065	0.1118	0.2397	0.078	0.9555	3.568
846381	M	15.85	23.95	103.7	782.7	0.08401	0.1002	0.09938	0.05364	0.1847	0.05338	0.4033	1.078
84667401	M	13.73	22.61	93.6	578.3	0.1131	0.2293	0.2128	0.08025	0.2069	0.07682	0.2121	1.169
84799002	M	14.54	27.54	96.73	658.8	0.1139	0.1595	0.1639	0.07364	0.2303	0.07077	0.37	1.033
848406	M	14.68	20.13	94.74	684.5	0.09867	0.072	0.07395	0.05259	0.1586	0.05922	0.4727	1.24
84862001	M	16.13	20.68	108.1	798.8	0.117	0.2022	0.1722	0.1028	0.2164	0.07356	0.5692	1.073
849014	M	19.81	22.15	130	1260	0.09831	0.1027	0.1479	0.09498	0.1582	0.05395	0.7582	1.017
8510426	B	13.54	14.36	87.46	566.3	0.09779	0.08129	0.06664	0.04781	0.1885	0.05766	0.2699	0.7886
8510653	B	13.08	15.71	85.63	520	0.1075	0.127	0.04568	0.0311	0.1967	0.06811	0.1852	0.7477
8510824	B	9.504	12.44	60.34	273.9	0.1024	0.06492	0.02956	0.02076	0.1815	0.06905	0.2773	0.9768
8511133	M	15.34	14.26	102.5	704.4	0.1073	0.2135	0.2077	0.09756	0.2521	0.07032	0.4388	0.7096
851509	M	21.16	23.04	137.2	1404	0.09428	0.1022	0.1097	0.08632	0.1769	0.05278	0.6917	1.127
852552	M	16.65	21.38	110	904.6	0.1121	0.1457	0.1525	0.0917	0.1995	0.0633	0.8068	0.9017
852631	M	17.14	16.4	116	912.7	0.1186	0.2276	0.2229	0.1401	0.304	0.07413	1.046	0.976
852763	M	14.58	21.53	97.41	644.8	0.1054	0.1868	0.1425	0.08783	0.2252	0.06924	0.2545	0.9832

Fig1 Dataset

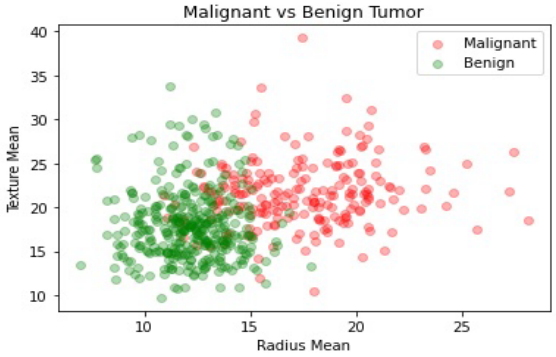

Fig 2:-Relationship between Texture and Radius Mean

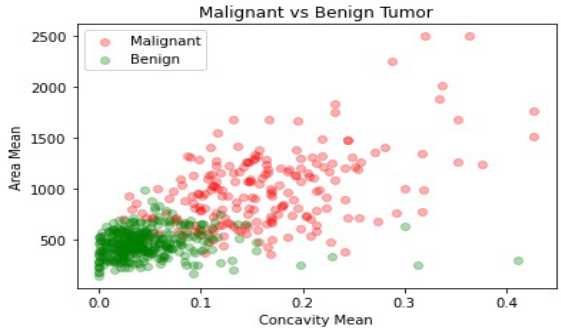

Fig 3:-Relationship between Area and Concavity Mean

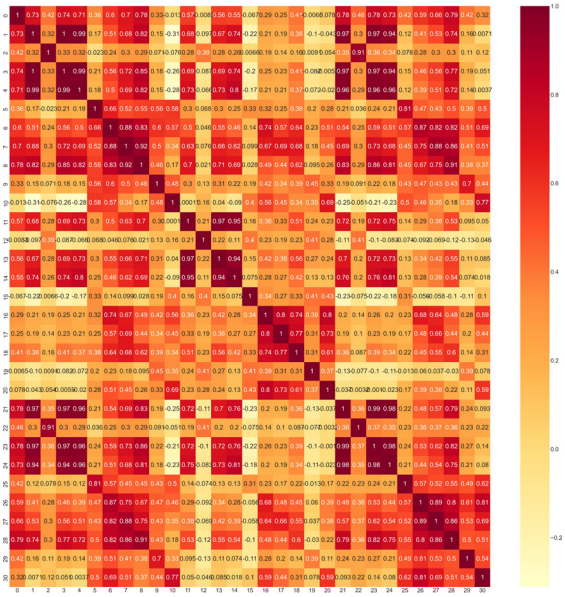

Fig 4:-Correlation Matrix

In Fig 4 colour grading was set to 'yellow red'. High correlation is shown by more red colour, while Low correlation is shown by more yellow colour. All diagonal elements have correlation value of 1 and are red since each feature is mapped to itself. Fig 5 shows the scatter plot of the new dataset.

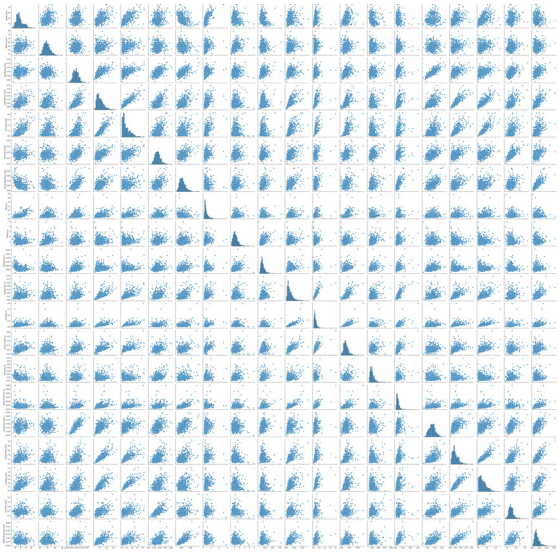

Fig 5:- Scatter Plot

Brief descriptions of various algorithms used in this study are described below.

Random Forest classifier

Random Forest contains a large number of decision trees, where each tree gives out a prediction and the one with highest number of votes will be given out as output(9). It works with the fundamental concept that a large number of Trees(models) working together will outperform any individual constituent models.

XGBoost classifier

XGBoost works under a gradient boosting framework and is also Decision Tree based. It was developed at University Of Washington in 2016. Similar to Random Forest, it is an ensemble learning algorithm. It's known for its handling of data types , distributions and the variety of hyper parameters that can be

tuned(10).

Adaboost classifier

AdaBoost is one of the first boosting algorithms created. It combines multiple weak learners into a single strong learner and can be used for both regression and classification. It works by giving more preference on ones more difficult to classify instances rather than on easily handled ones(11).

Decision tree classifier

Decision Tree Classifier comes under supervised learning techniques and is mainly used for classification. Its structure represents a tree where the internal nodes represent the features, the branches specify the decision rules and the leaf nodes present the outcome(12). Fig 6 illustrates the decision tree generated on this dataset.

Fig 6 :-Illustration of Decision Tree

K-nearest neighbours classifier

K-Nearest Neighbours or shortly KNN is also a supervised learning technique used for classification as well as regression. It can also be categorised under Lazy Learner Algorithms as doesn't immediately learn from the training data. It tires to calculates the similarity between new and trained data and put the new case into one of the categories(13).

Support vector machine classifier

Support Vector Machine(SVM) creates a best line or boundary that can separate N-dimensional space in categories so that new data can easily be put in one of the correct class. It chooses Extreme Vectors which help in generating a Hyperplane. These Extreme Vectors are called Support Vectors(14).

LightGBM

LightBGM share many similarities with XGBoost in features such as parse optimisation, parallel training, multiple loss functions and bagging. LightBGM grows trees leaf-wise instead of level- wise(15). It uses histogram based trees instead of Decision Trees. It was developed by Microsoft.

Logistic regression

Logistic Regression is a supervised learning algorithm and is used mainly for binary classification. It uses sigmoid function to classify the data and can easily determine the most effective attributes used for classification. It provides probable values between 0 and 1 (16).

Naive bayes classifier

Naive Bayes is a classification algorithm based on Bayes Theorem. It naively assumes independence among the features and the continuous values associated with each feature are assumed to be distributed according to a Gaussian distribution(17).

All the work was done using Jupyter Notebook, an interactive python notebook. All the algorithms used were performed using Scikit-learn machine learning library. Seaborn library was used to visualise the data.

Results and Discussion

Naive Bayes and Decision Tree Classifiers were the least performing models with an accuracy of 89.47% and 88.59% respectively. LightGBM achieved the highest accuracy of 98.24%. AdaBoost and XGBoost performed well with an accuracy of 96.49% and 97.36%. Fig 7 to Fig 15 present the confusion matrices of all algorithms used. Confusion Matrix gives us the number of True positive(TP) ,True negative(TN), False

positive(FP) and False negative(FN) instances.

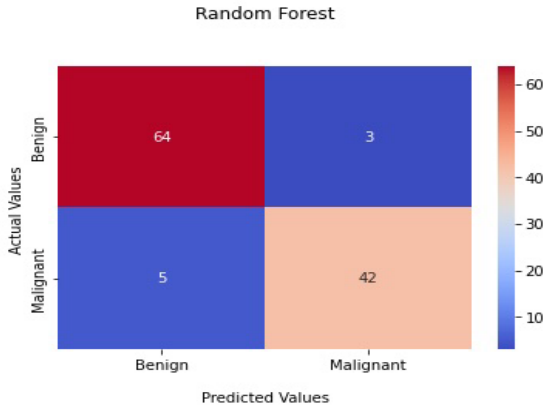

Fig 7

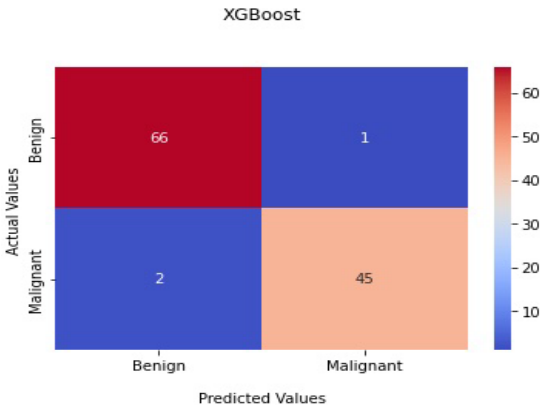

Fig 8

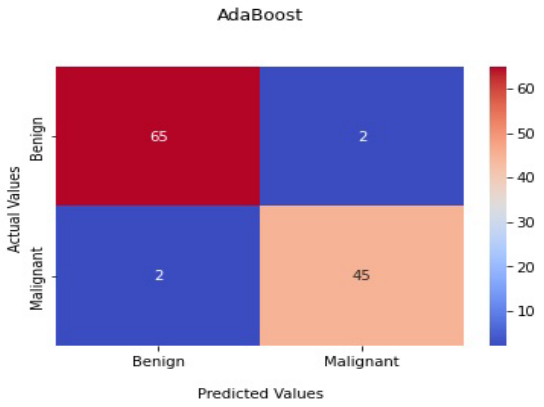

Fig 9

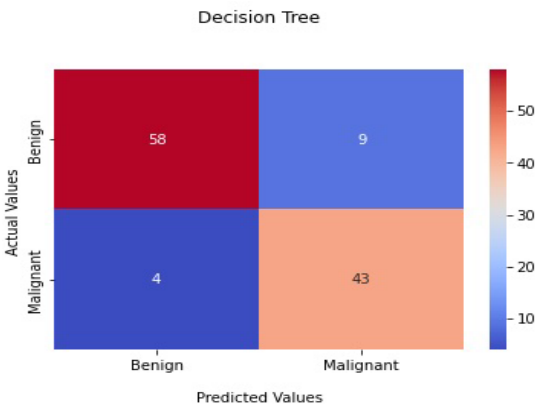

Fig 10

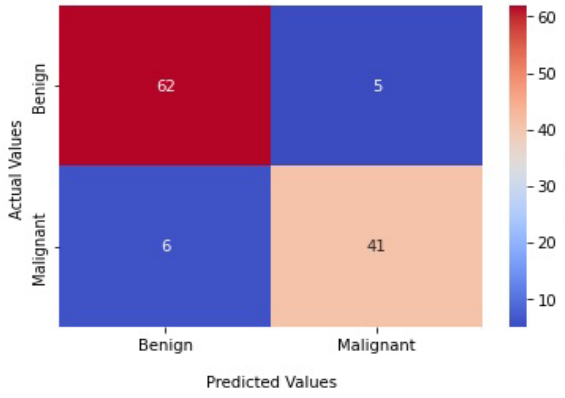

Fig 11

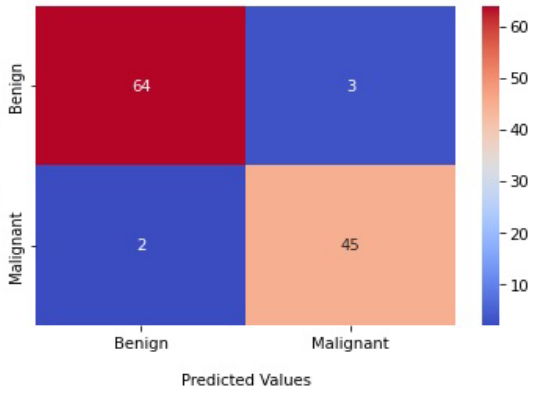

Fig 12

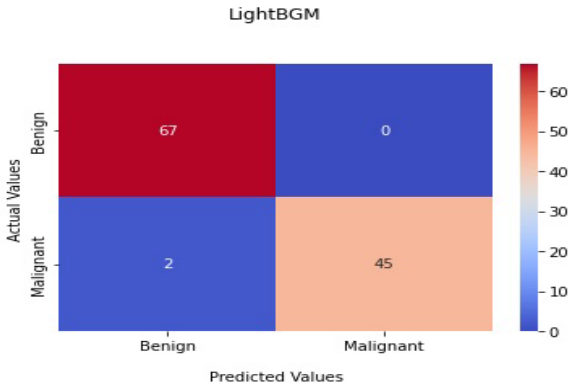

Fig 13

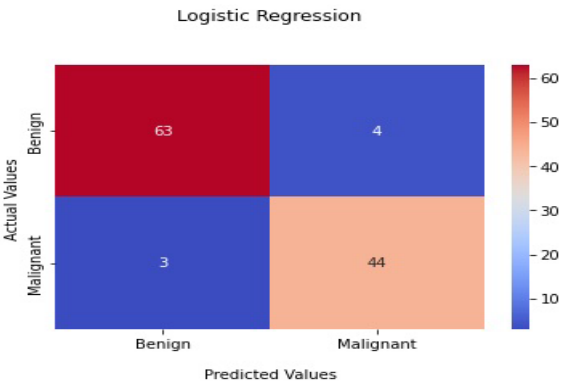

Fig 14

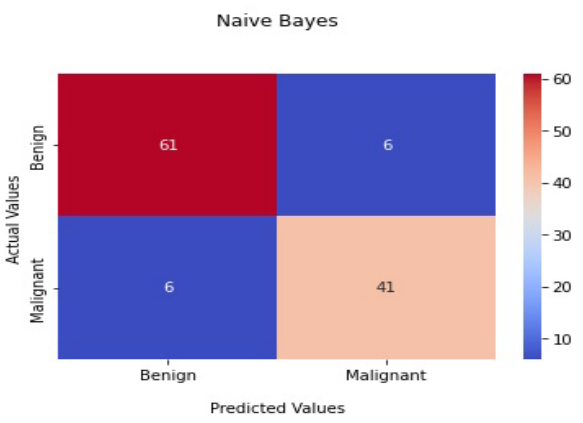

Fig 15

$$Accuracy = \frac{TP + TN}{TP + FP + FN + TN}$$

$$Precision = \frac{TP}{TP + FP}$$

$$recall = \frac{TP}{TP + FN}$$

$$F1 - Score = \frac{2 \times Precision \times recall}{Precision + recall}$$

Random Forest classifier has shown 42 True Positive, 64 True Negative, 3 False Positive and 5 False Negative instances. A Total of 106 instances have been correct out of 114, hence the accuracy is 92.98%.Precision, Recall and F1 Score were also calculated for each algorithm. Their Formulas are given Above. Each of these metrics were calculated for all the nine algorithms used and their values are given in Table 1. All values were compared graphically in Fig 16.

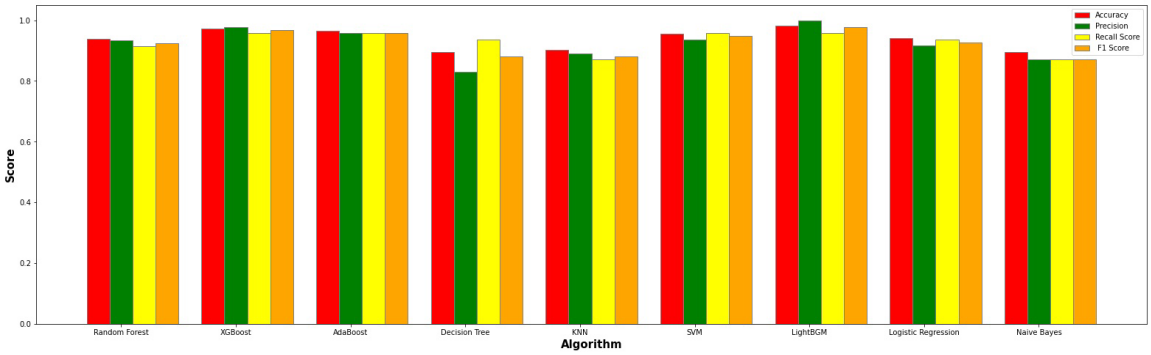

Fig 16:-Comparison of Metrics

Table 1:- Values Of Metrics

Algorithm	Accuracy	Precision	Recall Score	F1_Score
Random Forest	0.938596	0.934783	0.914894	0.924731
XGBoost	0.973684	0.978261	0.957447	0.967742
AdaBoost	0.964912	0.957447	0.957447	0.957447
Decision Tree	0.894737	0.830189	0.936170	0.880000
KNN	0.903509	0.891304	0.872340	0.881720
SVM	0.956140	0.937500	0.957447	0.947368
LightGBM	0.982456	1.000000	0.957447	0.978261
Logistic Regression	0.940659	0.916667	0.936170	0.926316
Naive Bayes	0.894737	0.872340	0.872340	0.872340

LightGBM scored the highest F1 Score of 97.82%, followed by XGBoost and AdaBoost with 96.77% and 95.74% respectively. SVM, AdaBoost, LightGBM and XGBoost achieved Recall Score of 95.74%. In all the four parameters, LightGBM performed better than the remaining algorithms. Also, boosting algorithms outperformed tree based algorithms in all parameters. ROC (Receiver Operating Characteristic) curves along with the AUC (Area Under The Curve) are presented in Fig 17-25.

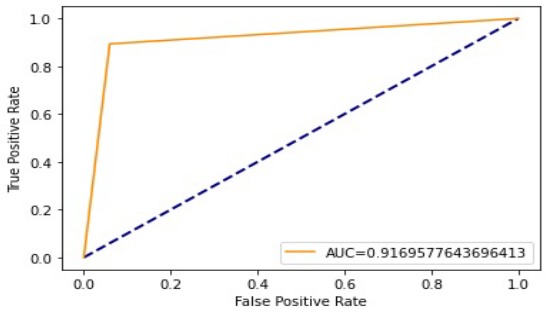

Fig 17:- Random Forest

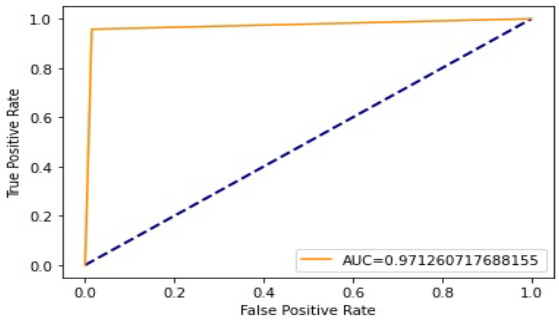

Fig 18:- XGBoost

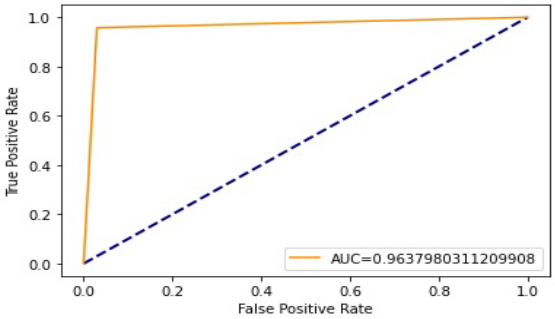

Fig 19:- AdaBoost

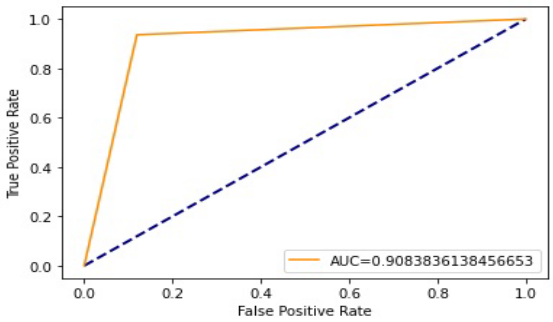

Fig 20:- Decision Tree

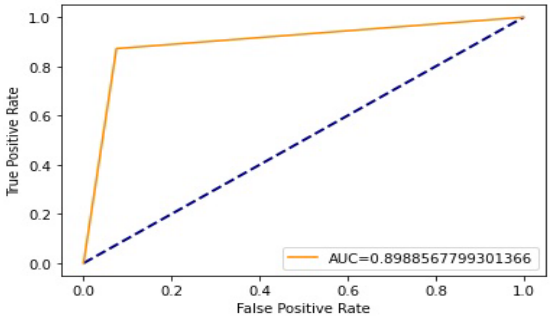

Fig 21:- KNN

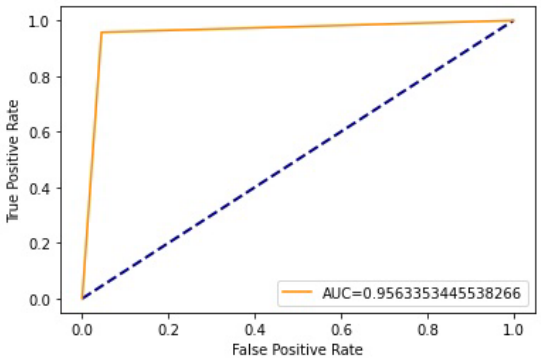

Fig 22:- SVM

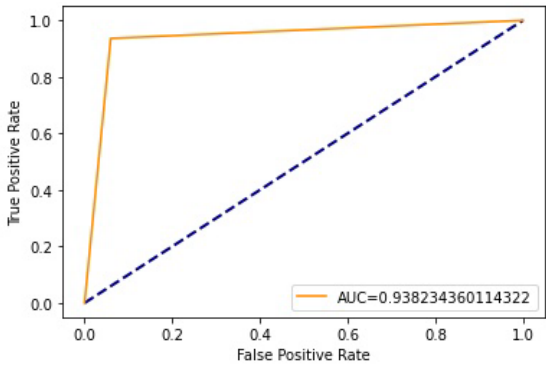

Fig 24:- Logistic Regression

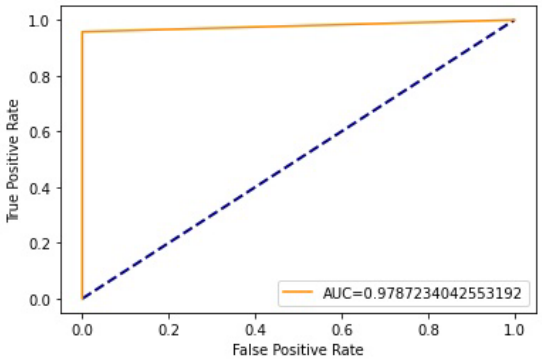

Fig 23:- LightGBM

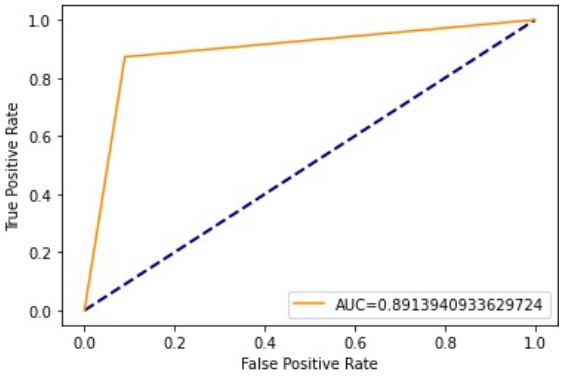

Fig 25:- Naive Bayes

ROC curves are used in binary classification and feature True Positive and False Positive rates on x and y axes respectively. A larger AUC is considered better. LightBGM has the highest AUC of 97.87% while Naive Bayes has the lowest of 89.13%.

Conclusion

Breast Cancer is one of the most frequently occurring cancers in the world. This study provides a comparative analysis of different machine learning algorithms used in detection of the disease. Most of the algorithms achieved an accuracy of score higher than 90%, proving that machine learning plays a crucial role in early diagnosis and automated detection of the disease. Boosting algorithms used in study (XGBoost, LightGBM and AdaBoost) performed superiorly.

References

(1) Greenlee RT, Hill-Harmon MD, Murry T, Thun M. Cancer Statistics, 2001. CA Cancer J Clin. 2001;51: 15

(2) Smith H, Kammerer-Doak D, Barbo D, Sarto G. Hormone Replacement Therapy in the Menopause: A Pro Opinion. CA—A Cancer Journal for Clinicians. 1996;46:343.

(3) Malone KE, Daling JR, Thompson JD, O'Brien CA, Francisco LV, Ostrander EA. BRCA1 mutations and breast cancer in the general population: analysis in women before age 35 years and in women before age 45 years with first-degree family history. JAMA. 1998;279:922–929.

(4) Mourouti N., Kontogianni M.D., Papavagelis C., Panagiotakos D.B. Diet

and breast cancer: A systematic review. Int. J. Food Sci. Nutr. 2015;66:1–42. doi: 10.3109/09637486.2014.950207. (PubMed) (CrossRef) (Google Scholar)

(5) Ward RC, Lourenco AP, Mainiero MB. Ultrasound-guided breast cancer cryoablation. Am J Roentgenol. 2019;213(3). doi: 10.2214/AJR.19.21329 (PubMed) (CrossRef) (Google Scholar) (Ref list))

(6) Obenauer S, Luftner-Nagel S, von Heyden D, Munzel U, Baum E, Grabbe E. Screen film vs full-field digital mammography: Image quality, detectability and characterization of lesions. Eur Radiol. 2002;12(7). doi: 10.1007/s00330-001-1269-y (PubMed) (CrossRef) (Google Scholar) (Ref list)

(7) Lughezzani G, Briganti A, Karakiewicz PI, et al. Predictive and prognostic models in radical prostatectomy candidates: A critical analysis of the literature. Eur Urol. 2010;58(5). doi: 10.1016/j.eururo.2010.07.034 (PMC free article) (PubMed) (CrossRef) (Google Scholar) (Ref list)

(8) Zhang Q, Zhao K, Song L, et al. A Novel Apoptosis-Related Gene Signature Predicts Biochemical Recurrence of Localized Prostate Cancer After Radical Prostatectomy. Front Genet. 2020;11. doi: 10.3389/fgene.2020.586376 (PMC free article) (PubMed) (CrossRef) (Google Scholar) (Ref list)

(9) Amaratunga D, Cabrera J, Lee Y-S (2008) Enriched random forests. Bioinformatics 24:2010–2014

(10) Liu, Jialin, Jinfa Wu, Siru Liu, Mengdie Li, Kunchang Hu, and Ke Li. "Predicting mortality of patients with acute kidney injury in the ICU using XGBoost model." Plos one 16, no. 2 (2021): e0246306.

(11) Robert E. Schapire. The strength of weak learnability. Machine Learning, 5(2):197-227, 1990

(12) Banu GR. A Role of decision Tree classification data Mining Technique in Diagnosing Thyroid disease. International Journal of Computer Sciences and Engineering. 2016;4(11):111-5.

(13) D. Wettschereck and D. Thomas G, "Locally adaptive nearest neighbour algorithms", Adv. Neural Inf. Process. Syst., pp. 184-186, 1994.

(14) Song Mingjun and S. Rajasekaran, "A greedy algorithm for gene selection based on SVM and correlation", International Journal of Bioinformatics Research and Applications, vol. 6, no. 3, pp. 296-307, 2010.

(15) Song, Jiazhi, Guixia Liu, Jingqing Jiang, Ping Zhang, and Yanchun Liang. "Prediction of Protein–ATP Binding Residues Based on Ensemble of Deep Convolutional Neural Networks and LightGBM Algorithm." International Journal of Molecular Sciences 22, no. 2 (2021): 939.

(16) Y. Bi and D. R. Jeske. The efficiency of logistic regression compared to normal discriminant analysis under class-conditional classification noise. Journal of Multivariate Analysis, 101(7):1622–1637, 2010

(17) P. Langley, W. Iba and K. Thompson, "An analysis of Bayesian Classifiers.," in Proceedings of the Tenth National Conference on Artificial Intelligence, San Jose, CA, 1992.

Current Trends in Biotechnology and Pharmacy
Vol. 16 (4) 490 - 499, Oct 2022, ISSN 0973-8916 (Print), 2230-7303 (Online)
10.5530/ctbp.2022.4.82

Formulation, Evaluation and Characterization of Mouth Dissolving Film of Cisapride

Prashant L. Pingale[1]*, Dattatray M. Shinkar[1], Sahebrao S. Boraste[1], Sunil V. Amrutkar[2]

[1*]Department of Pharmaceutics,
[2]Department of Pharmaceutical Chemistry
GES's Sir Dr. M. S. Gosavi College of Pharmaceutical Education and Research,
Nashik-42205, Maharashtra, India
*Corresponding Author : prashant.pingale@gmail.com

Abstract

Mouth dissolving films offer an attractive route for systemic drug delivery. MDFs are an alternative to fast dissolving tablets, Chewable tablet, due to their faster dissolution rate. Some drugs are absorbed from the mouth, pharynx and esophagus as the saliva passes down into the stomach. Fast mouth dissolving films have become popular as a new delivery system. They disintegrate or disintegrate in the oral cavity without the need to swallow or chew.

The objective of the present study was to develop mouth dissolving films (MDF) of Cisapride used to treat heartburn in patients with gastroesophageal reflux disease (GERD), with fast disintegration, optimum morphological properties, and mechanical strength. Lycoat RS 720, Hydroxypropylmethyl-cellulose 3cps were used as polymers and Glycerine as plasticizer. Films were prepared by solvent casting technique. Parameters like in-vitro disintegration time, tensile strength, content uniformity, folding endurance, swelling index, and in-vitro drug release were evaluated. *In-vitro* dissolution studies showed that 99% of Cisapride was released within 5 min with an average disintegration time of 60 sec. UV and FTIR spectrophotometry were used to identify drug-excipient interactions. Accelerated stability studies were performed as per ICH guidelines wherein the MDFs were stable for 2 months at 40 ± 2 °C and 75 ± 5% relative humidity.

Keywords: Cisapride, mouth-dissolving film, HPMC 3cps, Lycoat RS 720, Glycerine

Introduction

The oral route of drug administration is the very commonly and conveniently use for patient. Tablets and capsules represent the most widely used solid oral dosage forms. It is estimated that 35% of the general population, 30–40%of elderly nursing home patients and 25–50% of patients hospitalized for acute neuromuscular disorders and head injuries have dysphagia. Oral solid dosage forms are not ideal for elderly patients or those who have had surgery or radiation therapy to the head and neck [1,2].

Fast-dissolving oral drug delivery system is a novel solid dosage form, which disintegrate or dissolve in a few seconds after placement in the mouth. Offers substantial advantage over ordinary oral dosage form such as ease of administration, lack of requirement for. drinking water, and improved compliance [3].

Sublingual and buccal routes enhance the onset of action and improve the efficacy. They can be used for local and systemic delivery. Mouth dissolving films offer an attractive route for systemic drug delivery. There is a rising interest in the development of Mouth Dissolving film (MDFs). MDFs are an alternative to

fast dissolving tablets, Chewable tablet, due to their faster dissolution rate [4].

The oral mucosa (MDF) is an attractive and feasible site for drug delivery, with good permeability, easy ingestion and swallowing, pain avoidance and a wide surface area for absorption. Marketed MDF products have also become available, including Listerine, Chloraseptic and Triaminic [5].

Delivery system consist of a very thin oral strip, which is simply based on the patient's tongue. The film rapidly hydrates and adheres onto site of application. It then disintegrates and dissolves to release the medication [6].

A fast-dissolving drug delivery system is in the form of a solid tablet that disintegrates or disintegrates in the oral cavity without the need to swallow or chew. Some drugs are absorbed from the mouth, pharynx and esophagus as the saliva passes down into the stomach.Fast mouth dissolving films have become popular as a new delivery system. Since the sublingual mucosa is relatively permeable due to thin membrane and is highly perfused, rapid drug absorption and instant bioavailability is possible. This is beneficial in patients with dysphagia or difficulty in swallowing [7].

The fast-dissolving drug delivery system offers a giant leap forward in drug administration by providing a new and easy way of taking medication. Fast dissolving film is a thin film alleviates the fear of swallowing and the risk of choking commonly associated with a tablet.

Fast dissolving film is a thin film, with an area of 5-10 cm2, containing an active ingredient. The immediate dissolution, in water or saliva respectively, is reached through a special matrix. Drugs can be incorporated up to a single dose of 15 mg [8].

The faster the drug goes into the solution, quicker its absorption and onset of clinical effect. By altering the condition and formulation factors, it is possible to speed up dissolving rate in the mouth. Normally these films are soluble in water at room temperature and will break up in 30 sec and dissolve in one minute [9].

Fast dissolving films should be water soluble and disintegrate when in contact with saliva. Polymers selected for the study are Lycoat and HPMC-3 cps. Fast release film type of dosage form for Cisapride was thought worth to formulate.

The MDF is a thin, printable, low-moisture, non-tacky film that is convenient for labelling and flexible for easy packing, handling and application. The rapid hydration rate facilitates an almost immediate softening of the MDF upon application in the oral cavity [10].

Oral routes of drug administration have wide acceptance up to 50-60% of total dosage forms due to ease of ingestion and pain avoidance. Fast-dissolving films which dissolve/disintegrate in the mouth within a few seconds without additional water and the need to swallow are gaining interest as an alternative [11, 12].

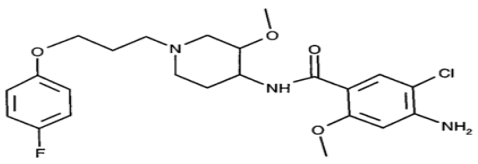

Cisapride

Figure 1: Structure of Cisapride

Molecular formula: $C_{23}H_{29}ClFN_3O_4$

IUPAC Name: 4-amino-5-chloro-N-[(3S,4R)-1-[3-(4-fluorophenoxy)propyl]-3-methoxypiperidin-4-yl]-2-methoxybenzamide

Material and Method

Cisapride was received as a gift sample from Healthy Life Pharma, Mumbai. HPMC was re-

ceived from Colorcon Asia Pvt. Ltd., Mumbai. Lycoat RS 720 was procured from Roquette Pharma, Mumbai. PEG 400 was received as a gift sample from PEG 400 (Central Drug House, Mumbai). All other excipients were purchased from local vendor and were of analytical grade.

UV-spectrophotometric calibration curve

The UV calibration curve of Cisapride was constructed in phosphate-buffered saline (PBS) at pH 6.8 (2.38 g Na_2HPO_4, 0.19 g KH-

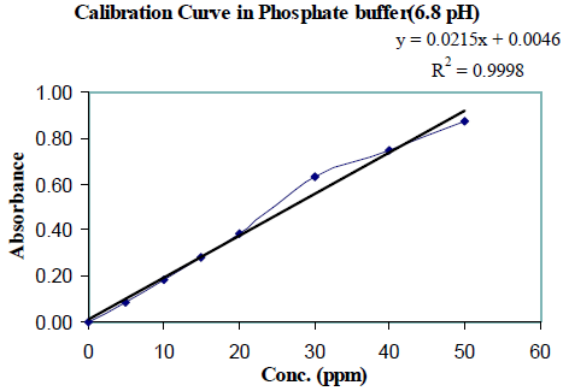

$_2PO_4$, and 8.00 g NaCl/1 L of distilled water)[13].

Figure2: Calibration curve of Cisapride in 6.8 buffer solution

Drug-excipients compatibility studies

Drug – Excipients studies were done to confirm the compatibility of Cisapride and other excipients used in the formulation. The drug alone and along with different excipients was mixed, sealed in clear glass vials, which were then charged into stability chambers[14].

Saturated solubility

The saturated solubility of Cisapride has been determined. A known amount of Cisapride (100 mg) was mixed with 10ml of distilled water in glass vials. The suspension was filtered through 0.45-µm membrane filter before analysis[15].

Formulation of fast dissolving films

Fast dissolving films of Cisapride were prepared by solvent casting technique. A flat square shaped, TLC applicator having surface area of 25 cm2 was fabricated for casting the films.

HPMC casting solution

The weighed quantities of polymer were preserved in distilled water in the HPMC casting solution. With distilled water, the volume was increased to 10 mL. Vacuum was used to release trapped air bubbles.

Lycoat as a casting solution

Lycoat was used as a casting solution, and it was made by dissolving weighed amounts of polymers in water and heating it on a water bath. The medication and flavour were dissolved in distilled water before being added to the aforementioned polymer solution, along with

Table 1: Formulation of Cisapride Mouth Dissolving film

Sr. No.	Ingredient (mg)	FC1	FC2	FC3	FC4	FC5	FC6	FC7	FC8	FC9
1	Cisapride	5	5	5	5	5	5	5	5	5
2	Lycoat RS 720	--	--	2	4	4	6	6	6	6
3	Glycerine	1	1.5	2.0	2.5	2.0	1.5	2.0	2.5	1
4	HPMC 3 cps	14.24	14.24	12.24	10.24	10.24	10.24	10.24	10.24	14.24
5	Ferric oxide red	0.03	0.03	0.03	0.03	0.03	0.03	0.03	0.03	0.03
6	PEG-400	--	0.03	--	--	2	2.4	2.4	2.4	2.4
7	Masking Agent (ml)	2	2	2	2	2	2	2	2	2
8	Purified water (ml)	19.23	19.23	17.23	17.23	17.23	19.23	19.23	19.23	19.23

the plasticizer propylene glycol, and well mixed to make a homogeneous mixture.HPMC and Lycoat combination casting solution, the casting solutions were made by dissolving weighed amounts of polymers in distilled water [16].

Preparation of fast dissolving films: The casting solution (10 ml) was poured into a glass mould and dried in a vacuum oven at 50°C for 24 hours to allow the solvent to evaporate. The patches were peeled off and cut into squares of 2.5 cm by 2.5 cm (6.25 cm^2). These patches were dried for two days in a desiccator before being wrapped in aluminium foil and put in self-sealing covers. Fast-dissolving films were made with various polymer ratios while keeping the plasticizer and sweetener concentrations constant [17,18]. Table 1 shows the formulation components used in preparation of Cisapride mouth dissolving film and physical and mechanical properties including tack test, tensile strength, folding endurance and disintegration time is shown in table 2.

Table 2: Physical and mechanical properties of Cisapride mouth dissolving films

Formulation code	Visual Appearance	TackTest	Tensile strength (kg/mm^2)	Folding endurance	Disintegration time
FC1	Transparent	Non-tacky	0.465±0.95	>100	78sec ±2.12
FC2	Semi-Transparent	Non-tacky	0.455±0.78	<100	191sec ±1.89
FC3	Non-Transparent	Non-tacky	0.412±0.11	<100	172sec ±1.45
FC4	Transparent	Non-tacky	0.423±0.18	<50	245sec ±1.50
FC5	Transparent	Non-tacky	0.430±0.48	<100	133sec ±1.30
FC6	Transparent	Non-tacky	0.405±0.50	<100	145sec ±3.60
FC7	Transparent	Non-tacky	0.490±0.45	<50	115sec ±2.90
FC8	Transparent	Non-tacky	0.480±0.40	<100	105sec ±1.50
FC9	Transparent	Slightly-tacky	0.376±0.75	<100	135sec ±2.15

Physical and chemical evaluation of film[19, 20]

Tack test

Tack refers to how well the film sticks to the attachment that has been pressed against the strip. The dryness is also determined by this test.

Tensile strength

Tensile strength is defined as maximum stress applied at which the film breaks. Basically, this test is performed to measure the mechanical strength of films. It can be calculated from applied load at rupture divided by the strip cross-sectional area given in the equation below:

Tensile strength = Load at breakage/ Strip thickness × Strip Width

Folding endurance

A piece of film is cut and repeatedly folded at the same location until it breaks to measure folding endurance. The folding endurance value is determined by the number of times the film could be folded at the same point without breaking. A film's typical folding endurance ranges from 100 to 150 folds.

Disintegration time

The disintegration time of a film is determined using disintegration apparatus stated in official pharmacopoeias. The disintegration time is usually a function of the film composition, as it changes with the formulation, and it typically

spans from 5 to 30 seconds. This test is commonly performed using the USP disintegration device. For estimating the disintegration period of orally rapid disintegrating films, there are no established recommendations available. There are two ways for determining the time it takes for a film to disintegrate.

Characterization of mouth dissolving films

Morphological Properties of Prepared Films

MDF homogeneity, colour, transparency, and surface were visually assessed. All of the formulas were wrapped in butter paper and subsequently aluminium foil, kept at room temperature (25^0C) with a relative humidity of 65 ±5% RH, and were tested periodically for 3 months.

Drug-Excipient Interaction Studies

To guarantee that there was no contact between the drug and the polymer or due to circumstances in the formulation process, the following interactions were investigated.

Tack Test

Tackiness was determined by gently pushing the film between fingertips and noting whether it was tacky or non-tacky.

Thickness Evaluation

The consistency of the film thickness is critical since it is directly related to the accuracy of dosage distribution in the film. The thickness of the film was measured using digital Vernier Calliper that were calibrated. At five different locations, the thickness was measured (four corners and one at centre).

Weight Variation

This test was carried out by cutting 6.25 cm^2 of film from the casted film at three separate locations. Weight of each film was determined using an electronic balance. For the weight variation research, three values were averaged.

Folding Endurance

The folding endurance of a film, which is related to its flexibility, was measured manually by strongly holding and folding the films through the centre multiple times. The value of folding endurance was defined as the number of folds on the same crease required to develop a crack in the film.

pH Evaluation

An acidic or alkaline pH might irritate the oral mucosa, the surface pH of the MDFs was evaluated to study possible side effects caused by a change in pH in vivo. The pH of the surface was measured with a pH metre.

The film was allowed to swell for 1 h at room temperature after being in contact with 1ml of distilled water. The pH was measured by placing the electrode on the film's surface, allowing it to equilibrate for 1 minute, and then recording the result.

Tensile Strength

The tensile strength of the films was determined using Universal Tensile Strength Tester (Dual Column) GT-C01-1 tiny tensile grips, as stated below: On the texture analyser, a 6.25 cm^2 sheet free of air bubbles or physical flaws was held longitudinally in the tensile grasp. The test was carried out using a crosshead speed of 2 mm/sec and a 6 mm initial grip separation from both sides until the film broke. For each film, all measurements were made in triplicate. The setting of texture analyser is done as follow:

Pre- test speed

1.50 mm/sec., Test speed: 2.00 mm/sec., Post-test speed: 10.00 mm/sec., Trigger force: 5.00 kg, Data acquisition rate: 200 pps.

In-vitro Disintegration of Films

In a petri dish containing 25 ml of phosphate buffer pH 6.8 at 37±0.5°C, the in-vitro disintegration time of 6.25 cm^2 films was visually evaluated. The time the film began to shatter or

disintegrate was recorded, and this is the film's disintegration time.

Percentage Moisture Loss

To check the integrity of films in the dry state, percentage moisture loss was computed. Films were cut into 6.25 cm^2, weighed precisely, and stored in desiccators with fused anhydrous calcium chloride. The films were removed and weighed again after 72 hours. The amount of moisture loss was determined by the decrease in the weight of the films. The percentage loss in moisture was calculated by using the following formula:

percentage moisture loss = (Initial weight - final weight) / (Initial weight) × 100

Percentage Moisture Absorption

By slicing the films into 6.25 cm^2 patches, the moisture uptake could be evaluated. These films were dehydrated for one day at room temperature in a desiccator containing a saturated potassium sulphate solution (relative humidity: 75%). It was discovered that the weight of the films had increased due to moisture absorption. The percentage gain in the moisture by the films was calculated using the following formula:

percentage moisture loss = (Initial weight - final weight) / (Initial weight) × 100

Swelling Index: On a 2% agar plate, a pre-weighed drug-loaded film was inserted. The weight of the film gradually increased until it reached a stable weight.

Drug Content Uniformity: The film (6.25 cm^2) was transferred into a graduated flaskcontaining 100 ml of distilled water. The flask was shaken for 4 h in a mechanicalshaker. Then the solution was filtered and after suitable dilutions with distilled water,the absorbance value was measured at 281 nm using the placebo patch solution asblank and the drug content was calculated.

Accelerated Stability Studies for Optimized Formulation: The ICH Q1A (R2) rules were followed for the accelerated stability studies. For the expedited stability research, the formulations FC7 and FC8 were chosen. Each film (6.25cm2) was wrapped with butter paper, then aluminium foil, before being placed in an aluminium pouch and heat-sealed. For two months, a stability study was conducted at 40±2°C and 75±5% RH. After a 15-day period, samples were taken out and analysed for physicochemical qualities. After two months of storage at 40±2°C and 75±5% RH, the similarity factor was used to investigate the influence of storage on physical appearance, in-vitro disintegration time, tensile strength, and drug content[21].

Results and Discussion:

Morphological Properties of Prepared MDFs: After three months of storage at room temperature (25°C) with a relative humidity of around 65±5%RH, the formulations showed no change in characteristics, including no crystallisation of the medication.

Drug-Excipient Interaction Studies: UV and FTIR studies were conducted to examine if there was any interaction between the drug and the excipients. A UV and FTIR scan of a physical mixture of drug and excipients exhibited peaks that were comparable to those of the pure drug, indicating that there was no interaction between the drug and the excipients, as shown in figure 3 and 4.

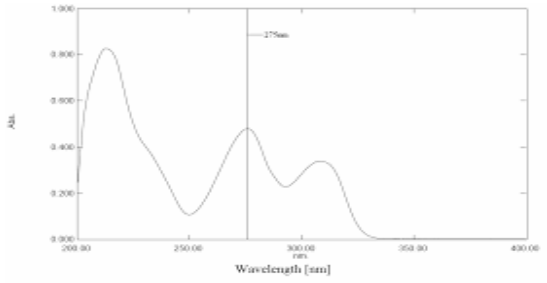

Figure 3: UV spectrum of drug and excipients in phosphate buffer pH 6.8

Table 3: Physico-chemical evaluation of Cisapride mouth dissolving film

Formulation code	Thickness (mm) ±SD	Weight variation (mg)	pH	% Moisture loss	% Moisture absorption
FC1	0.06±0.011	24.50±1.11	6.5±0.20	8.50± 0.55	7.75±0.30
FC2	0.07±0.014	26.50±1.60	6.4±0.30	8.73±0.45	8.11±0.35
FC3	0.08±0.013	28.75±1.25	6.5±0.20	8.24±0.31	9.56±0.45
FC4	0.09±0.009	29.25±1.57	6.4±0.25	8.11±0.25	10.90±0.26
FC5	0.08±0.008	31.50±1.80	6.9±0.30	6.55±0.23	11.98±0.40
FC6	0.07±0.013	30.25±1.55	7.1±0.15	5.85±0.19	12.18±0.35
FC7	0.08±0.011	32.75±1.71	7.3±0.25	4.45±0.21	13.11±0.30
FC8	0.09±0.007	31.50±1.55	7.4±0.30	4.15±0.19	14.15±0.25
FC9	0.09±0.013	29.25±1.61	7.4±0.20	5.27±0.20	14.23±0.40

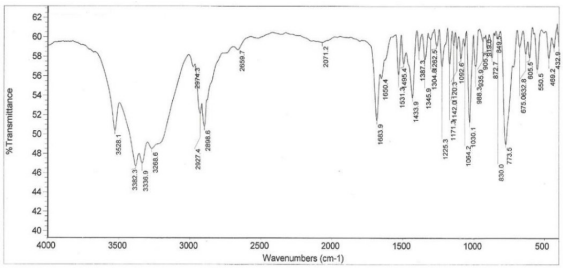

Figure 4: FTIR of drug and excipients

Surface Morphology Study by SEM:Cisapride showed crystalline structure while MDFs showed smooth surface without any scratches and transverse striations indicating that the drug is uniformly distributed. No crystals of the drug were observed in the prepared films Fig. 5 shows the results of SEM studies which were performed to assess the surface morphology of a drug and its preparation (MDFs).

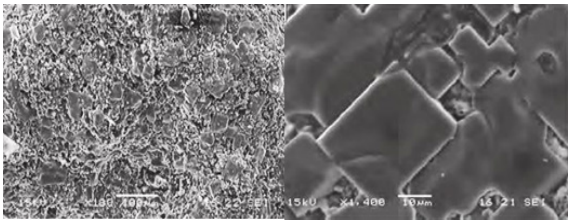

Figure 5: SEM image of drug and prepared film

Tack Test

Films F1 to F8 were non-tacky. The F9 was slightly tacky. This may be due to a lesser amount of glycerine. The results are shown in table 2.

Folding Endurance: As demonstrated in Table 2, the folding endurance of several MDFs ranged from 50 to 100.

Thickness evaluation

The consistency of the film thickness is critical since it is directly related to the accuracy of dosage distribution in the film. The thickness of the films rose as the amount of polymer increased, and was determined to be in the range of 0.06 to 0.09 mm, as shown in table 3.

Weight variation

The weight of the individual formulations was not significantly different from the average value in any of the batches. Weight variation as shown in table 3 for prepared film was found to be in the range of 24 to 32 mg.

pH evaluation

The pH of the surface was measured with a pH metre. The surface pH of prepared MDFs was found to be in the range of 6.1 to 7.5 in Table 3, indicating that they were in the neutral pH range and would not cause irritation when placed in the oral cavity.

Percentage moisture loss

To check the integrity of films in the dry state, percentage moisture loss was computed. Films were cut into 6.25 cm^2, weighed, and stored in desiccators with fused anhydrous calcium chloride. The films were removed and

reweighed after 72 hours, as shown in Table 3.

Percentage Moisture Absorption

The % moisture absorption test was used to determine the film›s physical stability or integrity in a humid environment. The moisture uptake of the films (n=3) was measured by exposing them to a 75%RH environment (saturated calcium chloride solution) at room temperature for one day, table 3 shows the results.

Swelling Index

The swelling index is used to measure the ability of hydrophilic polymers to absorb water after being hydrated. Drug release from a film is also affected by the rate and extent of film hydration and swelling. The amount of swelling was found to be directly proportional to the concentration of polymer and plasticizer in the current investigation, as shown in table 4.

Drug Content Uniformity: The content uniformity test was carried out to ensure that the medicine was distributed evenly. All of the formulas were tested for content homogeneity. The results showed that there was good homogeneity in drug content across all formulations, ranging from 91.50 to 99.05%. The drug concentration of the formulations is shown in Table 4.

Table 4: Swelling index and drug content of Cisapride mouth dissolving film

Formulation code	Swelling index	Drug content
FC1	41.50%±2.08	83.40±1.01
FC2	45.50%±1.50	93.30±1.14
FC3	52.45%±2.11	91.40±1.25
FC4	63.42%±1.45	78.20±1.75
FC5	69.42%±1.75	87.90±1.03
FC6	70.42%±2.10	92.30±1.19
FC7	83.22%±1.50	97.79±1.13
FC8	86.25%±1.25	99.15±1.11
FC9	80.25%±2.14	90.11±1.42

In-vitro Dissolution Study: The data reveals that the percentage of drug release at the end of 5th minute was between 65.10 to 96.2% for formulations F1 to F9. All formulations had a nearly identical release pattern, with rapid release in the first few minutes, followed by a steady release, and finally reaching a plateau level in around 5 minutes. Due to the various concentrations of polymer in each formulation, the rate of release during the early rapid release phase varied slightly between formulations. The greatest percentage drug release for Formulation F8 was 96.2 percent as shown in figure 6 and cumulative percent drug release from formulations FC1 to FC9 is shown in table 5.

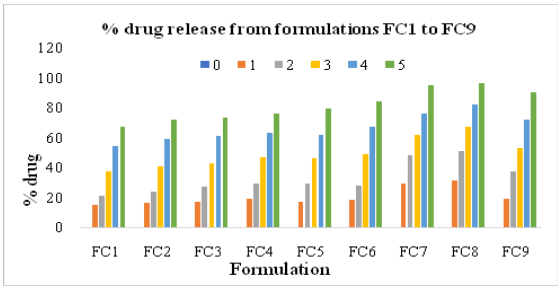

Figure 6: In-vitro percent drug release from formulations FC1 to FC9

Table 5: In-vitro percent drug release from formulations FC1 to FC9

Time (min.)	% Cumulative drug release								
	FC1	FC2	FC3	FC4	FC5	FC6	FC7	FC8	FC9
0	0	0	0	0	0	0	0	0	0
1	19.4	25.2	29.6	13.8	20.3	24.4	12.8	16.2	18.3
2	53.6	59.4	65.2	47.2	49.5	58.6	33.4	41.6	50.7
3	62.2	67.6	77.4	58.3	60.4	69.4	50.8	52.9	62.2
4	76.6	85.4	88.3	69.4	78.2	82.2	58.9	70.8	73.8
5	83.4	93.3	91.4	78.2	87.9	92.3	97.79	99.15	90.11

Table 6: Accelerated stability studies of formulations FC7 and FC8

Parameter	Appearance	Tensile Strength ($kg/mm^{2)}$		Disintegration Time (sec)		Drug Content (%)	
	FC7 and FC8	FC7	FC8	FC7	FC8	FC7	FC8
Initial	Transparent and both surfaces smooth	0.490 ±0.75	0.480 ±0.60	115sec ±1.15	105sec ±1.25	97.79	99.15
After 10 days	Transparent and both surfaces smooth	0.488 ±0.57	0.478 ±0.45	113 sec ±1.00	103 sec ±1.01	97.74	99.00
After 20 days	Transparent and both surfaces smooth	0.484 ±0.71	0.477 ±0.75	112 sec ±0.94	102 sec ±1.06	97.45	98.76
After 30 days	Transparent and both surfaces smooth	0.484 ±0.65	0.476 ±0.70	109 sec ±1.40	100 sec ±1.00	97.30	98.52
After 40 days	Transparent and both surfaces smooth	0.482 ±0.69	0.475 ±0.92	108 sec ±1.12	98 sec ±0.75	97.27	98.15
After 50 days	Transparent and both surfaces smooth	0.481 ±0.85	0.472 ±0.51	107 sec ±1.16	97 sec ±1.11	97.13	98.09
After 60 days	Transparent and both surfaces smooth	0.480 ±0.50	0.471 ±0.53	106 sec ±1.20	95 sec ±1.00	96.15	98.01

This could be due to the bigger proportion of the hydrophilic polymer expanding at a faster rate and to a greater extent. The drug release was minimal in Formulation F9. This could be owing to a higher polymer concentration but a lower plasticizer content.

Accelerated Stability Studies for Optimized Formulation:Stability studies of optimised formulations FC3 and FC6 were carried out at 40 ±2 °C and 75 ±5% RH for 2 months to detect the change in dosage form performance due to storage. After a 10-day period, samples were taken and physicochemical parameters were assessed. The batch's effect on storage was investigated using the similarity factor. It was inferred from the data in Table 6 that formulations F7 and F8 were stable and preserved their original qualities with slight modifications. Physically, there was no change in look or flexibility. Furthermore, there were no significant differences in disintegration time or drug content. As a result, the formulations were discovered to be stable.

Conclusion Cisapride is a gastro retentive agent; commonly a quick release dosage form will be highly suitable for having rapid onset of action. Water soluble polymers were chosen and films were formulated by solvent casting method. Some of these polymers individual not give films of desirable property. From the study, combination of two polymers i.e., HPMC 3 cps and Lycoat gave best films with required physical characteristics.

Cisapride MDFs were tested for stability at 40^0C / 75% RH for one month, did not show any change in morphology, content of the drug and dissolution. The mean thickness and weight of buccal polymeric patches increased with an increase in the amount of polymer weight.

Acknowledgement: None
Conflict of interest: None

References

1. Shariff, Z. B., Dahmash, D. T., Kirby, D. J., Missaghi, S., Rajabi-Siahboomi, A., & Maidment, I. D. (2020). Does the Formulation of Oral Solid Dosage Forms Affect Acceptance and Adherence in Older Patients? A Mixed Methods Systematic Review. Journal of the American Medical Directors Association. 21(8), 1015-1023.
2. Pawar, R., Sharma, R., Sharma, P., &Darwhekar, G. N. (2019). A Review on Mouth Dissolving Film. Journal of Drug Delivery and Therapeutics, 9(6), 206-210.
3. Hannan, P. A., Khan, J. A., Khan, A., &Safiullah, S. (2016). Oral dispersible system: A new approach in drug delivery system. Indian journal of pharmaceutical sciences, 78(1), 2.
4. Uddin, M. N., Allon, A., Roni, M. A., &Kou-

zi, S. (2019). Overview and future potential of fast dissolving buccal films as drug delivery system for vaccines. Journal of Pharmacy & Pharmaceutical Sciences, 22, 388-406.

5. Wertz, P. W. (2021). Roles of Lipids in the Permeability Barriers of Skin and Oral Mucosa. International Journal of Molecular Sciences, 22(10), 5229.
6. Patel, N. A., Shah, D. P., & Patel, T. J. (2016). A novel approach for buccal drug delivery system-buccal film. Pharma Science Monitor, 7(2).
7. Pingale, P. L., Rajput, A. P., & Bagade, S. B. (2020). Use of natural superdisintegrants in formulation of fast disintegrating tablet of atenolol. European Journal of Molecular & Clinical Medicine, 7(09), 3743-3752.
8. Pingale, P.L., Boraste, S. S., & Amrutkar, S. V. (2021). Formulation and evaluation of pravastatin fast disintegrating tablets using natural superdisintegrant. Journal of Medical Pharmaceutical & Allied Science, 10(3), 2977-2981.
9. Bala, R., Pawar, P., Khanna, S., & Arora, S. (2013). Orally dissolving strips: A new approach to oral drug delivery system. International journal of pharmaceutical investigation, 3(2), 67-76.
10. Alqahtani, M. S. (2021). Advances in oral drug delivery. Frontiers in Pharmacology, 12, 62.
11. Rada, S. K., & Kumari, A. (2019). Fast dissolving tablets: waterless patient compliance dosage forms. Journal of Drug Delivery and Therapeutics, 9(1), 303-317.
12. Kumar, R. S., & Ghosh, A. (2019). Fast dissolving tablets: patient compliance dosage forms.World Journal of Pharmacy and Pharmaceutical Sciences, 8(3), 280-300.
13. Prasad, N., Issarani, R., &Nagori, B. P. (2013). Ultraviolet spectrophotometric method for determination of glipizide in presence of liposomal/proliposomal turbidity. Journal of Spectroscopy, 836372, 1-5.
14. Pingale Prashant, L., & Nikhilitha, P. (2021). Effect of Natural Polymer on Release Retarding Rate of Glimepiride Sustained Release Tablet. Journal of Advanced Scientific Research, 12(1), 145-150.
15. Aghrbi, I., Fülöp, V., Jakab, G., Kállai-Szabó, N., Balogh, E., & Antal, I. (2021). Nanosuspension with improved saturated solubility and dissolution rate of cilostazol and effect of solidification on stability. Journal of Drug Delivery Science and Technology, 61, 102165.
16. Kathpalia, H., & Patil, A. (2017). Formulation and evaluation of orally disintegrating films of levocetirizine dihydrochloride. Indian Journal of Pharmaceutical Sciences, 79(2), 204-211.Alkahtani, M. E., Aodah, A. H., Abu Asab, O. A., Basit, A. W., Orlu, M., & Tawfik, E. A. (2021). Fabrication and Characterization of Fast-Dissolving Films Containing Escitalopram/Quetiapine for the Treatment of Major Depressive Disorder. Pharmaceutics, 13(6), 891.
17. Bala, R., & Sharma, S. (2018). Formulation optimization and evaluation of fast dissolving film of aprepitant by using design of experiment. Bulletin of Faculty of Pharmacy, Cairo University, 56(2), 159-168.
18. Raza, S. N., Kar, A. H., Wani, T. U., & Khan, N. A. (2019). Formulation and evaluation of mouth dissolving films of losartan potassium using 32 factorial design. International Journal of Pharmaceutical Sciences and Research, 10(3), 1402-1411.
19. Patel, M. A., & Pingale, P. L. (2014). Comparative effect of different high functionality excipients on various characteristics of vardenafil HCl tablets (BCS II drug). International Journal of Pharmaceutical Sciences and Research, 5(12), 5447-5551.
20. Chennuri, A., &Prasanthi, D. (2018). Solubility enhancement of aripiprazole by solid-self emulsifying drug delivery systems. International Journal of Pharmaceutical Sciences and Drug Research, 10(4), 233-245.

Current Trends in Biotechnology and Pharmacy
Vol. 16 (4) 500 - 510, Oct 2022, ISSN 0973-8916 (Print), 2230-7303 (Online)
10.5530/ctbp.2022.4.83

Is Olive Oil Consumption Suitable for Colorectal Cancer? *In Vivo* Preliminary Studies on Azoxymethane-Induced Colon Cancer in Rats

Sheba R David[1,2], Aida Batrisyia Mohd Taufik[2], Lim Ya Chee[2], Ashok Kumar Balaraman[3], Rajan Rajabalaya[2*]

[1]School of Pharmacy, University of Wyoming, Laramie, Wyoming, 82071 United States of America.
[2]PAPRSB Institute of Health Sciences, Universiti Brunei Darussalam, JalanTungku Link BE1410, Brunei Darussalam.

[3]MAHSA University, Bandar Saujana Putra, 42610 Jenjarom, Selangor, Malaysia

*Corresponding author: rajan.rajabalaya@ubd.edu.bn

Abstract

The incorporation of olive oil in the diet may have promoting or inhibitory effects on colorectal cancer (CRC). Objective: In this study, azoxymethane (AOM) was used to mimic CRC in rats and the effect of olive oil was correlated with the cancer progression in the colon of the rats. Design: Six weeks old Sprague-dawley male rats were randomized into 4 groups namely, naïve, indomethacin, saline and olive oil. Main outcome measures: This study was to investigate the effect of olive oil on preneoplastic cancer properties on the colonic mucosal surface for any tumors and the aberrant crypt foci (ACF). The induction AOM for the CRC by subcutaneous injection of 20 mg/kg.Rats were given 10 mg/kg b.w. of indomethacin dissolved in 0.9% saline by oral gavage for 4 weeks (28 days) as a positive control group.The negative control group was given 0.9% sodium chloride solution. Results: The experimental treatment compound, olive oil, was administered orally with a dosage of 7% daily food intake for 4 weeks (28 days). At week 6 (day 42), all animals were sacrificed by cervical dislocation and the colorectum was excised for histological examination.Histological sections were achieved using a microtome and histological sections were observed using a microscope. The mean body weights of the rats at 42 days are naïve – 238.5 ± 33.2, positive control – 251.5 ± 31.8, negative control – 231 ± 2.8 and treated group 262 ± 28.3. A total 3 ACF were found in the negative group compared to other groups. The crypts appeared regular with circular luminal openings and were arranged closely packed together in the naïve group. Crypts in the positive and treated group also had a similar appearance like naïve group.Conclusions: Olive oil inhibits the preneoplastic cancer properties ACF and maybe an incorporate into diet during CRC treatment or management.

Keywords: Preneoplastic, Olive oil, Aberrant crypt foci, Azoxymethane, Colorectal, Cancer.

Introduction

Colorectal cancer (CRC), also known as, colon cancer, rectal cancer or bowel cancer, is a heterogeneous disease that occurs in the inner lining of the colon and rectum.[1] Cancer remains to be a global cause of morbidity and mortality and the incidence continue to rise [2,3]According to many reports, CRC is the second most common cause of cancer in women and third in men.[1,3,4]The carcinogenesis is a multifaceted process that involves an abnormal growth of the mucosal surface termed as a polyp which develops at a slow rate into a premalignant lesion if left untreated.[1] Normal morphology of the colonic lining consists of crypts in which its bases contain regenerative

stem cells through a series of mechanisms, it will eventually extrude the epithelial cells and replace crypt cells every five days.[5] The presence of aberrant crypt foci (ACF) is remarked as a feature of possible CRC malignancy. ACF is defined as focal lesions formed specifically in the colonic mucosa that are composed of one to multiple crypts.[6] The first description of ACF was reported by Bird (1987) in which he performed a light microscopic examination of methylene blue-stained whole-mount preparations of AOM-treated mice colonic mucosa.[7] The carcinogens that specifically induce colon tumours in rats include aromatic amines, derivatives of cyacin such as 1,2-dimethylhydrazine (DMH) and its metabolite azoxymethane (AOM), alkylureas and heterocyclic amines such as 2-amino-1-methyl-6-phenylimidazo[4,5-b]pyridine (PhIP).[6,8–11]

Non-steroidal anti-inflammatory drugs (NSAIDs) such as aspirin, ibuprofen and sulindac are well reported to exhibit anti-neoplastic activity for colorectal tumours[12]epidemiological studies have demonstrated that continuous therapy with NSAIDs offers real promise of chemoprevention and adjunct therapy for colon cancer patients. Tumour growth is the result of complex regulation that determines the balance between cell proliferation and cell death. How NSAIDs affect this balance is important for understanding and improving treatment strategies and drug effectiveness. NSAIDs inhibit proliferation and impair the growth of colon cancer cell lines when tested in culture in vitro and many NSAIDs also prevent tumorigenesis and reduce tumour growth in animal models and in patients, but the relationship to inhibition of tumour cell proliferation is less convincing, principally due to gaps in the available data. High concentrations of NSAIDs are required in vitro to achieve cancer cell inhibition and growth retardation at varying time-points following treatment. However, the results from studies with colon cancer cell xenografts are promising and, together with better comparative data on anti-proliferative NSAID concentrations and doses (for in vitro and in vivo administration. It has demonstrated several actions at different phases of the Wnt pathway and effects on total β-catenin protein reduction, decreased nuclear localisation and decreased β-catenin/TCF binding resulting in suppressed cyclin expression.[13] A study performed and explored the significance of indomethacin in DMH-induced Sprague Dawley rats for a short term treatment of 3 weeks at doses 2 mg/kg and 1 mg/kg daily.[14] The experiment denotes satisfactory inhibition of ACF formation for the higher dose treated group while 1 mg/kg daily treatment did not produce significant statistical difference with the control.[13]

The cooking oils may contain numerous substances that can either protect against or promote for CRC development.[15] Vegetable oil is considered to possess more beneficial ingredients such as oleic acid than animal fat sources such as the trans fatty acid.[16]Olive oil is a rich source of biophenols and squalene such as oleuropein, flavonoids, phenolic acids, lignans, tyrosol and hydroxytyrosol.[17,18]Several anti-cancer investigations of *O. europeae*-extracts reported that erythrodiol, a triterpenoid of olives, exhibits anti-proliferative and apoptotic actions in HT-29 human adenocarcinoma cells. [19]The inhibitory effect olive oil observed in cancer cell lines has been linked with the blockade of the G2/M phase cell cycle through the inhibition of cyclic adenosine monophosphate (AMP) response element binding protein (CREB) phosphorylation resulting in a downstream reduction of COX-2 expression. Another study demonstrated the apoptotic activity of maslinic acid in HT29 human colon cancer cells via mitochondrial apoptotic pathway (Reyes-Zurita*et al.*, 2009).As mentioned by Chen & Huang (2009), CRC is the only cancer that can be prevented by selecting appropriate food and lifestyle.[20]

As the dietary intake of olive oil abundant with ω-9 MUFA had significantly inhibited the formation of ACF as well as decreased colonic arachidonate levels in AOM-induced

rat CRC model. [21,22] It was observed that AOM-induced colonic mucosa had significant increase in prostaglandin E_2 (PGE_2) concentration. However, olive oil treated rats had suppressed tumour growth mainly due to the regulation of COX-2 expression involving prostaglandin (PG) and caspase-3 synthesis that leads to apoptosis[23].

There are various studies on olive oil in relation to cancer, however in this study, we intend to observe the chemopreventive effect in the early stage of carcinogenesis and assess with an olive oil that is commercially available in which they can incorporate into their diet.This study involved the introduction of olive oil into AOM-induced rats to evaluate the action of olive oil on the quantity and size of polyps in colon. The outcome of this study is expected to provide nutritionists with a better comprehension on the effects of olive oil on colonic tumours, so a better and effective dietary pattern may be devised to eliminate the risk of nutritional deterioration in CRC patients.

Materials and Methods

Chemicals

The induction of CRC in rats was performed using carcinogen AOM purchased from Sigma Aldrich, St. Louis, MO. The drug indomethacin purchased from Promega, U.S.A. Olive oil which was produced by Borges Agricultural & Industrial Edible Oils in Tàrrega, Spain.

Animal experiment

The protocol of animal treatment was approved by the Animal Ethics Committee of Universiti Brunei Darussalam (UBD) and UBD Office of Safety, Health & Environment (OSHE). The research ethics for using animals were reviewed and approved by University Research Ethics Committee (UREC), Universiti Brunei Darussalam (Ref: UBD/OAVCR/UREC/Dec18-02). An five-weeks-old, male, Sprague Dawley rats which weighed between 100 to 150 grams (g), were kept under standard conditions of 27±2°C with 70-80% humidity and 12h light/12h darkness cycle. Furthermore, the animals were divided into 4 groups namely, naïve, indomethacin, saline and olive oil. In addition, each group consisted of 6 rats which were housed in one cage. The experiment protocol is summarised in Figure 1.Saline group was given 0.9% sodium chloride (NaCl) solution which represented the negative control group. The rodents were orally administered with 10 mg/kg b.w. of saline for 4 weeks (28 days). Indomethacin group acted as the positive control group and were given 10 mg/kg b.w. of indomethacin dissolved in 0.9% saline by oral gavage for 4 weeks (28 days).The experimental treatment olive oil group was administered orally with a dosage of 7% daily food intake for 4 weeks (28 days).

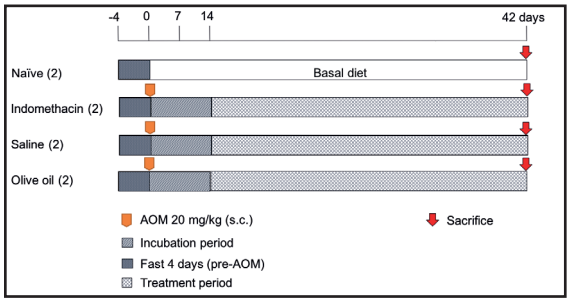

Figure 1 Experimental protocol for olive oil effect on CRC.

All rats were re-weighed before cancer induction on day 0 and each rat received 20 mg/kg body weight (b.w.) of AOM. All rats except naïve group received subcutaneous (s.c.) injection of AOM dissolved in physiological saline. The animals were allowed 2 weeks (14 days) of incubation period with access to food and water. On day 14, the animals began oral treatment which lasted for 4 weeks (28 days). Their body weights were measured weekly and macroscopically observed for the presence of rectal bleeding and diarrhoea. This group was neither given any carcinogen nor treatment compound. The naïve rats were only given basic food and water until they were sacrificed on day 42. Their body weights were recorded weekly and macro-

scopic observations were noted.

Macroscopic examination of ACF

After 24 hours of fixation, the colons were dipped in 0.2% methylene blue (Merck KGaA, Germany) in distilled water, then briefly washed with distilled water and placed on microscope slides with the mucosal surface uppermost. ACF was detected using light microscope (Olympus BX41, Japan) under 4x and 10x magnification.[6,24]distribution pattern along the colon and crypt multiplicity in 0.1% methylene-blue whole-mount preparations. ACF were distinguished from normal crypts by their larger size and elliptical shape. The incidence, distribution and morphology of colon tumors were recorded. The majority of ACF were present in the middle and distal colon of DMH-treated rats and their number increased with time. By the 4th week, 91.5% ACF were composed of one or two crypts and 8.5% had three or more crypts, while by the 30th week 46.9% ACF had three or more crypts. Thus, a progression of ACF consisting of multiple crypts was observed from the 4th to the 30th week. Nine well-differentiated adenocarcinomas were found in 10 rats by the 30th week. Seven tumors were located in the distal colon and two in the middle colon. No tumor was found in the proximal colon. The present data indicate that induction of ACF by DMH in the short-term (4 weeks The procedure involved counting the number of ACF in each colonic segment and evaluating the number of ACs in each ACF which was classified as either 1AC, 2ACs, 3ACs and ≥4ACs. After that, the tumours were prepared for haematoxylin and eosin staining for subsequent histopathological diagnosis.

Histological evaluation

Stained histological sections were observed using a microscope (Olympus BX41, Japan) at x10 and x20 magnifications. The cells were viewed on a computer using the software Olympus DP2-BSW and best representations of cells were photographed using a microscope digital camera (Olympus DP25, Japan). The histological classification was done according to a criteria described the cells may be categorised as normal, non-dysplastic ACF and dysplastic ACF.[5,25]The criteria for microscopic assessment was put into tabulated form below in Table 1.

Table 1. Criteria for microscopic classification.

Score	Criteria
0	Normal: straight test tube appearance, no serration, no branching.
1	Non-hyperplastic: enlarged crypts, lack significant abnormalities in epithelial cells, no mucin depletion.
2	Hyperplastic: larger and elongated crypts with side and apical branching, serrated lumen.
3	Dysplastic: nuclear stratification and enlargement, pleomorphism, hyperchromasia.

Statistical analysis

The data was statistically analysed using the GraphPad Prism software, Version 7. The numerical values for each group were expressed as mean±standard deviation (SD) and were subjected to unpaired *t*-test. The tumour multiplicity (number/rat) was expressed as mean±standard error of mean (SEM). For all cases, a value of $p<0.05$ was considered to be statistically significant.

Results and Discussion

General observations

The body weights were recorded each week for all groups. It was found that rats in all groups gradually gained weight throughout the experiment (Figure 2). However, inconsistency was found as the body weight was abruptly adjusted as seen in day 35 for naïve and positive,

and negative groups as well as day 42 for olive oil group. Rectal bleeding was not observed, but slight diarrhoea was noticed in the first week of treatment. Despite that, the rats consumed food as normal and were occasionally aggressive.

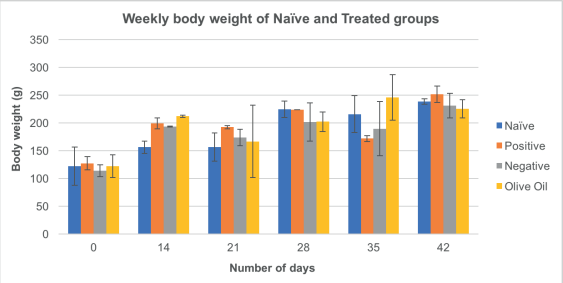

Figure 2. Effect of naïve and treated groups on body weight of Sprague Dawley rats.

Macroscopic evaluation

The mean length colon excised was 1.7 cm. The colon was divided into three portions in order to better manage for fixation and observing visible polyps. No visible neoplasm was detected in all groups. Figure 3 displays the normal appearance of rat colon with distinguishable features of proximal colon from distal regions.

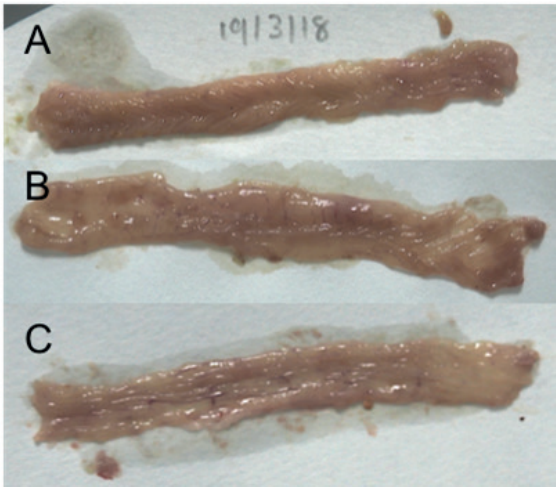

Figure 3. Macroscopic features of the colon. Whole colon was cut into 3 segments: (A) proximal, (B) middle and (C) distal. (A) Proximal colon can be easily distinguished due to visible foldings on mucosal surface. (B) Middle segment exhibits a transition from folded mucosa appearance of proximal to smooth mucosal surface in distal portion (C).

Effect of olive oil on ACF formation during initiation stages

Upon inspection under the microscope, it was found that negative and olive oil had an average of 0.5 and 4.5 of ACF respectively (Table 2) detected through the whole length of colon in each rat. Table 4 depicted that 0.5 ACFs in negative group contain 3ACs whereas olive oil had 4.0 of ACFs that contained 1AC and 0.5 ACFs with 2ACs. As the crypt multiplicity is higher in negative, formation and progression of ACF is more readily in this group than olive oil. As seen in figure 5, normal and positive groups exhibited normal configuration of crypts. Crypts in negative group displayed abnormal slit-like luminal opening, however this feature is not sufficient to consider as ACF. The best representation of an ACF is presented in negative (Figure 4) with obvious foci. Meanwhile, most slightly abnormal crypts found in olive oil group was not regarded as ACF.

Table 2. Effect of each treatment on AOM-induced colonic aberrant crypt foci (ACF) formation at week 6. Values are mean±SEM. No ACF were detected in naïve and positive groups.

Group	No. of ACF/ colon	Crypt multiplicity of ACF			
		1AC	2ACs	3ACs	≥4ACs
Naïve	0	-	-	-	-
Positive	0	-	-	-	-
Negative	0.5±0.5	0	0	0.5±0.5	0
Olive Oil	4.5±1.5	4.0±1.0	0.5±0.5	0	0

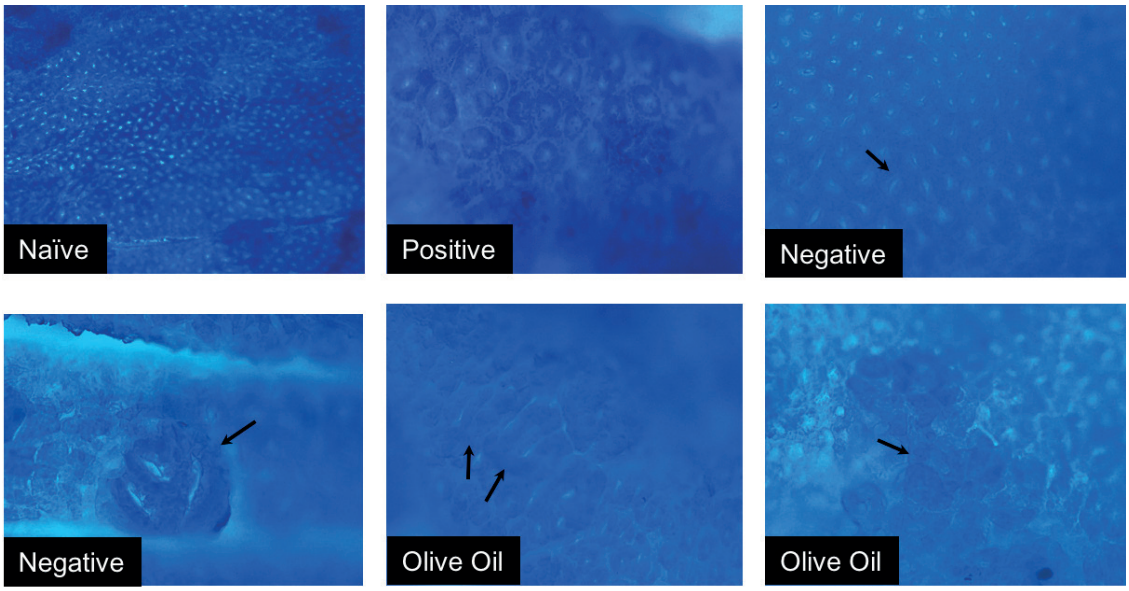

Figure4. A microscopic view of the whole mounts of methylene blue stained colonic showing presence of normal and aberrant crypts. No detection of ACF in naïve group and positive groups. Naïve at x4 magnification: exhibits crypts of similar size, round luminal opening and no significant abnormalities. Positive at x10 magnification: exhibits slight variation of crypt sizes with round luminal opening but no significant abnormalities. Negative at x10 magnification: most crypts had slit-like luminal opening (indicated with an arrow). Negative at x10 magnification: ACF detected was seen larger than normal and had thickened, darkened stain (indicated with an arrow). Olive oil at x10 magnification: exhibits increased dimensions with thicker and darker stain than normal (indicated with an arrow).

Non-hyperplastic cells were found in negative group only. The cells are indicated with arrows in Figure 5C and 5D. This finding supports the ACF that was macroscopically observed in Figure 4. Figures 5A and 5B illustrate the normal crypts as well as atypical crypts as seen in Figure 6 naïve, positive, negative slit-like lumen and olive oil. The microscopic scoring was based on numbering the categories normal (0), non-hyperplastic (1) and hyperplastic (2). The scoring values were averaged and presented in Figure 6. The naïve, positive and olive oil groups had normal scores in all colon segments while three segments in the negative group contributed to the mean 0.6 score. The negative group was found to be significantly different from naïve mean score. Whereas the olive oil aberrant crypt score is significantly lower than in negative control.cells. (D) Slight abnormal configuration of crypts with enlarged lumen (arrows).

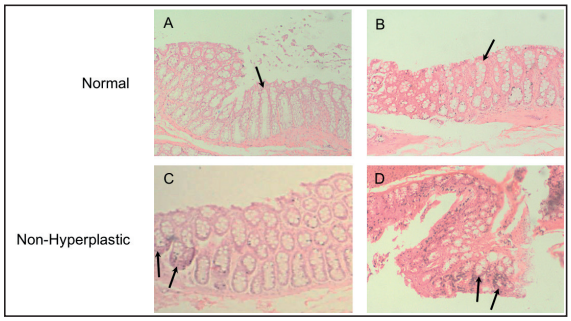

*Figure*5. A microscopic view of H&E staining detected for normal and non-hyperplastic histological category. (A, B) Normal mucosa showing characteristic straight test tube appearance, no serration and no branching indicated with an

arrow. (C) Crypts (arrows) are slightly enlarged but lack significant abnormalities in epithelial

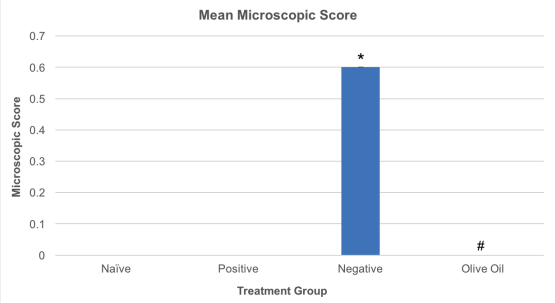

*Figure*6. Mean microscopic score of naïve and treated groups. Scoring is based on the criteria described by Alrawi et al. (2006) and Norlida & Phang (2010). Significant difference from naïve is denoted by *p<0.05 and from control is denoted by #p<0.05.

The use of animal models has become highly valuable for performing extensive investigative cancer studies due to its ability to demonstrate similar diseases in humans. The carcinogen AOM was used in this study due to its ability to promote cancer in the distal colon with high incidence in rats.There was no significance between the weekly weights gained in all groups. Several studies have attained similar insignificant weight gain of AOM-induced rats even in long-term experiments, however, there was no apparent explanation [26,27]6 weeks old, were injected once with one of five doses of azoxymethane. There was a dose response to the carcinogen as determined by weight gain and tumor induction. Rats given the three highest doses developed tumors of the gastrointestinal tract, auditory sebaceous glands, kidney, liver, and preputial gland, whereas rats receiving the lowest doses had tumors mainly of the intestine. Chronic liver lesions in high-dose rats were cirrhosis with megalocytosis, mild fibrosis, nodular hepatocellular hyperplasia, and hyperplasia of bile ductules.abstract":"BACKGROUND: Animal model studies have shown that the colon tumour promoting effect of dietary fat depends not only on the amount but on its fatty acid composition. With respect to this, the effect of n9 fatty acids, present in olive oil, on colon carcinogenesis has been scarcely investigated. AIMS: To assess the effect of an n9 fat diet on precancer events, carcinoma development, and changes in mucosal fatty acid composition and prostaglandin (PG. It is possible that the carcinogen itself did not affect the appetite of induced animals thereby carrying on with their typical food consumption. It is realised that weight is not an ultimate indicator of cancer symptom in animal models. However, the rats were observed to experience slight diarrhoea in the first week after induction which could be attributed to the metabolism of AOM irritating the mucosal lining as they are excreted in urine and faeces [20]. Even though the weights recorded in this experiment correlates with other studies, it was assumed that the values were inaccurate an unreliable on account of small population and fluctuating readings of the weighing balance. These issues can be overcome by increasing the population per group and using a weighing equipment with sensitive bearings.

The average length of colorectum documented is 1.8cm and the present study extracted an average length of 1.7cm [28]. This indicates that we are confident that we took into account appropriate parts for ACF observation. [11] Several studies have reported that AOM is able to stimulate ACF formation in colons as early as 5 weeks.[6,29] Since ACF detection is considered as biomarkers in short-term experiments, for that reason, the current study adopted an AOM-induced rat model that proceeded for 6 weeks. Even so, there were no visible neoplasms detected in all groups. ACF formation by AOM is well defined in distal part of colon and this corresponded to the locations of lesions we observed under the microscope. The indistinguishable inspection of polyps along the colonic mucosal surface could be argued on the basis of inadequate AOM dosage along with induction period, and misdetection of mucosal foldings with abnormal polyps. The severity of aberrant crypt formation may be improved by either in-

creasing the periodic injection to two injections a week for 2 weeks or once a week for the total experiment period 6 weeks [27,30]a constituent of olive oil, and a key intermediate in cholesterol synthesis may be regarded as partially responsible for the beneficial effects of olive oil, which include decreased mortality rates among populations with high olive oil consumption. Thus, in this study we have assessed the chemopreventive efficacy of squalene on azoxymethane (AOM.

The admittance of treatment compounds in day 14 after insufficient cancer induction could have restricted the growth of tumour. Additionally, the present experimental protocol could have created an ambiguity between the actions of test compounds affecting the carcinogenic potential of AOM from those that affected subsequent appearance and growth of lesions. This may be in which AOM was administered in two schedules of 15 mg/kg b.w. twice for 2 weeks and 30 mg/kg dose on day 7 only.[29] The test agent was given since the start of experiment at day 0 to 35 (5 weeks). Likewise, the study managed to detect few foci indistinguishable of the mechanisms mentioned previously. In order to confirm that ACF in the colon has been established before administrating test agent, a faction of rats should be sacrificed and inspected for polyp formation. This provides a basis for ACF count and multiplicity comparison in pre- and post-treatment administration[31]anti-oxidative, and anti-cancer properties but has poor bioavailability. Liquid crystals (LC.During the evaluation of this short-term investigation, it was observed that the positive control group did not develop any ACF and appeared normal as compared to negative control. Indomethacin is a potent NSAID known for its inhibitory effect on neoplastic growths. The research used a dosage of 3 mg/kg daily which was sufficient to prevent further growths as compared to the present study where 10 mg/kg b.w. daily was applied.[14,32]

It has been reported that ACF count and crypt multiplicity are predictive of colon tumour incidence. However, it was established that higher crypt multiplicity is indicative of malignancy and more aggressive tumour progression as opposed to high ACF counts. The negative control group exhibited a low number of ACF but with higher crypt multiplicity in comparison with olive oil group. The insignificant difference of ACF number and crypt multiplicity between olive oil and control groups suggests that dietary olive oil has a slight inhibitory effect on colon carcinogenesis. ACF with low crypt multiplicity is characterised as slower and less aggressive tumourigenesis. Since ACF was detected in negative control groups, microscopic observations displayed non-hyperplastic crypts in contrast with olive oil with morphologically normal crypts. Despite macroscopic observation of olive oil groups detected ACF growths, it was not reflected in microscopic examination. The morphogenesis of a colon tumour has been hypothesised to proceed in a top-down fashion whereby altered cells in the superficial mucosa proliferate laterally and downward to form new crypts adjacent to pre-existing normal crypts and eventually replace them [33]. It was assumed that technical skill errors in isolating abnormal tissue contributed to missed abnormal sections of tissues. The insufficient grade of abnormality in tissues may also cause the dismissal of aberrant categorisation. Tissue preparation could also contribute to the misdetection of crypts due to multi-layered tissue shaving leading to loss of aberrant compartment. This commercial 10% olive oil in the diet can significantly reduce the percentage of fragmented DNA, diminish ACF numbers and crypt multiplicity as well as induce apoptosis of tumour growths.[21,34]The present study utilised olive oil in the proportion of 7% of daily intake. This may account for the low inhibitory actions of olive oil on tumourigenesis in the study.

Low crypt multiplicity detected in the olive oil group showed promising significance of the compound in correcting DNA fragmentation that accounts for dysregulation of pathways

involved in cell proliferation and apoptosis. Although the present study did not manage to clarify the pathway olive oil predominantly affects, that may be due to high ω-9 MUFA as well as phenolic contents of olive oil might have a major influence in regulating Wnt pathways, subsequent COX-2 expression and arachidonate acid metabolism.[21,27,35]the effect of n9 fatty acids, present in olive oil, on colon carcinogenesis has been scarcely investigated. AIMS: To assess the effect of an n9 fat diet on precancer events, carcinoma development, and changes in mucosal fatty acid composition and prostaglandin (PG Furthermore, the present 6-week study has indicated that short-term experiments are inadequate to fully justify the questions of olive oil impact in early stages of cancer or even in high-risk individuals with predisposing mutations. Modulators of carcinogenesis such as COX-2, β-catenin, cyclin D1, Wnt 3, Wnt 5a and iNOSin the apoptotic activity and DNA fragmentation by western blotting should be investigated to recognise their roles in carcinogenesis.With these extensive findings, it would produce a highly reliable and credible outcome of the study to encourage nutritionists and the public to consume olive oil due to its potent beneficial properties during the CRC chemotherapy to avoid recurrence of cancer.

Conclusion

ACF formation is regarded as a precursor in CRC carcinogenesis of humans and rodents. Due to the ability to create a model that mirrors the disease in humans, the predictive value of ACF evaluation has become crucial in the context of anti-cancer drug evaluation. In this study illustrated that the dietary administration of olive oil in initiation stages of tumourigenesis has an inhibitive effect to some degree. The outcomes of the study emphasised the importance of conducting further investigations with olive oil, especially in long-term cancer models.

Acknowledgements

We sincerely thank PAPRSB Institute of Health Science, Universiti Brunei Darussalam for providing laboratory and animal facilities.

Competing interests

The authors declare that they have no competing interests.

References

1. Aran V, Victorino AP, Thuler LC, Ferreira CG. Colorectal Cancer: Epidemiology, Disease Mechanisms and Interventions to Reduce Onset and Mortality. Clin Colorectal Cancer. 2016;15(3):195–203.

2. Chong VH, Telisinghe PU, Bickle I, Abdullah MS, Lim E, Chong CF. Increasing Incidence of Colorectal Cancer, Starting at a Younger Age for Rectal Compared to Colon Cancer in Brunei Darussalam. Asian Pacific J Cancer Prev. 2015;16(12):5063–7.

3. Ferlay J, Soerjomataram I, Dikshit R, Eser S, Mathers C, Rebelo M, et al. Cancer incidence and mortality worldwide: Sources, methods and major patterns in GLOBOCAN 2012. Int J Cancer. 2015;136(5):E359–86.

4. Mustafa M, Menon J. Colorectal Cancer: Pathogenesis, Management and Prevention. IOSR J Dent Med Sci Ver IV. 2016;15(5):2279–861.

5. Alrawi SJ, Schiff M, Carroll RE, Dayton M, Gibbs JF, Kulavlat M, et al. Aberrant Crypt Foci. 2006;120:107–19.

6. Rodrigues MAM, Silva LAG, Salvadori DMF, De Camargo JL V, Montenegro MR. Aberrant crypt foci and colon cancer: Comparison between a short- and medium-term bioassay for colon carcinogenesis using dimethylhydrazine in Wistar rats. Brazilian J Med Biol Res. 2002;35(3):351–5.

7. Bird RP. Observation and quantification of

aberrant crypts in the murine colon treated with a colon carcinogen: Preliminary findings. Cancer Lett. 1987;37(2):147–51.

8. Reddy BS. Animal Models for Colon Cancer Chemoprevention. Science (80-). 2002;1:2002.

9. Johnson RL, Fleet JC. Animal Models of Colorectal Cancer. Cancer Metastasis Rev. 2013;32(1–2):39–61.

10. Doi K, Fujioka M, Sokuza Y, Ohnishi M, Gi M, Takeshita M, et al. Chemopreventive action by ethanol-extracted brazilian green propolis on post-initiation phase of inflammation-Associated rat colon tumorigenesis. In Vivo (Brooklyn). 2017;31(2):187–97.

11. Tudek B, Bird RP, Bruce WR. Foci of Aberrant Crypts in the Colons of Mice and Rats Exposed to Carcinogens Associated with Foods. Cancer Res. 1989;49(5):1236–40.

12. Ettarh R, Cullen A, Calamai A. NSAIDs and cell proliferation in colorectal cancer. Vol. 3, Pharmaceuticals. 2010. p. 2007–21.

13. Hull MA, Gardner SH, Hawcroft G. Activity of the non-steroidal anti-inflammatory drug indomethacin against colorectal cancer. Vol. 29, Cancer Treatment Reviews. 2003. p. 309–20.

14. Charalambous D, Farmer C, O'Brien PE. Sulindac and indomethacin inhibit formation of aberrant crypt foci in the colons of dimethyl hydrazine treated rats. J Gastroenterol Hepatol. 1996;11(1):88–92.

15. Czadek P. Chemoprevention of colorectal cancer. Polish Ann Med. 2016;23(1):75–9.

16. Food and Agriculture Organization (FAO). Fats and fatty acids in human nutrition. Report of an expert consultation. FAO Food Nutr Pap. 2010;91:1–166.

17. Fistonic I, Situm M, Bulat V, Harapin M, Fistonic N, Verbanac D. Olive oil biophenols and women's health. Med Glas (Zenica). 2012;9(1):1–9.

18. Hashmi MA, Khan A, Hanif M, Farooq U, Perveen S. Traditional Uses, Phytochemistry, and Pharmacology of Olea europaea(Olive). Evidence-Based Complement Altern Med. 2015;2015:1–29.

19. Orlando FA, Tan D, Baltodano JD, Khoury T, Gibbs JF, Hassid VJ, et al. Aberrant Crypt Foci as Precursors in Colorectal Cancer Progression. 2008;98(3):1–20.

20. Chen J, Huang XF. The signal pathways in azoxymethane-induced colon cancer and preventive implications. Cancer Biol Ther. 2009;8(14):1313–7.

21. Fujise T, Iwakiri R, Kakimoto T, Shiraishi R, Sakata Y, Wu B, et al. Long-term feeding of various fat diets modulates azoxymethane-induced colon carcinogenesis through Wnt/beta-catenin signaling in rats. Am J Physiol Gastrointest Liver Physiol. 2007;292(4):G1150–6.

22. Huan S, Lee F, Zulkipli IN, David SR, Ahmad SR, Ja'afar F, et al. A review on milk and its biological effects on human health : Neurological conditions , cardiovascular diseases and cancer. Int J Food Sci Nutr. 2018;3(6):84–9.

23. Happy A, Soumya M, Venkat Kumar S, Rajeshkumar S, Sheba RD, Lakshmi T, et al. Phyto-assisted synthesis of zinc oxide nanoparticles using Cassia alata and its antibacterial activity against Escherichia coli. Biochem Biophys Reports [Internet]. 2019 Mar;17:208–11. Available from: https://linkinghub.elsevier.com/retrieve/pii/S2405580818302292

24. Doi K, Wanibuchi H, Salim EI, Morimura K,

Kinoshita A, Kudoh S, et al. Lack of large intestinal carcinogenicity of 2-amino-1-methyl-6- phenylimidazo[4,5-b]pyridine at low doses in rats initiated with azoxymethane. Int J Cancer. 2005;115(6):870–8.

25. Norlida a O, Phang KS. Histomorphology of aberrant crypt foci in colorectal carcinoma. Malays J Pathol. 2010;32(2):111–6.

26. Ward JM. Dose Response to a Single Injection of Azoxymethane in Rats: Induction of Tumors in the Gastrointestinal Tract, Auditory Sebaceous Glands, Kidney, Liver and Preputial Gland. Vet Pathol. 1975;12(3):165–77.

27. Bartolí R, Fernández-Bañares F, Navarro E, Castellà E, Mañé J, Alvarez M, et al. Effect of olive oil on early and late events of colon carcinogenesis in rats: modulation of arachidonic acid metabolism and local prostaglandin E(2) synthesis. Gut. 2000;46(2):191–9.

28. Vdoviaková K, Petrovová E, Maloveská M, Krešáková L, Teleky J, Elias MZJ, et al. Surgical Anatomy of the Gastrointestinal Tract and Its Vasculature in the Laboratory Rat. Gastroenterol Res Pract. 2016;2016:1–11.

29. Pereira MA, Barnes LH, Rassman VL, Kelloff G V., Steele VE. Use of azoxymethane-induced foci of aberrant crypts in rat colon to identify potential cancer chemopreventive agents. Carcinogenesis. 1994;15(5):1049–54.

30. Rao C V, Newmark HL, Reddy BS. Chemopreventive effect of squalene on colon cancer. Carcinogenesis. 1998;19(2):287–90.

31. R David S, Akmar Binti Anwar N, Yian KR, Mai C-W, Das SK, Rajabalaya R. Development and Evaluation of Curcumin in Liquid Crystal Systems for Cervical Cancer. Sci Pharm [Internet]. 2020 Mar 23;88(1):15. Available from: https://www.mdpi.com/2218-0532/88/1/15

32. Rani S, Ahamed N, Rajaram S, Saluja R, Thenmozhi S, Murugesan T. Anti-diarrhoeal evaluation of Clerodendrum phlomidis Linn. leaf extract in rats. J Ethnopharmacol. 1999;68(1–3):315–9.

33. Fujise T, Iwakiri R, Shiraishi R, Wu B, Fujimoto K. Olives and Olive Oil in Health and Disease Prevention. Olives and Olive Oil in Health and Disease Prevention. 2010. 997–1004 p.

34. Zulkipli I, Rajabalaya R, David S, Idris A. Medicinal Plants: A Potential Source of Compounds for Targeting Cell Division. Drug Target Insights. 2015;9:9–19.

35. Gupta G, Singh R, David SR, Verma RK. Effect of rosiglitazone, a ppar-γ ligand on haloperidol-induced catalepsy. CNS Neurosci Ther. 2013;19(9):724–5.

Current Trends in Biotechnology and Pharmacy
Vol. 16 (4) 511 - 517, Oct 2022, ISSN 0973-8916 (Print), 2230-7303 (Online)
10.5530/ctbp.2022.4.84

India's International Collaboration in Biotechnology

Manohar Pathak[1] Atul Bhatt[1]N K Prasanna[2*]

Gujarat University, Ahmadabad-380009, Gujarat, India
CSIR- National Institute of Science Communication & Policy Research, New Delhi-110012
*Corresponding author: prasanna@niscpr.res.in

Abstract

This paper analyses 6451 research publications in the field of Biotechnology by Indian researchers in collaboration with other countries indexed in the web of Science core collections from 1975 to 2021. These 6451 publications received 228989 citations with 181 h-index. During the period the total number of publications from India are 33236 out of which 6451(19.40%) are in international collaboration. There were only 2 publications in 1973 which rose to 825 in the year 2021. Ashok Pandey from CSIR-IITR is the most productive author while CSIR is the leading organization in collaborating with international partners. Microalgae is the most frequent keyword, Journal Bioresource technology is the most preferred journal for publication. The United States, South Korea, and Peoples Republic of China is the most preferred country for collaboration by an Indian scholar.

Keywords: Biotechnology, Scientometric, Research evaluation, Collaboration

Introduction

Collaboration in research is seen as a proxy for quality in academia. Research collaboration is done to share the knowledge, resources, and tools to the worldwide research community to produce new findings and achievements. Due to rapid change in new knowledge in every domain of knowledge, it is rare to produce new knowledge or findings through individual efforts, therefore collaboration becomes necessary. In the field of Biotechnology, changes are so rapid that some of the developments cannot be imagined without the help of the industrial partners. Collaboration also occurs when a group or organization with the least research facility approaches the larger groups or well-established laboratories with greater research facilities. However, the major objective of research collaboration is to improve research quality by utilizing the research expertise in the field. In a field like Biotechnology, collaboration is required to meet the global challenges. New information and emerging technologies have created newer subdomains in the field of Biotechnology which is not possible for a single organization or research group to work upon.The field of Biotechnology is becoming wide and wide every year. From tissue culture to gene editing falls under the broad category of Biotechnology. In recent times PCR has been gain popularity in order to test the presence of Coronavirus. The application of PCR is an excellent example of research and innovation in the field of biotechnology. Especially in 21st-century research in life sciences and Biotechnology has made tremendous progress and innovations and major breakthrough have become continuous and its frequency is rising day by day leading to bioeconomy. There are many modes of collaboration

but collaboration identified through co-authorship has been studied by several researchers in detail. Zhao et al (2016)[1] studied characteristics of research collaboration in Biotechnology in China by analysing the publications indexed in SCIE. Patra and Chand (2005) [2]analysed the Biotechnology research profile of India. Payumo & Sutton (2015) [3] assessed collaboration among ASEAN countries in plant biotechnology. Earlier Pathak & Prasanna (2019) [4]analysed the international collaboration in Pharmaceutical Sciences for the period 2014-2018 and concluded that further study with a longer time range should be studied for wider insight. Garg *et al*[5], Basu and Kumar[6], Prakasan *et al*[7], Gupta and Dhawan[8], and Raina *et al*[9] used the Web of science to investigate collaboration patterns of Indian science. Pathak & Bharti[10,11] analysed the Indian Journal of Traditional knowledge and Botanical Survey of India output using the Web of Science as source of data.

Materials and Methods

Data for this study was retrieved from Web of Science-core Collection Database using advance search. Keyword Biotechnology was used in Research Area Category for the year range1945-2021. From the countries section India was selected and document types were restricted to Articles and Review. Retracted publications were excluded from the study. In this way 33226 results were retrieved. For further analysis, the publications which have India and any other countries in the address were selected exclusively. Collaboration was determined through co-authorship by the address given in the database.

Results and Discussion

The first publication in international collaboration appeared in the year 1973 and there were only 92 publications in collaboration with foreign countries upto the year 1990. In the next decades i.e. during 1991-2000 there was a significant increase in the number of publications in international collaboration. There were 395 publications during this period. There were 1300 publications during 2001-2010 which is more than 3 times from previous decades. The recent most years have witnessed the highest number of publications in association with foreign collaborators by Indian scholars in the field of biotechnology. 73% of total publications in international collaboration i.e. 4664 publications appeared during 2011-2021 which is evident that there is exponential decadal growth in international collaboration in the field of biotechnology. Figure 1 highlights the yearwise growth of publications in the field of biotechnology from India in international collaboration.

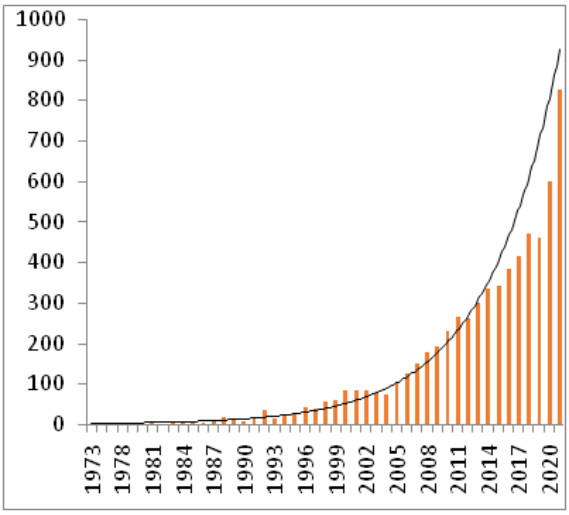

Figure-1: Year-wise growth of publications

There are 240 source titles or journals in which these 6451 research documents were published. There is 11 journals that published 100 or more research outputs by Indian authors in collaboration with International counterparts and contributes 2274 of 6451 publications. 50 % of the total publications were published in 23 journals. Table 1 enlist the list of productive journals with more than 100 publications Bioresource technology is the most productive journal which published 649 publications which are 10% of the total publications, followed by 3 biotech, with 219 publications Biomed research international with 212 publications There are 46 journals which published only one article. Thirteen journals pub-

lished 2 articles each. Eight journals published 3 articles each. Seventeen journals published 4 articles each.

Analysis of Productive authors suggests that Ashok Pandey from CSIR Indian institute of Toxicological research is the most productive author followed by Rajesh J Banu from the Central University of Tamil Nadu with 73 publications, Sunita Varjani from Gujarat Pollution Control Board with 41 publications, Raveendran Sindhu from TKM Institute of Technology Kollam Kerala with 37 publications and Hosakatte Niranjana Murthy, Karnataka University with 35 publications (Table 2). Among the authors from foreign countries, Rajeev K Varshney with 63 publications from Murdoch University is the most preferred author for collaboration by Indian Scientist, followed by Arivalagan Pugazhendhi from Ton Duc Thang University with 58 publications.

Among the organizations, CSIR India is the most productive organization with 844 publications is the most productive organizations followed by the Indian Institute of Technologies with 641 publications, the Indian Council of Agricultural Research with 372 publications, DBT India with 261 publications, the University of Delhi with 143 publications. Other productive organizations include Anna University, Banaras Hindu University, NIT, and Andhra University. Among the foreign organizations, King Saud University of Saudi Arabia is the most preferred organization with 202 publications followed by CGIAR with 173 publications, and ICRISAT with 140 publications respectively (Table 3, Figure 2).Table 4 enlists of the list of most preferred countries for collaboration by Indian researchers in the field of biotechnology. The USA with 1686 publications is the most preferred country for collaboration followed by South Korea 881publications, the Peoples Republic of China 509 publications, Germany 467 publications, and Saudi Arabia 450 publications. There are 130 countries that arein collaboration with India. Sixteen 16 countries have only one publication in collaboration with India which includes Afghanistan, Namibia, Hongkong, Zimbabwe, etc. 73 countries/regions have more than 10 publications each in collaboration with India. 25 countries have 100 or more publications in collaboration with India. The top four countries in collaboration with India have published ~55 % of the total publication in collaboration worldwideTable 5 highlights the most highly cited publications. It includes publications with more than 950 citations. There are six publications that have received more than 1000 citations. It is often opined that publications in international collaboration receive higher citations in comparison to publications not in collaboration. Publication entitled 1792 Nano based drug delivery systems: recent developments and future prospects by Patra et al published in Journal of Nanobiotechnology have received highest number of citations i.e 1792 followed by 1398 Microbial decolorization of textile-dye-containing effluents: A review by Banat et al published in Bioresource Technology with 1398 citations, 1379 Organic and inorganic contaminants removal from water with biochar, a renewable, low cost and sustainable adsorbent - A critical review by Mohan et al in Bioresource Technology with 1379 citations, 1231 Biomaterials based on chitin and chitosan in wound dressing applications by Jayakumar et al published in Biotechnology Advances with 1231 citations, 1201 Synthesis of metallic nanoparticles using plant extracts by Mittal et al in Biotechnology Ad-

Table 1: list of productive journals with more than 100 publications

Publication Titles	Record Count
Bioresource Technology	649
3 Biotech	219
Biomed Research International	212
Applied Biochemistry And Biotechnology	194
Process Biochemistry	175
Applied Microbiology And Biotechnology	156
Biosensors Bioelectronics	151
World Journal of Microbiology Biotechnology	142
Environmental Technology Innovation	133
Bmc Genomics	126
Human Vaccines Immunotherapeutics	117

Table 2: Authors from foreign countries

Total Citations	Title	Authors	Source Title
1792	Nano based drug delivery systems: recent developments and future prospects	Patra et al	Journal of Nanobiotechnology, 2018,16 -
1398	Microbial decolorization of textile-dye-containing effluents: A review	Banat et al	Bioresource Technology, 1996,58 217-227
1379	Organic and inorganic contaminants removal from water with biochar, a renewable, low cost and sustainable adsorbent - A critical review	Mohan et al	Bioresource Technology, 2014,160 191-202
1231	Biomaterials based on chitin and chitosan in wound dressing applications	Jayakumar et al	Biotechnology Advances, 2011,29 322-337
1201	Synthesis of metallic nanoparticles using plant extracts	Mittal et al	Biotechnology Advances, 2013,31 346-356
1063	Potential commercial applications of microbial surfactants	Banat et al	Applied Microbiology And Biotechnology, 2000, 53 495-508
965	Bacterial alkaline proteases: molecular approaches and industrial applications	Gupta et al	Applied Microbiology And Biotechnology, 2002,59 15-32
987	Photocatalytic degradation for environmental applications - a review	Bhatkhande et al	Journal of Chemical Technology And Biotechnology, 2002,77 102-116
972	Production, purification, characterization, and applications of lipases	Sharma et al	Biotechnology Advances, 2001,19 627-662
965	Mechanism of Salinity Tolerance in Plants: Physiological, Biochemical, and Molecular Characterization	Gupta& Huang	International Journal of Genomics, 2014,2014 -

Table 3: Authors from India

Authors	Affiliations	Publications
Ashok Pandey	Indian Instittue of Toxicological Research	154
Rajesh J Banu	Central University of Tamil Nadu	73
Sunita Varjani	Gujarat Pollution Control Board	41
Raveendran Sindhu	TKM Institute of Technology Kollam Kerala	37
Hosakatte Niranjana Murthy	Karnataka University	35

Table 4: Collaboration by Indian researchers

Affiliations	Publications
Council of Scientific and Industrial research	844
IIT system	641
Indian Council of Agricultural Research	372
DBT India	261
Delhi University	143

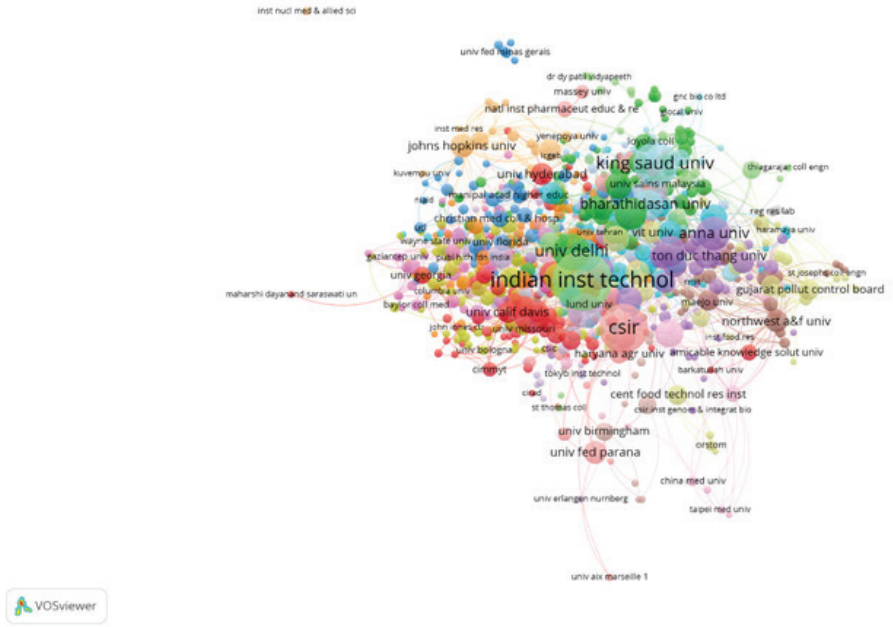

Figure 2: Co-authorship network of Organizations

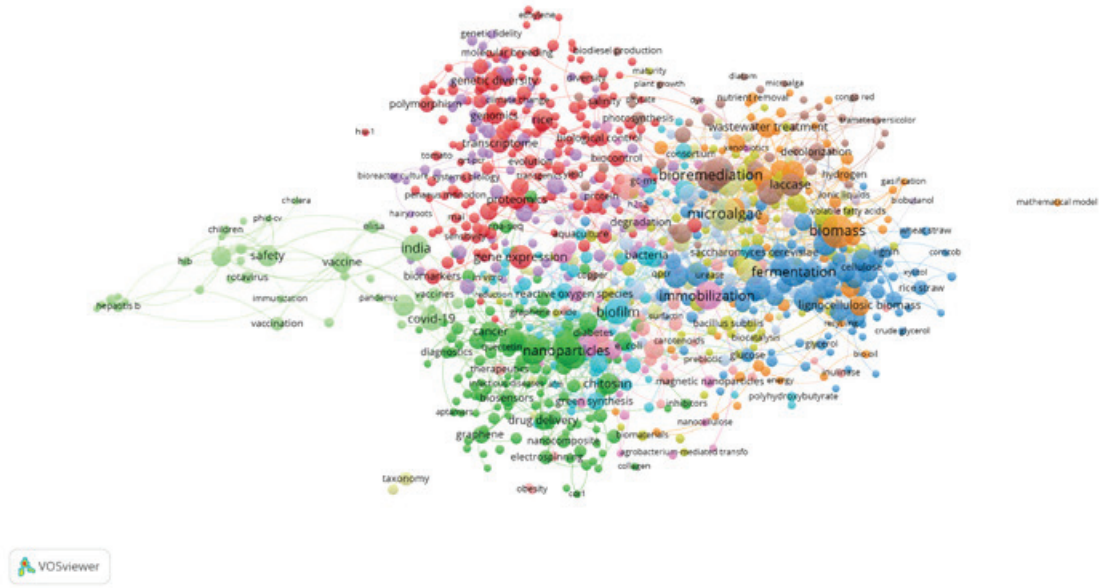

Figure 3: Keyword network

India's international collaboration in biotechnology

Table 5: Most highly cited publications

Countries/Regions	Record Count
USA	1686
South Korea	881
Peoples R China	509
Germany	467
Saudi Arabia	450
United Kingdom	404
Australia	402
Japan	347
Canada	279
France	258
Malaysia	219

vances with 1201 citations and 1063 Potential commercial applications of microbial surfactants by Banat et al published in Applied Microbiology And Biotechnology with 1063 citations are the most cited publications.

Analysis of keywords reveal that there are 853 total keywords provided by authors in these 6451 publications. Microalgae with 82 occurrences is the most frequent keyword provided by biomass with 81 occurrence, bioremediation with 74 occurrence, nanoparticles with 66 occurrence and biodegradation with 65 occurrences are the top 5 keywords on the basis of frequency. Figure 3 highlights the Keyword network.

Conclusion

It can be concluded that in recent decade international collaboration in Biotechnology has grown multi- fold and has shown exponential growth in terms of publications and citations. However, most of the contributing organizations are centrally funded Institutes. Some central universities have also been identified as a major contributor in Biotechnology research but state universities are lagging in collaboration. This may also happen because in state university researchers might not be aware of publishing their research in non-indexing journals. Publications in collaboration have been communicated in journals of high repute this also played a significant role in receiving a higher citation rates. This is only a preliminary investigation of international collaboration in Biotechnology from Indian scholars, more extensive study is required at the micro level to know the characteristics of international collaboration in Biotechnology. Comparative studies of similar countries or groups of countries may also be carried out to find greater insights.

References

1 Yong Zhao, Dong Li, Mingjie Han, Chenying Li & Dongmei Li, Characteristics of research collaboration in biotechnology in China: evidence from publications indexed in the SCIE. Scientometrics (2016) 107:1373–1387 DOI 10.1007/s11192-016-1898-1

2 Patrs SK & Chand Prakash, Biotechnology research profile of India, Scientometrics Vol. 63, No. 3 (2005) 583ñ597

3 Payumo JG & Sutton TC, A bibliometric assessment of ASEAN collaboration in plant biotechnology, Scientometrics (2015) 103:1043–1059 3–1059 DOI 10.1007/s11192-015-1582-x

4 Pathak Manohar & NK Prasanna, India's International Collaboration in Pharmaceutical Research Journal of Scientific & Industrial Research, 2019,78 ,738-741.

5 Garg K C, Kumar Suresh &Bebi, Collaboration Patterns of Indian Scientists in Organic Chemistry, *Curr Sci*, 114(2018) 1174-1180

6 Basu A &Vinu Kumar B S, International collaboration in Indian scientific paper, *Scientometrics*, 48 (2000) 381-402

7 Prakasan E R, Mohan Lalit, Girap Priya, Ganesh Surwase, Kademani B S & K Bhanumurthy, Scientometric facts on international collaborative Indian publications, *Curr Sci,* 106 (2014) 166-169

8 Gupta B M, Munshi U M & Mishra P K, S&T collaboration of India with other South Asian countries, *Curr Sci*,

83 (2002) 1201-1209

9 Raina Dhruv, Gupta B M & Kandhari Rohit,Collaboration in Indian physics: A case study of the macro and micro parametrization of sub-disciplines (1800–1950), *Scientometrics*, 33(1995) 295-314

10 Pathak M & Bharati KA, Botanical Survey of India (1971–2010): a scientometric analysis, *Curr Sci*, 107 (2014) 964-971

11 Pathak M & Bharati KA, Growing visibility and impact of Indian Journal of Traditional Knowledge, *Indian J Tradit Know* 17 (2018) 407-413

Current Trends in Biotechnology and Pharmacy
Vol. 16 (4) 518 - 528, Oct 2022, ISSN 0973-8916 (Print), 2230-7303 (Online)
10.5530/ctbp.2022.4.85

Evaluation of *In-vitro* Anticancer Effect of Hydroalcoholic Extract of Lepidagathis spinosa Wight Ex Nees.

Sutha Ponnusamy[1], Sangameswaran Balakrishnan[2]

[1]The Tamil Nadu Dr M.G.R Medical University, Guindy, Chennai-600032, Tamil Nadu, India.
[2]Department of Pharmacognosy, SSM College of Pharmacy, Erode- 638312, Tamil Nadu,
*Corresponding author: suthaharini3186@gmail.com

Abstract

People, for the most part in rustic environments and lately, those unsatisfied with usual medicine, use medicinal plants for their therapeutic effects.This ongoing study deals with the *in vitro* antioxidant and anticancer activity of hydroalcoholic extract of *L.spinosa* wight Ex Nees*.,* (*L.spinosa*) is a herb in the equatorial zone of Asia belonging to the family Acanthaceae. Total phenolic and flavonoid content was dogged**.** Antioxidant activity was valued by total antioxidant capacity, DPPH assay. By using MTT assay cell feasibility of total cell lines such as Rat skeletal muscle cell line (L6), Ehrlich Ascites Carcinoma (EAC), Human Breast cancer cells (MCF 7), Human Cervical cells (He La) and Human Hepatocellular carcinoma cell lines (Hep G2) were dignified against various doses of extracts. Isolate the active compound by using chromatographic performance. Hydroalcoholic extract of *L.spinosa* exposed more powerful activity against EAC & Hep G2 cell lines but average activity against MCF 7 & He La cell lines. The anticancer and antioxidant nature of the hydroalcoholic extract is due to the occurrence of numerous secondary metabolites like phenolic compounds, flavonoids, terpenoids, alkaloids, etc. The results obviously exposed the hydroalcoholic extract of *L.spinosa* as a good antioxidant with a significant anti-cancer effect.

Keywords*: L.spinosa*, Antioxidant, Anticancer, MTT assay, Compound isolation.

Introduction

Cancer is an important worldwide health problem commonly due to the absence of widespread and comprehensive primary detection methods, the related poor prognosis of patients diagnosed in later stages of the disease, and its increasing occurrence on a global scale. Definitely, the struggle to combat cancer is one of the greatest tasks of mankind(1).Almost 70% of deaths from cancer happen in low and middle-income countries. Opportunities to diminish the death rate from cancer through the finding of new drugs are benefiting from the advances in technology and knowledge on neoplastic disease (2).Recently, innovative methods of treating oncological diseases have appeared (nanotherapy, neutron capture, and low-intensity electroresonance therapy, and also, old methods are used – chemotherapy, radiation therapy, and surgery. Though, all of the overhead methods go with a number of side effects, which also negatively affect the patient's health(3). The present research and development personalized towards the detection of new antiproliferative agents from natural products have been buoyed by upgrading the science and technology of anticancer drug discovery. Antitumor drugs have also been linked with change of secondary malignancy(4).

According to the World Health

Organization (WHO), several countries, as well as developing countries, still use plants and natural source–associated products for therapeutic purposes. About 60% of anticancer agents have been initiated from natural sources globally. The nature-derived compounds are freely available, frequently more tolerated, and considered non-toxic to normal human cells (5). Various natural compounds such as terpenoids, alkaloids, lignans, tannins, quinones, phenolic acids, coumarins, and flavonoids have been initiated from plant sources that have major antioxidant activity and play a main part in the therapy of cancer. A number of studies have shown that antioxidant compounds demonstrate anti-inflammatory and ant carcinogenic activity. Natural antioxidant compounds can directly avoid the proliferation of cells and enhance the immune system (6). The development of cancer drugs from plant materials and their use in experimental practice is still a vital task. The occurrence of the above activities certifies the use of the inhibition and treatment of different cancer types such as skin, lung, stomach, liver, breast, prostate, and cervix cancers.

At present, more than 3,000 plants globally have anticancer properties. From the scientific perspective, the search for knowledge of the anticancer herbal raw materials is not new, on the other hand for the correct user, detailed phytochemical and pharmacological studies are forever essential (3). The ultimate aim of the study is to discover the antioxidant, cytotoxic activity of crude extract and the separation of the active constituent of hydroalcoholic extract of *L.spinosa* whole plant.

Materials and Methods

Plant collection and verification: The established and healthy whole plant of *L.spinosa* was collected from Tirunelveli district. The specimen was verified by

Dr.V.Chelladurai,M.Sc., Ph.D.,

Research Officer-Botany, Central Council for Research in Ayurveda & Siddha, Govt. of India. Tirunelveli, Tamil Nadu. In our college museum, the specimen has been placed.

Preparation of crude extracts: *L.spinosa* whole plant was collected and washed carefully. It was dried out in the air and sliced into small parts. Around 1 kg of dried entire plant *L. spinosa* was extracted in soxhlet consecutively with increasing polarity of solvents [petroleum ether (PE), chloroform (CH), ethyl acetate (EA), hydroalcohol (HA)]. All the extracts were evaporated using rotary vacuum evaporator. The whole thing was weighed and deposited for further use. All the used solvents were of analytical grade.

Preliminary phytochemical analysis of L.spinosa: Extracts were checked for the presence of phytochemicals with the standard procedure as defined in the textbook by Harborne A J (7).

Determination of total flavonoid content: Entire flavonoid content was analyzed via the aluminium chloride colorimetric technique(8).

Determination of total phenolic content: The phenolic content was assessed by Gallic acid equivalents (GAE/g) of dry plant material on the base of a standard curve of Gallic acid (2 - 64µg/mL) (8,9,10).

Antioxidant activity of crude extracts of Lepidagathis spinosa

Total antioxidant assay: The total antioxidant capacity of the test samples (PE,CH, EA, HA) was valued spectrophotometrically by the phosphomolybdenum method (11). Addition of 0.5 mL of extracts with 3 mL of reagent solution, incubated at 95°C for 90 min. After cooling, absorbance was measured at 695 nm by using a UV-Visible spectrophotometer against blank. The total antioxidant capacity is stated as the number of grams equivalent to ascorbic acid. Prepare the calibration curve by mixing ascorbic acid (10 – 80 µg/mL) with ethanol (12).

DPPH antioxidant assay DPPH antioxidant estimation is based on the capacity of antioxidants to decolorize 1, 1-diphenyl-2-picryl-hydrazyl. 0.135 mM DPPH was prepared in methanol. Various concentrations of test samples were mixed with 2.5 ml of DPPH solution. The absorbance of these solutions was measured at 517 nm and ascorbic acid as standard(13).

The capability of test samples to scavenge DPPH radical and control was calculated from the following formula:

% DPPH inhibition = [(OD of control - OD of test)/(OD of control)]×100

Preparation of test solution For MTT assay, serial two fold dilutions (3.125-50µg) were prepared from this assay.

Cell lines and culture medium Cell lines used for cytotoxicity screening were Rat skeletal muscle cell line (L6), Ehrlich's Ascites Carcinoma cell line (EAC), Human cervical cell line (He La), Human Breast cancer cells (MCF 7), and human hepatocellular carcinoma cells (Hep G2), and the cell lines acquired from National Centre for Cell Science (NCCS), Pune, India. Stock cell lines were cultured in a medium added with 10% inactivated New born calf serum, penicillin (100 IU/ml), and streptomycin (100 µg/ml) in a moistened atmosphere of 5% CO_2 at 37°C till confluent.

Procedure By using MTT assay measure cytotoxicity (loss of viable cells). This assay is founded on the metabolic reduction of the soluble MTT salt, 3-(4,5-dimethylthiazol-2-yl)-2,5-diphenyltetrazolium bromide which reflects the normal function of mitochondria dehydrogenase activity and cell viability, into an insoluble colored formazan product, which was measured spectrophotometrically. The activity of mitochondrial dehydrogenase of living cells rightly and proportionately represents the number of viable cells(14).

100µl of cell suspension of density 1 × 10^4 cells/well was positioned into each well of 96-well plates and incubated for 24h. After 24h, when a part of monolayer was formed, the supernatant was flicked off, with the help of a medium the monolayer was washed, add 100µl of different concentrations of test sample onto the partial monolayer in microtiter plates. Incubate the plate at 37°C for 24h in a 5% CO_2 atmosphere. After incubation, the test solutions in the wells were discarded and 100µl of MTT (1mg/ml of MTT in PBS) was added to each well. The plate was incubated for 4h at 37°C in a 5% CO_2 atmosphere. The supernatant was removed instead of that add 100µl of DMSO, the plate was gently shaken to solubilize the formed formazan. The absorbance was measured by means of a microplate reader at a wavelength of 570 nm (4,6).

The percentage of viability was calculated using the following formula:

% of viability = Sample abs/Control abs x 100

Where

Abs= Absorbance value

Isolation of active constituents Methanol used to dissolve the plant extract and adsorbed in silica gel 60 – 120. Evaporate the solvent, which was loaded into a silica gel column (100 – 200 mesh size), prepared in hexane. Elute the column with hexane followed by gradually increasing polarity with Hexane, Chloroform, Ethyl acetate, and Methanol. Absolutely 106 fractions were collected and examined under TLC. Related fractions were combined and the solvent was evaporated under reduced pressure. The resultant crude materials were refined by using activated charcoal in hot ethanol and crystallize the fractions (15). The acquired solid was submitted for Melting point, Mass spectra, FT-IR spectra, ^{13}C-NMR, and ^{1}H-NMR analysis.

Results and Discussion

Preliminary phytochemical studies of hydroalcoholic extract proven the presence of flavonoids, alkaloids, tannins, saponins, triterpenoids, and phenols, etc. Flavonoids, tannins, saponins and triterpenes have all been stated to possess antitumor activity (16,17,18,19). Flavonoids anticancer action has been connected with several mechanisms such as the variation of cell cycle arrest at the G1/S phase, Initiation of cyclin-dependent kinase inhibitors, anti-apoptotic gene downregulation, cell-survival kinase inhibition and inhibition of inflammatory transcription factors, and generation of Ca2+dependent apoptotic mechanism (20).

Results of the study presented that the phenolic compound of the tested extracts (PE, CH , EA, HA) differ from 5.62 to 33.53 GAE/g . Utmost phenolic compounds was identified in hydroalcoholic extract of *L.spinosa* at a 33.53 GAE/g. The amount of total flavonoid compounds was determined as the quercetin equivalent using an equation obtained from a standard quercetin graph (y = 0.003x + 0.2161, R^2 = 0.9709). The flavonoid content of the extracts varied from 0.74 to 19.63mgof quercetin. As shown in Table 1, excellent flavonoid content was found in the hydroalcoholic extract of

Table 1: Quantitative estimation of phytoconstituents present in various extracts of *Lepidagathis spinosa* wight ex Nees

Extract	Total phenol content (mg of GAE/gm of the plant extract)	Total flavonoids content (mg of QE/g of the plant extract)
LSPE	5.623188	0.744444
LSCH	14.25673	3.077778
LSEA	15.49896	6.744444
LSHA	33.53209	19.63333

Table:2 *Invitro* antioxidant activity of various extracts of*L.spinosa wight* ex Nees, whole plant

Extract	DPPH IC_{50} value	Total antioxidant capacity (mg/g)
LSPE	>320	4.03
LSCH	>320	16.23
LSEA	>320	21.73
LSHA	262.02	24.9

Table No:3. Assessment of cytotoxicity and cell viability for Hydroalcoholic extract of Lepidagathis spinosa whole plant on L6 cell line with MTT assay

S.No	Conc. (µg/ml)	% cell viability	% Cytotoxicity	IC_{50} Value (µg/ml)
	Control	100	0	>100
	3.125	98.772±007	1.228±0.024	
	6.25	97.299±005	2.711±0.032	
	12.5	94.879±0.004	5.120±0.048	
	25	91.898±0.005	8.120±0.039	
	50	87.969±0.006	12.030±0.059	

Table No:4 Assessment of cytotoxicity and cell viability for Hydroalcoholic extract of Lepidagathis spinosa whole plant on EAC cell line

S.No	Conc.(µg/ml)	% cell viability	% Cytotoxicity	IC_{50} Value (µg/ml)
1	Control	100	0	28.95
2	3.125	95.96±0.017	4.01±0.038	
3	6.25	82.92±0.012	17.08±0.025	
4	12.5	70.63±0.028	29.37±0.068	
5	25	56.54±0.009	43.46±0.083	
6	50	34.16±0.042	65.84±0.076	

Table No:5. Assessment of cytotoxicity and cell viability for Hydroalcoholic extract of Lepidagathis spinosa whole plant on MCF7 cell line using MTT assay

S.No	Conc.(µg/ml)	% cell viability	% Cytotoxicity	IC_{50} Value (µg/ml)
	Control	100	0	41.44
	3.125	95.28±0.011	4.72±0.058	
	6.25	86.92±0.012	13.08±0.045	
	12.5	71.50±0.012	28.50±0.028	
	25	63.75±0.006	36.25±0.059	
	50	42.458±0.006	57.54±0.072	

Table No:6. Assessment of cytotoxicity and cell viability for Hydroalcoholic extract of Lepidagathis spinosa whole plant on HEPG2 cell line

S.No	Conc.(µg/ml)	% cell viability	% Cytotoxicity	IC_{50} Value (µg/ml)
	Control	100	0	39.73
	3.125	96.168±0.0226	3.832±0.074	
	6.25	87.151±0.0226	12.849±0.026	
	12.5	76.201±0.0411	23.799±0.037	
	25	61.899±0.0133	38.101±0.014	
	50	41.173±0.0181	58.827±0.060	

Table No:7. Assessment of cytotoxicity and cell viability for Hydroalcoholic extract of Lepidagathis spinosa whole plant on HeLa cell

S.No	Conc.(µg/ml)	% cell viability	% Cytotoxicity	IC_{50} Value (µg/ml)
	Control	100	0	64.63
	3.125	98.208±0.00961	1.792±0.064	
	6.25	94.560±0.0106	5.44±0.088	
	12.5	80.424±0.009	19.576±0.032	
	25	65.196±0.008	34.804±0.046	
6.	50	53.266±0.0186	46.734±0.079	

L.spinosa.

In general, the phenolic content of the hydroalcoholic extract was extensively high, which could be a most important contributing factor to the strong antioxidant activity. Phenolic components are potential antioxidants and free radical terminators. They might decrease the risk of cardiovascular disease, and protect against urinary tract infections and cancer. They are also assumed to have an inhibitory effect on carcinogenesis. Flavonoids as one of the greatest and well-known groups of natural compounds are undoubtedly the most important natural phenolics. Phenolic compounds and flavonoids have a broad spectrum of chemical and biological actions, associated with antioxidative action in biological systems, acting as scavengers of singlet oxygen and free radicals (20,21,22).

Total antioxidant capacity The assessment of total antioxidant contents between the different extracts was revealed. Total antioxidant capacity in the test samples (PE, CH, EA, HA) by means of the calibration curve, was found to be 4.03, 16.23, 21.73, 24.96mg/g ascorbic acid. The principle of this assay comprises the activity of an antioxidant compound which leads to the reduction of the hexavalent form of

molybdenum [Mo (VI)] to pentavalent form [Mo (V)], and the development of a green phosphate/ Mo (V) complex at acidic pH and at a higher temperature. This is spectrophotometrically measured at 695 nm (13).

DPPH assay DPPH is a constant nitrogen-centered free radical, generally intended for testing radical scavenging activity of the compound or plant extracts. The violet color of the DPPH radical was reduced to yellow-colored diphenylpicrylhydrazine radical when they accept an electron from an antioxidant compound which was measured colorimetrically. Constituents which are able to make this type of reaction can be considered antioxidants and then radical scavengers. Hydroalcoholic extract of *L.spinosa* exhibited good antioxidant activity compared to others (21). The reports were presented in table 2. In a concentration-dependent manner, DPPH scavenging was increased and compared to ascorbic acid used as the positive antioxidant control. Medium inhibitory concentration (IC_{50}) value for standard ascorbic acid was 21.06µg/ml, in plant extracts hydro alcohol extract of *Lepidagathis spinosa* (LPHA) had the lesser percentage inhibition (IC_{50}-262.02 µg/ml).)

MTT assay Hydroalcoholic extract of the whole plant of *Lepidagathis spinosa* was screened for cytotoxic properties on L6, EAC, MCF, He La and Hep G2 cells lines by MTT Assay. The hydroalcoholic extract did not expose any cytotoxicity against the normal L6 cell line. Among EAC, Hep G2, MCF 7, and He La cell lines exposed significant cytotoxicity with the IC_{50} value of 28.95 µg/ml, 39.73µg/ml, 41.44 µg/ml, and 64.63 µg/ ml. Hydroalcoholic extract shows good activity against EAC (Experimental tumor model), among the human cell lines the hydroalcoholic extract showed significant cytotoxicity against Hep G2 cell line followed by moderate activity against MCF 7, He La cell lines as shown in Tables and Figures. Flavonoids possess good antimutagenic and antimalignant result. Furthermore, they have a chemopreventive character in cancer through their effects on signal transduction in cell proliferation in addition to inhibition of neovascularization (23,24).

The hydrpalcoholic extract of *Lepidagathis spinosa* wight ex Nees., has more significant anticancer activity, it is mainly because of the phytoconstituents present in the extract. The phytochemical study revealed the presence of various phytoconstituents like flavonoids, phenolic compounds, alkaloids, triterpenoids, etc.

Compound isolation Since plant extracts normally occur as a mixture of different types of bioactive compounds or phytochemicals with different polarities, their separation remains a major challenge for the bioactive compound identification and characterization process. In isolating these bioactive compounds, it is common practice to use a variety of different separation methods, such as TLC, column chromatography, etc., to obtain pure compounds.

Figure No:1. Effect of hydroalcoholic extract of Lepidagathis spinosa whole plant on L6 cell line.

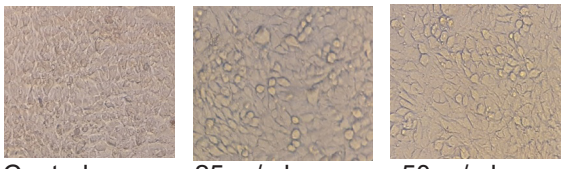

Control 25µg/ml 50µg/ml

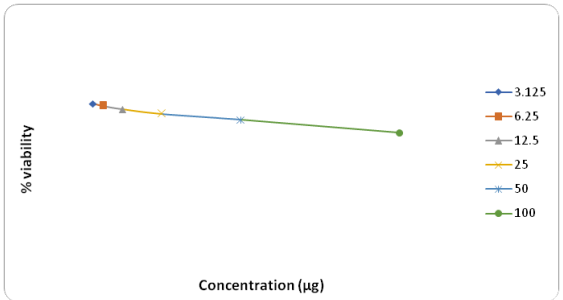

Figure No: 2. Assessment of cytotoxicity and cell viability for hydroalcoholic extract of Lepidagathis spinosa whole plant on L6 cell line

Figure No:3. Effect of hydroalcoholic extract of Lepidagathis spinosa whole plant on EAC cell line

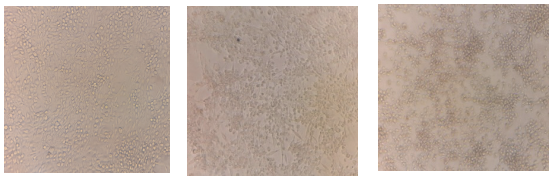

Control 25 µg/ml 50 µg/ml

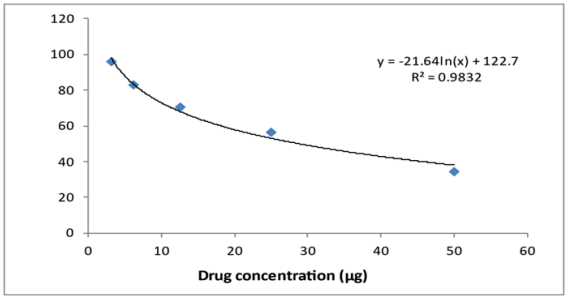

Figure No:4. Assessment of cytotoxicity and cell viability for Hydroalcoholic extract of Lepidagathis spinosa whole plant on EAC cell line

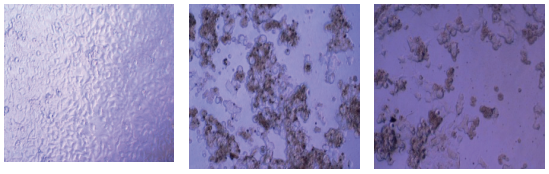

Control 25 µg/ml 50 µg/ml

Figure No:5. Effect of hydroalcoholic extract of Lepidagathis spinosa whole plant on MCF7 cell line using MTT assay

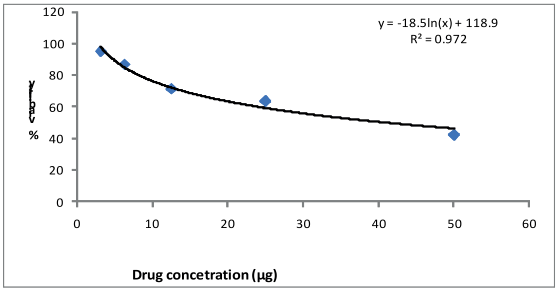

Figure No: 6. Assessment of Hydroalcoholic extract of Lepidagathis spinosa whole plant on MCF7 cell line

Figure No: 7. Effect of hydroalcoholic extract of Lepidagathis spinosa whole plant on HEPG2 cell line

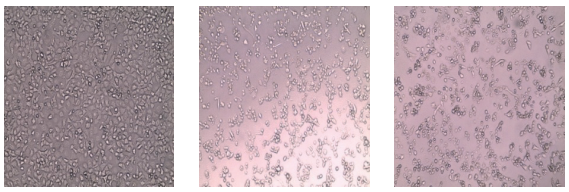

Control 25 µg/ml 50 µg/ml

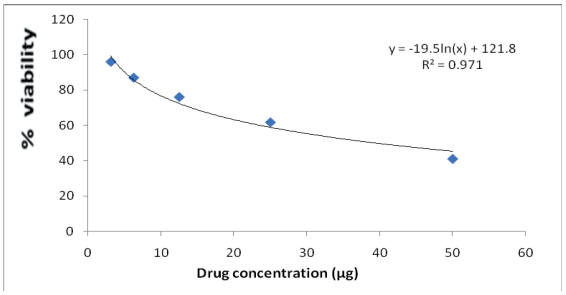

Figure No: 8. Assessment 0f cytotoxicity and cell viability of hydroalcoholic extract of Lepidagathis spinosa whole plant on HEP G2 cell line.

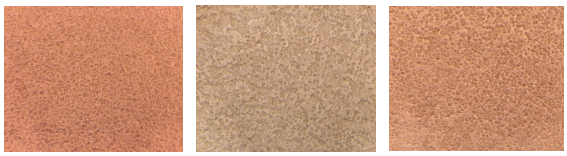

Control 25 µg/ml 50 µg/ml

Figure No: 9. Effect ofhydroalcoholic extract of Lepidagathis spinosa whole plant on HeLa cell line

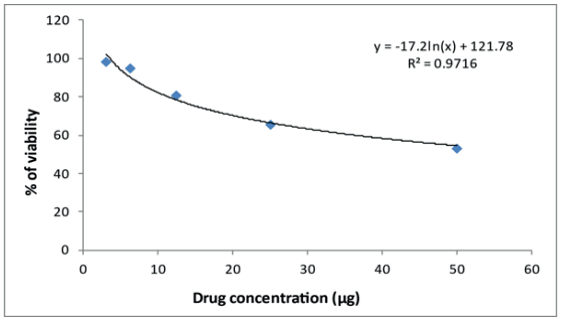

Figure No: 10 Assessment of cytotoxicity and cell viability for hydroalcoholic extract of Lepidagathis spinosa whole plant on HeLa cell line

The pure compounds are then used for structure and biological activity determination.

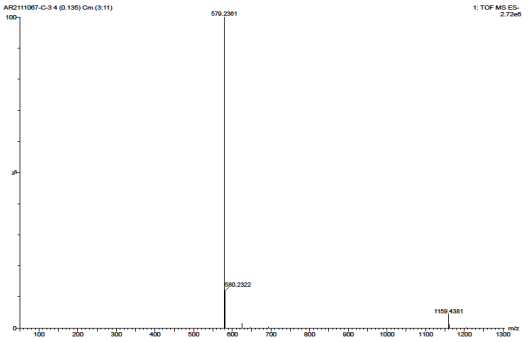

Figure No: 11 Mass spectrum of isolated compound

Fourier-transform infrared spectroscopy (FTIR) can also be used to achieve and promote the detection of bioactive compounds in addition to this phytochemical screening assay. Data from a broad range of spectroscopic techniques such as Nuclear Magnetic Resonance (NMR), Mass spectroscopy andInfrared (IR) are used to determine the structure of natural products. Spectroscopy's basic concept is to transfer electromagnetic radiation through an organic compound that absorbs some, but not all, of the radiation. A spectrum can be generated

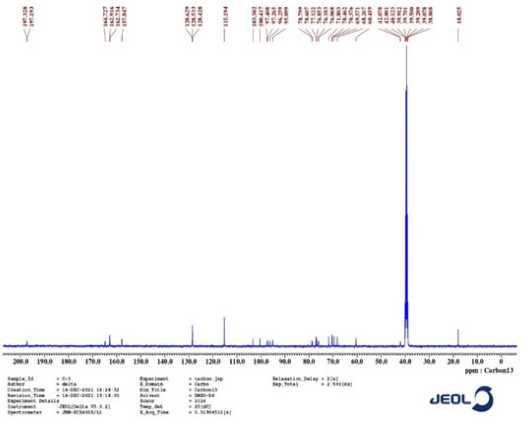

Figure No: 12 ^{13}C-NMR spectrum of isolated Compound

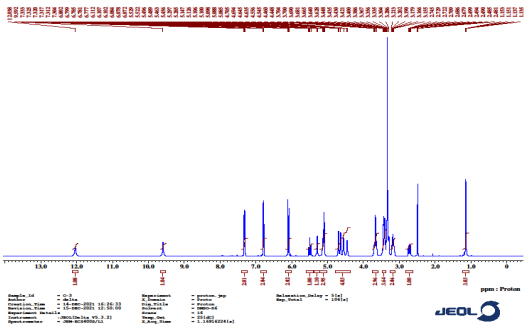

Figure No: 13 ^{1}H NMR spectrum of isolated compound

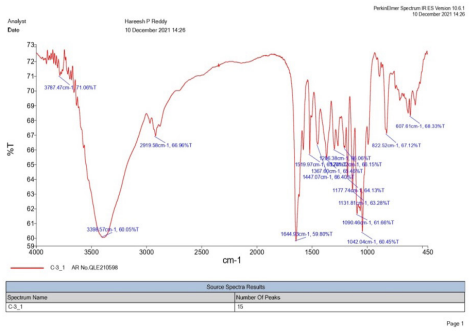

Figure No: 14 IR spectrum of isolated compound

by measuring the amount of absorption of electromagnetic radiation. The spectrum in a compound is unique to such bonds. The composition of the natural compound can be defined based on these spectrums.(24).

Pale yellow colour solid, m.p. 163 - 164 °C; C27H32O14 ;EI-MS m/z: 579.23 (M-H)-

1H-NMR (DMSO-d6): δ ppm: δ 12.03 (s, 1H, -OH), 9.59 (s, 1H, -OH), 7.30 -7.33 (m, 2H, H-2' and H6'), 6.77 – 6.80 (m, 2H, H-3' & H-5'), 6.07 – 6.11 (m, 2H, H-8 H-6), 5.45 – 5.52 (m, 1H, H-2), 5.28 – 5.29 (d, 1H, H-1'"), 5.08 – 5.14 (d, 1H, H-1"), 4.69 – 4.70 (d, 1H, Ha-6"), 4.63 – 4.64 (d, 1H, Hb-6"), 4.54 – 4.55 (d, 1H, H-5'"), 4.44 – 4.46 (d, 1H, H-5"), 3.62 – 3.71 (m,2H, H-3'", H-3"), 3.42 – 3.47 (m,2H, H-2", H-2'"), 3.15 – 3.21 (m,2H, H-4'", H-4"), 2.67 – 2.75

(m,2H, Ha-3, Hb-3), 1.13 – 1.15 (dd, 3H, CH3-6'").

13C-NMR (DMSO-d6):δ 197.32 (C-4,), 164.72 (C-7), 162.91 (C-5), 162.73 (C-9), 157.84 (C-4'), 128.62 (C-1'), 128.53, 128.42 (C-2' and C-6'), 115.19 (C-3' and C-5'), 103.30 (C-10), 100.41 (C-1"), 97.40 (C-1'"), 96.25 (C-6), 95.09 (C-8), 78.79 (C-2), 78.60 (C-2"), 77.12 (C-5"), 76.18 (C-3"), 71.80 (C-4'"), 70.46 (C-2'" and C-3'"), 69.57 (C4"), 68.26 (C-5'"), 60.41 (C-6"), 42.07 (C-3), 18.02 (C-6'").

FT-IR (KBr cm-1):3398 cm^{-1} (-OH stretching) ; 1296 cm^{-1} (-C-O bending);644 cm^{-1} (-C=O stretching); 1519 cm^{-1} (-C=C stretching); 1447 cm^{-1} (-CH bending) ; 1367 cm^{-1} (-CH bending), , 1090 cm^{-1} (-C-O stretching). 2919 cm^{-1} (-CH stretching).

The ^{1}H-NMR spectrum revealed signals at *δ* 12.03 and 9.59 showing the presence of aromatic hydroxyl group. A multiplet of protons at δ 6.11 to 7.30 were allotted to aromatic protons declaring a flavonoid ring system. Protons from 1.13 to 4.63 typical signal observed and suggesting the presence of sugar moiety.

The ^{13}C-NMR spectrum showed 27 carbons which included carbon at 164.72 and 162.91 was a characteristic of carbon attached with hydroxyl moiety. Carbon from 18.02to100.41 representing the presence of sugar moiety.

FTIR spectrum showed absorption band at wave number region 3398 cm^{-1} for the shifting vibration of hydroxyl group (OH), wavelength region of 2919 cm^{-1} was a C-H group of aromatic ring, wave length region of 1519 cm^{-1} shows the C=C bond of the aromatic ring,the wavelength region of 1447 cm^{-1} was a C-H bond in the CH_2 group, then the absorption band number in the wave length region 1367 cm^{-1} was the C-H bond of the CH_3. The wavelength region of 1090 cm^{-1} is the C-O-C bonds of the ether. Based on these data it can be estimated that the tested compound contains a hydroxy group (−OH), aromatic cyclic groups (C=C), CH_2, CH_3, and ether groups.

The molecular weight of the separated compound ascertained by high-resolution

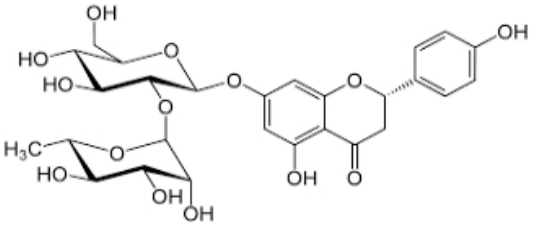

mass spectrometry and the molecular ion peak appearing at m/z 579.23 (M-1).

This pattern of the spectrum was identical with that of compound naringin [1]. The structure of compound-1 as given below

Conclusion

In the system of folk and clinical medicine of different countries, herbal plants have always been played a major role in prevention and treatment of cancer and other diseases. Hydroalcoholic extract of *Lepidagathis spinosa* has more significant anticancer activity, it is mainly because of the phytoconstituents present in it. Also, it is rich in flavonoid and phenolic content, and possess good antioxidant activity in the experimental and human cancer cell line. Using column chromatography the active compound was isolated and elucidated it is similar to Naringin. In the future, the investigation can be extended using *invivo* on a particular cell line and also need to study the mechanism of action of isolated compound.

Acknowledgments: We are grateful The Tamil Nadu Dr M.G.R Medical University,Chennai, Tamil Nadu, India for supporting this research.

Conflict of Interests: The authors state that there is no potential conflict of interest.

Reference:

1. Divisi, D., Di Tommaso,S., Salvemini, S. (2006). Diet and cancer. Acta Biomedica,

77(2): 118-123.

2. Vinod kumar Nelson, Nalini Kanta Sahoo, Madhusmita Sahu , Hari hara Sudhan. (2020). In vitro anticancer activity of Eclipta alba whole plant extract on colon cancer cell HCT-116.BMC Complementary Medicine and Therapies,20(355):2-8.

3. Olha Mykhailenko, Roman Lesyk Finiuk, Rostyslav Stoika, Tetyana Yushchenko,Anna Ocheretuiuk,Valentina Vaschuk, Volodymyr Mishchenko, Victoriya Georgiyants.(2020). Invitro anticancer activity screening of Iridaceae plant extracts. Journal of Applied Pharmaceutical Science, 10(7):059-063.

4. Abidemi, J. Akindele, Zahoor ,A. Wani, Sadhana Sharma, Girish Mahajan, Naresh, K. Satti, Olufunmilayo, O. Adeyemi, Dilip, M. Mondhe, and Ajit, K. Saxena. (2015).In vitro and in vivo anticancer activity of root extracts of Sansevieria liberica Gerome and Labroy (Agavaceae). Evidence-Based Complementary and Alternative Medicine.2015:1-11.

5. Shakirah Razali ,Al'ainaYuhainisFirus Khan , Alfi Khatib, Qamar Uddin Ahmed , Ridhwan Abdul Wahab and Zainul Amiruddin Zakaria.(2021). An In vitro anticancer activity evaluation of Neolamarckiacadamba (Roxb.) Bosser leaves' extract and its metabolite profile. Frontiers in Pharmacology,12:1-11.

6. Manoharan Dhanalakshmi, Subramaniam AnandaThangadurai.(2020).Evaluation of anticancer effect of ethanolic extract of LepidagathispungensNees., whole plant by MTT assay- An in vitro study. European Journal of Molecular & Clinical Medicine, 07(08):1027-1038.

7. Harborne, A.J. (1998). Phytochemical methods: A guide to modern techniques of plant analysis (3rd ed),Springer Science and Business Media London,pp.20-70.

8. Sushant Aryal , Manoj Kumar Baniya, Krisha Danekhu , Puspa Kunwar, Roshani Gurung, Niranjan Koirala. (2019).Total phenolic content, flavonoid content and antioxidant potential of wild vegetables from western Nepal.Plants, 8(4): 96.

9. Perumal, P., and Saravana bhavan, K.(2018). Antidiabetic and antioxidant activities of ethanolic extract of Piper betle L. leaves in catfish, Clarias gariepinus. Asian Journal of Pharmacy& Clinical Research, 11(3):194-198.

10. Elin Novia Sembiring, Berna Elya, Rani Sauriasari. (2018). Phytochemical screening, total flavonoid and total phenolic content and antioxidant activity of different parts of Caesalpinia bonduc (L.) Roxb. Pharmacognosy Journal, 10(1): 123-127.

11. Riffat Batool, Ejaz Aziz, Javed Iqbal, Hina Salahuddin, Benny Tan and SairaTabassum In vitro antioxidant and anti-cancer activities and phytochemical analysis of Commelinabenghalensis L. root extracts. Asian Pacific Journal of Tropical Biomedicine, 10(9):417-424.

12. Prieto, P., Pineda, M., Anguilar, M.(1999). Analytical Biochemistry,269: 337- 341.

13. Olorunjuwon Olugbami,J., Michael, A., Gbadegesin, Oyeronke, A., Odunola. (2015).In vitro free radical scavenging and antioxidant properties of ethanol extract of Terminalia glaucescens.Pharmacognosy Research,7(1): 49–56.

14. Sara Soltanian, Mahboubeh Sheikhbahaei, Neda Mohamadi.(2017).Cytotoxicity evaluation of methanol extracts of some medicinal plants on P19 embryonal carcinoma cells. Journal of Applied

Pharmaceutical Science,7 (07):142-149.

15. Mauricio M. Victor,JorgeM. David, Maria C.K. Sakukuma, Elivana L. França and Anna V.J. Nunes. (2017). A simple and efficient process for the extraction of naringin from grapefruit peel waste. Green Process Synthesis, 7: 524–529.

16. Chun -Lin Ye,Yu Liu,Dong -Zhi Wei. (2007). Antioxidant and anticancer activity of 3' formyl-4', 6'- dihydroxy-2'-methoxy-5'-methylchalcone and (2S)-8-formyl-5-hydroxy-7-methoxy-6- methylflavanone. Journal of Pharmacy and Pharmacology,59 (4): 553-559.

17. Ferguson, P.J., Kurowska, E.M., Freeman, D.J., Chambers, A.F. and Koropatnick, J.(2006). In vivo inhibition of growth of human tumor lines by flavonoid fractions from cranberry extract. Nutrition and Cancer,56(1): 86-94.

18. Lemeshko, V.V., Haridas, V., Quijano Perez, J.C. and Gutterman, J.U. Avicins. (2006). Natural anticancer saponins, permeabilize mitochondrial membranes. Archives of Biochemistry and Biophysics, 454(2): 114-122.

19. Roy, M.K., Kobori, M., Takenaka, M., Nakahara, K., Shinmoto, H., Isobe, S. and Tsushida, T.(2006). Antiproliferative effect on human cancer cell lines after treatement with nimbolide extracted from an edible part of the Neem tree (Azadirachta indica). Phytotherapy Research, 21(3): 245-250.

20. Ashafa, A. O. T., Grierson ,D. S., Afolayan ,A. J. (2010). In vitro antioxidant activity of extracts from the leaves of Felicia muricata thunb. An underutilized medicinal plant in the eastern cape province, South Africa. African Journalof Traditional Complementary and Alternative Medicine, 7(4):296-302.

21. Marijana Kosanic, Branislav Rankovic, Jelena Vukojevic.(2011).Antioxidant properties of some lichen specie. Journal of Food Science and Technology, 48(5):584–590.

22. Vadivukkarasi Sasikumar and Pavithra Kalaisezhiyen.(2015). Evaluation of free radical scavenging activity of various leaf extracts from Kedrostis foetidissima (Jacq.) Cogn., Food Science and Human Wellness,4(1): 42-46.

23. Ludmila, G., Korkina,Igor, B. Afanas'Ev. (1996).Antioxidant and Chelating Properties of Flavonoids. Advances in Pharmacology,38:151-163.

24. Fazlul, H. Sarkar, Yiwei Li. (2004). Cell signaling pathways altered by natural chemopreventive agents. Mutation Research, 555(1-2): 53–64.

25. Rajendran Raja Priya, Nawas Bhaduhsha, Veramuthu Manivannan, Thanthoni Gunasekaran. (2020).Extraction and isolation of bioactive compounds from a therapeutic medicinal plant – Sennaalata (l.) roxb. PalArch's Journal of Archaeology of Egypt/Egyptology, 17(12): 1569-1577.

Current Trends in Biotechnology and Pharmacy
Vol. 16 (4) 529 - 539, Oct 2022, ISSN 0973-8916 (Print), 2230-7303 (Online)
10.5530/ctbp.2022.4.86

In-Silico Investigation of Plant-Derived Natural Allosteric Compounds Towards Enhanced Drug-Protein Interaction of MOA Protein Complex in Depression Based on Molecular Docking and Molecular Dynamic Simulation Approaches

Abhimanyu[1+] , Poornima Srivastava[1+],Chakresh Kumar Jain[1*],

[1]Department of Biotechnology, Jaypee Institute of Information Technology, A-10, Sector -62 NOIDA, India, 201307.

*Corresponding author :ckj522@yahoo.com

Abstract

Allostery is an effective method of controlling the function of biological macromolecules and currently gaining more attention in the realm of drug development due to the unique characteristics of allosteric modulators, such as good selectivity and low toxicity. These qualities are critical for both the creation of the allosteric concept and the evaluation of allosteric interactions. Primarily, allosteric modulators are responsible for boosting efficacy and reducing the drug's catastrophic effects. Since the chemical compounds have always proven to cause side effects in the body. Hence, the discovery of an alternative natural allosteric compound instead of chemical allosteric compounds for enhancement of drug efficacy and regulating drug dosage is the major challenge in modern drug discovery, especially for diseases *i.e.,* cancer, Parkinson's, mental disorder, etc. where the long-term treatments are recommended. In this research paper *in-silico* based comparative interaction/molecular docking and dynamics study of FDA-approved Antidepressant drugs i.e., isocarboxazid Phenelzine, Selegiline, Tranylcypromine, etc with potential drug target protein [PDB ID: 2Z5X] MAO enzymes for major depressive disorder have been conducted. Various drug compounds complexed with protein have been analyzed by performing molecular docking. The site-directed docking /interaction energy for the Isocarboxazid drug complexed with protein target was performed with a docking score -8.6 kcal/mol using Autodockvina. The chemical allosteric compound (ID ASD01720151,) was retrieved from the Allosteric database (ASD) through virtual screening and docked at the predicted allosteric site by PASSER computational tool where the best docking/ interaction energy was found -11.8 kcal/mol. The final site-directed docking was performed on the complex (target protein-natural allosteric compound) with Isocarboxazid drug and the interaction energy was found better i.e., -8.7 kcal/mol. Finally, the simulation performed which reveals the stability of the final docked structure and supports the usage of the natural compound as an alternative allosteric compound for enhancement of drug binding. The work can be extended with wet lab-based experimentation for better understanding and validation

Keywords: Allosteric compound, Molecular docking, Homaline, Major Depressive Disorder, Molecular dynamic simulations

Introduction

Evolution has endowed organisms with intricate molecular mechanism networks that enable very effective reactions to environmental changes over billions of years. The majority of these processes rely on structure-switching biomolecules that change conformation in response to the stimulus.

Allostery is one of the most significant naturally occurring ways in which a stimulus causes the target biomolecule's structural alterations and functional modulation (1). Noncovalent events such as ion, small molecule, ribonucleic acid (RNA), deoxyribonucleic acid (DNA), or protein binding (2, 3, 4); covalent events such as phosphorylation, glycation,Rossetti, Marianna, and Alessandro Porchetta. "Allosterically regulated DNA-based switches: From design to bioanalytical applications." Analyticachimicaacta 1012 (2018): 30-41. nitration (5, 6, 7, 8) and light absorption (9) cause it. The allosteric disruption (such as the binding of an effector) usually happens at a position distant from the target biomolecule's active site (10). Allostery occurs in all dynamic proteins, multimolecular assemblies, RNA and DNA polymers, and multimolecular assemblies (11). Allosteric regulation is a common method in nature for controlling cellular activities by adjusting biomolecule affinities. To govern their activity, several important proteins use allosteric regulation. The negative allosteric regulation of hemoglobin by 2,3-bisphosphoglycerate (12) is one of the best examples. Allosteric modulators might be a new kind of medicine that is both effective and safe. The capacity of an allosteric modulator to modify the substrate/receptor affinity in a very predictable manner is one of its key advantages. As a result, large dosages of allosteric modulators can be given with minimal risk of harm dependent on the target (13). Furthermore, because the allosteric site is far from the receptor/substrate contact, allosteric modulation has no effect on the biomolecule's substrate specificity. Several effective allosteric modulators have been authorized as marketed medications by the US Food and Drug Administration (FDA) namely, Nevirapine, Maraviroc, Benzodiazepines, Cinacalcet, and more. These allosteric medications interact with important proteins such as ion channels, enzymes, and G protein-coupled receptors, among others (GPCRs) (13). Isocarboxazid is an antidepressant that is a non-selective and irreversible monoamine oxidase inhibitor known as MAOI, belonging to the hydrazine family (14). It is one of just three traditional MAOIs still accessible for therapeutic use in the treatment of depressive diseases in the United States, along with tranylcypromine and phenelzine, despite the fact that it is not as widely used as the others (15, 16). Isocarboxazidis mostly utilized to treat depression and anxiety. It is also being studied for the treatment of Parkinson's disease (17), schizophrenia, and other dementia-related conditions (18). The monoamine neurotransmitters norepinephrine, serotonin, and dopamine are elevated in the brain by isocarboxazid and other MAOIs (19). Some of the major pathways of MDD that are targeted by isocarboxazid are the Estrogen signaling pathway, Tryptophan metabolism, Folate biosynthesis, Metabolic pathways, and Serotonergic synapse (http://www.genome.ad.jp/kegg/). The (MAO) Monoamine oxidase enzymes regulate the catabolism of the biogenic trace amines and monoamine neurotransmitters as well as human behavior. The processes that control MAO, on the other hand, remain unknown. Many transcription factor proteins have been postulated to influence MAO gene transcription, although the evidence for these ideas is unclear (20). The (MAO-A, -B) Monoamine oxidases mediate and modify intracellular signal pathways that determine whether neuronal cells live or die. MAO-A has been linked to the formation of synaptic activity, neuronal architecture, and the emergence of mental diseases such as depression and antisocial-aggressive behavioral problems [21]. MAO-B is a protein that creates hydrogen peroxide and is involved in neuronal loss in neurodegenerative illnesses including Parkinson's and Alzheimer's (22). As with growing cases of depression-associated disorders, the need for efficient antidepressant drugs is increasing, and the number of young people diagnosed with depression has increased for unknown causes at this time. While environmental and genetic variables also play a significant part. Although there are some FDA-approved drugs in the market being used for treating patients with such conditions, these drugs come with devastating side effects such as hair loss, anemia, skin rashes, nausea, fatigue,

weakness, and diarrhea (23). Hence, there is an urgent need for a solution to overcome this problem and make the drug more efficient with fewer side effects.

Materials and Methods

Preparation of protein structure

The crystal structure of the human monoamine oxidase A with Harmine(2Z5X) was downloaded from the protein data bank www.rcsb.org (25). The total structure weight was 59.97 kDa while the total atom present was 4397.Complexes that were bound with protein molecules were removed and all the preprocessing of the protein structure was performed using Autodock software (version 4.2.6). Polar hydrogens were added, with no bond order, and gasteiger charges were added. After the preprocessing step, the appropriate formatting of the protein structure was formed for further analysis via autodockvina version 1.2.0 (26). Autodockvina is a command-line-based tool for performing molecular docking.

Preparation of ligand and allosteric structures

Preparation of ligand

The structure of different ligands was downloaded, after rigorous literature mining through Pubmed(https://pubmed.ncbi.nlm.nih.gov/30165565/). There were 4 ligands that were selected for further studies namely Isocarboxazid, Phenelzine, Selegiline, and Tranylcypromine.

Preparation of allosteric compound

The allosteric activators of oxidoreductase were downloaded from the allosteric database (22). ASD is a central repository that has offered complete information on allosteric control and regulation, which is available online at ASD database(24, 27). There were a total of 103 oxidoreductases available. Conversion of the allosteric compounds into suitable format was generated using open babel software (28)

Preparation of natural compounds

The activated natural compounds were taken from the Lotus natural database(29) with the Tanimoto similarity threshold score of 75. While the conversion of suitable format was generated using openbabel(28).

Identification of active site on protein

The active site prediction on the target protein was done by the castp server (30). CASTp is an online server-based prediction tool that provides resources for locating, delineating, and measuring concave surface regions on the 3d structure of the protein.

Identification of allosteric site on protein

The allosteric site was predicted on the target protein via passerCLI(31) which is a command-line interface-based package available on GitHub. It is a package based on the ensemble learning technique, consisting of a convolutional neural network and extreme gradient boosting. the algorithm used in identifying the allosteric site is FPocket algorithm

Molecular docking and its analysis

Molecular docking of protein-ligand was performed using the software autodock with center coordinate (X,Y,Z [A^0] = 38.8781, 26.2673, -19.7061) and center coordinates (31.3540, 35.3858, 34.5375). While that of the docking between protein and allosteric compound are also same(X,Y,Z [A^0]= 38.8781, 26.2673, -19.7061) and center coordinates (31.3540, 35.3858, 34.5375) with exhaustiveness 8.0 as both the active site and allosteric site lies nearby according to the prediction software. For better visualization of the docked structure PyMolsoftware(32) was used. Whereas, the two-dimensional interactions between both the docked compounds were identified using ligplot + software(33).

Admet property

ADMET stands for absorption, distribution, metabolism, excretion, and toxicity. These properties are used to identify

the likeliness of a drug. These properties are based on its pharmacokinetics calculations which act as a key feature to identify the activity of a drug inside the body. By the identification of these properties, one is able to find out the undesirable toxicity and features of a compound. The program ADMETSAR2.0 was used to do the ADMET analysis (34)

Pass analysis

The program PASS predicts the action of several ligands, allowing us to find an antiviral activity (35). PASS is a software that uses a computational technique to predict different sorts of physiological responses for distinct phytoconstituent molecules. It provides findings based on likely activity and probable inactivity, i.e. (Pa) and (Pa) (Pi). Those compounds with a higher Pa than Pi are the ones we can address for future medicinal uses.

Molecular dynamic simulation

For the molecular dynamic simulation iMODSserver(36) which is available online was explored.This server is used for the predictions of protein flexibility. The web server is comprised of a number of ASP, Java, PHP, JavaScript and Perl components. It is a powerful molecular dynamics modeling tool that could be used to examine the structural dynamics of protein complexes quickly and easily. It predicts deformability, eigenvalues, and other parameters. The ability of a complex or a protein to deform at each of its amino acid residues determines the deformability. The eigenvalue is proportional to the amount of energy required to distort (deform) a certain structure, and the lower the eigenvalue, the easier the complex is to deform. Furthermore, the eigenvalue also indicates the protein complex's motion stiffness.

Results and Discusion

Identification of the allosteric site

The allosteric sites was identified using Passer packages which show various poses and sites which can be an allosteric site of the protein. On the basis of the best pocket size and score, pocket 1 has been selected with the best pocket score of 0.866.

Identification of the active site

The active site of the protein was identified using the online tool CastP. The id of the protein structure was provided in the server and the server itself provides the best active site sites for further analysis.

Molecular docking and analysis of target prediction

The docking of the protein and ligand was performed by the software Autodock whereas virtual screening of the molecules was performed using the software pyrx.

Identification of suitable allosteric compound: -

The compounds that were downloaded from the allosteric database were thoroughly screened using Pyrx software and out of 103 downloaded activators the best allosteric activator identified was an isocitrate dehydrogenase with an ASD id ASD01720151, having the best affinity docking score -11.8.

Identification of suitable Ligand: - After performing molecular docking we were able to find that out of Isocarboxazid, Phenelzine, Selegiline, and Tranylcypromine, the ligand Isocarboxazid has the best docking score (-8.6 K cal/mol) and was suitable for further analysis as shown in table 1.

Table1. The docking score between different ligand compounds with Protein structure

S.no.	Pro-tein	Ligand	Pub-chem id	Docking score
1	2Z5X	Isocarbox-azid	3759	-8.6
2	2Z5X	Phenelzine	3675	-6.7
3	2Z5X	Selegiline	26757	-7.6
4	2Z5X	Tranylcy-promine	19493	-6.3

Identification of the natural compound

The natural compound was taken from the lotus database whereas the similarities score i.e., the Tanimoto similarity was set at 75%, there were 12 hits results were identified as having Tanimoto similarity of more than 75% on those 12 results a virtual screening have been performed and out of which the structure homaline, having lotus id LTS0214462 shows the best Docking score -10.1 and was taken for further experimentation.

Process of the experimentation

The Identification of a natural compound as a substitute for an allosteric compound was performed using molecular docking. In the initial step, the molecular docking was performed between chemical allosteric compounds and protein molecules, by using the virtual screening software Pyrx. The docking score obtained was -11.8kcal/mol of the allosteric compound with an id ASD01720151. Again molecular docking has been performed with the protein structure (2z5x) and different ligands in which the ligand Isocarboxazid shows the highest affinity with a score -8.6kcal/mol.

After performing docking between both the molecules a complex has been formed between protein and allosteric compound. This complex structure has been used for further experimentation, a molecular docking has been performed between complex and ligand isocarboxazid with a docking score of -9.0. From this score, we can identify that the allosteric compound performs its activity, and due to this better Docking score was obtained. But as the allosteric compound is a chemical compound, we have to find another compound that can be a good substitute for the chemical compound and have less toxicity.

So, for the identification of the natural compound, through literature mining and from various databases we were able to find out the best Tonimoto structure has the best structural similarity with the chemical compound. Again, performing molecular Docking with the same environment and coordinate file we were able to find that the Docking score between the protein and natural allosteric compound was -10.1. as we have earlier found out the Docking score between the protein and ligand was -8.6. Now again we made a complex structure between a protein and natural allosteric compound and performed docking between the complex structure and the ligand, the docking score was -8.7 kcal/mol as detailed in and table no.2,3. The pictorial representation of the docking is shown in fig1, fig 2 and interaction was shown in fig 3

Table2: Docking between protein and ligands(chemical allosteric)

Protein	Ligand	Energy score	Method
2z5x	Isocarboxazid	-8.6 kcal/mol	Autodockvina
2z5x	ASD01720151	-11.8 kcal/mol	Autodockvina
Complex (2z5x+ ASD01720151)	Isocarboxazid	-9.0 kcal/mol	Autodockvina

Table3: Docking between protein and ligand(natural allosteric)

Protein	Ligand	Energy score	Method
2z5x	Isocarboxazid	-8.6 kcal/mol	Autodockvina
2z5x	Homaline	-10.1 kcal/mol	Autodockvina
Complex (2z5x+Homaline)	Isocarboxazid	-8.7 kcal/mol	Autodockvina

1.Below are the images of the docked compounds (chemical allosteric)

A B C

Fig1. illustrations of these images are as follows- (A) image shows the docking between the drug and the target protein, where red-colored molecule depicts the and green depicts the. (B) image shows the docking of the allosteric compound on the identified allosteric site of the target protein (C) Depicts the docking of the complex having the chemical allosteric compound and the target protein with the ligand molecule, where red-colored molecule depicts the and where the red-colored molecule depicts the and green depicts the, and the yellow, green depicts the, and the yellow.

1.Below are the images of the docked compounds (chemical allosteric)

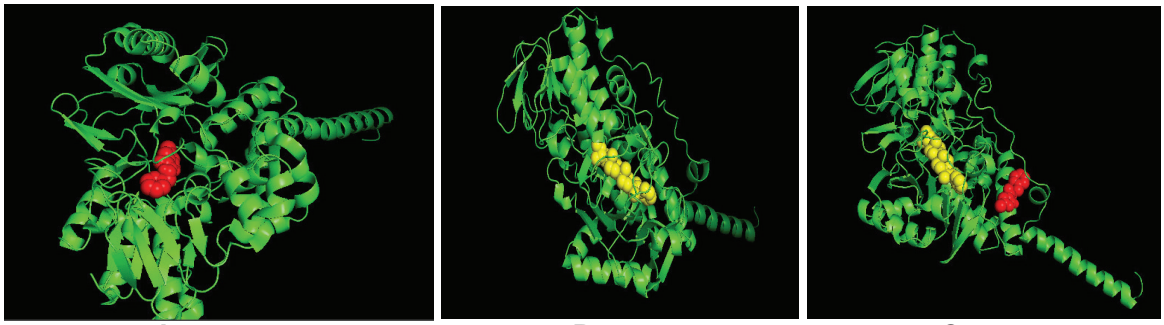

A B C

Fig2. illustrations of these images are as follows- (A) image shows the docking between the drug (red color) and the target protein (green color). (B)docking of the natural allosteric compound (yellow color) on the allosteric site of the target protein (green color). (c)Depicts the docking of the complex having the natural allosteric compound (yellow) and the target protein(green) with the ligand molecule (red color).

2D interaction between the docked protein, ligand, and natural allosteric compound

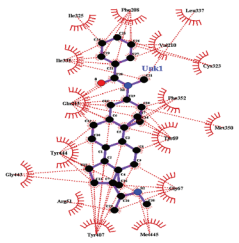

Protein-ligand interaction(allosteric)

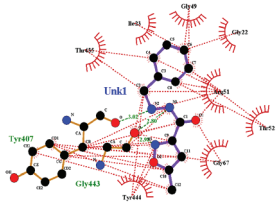

Protein-ligand interaction(active compound)

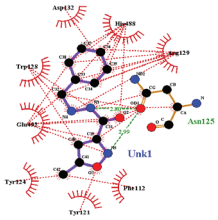

Protein+allosteric+ligand interaction

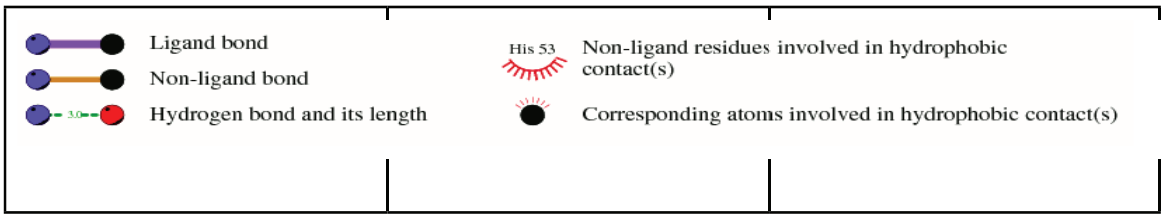

Fig 3. Two-dimensional representation of H-bonds and hydrophobic interactions between protein and allosteric compound, protein and ligand, protein and allosteric complex+ligand. Ligands are colored and represented in Purple color, H bonds are shown in green dotted lines, red stellations show hydrophobic interactions, and bonds of proteins are represented in brown color.

ADMET Properties of allosteric compound:-

ADMET properties are required to identify how a compound works as a ligand. After performing ADMET analysis the natural compound compounds follow the Lipinski rule and show good admit property but natural compounds showed better results and were also non-toxic in nature, also it does not penetrate the Blood-Brain Barrier as shown in table 4.

Table 4. Different ADMET properties of allosteric compounds where HIA stands for human intestinal absorption, BBB stands for Blood-Brain Barrier.

S.no.	Properties	Allosteric compound	Natural compound
1 Molecular weight, 484.280			450.360
2	Lipinski Rule	Accepted	Accepted
3	Caco-2 Permeability	-5.674	-4.695
4	BBB Penetration	Penetrate	Not penetrate
5	AMES Toxicity	Toxic	Non-toxic
6	HIA (Human intestinal absorption)	Low absorption	High absorption
7	Acute Toxicity Rule	0 alert	0 alert

Prediction of the antidepressant activity by Pass analysis

PASS is defined as Prediction of Activity Spectra for Substances. PASS analysis can be helpful In determining biologically active spectra of phyto-constituents. Here Pa is the probability of a compound to be active and shows chances of being an active compound whereas Pi represents the probability of a compound to be inactive which estimates that the compound belongs to the sub-class of the inactive compound. Here various activities have been shown in which PASS prediction of the natural compound shows a good response as shown in table 5

Table 5: Table shows the values of Pa, Pi with activities of compound

Pa	Pi	Activity
0,319	0,008	MAO inhibitor
0,106	0,018	MAO B inhibitor
0,071	0,044	MAO A inhibitor
0,591	0,127	Phobic disorders treatment
0,554	0,021	Neurodegenerative diseases treatment
0,275	0,179	Dementia treatment

Molecular dynamic simulation

The results of Molecular Dynamics Simulation are shown in Figure 4a and 4b. The

deformability graph indicates that the peaks in the graphs correlate to deformable regions in the protein (Figure 4a). In Figure 4b, the eigenvalue of the complex is shown. The eigenvalue of the docked complex was predicted to be 1.038932e-05.

According to the molecular dynamics simulation study of the docked complex, the complex Figure 4a has a lot of deformability potential as well as has a low eigenvalue of 1.038932e-05, which illustrates that the lower the eigenvalue, the easier the deformation of the complex would be Figure 4b, it also depicts the protein complex's motion stiffness.

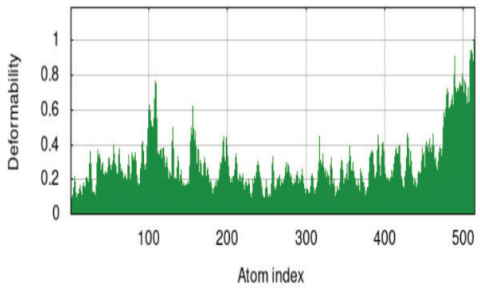

Figure 4a. Result of molecular dynamics simulation shows the graph of deformability

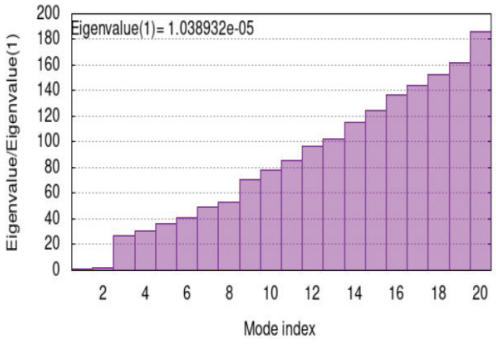

Figure 4b. Result of molecular dynamics simulation shows the graph of eigenvalue

Mental disorders are increasing rapidly and everyone in the entire world is suffering from one kind of mental disorder. There are many of the FDA approved drugs are available having good responses against mental disorders but are time-consuming and have low response rates for increasing the response rate allosteric compounds can be a good option, in this study we are able to identify the natural compound which can be used as an alternative of the chemical allosteric compound having an effect on the activity of the drug. In this approach, we have used different in silico methods like molecular docking, molecular simulation, etc., and on the basis of which the natural allosteric compounds were identified. The FDA-approved drug that has been used for this study is isocarboxazid while the chemical allosteric compound identified after performing virtual screening was an isocitrate dehydrogenase. This compound is further used to identify the natural compound as an alternative to the chemical allosteric compounds. With the growing scenario, the urgent need to replace chemical compounds with natural ones is increasing at a faster pace. Thus, in our study, we investigated an alternative of the chemical allosteric compound with a natural allosteric modulator**.**

Our study demonstrates that the natural allosteric compound could play a crucial role in increasing its efficacy and effectiveness.

Future direction or limitation

Biological screening of the natural allosteric compound is a key aspect of identifying and increasing the effect of the drug(37). The Monoamine oxidase(MAO) enzyme is a prevalent target for many depressive disorders. As this enzyme somehow plays a major role in various depressive disorders and neurodegenerative disorders. Potential therapeutics are required to suppress this enzyme activity. Isocarboxazid is such a drug which is an antidepressant(monoamine oxidase inhibitor), the activity of this drug can be enhanced by using an allosteric compound but outcomes and side effects of the allosteric could be a problem, To overcome the negative effects of the allosteric compound natural

compound can be an alternate. As the activity of the drug can be enhanced it could also be used in treating different diseases like parkinson's (38), and bipolar disorder(39) in which MAO is involved . one of the limitations of using the drug and allosteric compound is the amount of drug provided and its response rate. Wet lab-based experimentation would be required for proper validation.

Acknowledgement

We are thankful for Prof Shweta Dang for academic suggestions and Jaypee Institute of Information Technology for facilitating the necessary support.

Conflict of Interest: Authors declares no conflict of Interest

References

1. Rossetti, M., &Porchetta, A. (2018). Allosterically regulated DNA-based switches: From design to bioanalytical applications. *Analyticachimicaacta*, *1012*, 30–41..
2. Csermely, P., Palotai, R., &Nussinov, R. (2010). Induced fit, conformational selection and independent dynamic segments: an extended view of binding events. *Trends in biochemical sciences*, *35*(10), 539–546.
3. Cui, Q., &Karplus, M. (2008). Allostery and cooperativity revisited. Protein science : a publication of the Protein Society, 17(8), 1295–1307.
4. Pan, Y., Tsai, C. J., Ma, B., &Nussinov, R. (2010). Mechanisms of transcription factor selectivity. Trends in genetics : TIG, 26(2), 75–83.
5. Bah, A., Vernon, R. M., Siddiqui, Z., Krzeminski, M., Muhandiram, R., Zhao, C., Sonenberg, N., Kay, L. E., & Forman-Kay, J. D. (2015). Folding of an intrinsically disordered protein by phosphorylation as a regulatory switch. Nature, 519(7541), 106–109.
6. Gustavsson, M., Verardi, R., Mullen, D. G., Mote, K. R., Traaseth, N. J., Gopinath, T., &Veglia, G. (2013). Allosteric regulation of SERCA by phosphorylation-mediated conformational shift of phospholamban. Proceedings of the National Academy of Sciences of the United States of America, 110(43), 17338–17343.
7. Sevcsik, E., Trexler, A. J., Dunn, J. M., & Rhoades, E. (2011). Allostery in a disordered protein: oxidative modifications to α-synuclein act distally to regulate membrane binding. *Journal of the American Chemical Society*, *133*(18), 7152–7158.
8. Subedi, G. P., Hanson, Q. M., & Barb, A. W. (2014). Restricted motion of the conserved immunoglobulin G1 N-glycan is essential for efficient FcγRIIIa binding. Structure (London, England : 1993), 22(10), 1478–1488.
9. Strickland, D., Moffat, K., &Sosnick, T. R. (2008). Light-activated DNA binding in a designed allosteric protein. Proceedings of the National Academy of Sciences of the United States of America, 105(31), 10709–10714.
10. Changeux J. P. (2012). Allostery and the Monod-Wyman-Changeux model after 50 years. Annual review of biophysics, 41, 103–133.
11. Lechtenberg, B. C., Freund, S. M., & Huntington, J. A. (2012). An ensemble view of thrombin allostery. *Biological chemistry*, *393*(9), 889–898.
12. MONOD, J., WYMAN, J., & CHANGEUX, J. P. (1965). ON THE NATURE OF ALLOSTERIC TRANSITIONS: A PLAUSIBLE MODEL. *Journal of molecular biology*, *12*, 88–118.
13. Zhang, J., &Nussinov, R. (Eds.). (2019).

Protein allostery in drug discovery. Singapore: Springer.

14. Fagervall, I., & Ross, S. B. (1986). Inhibition of mono amine oxidase in monoaminergic neurones in the rat brain by irreversible inhibitors. Biochemical pharmacology, 35(8), 1381-1387.

15. David Rosenberg (21 August 2013). Pocket Guide For The Textbook Of Pharmacotherapy For Child And Adolescent Psychiatric Disorders. Routledge. pp. 176–. ISBN 978-1-134-86002-9.

16. Rosenbaum, J. F., Arana, G. W., Hyman, S. E., Labbate, L. A., Fava, M., & Williams, M. L. (2007). Handbook of psychiatric drug therapy. J Clin Psychiatry, 68(2).

17. DARLING HF. Isocarboxazid (Marplan) in ambulatory psychiatric patients. American Journal of Psychiatry. 1959 Oct;116(4):355-6.

18. Riederer, P., &Laux, G. (2011). MAO-inhibitors in Parkinson's Disease. Experimental neurobiology, 20(1), 1–17..

19. Volz, H. P., &Gleiter, C. H. (1998). Monoamine oxidase inhibitors. A perspective on their use in the elderly. Drugs & aging, 13(5), 341–355

20. Liu, C. H., Ren, J., & Liu, P. K. (2016). Amphetamine manipulates monoamine oxidase-A level and behavior using theranosticaptamers of transcription factors AP-1/NF-kB. Journal of biomedical science, 23, 21.

21. Son, S. Y., Ma, J., Kondou, Y., Yoshimura, M., Yamashita, E., &Tsukihara, T. (2008). Structure of human monoamine oxidase A at 2.2-A resolution: the control of opening the entry for substrates/inhibitors. Proceedings of the National Academy of Sciences of the United States of America, 105(15), 5739–5744.

22. Naoi, M., Maruyama, W., &Shamoto-Nagai, M. (2018). Type A and B monoamine oxidases distinctly modulate signal transduction pathway and gene expression to regulate brain function and survival of neurons. Journal of neural transmission (Vienna, Austria : 1996), 125(11), 1635–1650.

23. Zisook S. (1984). Side effects of isocarboxazid. The Journal of clinical psychiatry, 45(7 Pt 2), 53–58.

24. Liu, X., Lu, S., Song, K., Shen, Q., Ni, D., Li, Q., He, X., Zhang, H., Wang, Q., Chen, Y., Li, X., Wu, J., Sheng, C., Chen, G., Liu, Y., Lu, X., & Zhang, J. (2020). Unraveling allosteric landscapes of allosterome with ASD. Nucleic acids research, 48(D1), D394–D401.

25. Berman, H. M., Westbrook, J., Feng, Z., Gilliland, G., Bhat, T. N., Weissig, H., Shindyalov, I. N., & Bourne, P. E. (2000). The Protein Data Bank. Nucleic acids research, 28(1), 235–242.

26. Morris, G. M., Huey, R., Lindstrom, W., Sanner, M. F., Belew, R. K., Goodsell, D. S., & Olson, A. J. (2009). AutoDock4 and AutoDockTools4: Automated docking with selective receptor flexibility. Journal of computational chemistry, 30(16), 2785–2791.

27. Huang, Z., Zhu, L., Cao, Y., Wu, G., Liu, X., Chen, Y., Wang, Q., Shi, T., Zhao, Y., Wang, Y., Li, W., Li, Y., Chen, H., Chen, G., & Zhang, J. (2011). ASD: a comprehensive database of allosteric proteins and modulators. Nucleic acids research, 39(Database issue), D663–D669.

28. O'Boyle, N. M., Banck, M., James, C. A., Morley, C., Vandermeersch, T., & Hutchison, G. R. (2011). Open Babel: An open chemical toolbox. Journal of

cheminformatics, 3, 33.

29. Lotus.naturalproducts.net. 2022. LOTUS: Natural Products Online. [online] Available at: <https://lotus.naturalproducts.net/documentation> [Accessed 12 May 2022].

30. Tian, W., Chen, C., Lei, X., Zhao, J., & Liang, J. (2018). CASTp 3.0: computed atlas of surface topography of proteins. Nucleic acids research, 46(W1), W363–W367.

31. Tian, H., Jiang, X., & Tao, P. (2021). PASSer: Prediction of Allosteric Sites Server. Machine learning: science and technology, 2(3), 035015.

32. Seeliger, D., & de Groot, B. L. (2010). Ligand docking and binding site analysis with PyMOL and Autodock/Vina. Journal of computer-aided molecular design, 24(5), 417–422.

33. Laskowski, R. A., &Swindells, M. B. (2011). LigPlot+: multiple ligand-protein interaction diagrams for drug discovery. *Journal of chemical information and modeling*, *51*(10), 2778–2786.

34. Yang, H., Lou, C., Sun, L., Li, J., Cai, Y., Wang, Z., Li, W., Liu, G., & Tang, Y. (2019). admetSAR 2.0: web-service for prediction and optimization of chemical ADMET properties. *Bioinformatics (Oxford, England)*, *35*(6), 1067–1069.

35. Examples. Way2drug.com. (2022). Retrieved 12 May 2022, from http://way2drug.com/PassOnline/ex.php.

36. López-Blanco, J. R., Aliaga, J. I., Quintana-Ortí, E. S., &Chacón, P. (2014). iMODS: internal coordinates normal mode analysis server. Nucleic acids research, 42(Web Server issue), W271–W276.

37. SarathKumar, B., & Lakshmi, B. S. (2019). In silico investigations on the binding efficacy and allosteric mechanism of six different natural product compounds towards PTP1B inhibition through docking and molecular dynamics simulations. Journal of molecular modeling, 25(9), 272.

38. Riederer, P., &Laux, G. (2011). MAO-inhibitors in Parkinson's Disease. Experimental neurobiology, 20(1), 1–17.

39. Mallinger, A. G., Frank, E., Thase, M. E., Barwell, M. M., Diazgranados, N., Luckenbaugh, D. A., &Kupfer, D. J. (2009). Revisiting the effectiveness of standard antidepressants in bipolar disorder: are monoamine oxidase inhibitors superior?. Psychopharmacology bulletin, 42(2), 64–74.

Current Trends in Biotechnology and Pharmacy
Vol. 16 (4) 540 - 552, Oct 2022, ISSN 0973-8916 (Print), 2230-7303 (Online)
10.5530/ctbp.2022.4.87

Vernonia amygdalina Leaf Extract Protects Against carbon tetrachloride-induced hepatotoxicity and Nephrotoxicity: Possible Potential in the Management of Liver and Kidney Diseases

Temidayo Ogunmoyole[1], Yetunde Apanisile[2],OmowumiJayeola Makun[3], Olaitan Daniel Johnson[4], Yusuff Adewale Akeem

[5]1*Department of Medical Biochemistry, College of Medicine, Ekiti State University, Ado Ekiti, Ekiti State, Nigeria.
[2]Department of Science Laboratory Technology, Faculty of Science, Ekiti State University, Ado Ekiti, Ekiti State, Nigeria
[3]Department of Environmental Management and Toxicology, Federal University of Petroleum Resources, Effurun, Delta State, Nigeria
[4]Department of Science Laboratory Technology, School of Applied Sciences and Technology, Auchi Polytechnic, Auchi, Edo State, Nigeria

[5]Department of Biochemistry, Federal University of technology, Akure, Ondo State, Nigeria

*Corresponding author: ogunmoyoledayo@yahoo.com

Abstract

The rising prevalence of liver and kidney diseases is worrisome and constitutes a major threat to public health. The present study investigates the medicinal potentials of *Vernonia amygdalina* leaves in the management of liver and kidney diseases. Albino rats were randomly divided into five groups of 5 animals each. All experimental animals, except group I, were exposed to 3 ml/kg b.w of CCl_4 and administered different treatments. Groups III, IV and V each were treated with 50 mg/kg b.w, 100 mg/kg b.w. of bitter leaf extract and 100 mg/kg b.w. of silymarin respectively. Group II animals were left untreated after exposure to toxicant. Activities of creatine kinase (CK), aspartate amino transferase (AST), alanine amino transferase (ALT), alkaline phosphatase (ALP), as well as level of urea, uric acid and bilirubin were determined in the serum and tissue homogenates. Lipid profile as well as activities of superoxide dismutase (SOD) and catalase (CAT) were also determined. Exposure to CCl_4 resulted in significant increase in CK, AST, ALP, ALT as well as bilirubin, urea and uric acid relative to the control. Lipid profile was deranged, activities of SOD and CAT were markedly inhibited and level of GSH significantly depleted. However, treatment with *V. amygdalina* reversed the toxic trend in a dose dependent manner comparable to animals treated with silymarin. In conclusion, *V. amygdalina* leaf extract restored deranged lipid profile, distorted histoarchitecture as well as liver and kidney function markers. Hence, the plant is a potential candidate for the management of liver and kidney diseases.

Keywords: *Vernonia amygdalina*, animals, biomarkers, carbon tetrachloride, diseases.

Introduction

Since antiquity, nature has provided man with basic requirements such as healthcare, food, shelter as well as other necessities of human existence. Globally, medicinal plants occupy a central space and has dominated the healthcare system of developing countries where a very large percentage of the population depends on plants for therapy. As it stands, several developed and well industrialized nations of the world are fast embracing the use of herbal extracts as complimentary therapy (1). Medicinal plants are not just important for healthcare but as an assured hope for the development of future medicines. At the moment, only about one-third of human diseases has readily available and efficacious therapy. There

is therefore a dire need for medicinal plants with proven potency and safety that can serve as panacea to the menace of several diseases (2). The World Health organization (WHO) has endorsed and promoted the inclusion of herbal medicines in National healthcare programs due to ease of access, affordability and safety (3). Consequently, collaborative research efforts in the area of screening of plants extracts has led to the identification of pharmacologically active agents that can be exploited as drugs for the management of diseases (4).

Chronic liver disease (CLD) constitutes a major threat to global public health, causing increasing mortality and morbidity worldwide.(5) Between 1980 and 2010, mortality as a result of liver disease increased by 46 % globally (6) with higher prevalence in the developing nations including Africa. (7). Similarly, the global disease burden report of 2010 ranked chronic kidney disease as 27th on the list of causes of global death in 1990. However, in 2010, chronic kidney disease rose to 18th position on the list (7) This rise in burden was second to HIV/AIDS. According to the report, the overall premature mortality was estimated at 82% which was third largest behind diabetes (93%) and HIV/AIDS (396%). Considering this data that threatens global health as well as the sustainable development goal (8), there is a dire need to leverage on potent medicinal plants that could serve as complimentary therapy to stem-down the tide of these diseases.

Vernonia amygdalina is a leafy vegetable widely noted for its bitter taste, hence its popularly called 'bitter leaf'. Its leaves are normally employed in cooking delicious vegetable soup usually recommended for treating several ailments. *V. amygdalina* has been widely studied due to its versatile medicinal relevance such as in the treatment of diabetes, hypertension, and infertility (9). Recent scientific evidences have given credence to its numerous medicinal benefits such as anti-obesity (10), antioxidant (11), anticarcinogenic (12), antihyperglycemic (13), anti-sickling (14) and in the management of cardiovascular disorders (15). Reports have indicated that leaf extract of *Vernonia amygdalina* protects against brain degeneration thereby enhancing memory (16). Besides, extract of *V. amygdalina* Del leaf exhibits anti-helmintic, anti-parasitic and antimicrobial properties (17).

I n view of the rising burden of liver and kidney diseases, there is a dire need to investigate the potentials of *V. amygdalina* extract in the management of these diseases. Hence, this study.

Materials and Methods

Plant Materials

*Vernonia amygdalina*leaves was obtained from a private farm in Ado Ekiti, air dried in the laboratory, pulverized and then stored in an air-tight container.

Reagents and chemicals

All biochemical kits were of analytical grade obtained from Randox laboratories, UK.

Extraction of the extract

Bitter leaves were air-dried at room temperature and pulverized to obtain fine powder using a blender. 500 g each of the powdered leaves of V. amygdalina was soaked in 5000 ml of distilled water for 72 hours to allow for extraction. It was then filtered using a cheese cloth, and freeze-dried to obtain the dried extract. The extract was kept in a closed container and kept inside the fridge at 4^0C for further studies

Animals protocol

Twenty-five (25) male wistar albino rats weighing 180 – 200 g were acclimatized for two weeks, housed in clean wire meshed cages under standard conditions temperature (24 ± 1^{o}C), relative humidity, and 12 / 12-hour light and dark cycle. They were allowed to have free access to food (commercial palletized diet from Vital Feed Mill) and drinking water daily. The rat beddings were changed and replaced every day throughout the experimental period.

Animal grouping and treatment

Experimental animals were administered different treatments as shown in Table 1.

Table 1. Animal treatment

Groups	Treatment
I	Distilled water only for 14 days
II	Single intraperitoneal injection of 3 ml CCl_4/kg body weight
III	3 ml CCl_4 + 50 mg/kg *Vernonia amygdalina* extract for 14 days
IV	3 ml CCl_4 + 100 mg/kg *Vernonia amygdalina* extract for 14 days
V	3 ml CCl_4 + 100 mg/kg silymarin for 14 days

Dissection of rats

The animals were decapitated under very light anesthesia to obtain the liver, kidney and heart, while whole blood was collected by cardiac puncture allowed to stand for 1 hour in an EDTA bottle. Serum was prepared by centrifugation at 3000 rpm for 15 min at 25°C. The clear supernatant was collected and used for the estimation of serum biochemical parameters.

Preparation of homogenates

The liver, heart and kidney were excised using scissors and forceps. They were trimmed of fatty tissue, washed in distilled water, blotted with filter paper and weighed. They were then chopped into bits and homogenized in ten volumes of the homogenizing phosphate buffer (pH 7.4) using a Teflon homogenizer. The resulting homogenates were centrifuged at 3000 rpm at 4°C for 30 mins. The supernatant obtained was collected and stored under 4^0C and then used for biochemical analyses.

Determination of serum creatine kinase (Ck-Mb) activity

Creatine kinase was measured by the method of Mattenheimer (18). One thousand microliters of imidazole buffer (10 mM, pH 6.6), containing creatine phosphate (30 mM), glucose (20 mM), N-acetyl-cysteine (20 mM), magnesium acetate (10 mM), ethylene diaminetetraacetic acid (2 mM), ADP (2 mM), NADP (2 mM), AMP (5 mM), DAPP (10 µM), G6PDH (≥2.0 ku/L) and HK(≥2.15 ku/L)) was incubated in a thermostatic cuvette at 37 °C after the addition of 50 µl of serum. Absorbance at 340 nm of the resulting mixture was read immediately for 5 min at 30 sec interval. Change in absorbance per minute was estimated while enzyme activity was determined as:)

Assay of aspartate aminotransferase (AST) activity

AST activity was determined following the principle described by Reitman and Frankel (19). Briefly, 0.1 ml of organs homogenates as well as serum was mixed separately with phosphate buffer (100 mmol/L, pH 7.4), L-aspartate (100 mmol/L), and α-oxoglutarate (2 mmol/L) and the mixture incubated for exactly 30 min at 37°C. Five hundred microliters of 2,4-dinitrphenylhydrazine (2mmol/L) was added to the reaction mixture and allowed to stand for exactly 20 min at 25 °C. Five milliliter of NaOH (0.4 mol/L) was then added and the absorbance of the mixture read after 5 min at 546 nm against the reagent blank.

Assay of alanine amino transferase (ALT) activity

The principle described by Reitman and Frankel (19) was followed in the assay of ALT using commercially available assay kit (Randox laboratories, UK) according to the instructions of the manufacturer. Five hundred microliter of reagent I (R1) containing phosphate buffer (100 mmol/l, pH 7.4), L-alanine (200 mmol/l) and α-oxoglutarate (2.0 mol/l) was added to 0.1 ml of serum in a test tube and the mixture was incubated at 37°C for 30 min. Exactly 0.5 ml of R2 containing 2, 4-dinitrophenylhydrazine (2.0 mmol/l) was added and the solution incubated again at 20°C for 20 min. Finally, 5 ml of NaOH was added and the solution was allowed to stand for 5 min at 25°C and the absorbance was read at 546 nm. Activity of ALT was obtained

from the standard curve provided in the kit.

Assay of alkaline phosphatase (ALP) activity

Assay of serum ALP was based on the method of Englehardt*et al*. (20) using commercial assay kits (Randox laboratories, UK) according to the instructions of the manufacturer. Exactly 1.0 ml of the reagent (1 mol/l diethanolamine buffer pH 9.8, 0.5 mmol/l $MgCl_2$; substrate: 10 mmol/l p-nitrophenol phosphate) was added to 0.02 ml of the serum sample and mixed. The absorbance was taken at 405 nm for 3 minutes at intervals of 1 minute. ALP activity was determined as shown

Serum Lipid Profile

Estimation of total cholesterol level

Total cholesterol level was determined based on the method of Trinder (21) using commercially available kits (Randox laboratories, UK). Ten microliters (10 µl) of standard and 10 µl serum samples were measured into labeled test tubes. One milliliter (1 ml) of working reagent containing; Pipes buffer (80 mmol/l at pH 6.8), 4-aminoantipyrine (0.25 mmol/l), phenol (6 mmol/l), peroxidase (≥ 0.5 U/ml), cholesterol esterase ion (≥0.15 U/ml) and cholesterol oxidase (0.10 U/ml) was added into all the tubes. The test tubes were mixed thoroughly and incubated for 10 min at 25 °C. Absorbance of the sample (Asample) was read at 500 nm against the reagent blank.

Cholesterol concentration (mg/dl) was calculated as follows:

Evaluation of concentration of triglyceride

Triglycerides level was determined based on the method of Tietz (22) using commercially available kits (Randox laboratories, UK). Triglyceride standard (10 µl) and serum (10 µl) were measured into labeled test tubes. One milliliter of the working reagents; R1a (buffer) containing Pipes buffer (40 mmol/l, pH 7.6), 4-chloro-phenol (5.5 mmol/l), magnesium-ion (17.5 mmol/l); R1b (enzyme reagent containing 4-amino phenazone (0.5 mmol/l), ATP (1.0 mmol/l), lipase ((≥150 U/ml), glycerol-kinase ((≥0.4U/ml), glycerol-3-phosphate oxidase ((≥1.5 U/ml) and peroxidase (≥0.5 U/ml)was added into all the tubes. The test tubes were mixed thoroughly and incubated for 10 min at room temperature. Absorbance was taken at 546 nm against the blank (Tietz, 1990).

High Density Lipoprotein (HDL-c)-Cholesterol Assay

High-density lipoprotein cholesterol was determined by the method of Grove (23) in two stages:

Precipitation

Reaction mixture containing 200 µl of the serum, 200 µl of the cholesterol standard, 500 µl of the diluted precipitant R1 (0.55 mM phosphotungstic acid, 25 mM magnesium chloride) was mixed together and allowed to stand for 10 min at room temperature. It was then centrifuged for 10 min at 4000 rpm to obtain a clear supernatant. The clear supernatant was separated off within 2 h and the cholesterol content was determined by the CHOD-PAP reaction method.

Cholesterol CHOD-PAP Assay

One milliliter of cholesterol reagent was added to 100 µl of the sample supernatant in a test tube. The standard test tube contained 100 µl of the cholesterol standard supernatant and 1 ml of cholesterol reagent. The reagent mixture was mixed thoroughly and incubated for 10 min at 25°C. The absorbance of the sample (A_{sample}) and standard ($A_{standard}$) was then measured at 500 nm against the reagent blank within 1 h.

Low Density Lipoprotein (LDL) - Cholesterol Determination

The concentration of low-density lipoprotein in the serum was calculated using the formula of Friedwald et al. (1972) (24) :

Antioxidant assay

Determination of catalase activity

This experiment was carried out according to the method described by Sinha (25). Two hundred microliters of serum and organs homogenates was mixed separately with 0.8 ml of distilled H_2O to give 1 in 5 dilution of the sample. The assay mixture contained 2 ml of solution (800 µmol) and 2.5 ml of phosphate buffer in a 10 ml flat bottom flask. Properly diluted enzyme preparation (0.5 ml) was rapidly mixed with the reaction mixture by a gentle swirling motion. The reaction was run at room temperature. A 1 ml portion of the reaction mixture was withdrawn and blown into 1 ml dichromate/acetic acid reagent at 60 seconds intervals. The hydrogen peroxide content of the withdrawn sample was determined by the method described below.

Calculation

Concentration of H_2O_2 remaining was extrapolated from the standard curve for catalase activity.

Determination of superoxide dismutase (SOD) activity

The level of SOD activity was determined by the method of Misra and Fridovich (26). Ten-fold dilution of the sample was prepared**.** An aliquot of the diluted sample was added to 2.5 ml of 0.05 M carbonate buffer (pH 10.2) to equilibrate in a spectrophotometer. Reaction was initiated by the addition of 0.3 ml of freshly prepared 0.3 mM adrenaline to the mixture which was quickly mixed by inversion. The reference cuvette contained 2.5 ml buffer, 0.3 ml of substrate (adrenaline) and 0.2 ml of water. The increase in absorbance at 480 nm was monitored every 30 seconds for 150 seconds.

Determination of Reduced Glutathione (GSH) Level

The method of Beutler et al. (27) was followed in estimating the level of reduced glutathione (GSH). Exactly 0.2 ml of supernatant was added to 1.8 ml of distilled water followed by the addition of 3 ml of the precipitating solution and then shaken thoroughly. The mixture was then allowed to stand for 5 min and then filtered. One milliliter of filtrate was added of 4 ml of 0.1 M phosphate buffer pH 7.4. Finally, 0.5 ml of the Ellman reagent was added. A blank was prepared with 4 ml of the 0.1 M phosphate buffer, 1 ml of diluted precipitating solution (3parts to 2 parts of distilled water) and 0.5 ml of the Ellman reagent. The absorbance was measured at 412 nm against reagent blank. Level of GSH in the serum was obtained from the standard curve.

Determination of Total Protein (TP) in Serum

The Biuret method described by Weichselbaum (28) was employed in the determination of total protein in the serum using commercially available kits (Randox laboratories, UK). One milliliter of Reagent R1 containing sodium hydroxide (100 mmol/l), Na-K-tartrate (18 mmol/l), potassium iodide (15 mmol/l) and cupric sulphate (6 mmol/l) was added to 0.02 ml of the serum sample. The reaction mixture was incubated at 25°C and absorbance measured against the reagent blank at 546 nm.

Statistical Analysis

All values are expressed as mean ± SD. Statistical evaluation was done using One Way Analysis of Variance (ANOVA) followed by Duncan's Multiple Range Test (DMRT) by using SPSS 11.09 for windows (Anthony and Richard, 2006). The significance level was set at $p < 0.05$.

Result and Discussion

Table 1. shows the treatment protocol adopted for the experimental animals. Animals in group II were exposed to 3ml/kg bw of CCl_4 but not treated with the extracted, while groups III, IV and V animals were exposed to 3ml/kg bw of CCl_4 and treated with 50, 100 mg/kg bw of *V. amygdalina* leaf extract and 100mg/kg bw of silymarin respectively. Group I animals received distilled water only and were not exposed to the toxicant at all. Exposure to CCl_4 caused a marked derangement in lipid profile (cholesterol, triglyceride, HDL-c and LDL-c) regardless of the organ involved (Table 2a-d). Treatment with *V. amygdalina* resulted in the restoration of the

lipid profile in a dose dependent fashion comparable to animals treated with silymarin. Serum level of alkaline phosphatase (ALP), alanine aminotransferase (ALT) and aspartate aminotransferase (AST) as well as bilirubin were significantly raised relative to control animals (Table 3a-d). However, treatment of intoxicated animals with graded doses of *V. amygdalina* led to a restoration of the marker enzymes in a manner comparable with animals treated with silymarin (Table 3a-d). Urea, and uric acid as well as total bilirubin were elevated following exposure to CCl_4 (Table 3a-d). Administration of the leaf extract of *V. amygdalina* reversed the trend to a level comparable with animals that were not exposed to the toxicant (Table 3a-d). Activity of superoxide dismutase, catalase and creatine kinase were significantly depleted when animals were exposed to CCl_4 but activity were restored to levels comparable with animals treated with silymarin following treatment with leaf extract of *V. amygdalina* (Table 4a-d). Reduced glutathione (GSH) was markedly decreased in the serum of animals exposed to CCl_4. However, GSH level was restored in the exposed animals following treatment with graded doses of V. amygdalina leaves extract. Administration of CCl_4 caused a marked distortion in hepatic, renal and cardiac histoarchitecture but the distortion was reversed by treatment with *V. amygdalina* leaves extract (Table 4a-d).Histomicrographof liver tissue of experimental animals under different

(a) Serum

Parameter	I	II	III	IV	V
T. Chol (mg/dl)	73.28±1.84[a]	140.21±0.00[b]	79.61±0.25[a]	69.17±0.31[a]	77.76±0.96[a]
Trig (mg/dl)	23.05±1.30[a]	46.22±1.18[b]	27.17±1.39[a]	26.25±0.11[a]	25.35±0.81[a]
HDL (mg/dl)	15.91±0.68[a]	10.10±0.04[b]	10.38±0.20[b]	11.87±0.05[a]	13.35±0.28[a]
LDL (mg/dl)	54.10±4.53[a]	120.87±0.46[b]	13.74±0.31[a]	12.05±0.38[a]	59.34±1.22[a]

(b) Liver

Parameter	I	II	III	IV	V
T. Chol (mg/dl)	72.96±1.01[a]	119.75±1.52[b]	83.67±1.26[a]	95.48±1.77[a]	86.63±1.95[a]
Trig. (mg/dl)	1.40±0.16[a]	25.8±0.27[b]	8.57±1.63[a]	1.07±1.12[a]	1.20±0.92[a]
HDL (mg/dl)	53.62±0.11[a]	34.19±0.10[b]	40.13±0.08[a]	49.42±0.30[a]	36.29±0.08[a]
LDL(mg/dl)	6.53±1.06[a]	67.44±3.41[b]	27.82±1.26[a]	13.84±1.69[a]	6.26±1.76[a]

(c) Kidney

Parameter	I	II	III	IV	V
T. Chol (mg/dl)	30.58±0.50[a]	57.46±0.76[b]	42.55±1.13[a]	42.11±1.58[a]	34.65±0.95[a]
Trig. (mg/dl)	17.34±0.09[a]	36.17±0.20[b]	32.01±0.38[a]	33.79±15.00[a]	34.81±0.44[a]
HDL (mg/dl)	11.27±0.19[a]	8.31±0.01[b]	9.61±0.24[a]	10.13±0.09[a]	10.47±0.23[a]
LDL (mg/dl)	16.11±0.57[a]	41.93±0.74[b]	28.01±1.03[a]	25.22±4.18[a]	19.19±0.75[a]

(d) Heart

Parameter	I	II	III	IV	V
T. Chol (mg/dl)	23.96±1.80[a]	38.49±0.65[b]	28.89±0.00[a]	22.11±0.79[a]	23.08±2.53[a]
Trig (mg/dl)	7.75±0.65[a]	11.6±0.50[b]	9.65±0.20[a]	9.89±0.08[a]	8.22±0.04[a]
HDL (mg/dl)	6.40±0.07[a]	3.57±0.11[b]	4.71±0.29[a]	4.91±0.02[a]	5.70±0.14[a]
LDL (mg/dl)	16.01±1.71[a]	32.6±0.68[b]	24.25±0.28[a]	15.95±0.01[a]	15.73±2.53[a]

treatment is as shown in Figure 1A-D.

Table 2. Effect of V. amygdalina leaf extract on lipid profile in the serum, liver, kidney and heart of CCl_4-exposed rat

Data represent mean ± SEM of experiment performed in triplicate. I – administered water only; II- administered CCl_4 only; III- treated with V.amygdalina at 50 mg/kg bw after exposure; treated with V.amygdalina at 100 mg/kg bw after exposure; V- treated with silymarin at 100 mg/kg bw after exposure. 'b' represents significant difference from the control 'a' at P=0.05

(a) Serum

Parameter	I	II	III	IV	V
ALP (U/L)	85.37±0.00[a]	145.96±0.00[b]	109.61±0.00[a]	92.46±1.07[a]	96.39±0.00[a]
ALT (U/L)	66.09±0.88[a]	106.69±1.72[b]	79.51±0.65[a]	69.69±2.25[a]	66.92±0.46[a]
AST (U/L)	75.19±1.06[a]	113.01±1.08[b]	78.20±0.87[a]	69.41±1.44[a]	73.36±0.49[a]
T. BIL (mg/dl)	63.73±0.43[a]	102.48±0.36[b]	78.34±0.38[a]	72.33±0.88[a]	68.11±0.67[a]
UREA (mg/dl)	42.80±0.68[a]	99.61±0.66[b]	72.69±0.00[a]	57.12±0.82[a]	50.77±0.57[a]
CK (U/L)	41.73±1.41[a]	62.93±2.34[b]	46.18±1.86[a]	42.29±1.44[a]	13.93±2.10[a]
URIC (mg/dl)	28.40±0.10[a]	50.80±0.23[b]	33.77±0.66[a]	26.35±0.14[a]	31.11±0.53[a]

(b) Liver

Parameter	I	II	III	IV	V
ALP (U/L)	55.08±0.00[a]	112.91±0.00[b]	97.08±1.60[a]	60.59±34.98[a]	65.41±1.38[a]
ALT (U/L)	44.99±3.23[a]	116.55±3.18[b]	89.32±1.10[a]	83.21±0.39[a]	66.03±0.96[a]
AST (U/L)	69.07±1.55[a]	104.59±4.32[b]	77.57±0.83[a]	75.02±1.01[a]	68.64±1.74[a]
T. BIL (mg/dl)	24.85±1.28[a]	46.48±0.18[b]	37.20±0.576[a]	28.67±0.061[a]	26.65±1.15[a]

(c) Kidney

Parameter	I	II	III	IV	V
ALP (U/L)	85.37±0.00[a]	145.96±0.00[b]	14.70±41.31[a]	93.64±0.00[a]	96.39±0.00[a]
ALT (U/L)	56.14±0.94[a]	158.71±7.56[b]	64.20±0.87[a]	58.43±2.25[a]	64.06±0.97[a]
AST (U/L)	69.58±1.28[a]	99.74±1.08[b]	93.03±1.55[a]	89.12±1.06[a]	75.27±1.47[a]
UREA (mg/dl)	52.69±0.67[a]	93.08±0.00[b]	71.83±50.18[a]	65.77±0.00[a]	58.85±0.00[a]
URIC (mg/dl)	24.36±0.29[a]	50.48±0.33[b]	41.63±0.44[a]	32.50±0.41[a]	25.55±0.55[a]

(d) Heart

Parameter	I	II	III	IV	V
ALP (U/L)	23.87±1.59[a]	38.56±0.00[b]	34.43±1.5[9]	27.54±0.00[a]	27.54±0.00[a]
ALT (U/L)	2.18±0.49[a]	15.05±0.39[b]	11.48±0.72[a]	6.13±0.26[a]	4.56±0.47[a]
AST (U/L)	11.97±0.77[a]	27.09±1.44[b]	21.86±1.57[a]	14.34±0.00[a]	9.88±1.05[a]
CK (U/L)	51.88±1.41[a]	83.91±1.17[a]	54±0.01[a]	50.16±0.01[a]	41.45±1.11[a]

Table 3: Effect of V. amygdalina leaf extract on selected biomarkers in organs of CCl_4 exposed rat

Data represent mean ± SEM of experiment performed in triplicate. I – administered water only; II- administered CCl_4 only; III- treated with V.amygdalina at 50 mg/kg bw after exposure; treated with

(a) Serum

Parameter	I	II	III	IV	V
SOD (U/mg protein)	8.47±0.49[a]	5.02±0.35[b]	5.17±1.68[a]	6.20±0.95[a]	7.80±1.04[a]
CAT (U/mg protein)	4.36±0.18[a]	1.84±0.05[b]	1.92±0.62[a]	2.44±0.14[a]	3.77±0.60[a]
GSH (mM/g tissue)	6.81±1.10[a]	4.53±1.22[b]	5.27±0.65[a]	5.88±0.32[a]	6.04±0.87[a]
TP (mg/ml)	3.75±0.20[a]	1.67±0.60[b]	2.73±0.27[a]	3.02±0.81[a]	2.59±0.18[a]

(b) Liver

Parameter	I	II	III	IV	V
SOD (U/mg protein)	2.04±0.10[a]	1.42±0.42[b]	1.37±0.17[a]	1.79±0.29[a]	2.11±0.32[a]
CAT (U/mg protein)	1.14±0.13[a]	0.26±0.21[b]	0.28±1.21[a]	0.61±0.67[a]	0.97±0.22[a]
GSH (mM/g tissue)	1.93±0.03[a]	0.39±0.01[b]	0.92±0.18[a]	1.16±0.01[a]	1.79±0.03[a]

(c) Kidney

Parameter	I	II	III	IV	V
SOD (U/mg protein)	5.26±0.02[a]	2.28±0.12[b]	2.95±0.63[a]	3.46±0.44[a]	3.62±0.21[a]
CAT (U/mg protein)	1.36±0.11[a]	0.64±0.07[b]	0.77±0.19[a]	1.05±0.31[a]	1.47±0.60[a]
GSH (mM/g tissue)	2.52±0.17[a]	0.93±0.02[b]	1.56±0.87[a]	1.93±0.09[a]	1.95±0.04[a]
TP (mg/ml)	2.97±0.02[a]	2.14±0.01[b]	2.22±0.13[a]	2.37±0.17[a]	2.74±0.11[a]

(d) Heart

Parameter	I	II	III	IV	V
SOD (U/mg protein)	4.31±1.47[a]	2.08±0.75[b]	2.35±0.49[a]	3.63±1.27[a]	4.22±0.43[a]
CAT (U/mg protein)	3.16±0.10[a]	1.90±0.15[b]	2.27±0.19[a]	2.89±0.41[a]	3.02±0.23[a]
GSH (mM/g tissue)	3.89±0.03[a]	1.05±0.05[b]	2.15±1.40[a]	3.24±1.84[a]	2.65±0.02[a]
TP (mg/ml)	6.47±1.21[a]	2.43±0.68[b]	2.77±1.01[a]	3.37±1.17[a]	5.43±1.84[a]

V.amygdalina at 100 mg/kg bw after exposure; V- treated with silymarin at 100 mg/kg bw after exposure. 'b' represents significant difference from the control 'a' at P=0.05 **Table 4: Effect of V. amygdalina leaf on reduced glutathione, total protein and selected antioxidant enzymes activity in CCl_4-exposed rats**

Vernonia amygdalina leaf extract protects against carbon tetrachloride-induced hepatotoxicity

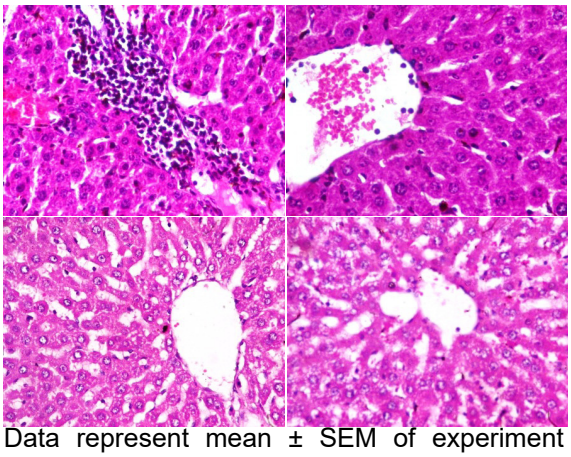

Data represent mean ± SEM of experiment performed in triplicate. I – administered water only; II- administered CCl_4 only; III- treated with V.amygdalina at 50 mg/kg bw after exposure; treated with V.amygdalina at 100 mg/kg bw after exposure; V- treated with silymarin at 100 mg/kg bw after exposure. 'b' represent significant difference from the control 'a' at P=0.05

Figures 1A-D: Histoarchitecture of liver tissue slices of experimental animals under different experimental treatments at a magnification (x400).

1A: Photomicrograph of liver slices of animals that were not exposed to carbon tetrachloride toxicity at all: It shows no sign of histological distortion of the hepatocytes. Tissue histomorphology was normal and nuclei rightly located in the cytoplasm.

1B: Photomicrograph of liver slices of animals exposed to CCl_4 3 ml /kg bw without treatment. It showed fatty liver with cholestasis.

1C: Photomicrograph of liver slices of animals treated with *V. amygdalina* (100 mg/kg bw) after exposure to CCl_4: It showed no sign of distorted hepatic histoarchitecture.

1D: Photomicrograph of liver slices of animals treated with silymarin at 100 mg/kg bw after initial exposure to CCl_4. It showed unperturbed hepatic histomorphology without any sign of histopathological distortion

DISCUSSION

The ever-increasing global burden of liver and kidney diseases calls for concerted efforts at stemming the tide which may threaten public health if left unchecked. Attainment of the sustainable development goal (SDG) on health requires not only the conventional drugs but the complementary effort of herbal medicines. Animal models of liver and kidney diseases has been routinely used to assess the therapeutic potentials of medicinal plants in managing such diseases. Derangement of lipid profile is a potent toxicity mechanism of several toxicants. Hyperlipidemia has been identified as a major culprit in the onset and progression of cardiovascular diseases (29). Routinely, notable signs of toxicity include: high cholesterol, high triglycerides, high LDL and depleted HDL in exposed animals (29). In the present study, exposure of experimental animals to carbon tetrachloride (Table 1) caused a marked derangement in the lipid profile regardless of the organ involved (Table 2a-d). Specifically, there was a surge in cholesterol level in the liver, kidney heart and serum following exposure to CCl_4. This observation implies that CCl_4 triggered a derangement in critical membrane lipid leading to a compromise in membrane function. However, treatment with *V. amygdalina* leaf extract restored the cholesterol level back to a level comparable with animals treated with silymarin. Undoubtedly, such effect could be linked with the flavonoid and other polyphenols present in the extract. Triglyceride level in the serum and organs homogenates was significantly increased following exposure of experimental animals to CCl_4 (Table 2a-d). However, treatment with *V. amygdalina* leaf extract reversed the trend in a manner that was dose-dependent and comparable to animals treated with silymarin. This further suggests the potential of the plant as an efficacious alternative in the management of multiple organ diseases. Level of high-density lipoprotein has been used to predict the antioxidant status and overall well-being of an animals. In the present study, CCl_4 exposure caused a marked depletion in the level of HDL in the serum, liver, kidney and heart homogenates of experimental animals. This observation points to the free-radical induced depletion of

antioxidants in the animals. Administration of *V. amygdalina*extract relieved the oxidative stress on the organs as the level of HDL was restored to normal. Detailed phytochemical contents of the leaf extract of *V. amygdalina* has been reported. The relief obtained by experimental animals following treatment with the plant extract can be attributed to the flavonoid and polyphenolic content of the plant. On the other hand, low density lipoprotein (LDL) otherwise called 'bad cholesterol' was increased following exposure to CCl_4. Administration of *V. amygdalina* extract brought the LDL level back to basal comparable to silymarin. Invariably, the surge in LDL was due to increased free radicals triggered by the toxicant. Treatment of intoxicated animals with *V. amygdalina* extract relieved the toxicity imposed by CCl_4, further buttressing its potential in the management of diseases related to these organs. Treatment of CCl_4- exposed animals with *V. amygdalina* leaves resulted in a dose-dependent reversal of total cholesterol, triglycerides and LDL-cholesterol in a manner comparable to the negative control and animals treated with the standard drug (Table 2a-d). This is due to the presence of bioactive ingredients such as flavonoids in the extract.

Monitoring the integrity of liver and kidney involves the assessment of specific biomarkers such as ALP, ALT and AST (30). Whenever there is an unusual increase in the level of these biomarkers in the blood, hepatic injury can be inferred (31). In the present study, the significant increase in ALP in the serum and organs homogenates following exposure to CCl_4 toxicity (Table 3a-d) could be as a result of obstruction in bile flow, heart failure, dehydration and decrease in renal blood flow (32). The most fundamental explanation is that CCl_4 deranged the membrane lipid profile, hence, these biomarkers that are normally compartmentalized within membrane bound cell, got leaked into the bloodstream, leading to an elevation in their level in the serum. Treatment with *V. amygdalina* leaves extract caused a dose-dependent restoration of these biomarkers suggesting a curative effect on the organ injury caused by the toxicant. This effect can be linked to the presence of antioxidant phytochemicals present in the extract. Bilirubin is a product of heme degradation in the spleen, liver and bone marrow. Under normal circumstance, bilirubin is conjugated with glucuronic acid to form a soluble product that is excreted. An unusually high bilirubin is a typical of an injured liver or too high level of heme degradation. Serum and liver bilirubin levels of experimental rats exposed to CCl_4 toxicity were significantly increased relative to the control. This perhaps suggests that the toxicant upregulates heme degradation causing a derangement in the process. It can also be traced to the free radical induced oxidative injury on the hepatocytes. Administration of *V. amygdalina* leaves extract relieved the toxicity imposed by the toxicant restoring the bilirubin level to that comparable with animals that were not exposed at all (Table 3a-d). This indicates the potential of the plant as therapeutic remedy for liver diseases.

Urea, one of the products of nitrogen metabolism in mammals has been employed as a routine marker for chronic kidney diseases (33). In the present study, intoxicated animals that were treated with graded doses of V. amygdalina showed signs of recovery as indicated in the reversal of urea to levels comparable with animals treated with silymarin (Table 3a-d). This suggests the presence of antioxidant phytochemicals such as flavonoids and other polyphenols in the extract which produced the observed effect. It also implies the possible therapeutic relevance of the plant in the management of kidney diseases.

Uric acid, the product of purine degradation in humans has been suggested as central to the development of gout (34). Recent reports have suggested an intricate link between high serum level of uric acid and certain pathological conditions such as hypertension, diabetes, obesity and renal insufficiency (34). In the present study, exposure of experimental animals to CCl_4 caused a surge in the serum level of uric acid relative to the control. *V. amygdalina* showed a potent ameliorative effect when administered to animals under the toxic effect of CCl_4. Uric acid level dropped back to levels comparable to

animals that were not exposed to the toxicant, following treatment with *V. amygdalina* leaves extract (Table 3a-d). This suggests the potential of the plant in the management of chronic kidney disease.

Antioxidant enzymes such as superoxide dismutase and catalase (CAT) are critical in shielding the physiological system from the menace of free radicals (35). In terms of mechanism, SOD dismutates superoxide radicals converting it to hydrogen peroxide which is scavenged by catalase (36). In the present study, exposure of experimental animals to CCl_4 resulted in depletion in the level of SOD and catalase in the serum and organs homogenates (Table 4a-d). This is probably due to the surge in the level of superoxide anion radicals occasioned by the toxicant. However, treatment with *V. amygdalina* extract caused a restoration of SOD and CAT levels to that comparable with normal animals (Table 4a-d). This implies that certain phytochemicals in the extract exhibited potent antioxidant activity in scavenging both superoxide anions and breaking hydrogen peroxide viz-a-viz the activation of SOD and catalase respectively. This observation can be attributed to the flavonoids and polyphenols present in the extract.

Reduced glutathione GSH is a non-enzymic thiol often used to measure the health status of organism. Any specie that depletes the GSH level of an organism is toxic. In the present study, administration of CCl_4 depleted the GSH level in the serum and organs homogenates suggesting the multiorgan toxicity of CCl_4 (Table 4a-d). However, treatment with *V. amygdalina* leaves extract restored the GSH level in a dose dependent manner comparable to animals treated with silymarin. This suggests that potential of *V. amygdalina* leaves in the management of multiorgan disorders.

Hepatic histoarchitecture distorted by exposure to $CCl_4$was restored by treatment with *V. amygdalina* leaf extract (Figure 1A-D). This is an indication that the oxidative injury inflicted on the liver by $CCl_4$was healed by phytochemical present in the extract, suggesting the medicinal potential of the plant in the treatment of liver diseases.

Conclusion

V. amygdalina leaf extract restored deranged lipid profile, reactivates inhibited antioxidant enzymes and reversed oxidative injury to liver, kidney and heart. Distorted histoarchitecture of the hepatic, renal and cardiac tissues were also restored following treatment with *V. amygdalina*(Figure 1A-D). Hence, the plant is a potential therapeutic agent that can be exploited in the management of diseases relating to these critical organs.

Acknowledgements: Authors wish to acknowledge the support of MrOyelade of the Federal Polytechnic Ado Ekiti.

Declaration of Interest Statement: Authors declare that there is no conflict of interest of any kind.

Funding: The study did not receive any financial support for its execution

References

1. Fakim, A.G. Medicinal plants: Traditions of yesterday and drugs of tomorrow. *Molecular aspects of medicine*, **2006**, 27, 1-93.

2. Hamburger, M. and Hostettmann, K. Bioactivity in plants: the link between phytochemistry and medicine. *Phytochemistry*, **1991** 30, 3864-3874.

3. Singh, P. and Singh, C. L. Chemical investigations of *Clerodendraonfragrans*. *Journal of Indian Chemical Society*, **1981**, 58: 626-627.

4. Rastogi, P. R. and Meharotra, B. N. In Compendium of Indian Medicinal Plants. Vol. I, 339; a) (**1993**) III: 194. PID, CSIR, New Delhi, India.

5. Marcellin, P.; Kutala B.K. Liver diseases: a major, neglected global public health problem requiring urgent actions and large-scale screening. *Liver Int***2018**,38 (Suppl 1):2–6. https://doi.org/10.1111/liv.13682.

6. Mokdad, A.A.; Lopez, A.D.; Shahraz, S.; Lozano, R.; Mokdad, A.H.; Stanaway, J. Liver cirrhosis mortality in 187 countries between 1980 and 2010: a systematic analysis. *BMC Med***2014**;12:145, PMID: 25242656.

7. Stepanova, M.; De Avila, L.; Afendy, M.; Younossi, I.; Pham, H.; Cable, R. Direct and indirect economic burden of chronic liver disease in the United States. *Clin Gastroenterol Hepatol.,* **2017**, 15. 759–766.e5 https://doi.org/10.1016/j.cgh.2016.07.020

8. Levin, A.; Tonelli, M.; Bonventre, J.; Coresh, J; Donner, J.A. Fogo, A.B ISN Global Kidney Health Summit participants. Global kidney health 2017 and beyond: a roadmap for closing gaps in care, research, and policy. *Lancet.***2017**, 390(10105):1888–917. doi: http://dx.doi.org/10.1016/S0140-6736(17)30788-2 PMID: 28434650

9. Kassebaum, N. J.; Arora, M.; Barber, R.M.; Bhutta, Z.A.; Brown J, Carter A.; GBD 2015 DALYs and HALE Collaborators. Global, regional, and national disability-adjusted life-years (DALYs) for 315 diseases and injuries and healthy life expectancy (HALE), 1990-2015: a systematic analysis for the Global Burden of Disease Study 2015. *Lancet*. **2016** 10 8;388(10053):1603–58. doi: http://dx.doi.org/10.1016/S0140-6736(16)31460-X PMID: 27733283

10. Farombi, E. O.; Owoeye, O. Antioxidative and Chemopreventive Properties of Vernonia amygdalina and Garcinia biflavonoid. *International Journal of Environmental Research and Public Health*, **2011,** 8, 2533–2555.

11. Adesanoye, O. A; Farombi, E. O. Hepatoprotective Effects of Vernonia amygdalina (Astereaceae) in Rats Treated with Carbon Tetrachloride. *Experimental and Toxicologic Pathology*, 2010, 62(2), 197–206.

12. Wong, F. C.; Woo, C. C.; Hsu, A; Tan, B. K. H. The Anti-Cancer Activities of Vernonia amygdalina Extract in Human Breast Cancer Cell Lines Are Mediated through Caspase-Dependent and p53-Independent Pathways. *PLOS ONE*, **2013**, 8(10): 1–15.

13. Jan Mohamed, H. J.; Yap, R. W.; Loy, S. L.; Norris, S. A.; Biesma, R, A. -H. J. Prevalence and Determinants of Overweight, Obesity, and Type 2 Diabetes mellitus in Adults in Malaysia. *Asia Pacific Journal Public Health*, **2015**, 27(2): 123–135.

14. Egharevba, C.; Osayemwenre, E.; Imieje, V.; Ahomafor, J.; Akunyuli, C.; Udu-Cosi, A. A.; Theophilus, O.; James, O.; Ali, I.; Falodun, A. Significance of Bitter Leaf (Vernonia amgdalina) In Tropical Diseases and Beyond: A Review. *Malaria Chemotherapy Control and Elimination*, **2014**, 3(1), 1–10.

15. Abdulmalik, O.; Oladapo, O.O.; Bolaji, M.O. Effect of aqueous extract of Vernonia amygdalina on atherosclerosis in rabbits. ARYA *Atherosclerosis*, **2016**, 12(1), 35.

16. Osaretin, A. T.; Ebuehi, M.; Olufemi, A. Neurochemical Impact of the Aqueous Extract of *Vernonia amygdalina* and *Talinum triangulare*on Learning and Memory in Male Wistar Rats.*International Journal of Brain and Cognitive Sciences*, **2017**, 6(5), 81-88. DOI: 10.5923/j.ijbcs.20170605.01

17. Anibijuwon, I. I.; Oladejo, B. O.; Adetitun, D. O.; Kolawole, O. M. Antimicrobial Activities of Vernonia amygdalina against Oral Microbes. *Global Journal of Pharm*acology, **2012**, 6(3), 178–185.

18. Mattenheimer, H. Urinary enzyme measurements in the diagnosis of renal disorders. *AnnClin Lab Sci*., **1981**,11(3),189–201.

19. Reitman, S.; Frankel, S. Glutamic – pyruvate transaminase assay by colorimetric

method. *Am J Clin Pathol.***1957**, 28, 56–60.

20. Englehardt, A. Measurement of alkaline phosphatase. *Aerztl Labor*,1**970**, 16, 42.

21. Trinder, H. A. simple Turbidimetric method for the determination of serum cholesterol. Ann din Biochem., **1969**,6, 165.

22. Tietz, N.W. Clinical guide to laboratory tests. 3rd ed. Philadelphia: Saunders and Co. Publishers; **1995**.

23. Grove, T.H. Effect of reagent pH on determination of high-density lipoprotein cholesterol by precipitation with sodium phosphotungstate-magnesium. *Clin Chem*., **1979**, 25(4), 560–4.

24. Friedewald, W. T.; Levy, R.I.; Fredrickson, D.S. Estimation of the concentration of low-density lipoprotein cholesterol in plasma, without use of their preparative ultracentrifuge. *Clin Chem*. **1972**,18, 499–502.

25. Sinha, A.K. Colorimetric assay of catalase. *Anal Biochem*., **1972**, 47, 89–94.

26. Misra, H.P. The role of superoxide anion in the autoxidation of epinephrine and a simple assay for superoxide dismutase. *J Biol Chem*., **1972**, 247(15), 3170–5.

27. Beutler, E.; Duron, O.; Kelly, B.M. Improved method for the determination of blood glutathione. *J Lab Clin Med*., **1963**, 61, 882–90.

28. Weichselbaum, T. E. An accurate and rapid method for the determination of protein in small amount of blood, serum. *Am J Clin Pathol*., **1995**, 16, 40.

29. Ugwu, P.C.; Okechukwu, F.C.; Nwodo, O. E.; Joshua Parker, E.; Odo Christian, C; Ossai Emmanuel, Effect of Ethanol Leaf Extract of Moringa Oleifera on Lipid Profile of Mice, *Res. J. Pharm. Biol. Chem. Sci*. **2013**, 4 (1), 1324–1332.

30. Kaniaw, R.K.; Esmail, S.K. Hepatorenal function markers alteration in aged and aged related disease in human. *Indian J Public Health Res Dev*., **2020,**11, 844–9.

31. Udem, S.C.; Obidoa, O.; Asuzu, I.U. Acute and chronic toxicity studies of erythrinasenegalensis stem bark extract in mice*, Comp. Clin. Pathol*. **2009,** 19, 275–282.

32. Whitby, L.G.; Percy-Robb, I.W.; Smith, A.F. Enzymes test in diagnosis, Lecture notes On Clinical Chemistry, 3rd ed., Blackwell Sci. Publication, London, **1984**, pp. 138–168 .

33. Claudio, B.; Enrico, A.; Richard, J.; Jan, T.K.; Empar, L.; Giuseppe, M.; Josep, R.; Stack, A.G.; Konstantinos P.T. Hyperuricaemia and gout in cardiovascular, metabolic and kidney disease. *Eur J Intern Med.***2020**,80, 1–11 ISSN 0953–6205. https://doi.org/10.1016/j.ejim.2020.07.006.

34. Xiong, Q.; Liu, J.; Xu, Y. Effects of uric acid on diabetes mellitus and its chronic complications. *Int J Endocrinol.***2019**. https://doi.org/10.1155/2019/9691345.

35. Nandi, A.; Liang-Jun, Y.; Chandan, K.J; Nilanjana D. Role of catalase in oxidative stress- and age-associated degenerative diseases. *Oxidative Med Cell Longev*. **2019**. https://doi.org/10.1155/2019/9613090.

36. Zhang, L.B.; Feng, M.G. Antioxidant enzymes and their contributions to biological control potential of fungal insect pathogens. *Appl Microbiol Biotechnol*. **2018**,102,4995–5004. https://doi.org/10.1007/s00253-018-9033-2.

Current Trends in Biotechnology and Pharmacy
Vol. 16 (4) 553 - 561, Oct 2022, ISSN 0973-8916 (Print), 2230-7303 (Online)
10.5530/ctbp.2022.4.88

Efficacy of Entomopathogenic Fungi *Beauveria bassiana* in Pest Management

Srivani MVK[1], Jalaja N[2]
[1]Department of Chemistry, Vignan's Foundation for Science Technology and Research (Deemed to be University), Vadlamudi, Guntur 522 213, Andhra Pradesh
[2]Department of Biotechnology, Vignans Foundation for Science Technology and Research (Deemed to be University), Vadlamudi, Guntur 522 213, Andhra Pradesh
*Corresponding author: sriani77@gmail.com

Abstract

Indiscriminate application of chemical pesticides to the crops is a major threat today to the environment. Chemical pesticides degrade the environmental quality and drastically affect human health. To address this issue, many studies have been conducted which recommend the use of biopesticides and highlighted the importance of entomopathogenic fungi as biocontrol agents. Application of *Beauveria bassiana* has been found to protect many crops from pests and prevent the dreadful impacts on environmental degradation. Biocontrol agents also play an important role in preventing environmental pollution and therefore used as a component of integrated pest management. Biocontrol agents help for sustainable agroecosystems mostly in tropical regions. It is found naturally, it is cost effective, eco-friendly with antimicrobial properties. The main aim of this review is to outline the importance of *Beauveria bassiana* and highlight its role in controlling the multiple pests and in minimizing the final yield losses.

Keywords: Biopesticide, *Beauveria bassiana*, Mycoinsecticides, Pest control

Introduction

Introducing chemical pesticides into agricultural ecosystems is a serious issue today. Synthetic pesticides are certainly detrimental to the biodiversity as well as environment. They may kill natural enemies of pests, which ultimately would result in the outbreak of pests. Pesticide residues on crops that are being exported are not permissible if they exceed the limits (1). Biopesticides are used to control pests and approximately 175 registered biopesticide ingredients and 700 products are present in the market. The biopesticide market is valued around $200 million in the United States and may increase further. Pesticides also affect predators and insect pollinators that are beneficial to the ecosystem. Insects and pathogens develop resistance to such chemical pesticides within no time by changing their genetic constitution (2). Pesticides contain harmful chemicals that may impact human and environmental health. Pesticide residues enter the foodchain and results in ecological imbalance. This has necessitated the use of biopesticides such as entomopathogenic fungi (EPF) for controlling the insect pests (3). In the tropical and subtropical regions, multiscale microbial diversity infects arthropods and other insects by acting as parasites (4,5). *Beauveria bassiana*, *Metarhizium anisopliae*, *Verticillum hirsutella, Lecanicillium, Isaria* are the commercially available genera which are being used on a wider scale to control insect pests (6,7). Many biopesticides were developed

during the past few years that can concentrate on only target species and eliminate them. They are less toxic than conventional pesticides and thus help to increase the produce. The fungus infects sucking pests like white flies, aphids, thrips, weevils, mealy bugs, and leaf hopper. Many strains that have originated from this genus help in controlling a variety of insects. Toxic substances like bassianolide, beauverolides, bassianin, beauvericin, tenellin, oxalic acid and oosporein produced by these fungi kill the pests. Smallholder farmers cannot afford to buy chemical pesticides and at the same time, they need their food grains with minimum levels of toxicity. In this paper, *B. bassiana*, an entomopathogeneic fungus is reviewed.

Advantages of biopesticides

Microbial biopesticides are biologically toxic substances that come from microorganisms like bacteria and fungi. Global biopesticide production has crossed 3000 tonnes per year. Global market for biopesticides is valued at 3.0 billion US$. This accounts for nearly 5% of the total pesticide market (8,9). The market share of biopesticides may grow further by 2050 equal to that of chemical pesticides (10,11). Biopesticides are cheaper and can avoid resistance problems. Biopesticides kill a variety of pests like locusts, grass hoppers, white flies and termites. They replace the hazardous chemical substances and promote sustainable agriculture. *B. bassiana* is environmentally friendly mycoinsecticide that produces both enzymes and secondary metabolites that play an important role in the biological control of pests. There are thousands of fungal species that can kill insects, spiders and mites (9). Use of biopesticides does not lead to resistance build-up in target pests. *B. bassiana* is one of the best entomopathogenic fungi to control insect pests (12). Different strains of *B. bassiana* play a pivotal role in killing different types of pests. Biological metabolic compounds like tennelin, bassianin, pyridovericin, pyridomacrolidin non-peptide pigment oosporein, non-ribosomally synthesized cyclodepsipeptides (beauvercins and allobeauvercins, bassianolides), and BpL lectin) are being used in industrial, pharmaceutical and agricultural industries. Alkaloids like tennelin (II), bassianin (III) pyridovericin (IV) and pyridomacrolidin (V) are found in *B. bassiana* but their exact function is unknown till now (Table 1).

Brief history, taxonomy and morphology b. bassiana

B. bassiana belongs to the Kingdom Fungi, phylum Ascomycota, class Sordariomycetes, order hypocreales and family Clavicipitaceae (13,14). It was discovered by Bassi Agostino of Lodi, Italy, in 1835 and its role in killing pests (15), though others considered that it belongs to Cordycipitaceae or Ophiocordicipitaceae (16,17). The fungus is a saprophyte, and of terrigenous origin. It infects many insect orders like Lepidoptera, Hemiptera, Coleoptera, Hymenoptera, Homoptera, and Orthoptera (18,19). The spores of this fungus are called conidia which are white to yellowish in colour with septal filaments. Diverse types of conidia are produced by *B. bassiana* with different environmental conditions. The diameter of hyphae varies from 2.5 µm to 25 µm. Both conidiophores and blastophores are infectious organs (19,20,21).

Mode of action of the fungus

Mascarin and Jaronski (22) have studied in detail about the mode of infection of *B. bassiana*. Conidia are generally dispersed either by wind or rain or even by arthropod vectors which helps the asexual spores to colonize on the susceptible hosts (23). Infection of the fungus on the host is generally by adhesion, germination, differentiation, penetration and dissemination. Conidia first recognize the host cuticle cells by electrostatic and chemical forces which then produce mucilage and germinate (22,24,25). Under ideal conditions, conidia germinate, pegs penetrate into the cuticle. The germ tub now forms a structure called an enlarged cell or appressorium (24,25). Penetration peg secrets hydrolytic enzymes

such as proteases, chitinases, lipases which then dissolve the cuticle for easy penetration into insect hemolymph. The fungus grows into a single-celled organism and starts destroying the host tissues. The conidia produced from the dead host are generally carried away with the air and are capable of infecting other hosts (26,27). The fungus also produces toxins like beauvericin, beauverolides, bassinolides and isarolides which can help in the invasion of the fungus (28). Once the insect dies, the fungus now starts producing a secondary metabolite called oosporein. Initially it was believed that it functions as an insect toxin. Now it appears that this compound functions after the death of the host to counter any bacterial competition on the host corpse. This permits the fungus to utilize the nutrients and also complete the life cycle (25). Production of oosporein is modulated by a cascade of transcription factors with BbSmr1 (putative methyltransferase) acting at the upstream as a negative regulator, but triggering other genes associated in the oosporein synthesis (29,30).

S. No		Strain	Effects
1		Bba 5653	Virulent to diamond back moth and kills cater pillars
		19, 1205, 1215	Controls F. oxysporum, f.ps lycopersici race 3 in tomato plants
		Bb GHA strain	Kills variety of insects and weakens insects outer coat and kill them
		CNPMF 407, CNPMF 218, and CNPMF 416	Play an important role in preventing pests. CNPMF 218 controls C. sordidus (banana weevil)
		Bb (202)	Kills plant sucking insects (31)
		PPRI 5339	Mortality of eggs and motile stages (valuation of two entomopathogenic fungi, *B. bassiana* and *Metarhizium anisopliae*, for the control of carmine spider mite, *Tetranychus cinnabarinus* (Boisduval) under greenhouse conditions.
		B. bassian a 146 strain	Effects eggs and larvae of Castniid Palm borer
		Native strain of B.bassian a NI8ARSEF8889	Shows effect on on green lace wigs, Chrysoperla rufilabris
		B. bassiana GHA (ARSEF3620, ATCC74250) GHA	Fungal biocontrol agents Effects insects and pests
		B.b -COO1	Infects T. infetants (32)
2	Bioactive metabolic compounds	N-decane,1-pentadecene, alkylbenzene derivatives and methyl -alkyl ketones (33) B. bassiana extracts of ethyl acetate and acetone	Shows antimicrobial,snailicidal and antioxidant activities

Efficacy of entomopathogenic fungi *Beauveria bassiana* in pest management

3	Biologically active metabolites	Tennelin, bassianin, pyridovericin, pyridomacrolidin Non-peptide pigment oosporein Non-ribosomally synthesized cyclodepsipeptides (beauvercins and allobeauvercins, bassianolides), and BpL lectin) Beauvericin A (2) and beauvericin A (3) two novel cyclodepsipepdide analogues (35) B. bassiana-22 B. bassiana- 28	Used in industrial, pharmaceutical and agriculture industries (34) Act against Gram positive bacteria and mycobacteria Effects different stages of larvae and targets several insects like root weevils, plant hoppers, spittle bugs, white grubs. Effective against CX. Quinquefasciatus pupae (36)
4	Volatile organic compounds	Diisopropyl naphthalenes Ethanol sesquiterpenes benzene acetal dehyde 1-pentadecene and methyl alkyl ketones (33)	Used as tool for detection of fungusbased on their characteristic capillary gas chromatography and mass spectrometry
5	Alkaloids	Alkaloids like tennelin (II), bassianin (III) pyridovericin (IV) and pyridomacrolidin (V) have been identified Tennelin (II), bassianin (III) (37), pyridovericin (IV) and pyridomacrolidin (V) have been found (38,39)	Exact role in fungal interaction with the host is unknown till now
6	Pigments	2-pyridone alkaloids tennelin (II) and bassianin (III), a red pigment-dibenzoquinone pigment oosporein (VI) (40)	They have antimicrobial and antiviral properties. They are yellow in colour.

Table 1. Beauveria bassiana compounds and their activities

Applications of beauveria bassiana

Spores of *B. bassiana* do not develop at high temperatures, and optimum is 18 and 29 ^{0}C. It can be used in association with other natural enemies, pathogens and pesticides (41,42,43). Spores produced by the fungus are applied to the affected crops in the form of emulsified suspension or wet powder. Fungal conidia treated with oosporein has been found highly effective against Aphididae, Cercopidae, Coleoptera, Delphaacidae, and Lepidoptera (44,45). Further, protein extract of the *B. bassiana* as granule can be mixed with inorganic material or emulsifiable concentrates.

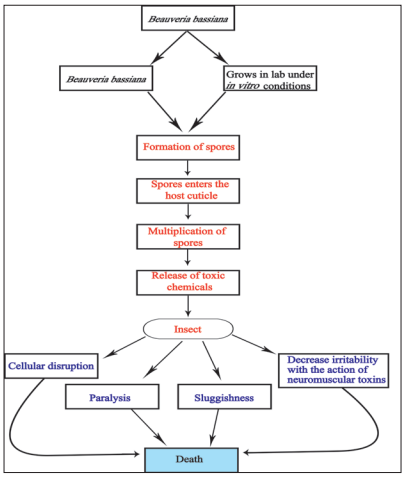

Such formulations have been found effective against many insect pests (46).

Figure 1. Flow chart depicts the mechanism of action of Beauveria bassiana in killing the pests.

Genetic tinkering and fungal toxicity improvement

It is vital for us to improve the fungus genetically so that it can survive under harsh environments like heavy rain, photooxidative stress and ultraviolet light (47). Glare et al. (48) stressed the need for finding out the genes associated with virulence. Though genetic diversity among *B. bassiana* isolates is very high (49), finding target genes is still a challenge. It appears that protease-related genes and their transcription factors are crucial for improving the virulence of *B. bassiana*. Screening of the differentilly expressed genes has been carried out (50,51), which may help to scrutinize mutants and the associated virulence genes. It is now possible to obtain lines with better virulence by gene manipulation techniques such as CRISPR-Cas9 (52,53). Protein engineering can also be thought over for modulating the target proteins and to obtain strains with superior virulence to insect pests (54).

Conclusions

One of the most interesting integrated pest management practices is the use of *B. bassiana* entomopathogenic fungus which kills diverse types of insects in agricultural crops. It is found naturally in soil and can be cultured in the aboratory on a large scale. The insecticidal activity of *B. bassiana* is rapid compared to other fungi and an added advantage of this fungus is, conidia can be preserved for a long time. It is very simple to culture and strains of *B. bassiana* can be maintained in a laboratory conditions. It does not harm mammals, birds and human beings and other non-target organisms. So, the organism can be used effectively against a wide spectrum of insect pests for sustainable development. Its extract if sprayed on crop plants as an elicitor might help them to protect against insect pathogens. Bioactive compounds like oosporein, oxalic acid and tenellin must be exploited as emulsified wet powder. Further, strategies must be evolved to make genetically modified *B. bassiana* that is highly virulent to insects, but does not harm the environment.

Availability of data and materials The material used in this manuscript is available with the author.

Competing interest Authors declare no competing interest.

Funding This manuscript is not financially supported by any external funding agency.

Acknowledgements I thank the management of Vignan's Foundation for Science Technology and Research (deemed to be university) for their encouragement.

References

1. Bailey A., Chandler, D., Grant, W. P., Greaves, J., Prince, G., Tatchell, M (2010). Biopesticides: pest management and regulation (Wallingford, UK: CABI). doi: 10.1079/9781845935597.0000

2. Akutse KS, Subramanian S, Maniania NK, Dubois T and Ekesi S (2020) Biopesticide research and product development in Africa for sustainable agriculture and food security – experiences from the international centre of insect physiology and ecology (icipe). Front. Sustain. Food Syst. 4, 563016. doi: 10.3389/fsufs.2020.563016

3. Inglis GD, Goettel MS, Butt TM, Strasser H (2001) Use of hyphomycetous fungi for managing insect pests. In: Butt TM, Jackson C, Magan N (eds). Fungi as biocontrol agents. Progress, problems and potential. CABI Publishing Wallingford. Pp. 23-69.

4. Thompson, L. R., Sanders, J. G., McDonald, D., Amir, A., Ladau, J., Locey, K. J., et al. (2017). A communal catalogue reveals Earth's multiscale microbial

diversity. Nature 551, 457-463. doi: 10.1038/nature24621

5. Mahe, F., de Vargas, C., Bass, D., Czech, L., Stamatakis, A., Lara, E., et al. (2017). Parasites dominate hyperdiverse soil protist communities in Neotropical rainforests. Nat. Ecol. Evol. 1, 0091. doi: 10.1038/s41559-017-0091

6. Kumar KK., Sridhar, J., Murali-Baskaran, RK., Senthil-Nathan, S., Kaushal, P., Dara, SK., et al. (2018). Microbial biopesticides for insect pest management in India: current status and future prospects. J. Invertebr. Pathol. 165, 74-81. doi: 10.1016/j.jip.2018.10.008

7. Mascarin GM., Lopes, R. B., Delalibera, I., Fernandes, EKK., Luz, C., Faria, M. (2019). Current status and perspectives of fungal entomopathogens used for microbial control of arthropod pests in Brazil. J. Invertebr. Pathol. 165, 46-53. doi: 10.1016/j.jip.2018.01.001

8. Marrone PG (2014). The market and potential for biopesticides. In Biopesticides: State of the art and future opportunities. Eds AD Gross, JR Coats, SO Duke, JN Seiber (Washington DC, USA: American Chemical Society), 245-258.

9. Ebani VV, Mancianti F (2021). Entomopathogenic fungi and bacteria in a veterinary perspective. Biology (Basel). 10(6): 479. doi: 10.3390/biology10060479.

10. Olson S. (2015). An analysis of the biopesticide market now and where is going. Outlook. Pest Manag. 26, 203-206. doi: 10.1564/v26_oct_04

11. Dalmas, CA, Koutroubas, SD (2018). Current status and recent developments in biopesticide use. Agriculture 8, 13. doi: 10.3390/agriculture8010013

12. Thomas MB, Read AF (2007). Can fungal biopesticides control malaria? Nat. Rev. Microbiol. 5, 377-383.

13. Sung JM, Lee JO, Humber RA, et al. (2006). *Cordyceps bassiana* and production of stromata in vitro showing *Beauveria anamorph* in Korea. Mycobiology. 34, 1-6.

14. Halouane F (2008). Basic research on the entomopathogen *Beauveria bassiana* (Bals.-Criv.) Vuill. (Ascomycota: Hypocreales): bioecology, production and application on *Schistocerca gregaria* (Forskål, 1775) and *Locusta migratoria* (Linné, 1758) (Orthoptera, Acrididae). http://hdl.handle.net/123456789/784.

15. Lord JC (2005) From Metchnikoff to Monsanto and beyond: the path of microbial control. J Invertebr Pathol. 89, 19-29.

16. Sensagent (2000-2016). Online encyclopedia, dictionary Parisien. Paris: Sensagent; 2000-2016.

17. Vigneshwaran V (2015). Entamopathogenic fungi as biocontrol agents – a special focus on *Beauveria bassiana* and *Hirsutella*. https://www.slideshare.net/VigneshWaran16/entamopathogenic-fungi-as-biocontrol-agents-a-special focus-on-beauveria-bassiana-and-hirsutella. Access 1 Dec 2019.

18. Li ZZ, Li CR, Huang B, et al. (2001). Discovery and demonstration of the teleomorph of *Beauveria bassiana* (Bals.) Vuill., an important entomogenous fungus. Chin Sci Bull. 46, 751-753.

19. Sabbahi R (2008). Use of the entomopathogenic fungus *Beauveria bassiana* in a strategy of phytosanitary management of the main insect pests in strawberry plantations. University of Quebec, Quebec, Canada.

20. Weiser J (1972). *Beauveria Vuill*. In:

Table 5: Most highly cited publications

Nemoci H, editor. Insect diseases. Prag, Czech: Academic Press; pp. 361-377.

21. Lipa JJ (1975). White muscardine (*Beauveria* sp.). In: Lipa JJ, editor. An outline of insect pathology. Warsaw: Foreign Sciences Publications. Dept NCSTEI; pp. 139-142.

22. Mascarin MG, Jaronski TS (2016). The production and uses of *Beauveria bassiana* as a microbial insecticide. World J Microbiol Biotechnol. 32, 1-26.

23. Ortiz-Urquiza A, Keyhani NO (2013). Action on the surface: entomopathogenic fungi versus the insect cuticle. Insects 4, 357-374. https://doi.org/10.3390/insects4030357.

24. Wraight RJ, Roberts DW (1987). Insect control effort with fungi. Dev Ind Microbiol. 28, 77-87.

25. De Kouassi M (2001). The possibilities of microbiological control, Vertigo. The Electronic Journal in Environmental Science Online 2, 1-18. https://doi.org/10.4000/vertigo.4091.

26. Feng P., Shang, Y., Cen, K., Wang, C (2015). Fungal biosynthesis of the bibenzoquinone oosporein to evade insect immunity. Proc. Natl. Acad. Sci. U.S.A. 112, 11365-11370. doi: 10.1073/pnas.1503200112

27. Pedrini N (2018). Molecular interactions between entomopathogenic fungi (Hypocreales) and their insect host: perspectives from stressful cuticle and hemolymph battlefields and the potential of dual RNA sequencing for future studies. Fungal. Biol. 122, 538-545. doi: 10.1016/j.funbio.2017.10.003.

28. Hajek AE, St. Leger RJ (1994). Interactions between fungal pathogens and insect hosts. Annu. Rev. Entomol. 39, 293-322

29. Qin Y., Ortiz-Urquiza, A., Keyhani NO (2014). A putative methyltransferase, mtrA, contributes to development, spore viability, protein secretion and virulence in the entomopathogenic fungus *Beauveria bassiana*. Microbiology 160, 2526-2537. doi: 10.1099/mic.0.078469-0.

30. Fan Y, Liu X, Keyhani NO, Tang G, Pei Y, Zhang W, Tong S (2017). Regulatory cascade and biological activity of *Beauveria bassiana* oosporein that limits bacterial growth after host death. Proc. Natl. Acad. Sci. USA 114, E1578-E1586. doi: 10.1073/pnas.1616543114.

31. Ali BG, Wang B, Cao N, Hua FL (2018) Pathogenicity of *Beauveria bassiana* strain 202 against sap-sucking insect pests. Plant Protection Science 54, 111-117.

32. Baldiviezo LV et al. (2020) Isolation of *Beauveria bassiana* from the Chagas disease vector *Triatoma infestans* in the Gran Chaco region of Argentina: Assessment of gene expression during host-pathogen interaction. Journal of Fungi 64, 219.

33. Crespo R, Pedrini N, Juárez MP, Dal Bello GM (2008). Volatile organic compounds released by the entomopathogenic fungus *Beauveria bassiana*. Microbiol Res. 163: 148-151.

34. Xu Y, Orozco R, Kithsiri WEM, Espinosa AP, Leslie GAA, Patricia SS, Molnár I (2009) Biosynthesis of the cyclooligomer depsipeptide bassianolide, an insecticidal virulence factor of *Beauveria bassiana*. Fungal Genet Biol 46, 353-364.

35. Gupta S, Montllor C, Hwang YS (1995). Isolation of novel beauvericin analogues from the fungus *Beauveria bassiana*. J.

Nat. Prod. 58, 733-738.

36. Vivekanandhan P, et al. (2018) Toxicity of *Beauveria bassiana*-28 mycelial extracts on larvae of *Culex quinquefasciatus* mosquito (Diptera: Culicidae). International journal of Environmental Research and Public Health 15, 440

37. Wat CK, Mcinnes AG, Smith DG, Wright JLC, Vining LC (1977). The yellow pigments of *Beauveria* species. Structures of tenellin and bassianin. Canad J Chem. 55, 4090-4098.

38. Takahashi S, Kakinuma N, Uchida K, Hashimoto R, Yanagisawa T, Nakagawa A (1998a) Pyridovericin and pyridomacrolidin: novel metabolites from entomopathogenic fungi *Beauveria bassiana*. J Antibiotics 51, 596-598.

39. Takahashi S, Uchida K, Kakinuma N, Hashimoto R, Yanagisawa T, Nakagawa A (1998b) The structures of pyridovericin and pyridomacrolidin, new metabolites from the entomopathogenic fungus, *Beauveria bassiana*. J Antibiotics 51, 1051-1054.

40. Basyouni SHE, Brewer D, Vining LC (1968) Pigments of the genus *Beauveria*. Canad J Botany 46, 441-448

41. Shipp JL, Zhang Y, Hunt DWA, Ferguson G (2003) Influence of humidity and greenhouse microclimate on the efficacy of *Beauveria bassiana* (Balsamo) for control of greenhouse arthropod pests. Environ Entomol 32, 1154-1163

42. Goettel MS, Poprawski TJ, Vandenberg JD, Li Z, Roberts DW (1990). Safety to non-target invertebrates of fungal biocontrol agents. In: Laird M, Lacey LA, Davidson EW (eds) Safety of microbial insecticides. CRC, Boca Raton, FL, 209-232.

43. Kouassi M, Coderre D, Todorova SI (2003) Compatibility of zineb, dimethoate and *Beauveria bassiana* (Balsamo) Vuillemin against tarnished plant bug (Hemiptera: Miridae). J Entomol Sci. 38, 359-367

44. Eyal J (1993). Novel toxin producing fungal pathogen and uses. European Patent No. 0570089A1. European Patent Office

45. Eyal J, Mabud MA, Fischbein KL, Walter JF, Osborne LS, Landa Z (1994). Assessment of *Beauveria bassiana* Nov. EO-1 strain, which produces a red pigment for microbial control. Appl Biochem Biotechnol. 44, 65-80.

46. Leckie B, Stewart C (2006). Insecticidal compositions and methods of using the same. U.S. Patent 20070044179 A1.

47. St Leger RJ., Wang C (2010). Genetic engineering of fungal biocontrol agents to achieve greater efficacy against insect pests. Appl. Microbiol. Biotechnol. 85, 901-907. doi: 10.1007/s00253-009-2306-z.

48. Glare, T., Campbell, M., Biggs, P., Winter, D., Durrant, A., McKinnon, A., et al. (2020). Mitochondrial evolution in the entomopathogenic fungal genus *Beauveria*. Arch. Insect. Biochem. Physiol. 105, e21754. doi: 10.1002/arch.21754.

49. Lee S.J., Lee, MR., Kim, S., Kim, JC., Park, SE., Li, D., et al. (2018). Genomic analysis of the insect-killing fungus *Beauveria bassiana* JEF-007 as a biopesticide. Sci. Rep. 8, 12388. doi: 10.1038/s41598-018-30856-1.

50. Luo Z, Li Y, Mousa J, Bruner S, Zhang Y, Pei Y, Keyhani NO. (2015). *Bbmsn2* acts as a pH-dependent negative regulator of secondary metabolite production in the entomopathogenic fungus *Beauveria bassiana*. Environ Microbiol. 17, 1189–

1202.

51. Rangel, D. E., Braga, G. U., Fernandes, ÉK., Keyser, C. A., Hallsworth, J. E., Roberts, D. W. (2015b). Stress tolerance and virulence of insect-pathogenic fungi are determined by environmental conditions during conidial formation. Curr. Genet. 61, 383-404.

52. Xiao, G., Ying, S. H., Zheng, P., Wang, Z. L., Zhang, S., Xie, X. Q., et al. (2012). Genomic perspectives on the evolution of fungal entomopathogenicity in *Beauveria bassiana*. Sci. Rep. 2:483. doi: 10.1038/srep00483

53. Raya-Díaz, S., Sánchez-Rodríguez, A.R., Segura-Fernández, J.M., Del Campillo, MDC., Quesada-Moraga, E. (2017). Entomopathogenic fungi based mechanisms for improved Fe nutrition in sorghum plants grown on calcareous substrates. PLoS One 12, e0185903. doi: 10.1371/journal.pone. 0185903.

54. Wang H, Peng H, Li W, Cheng P and Gong M (2021) The toxins of *Beauveria bassiana* and the strategies to improve their virulence to insects. Front. Microbiol. 12, 705343. doi: 10.3389/fmicb.2021.705343

Current Trends in Biotechnology and Pharmacy
Vol. 16 (4) 562 - 576, Oct 2022, ISSN 0973-8916 (Print), 2230-7303 (Online)
10.5530/ctbp.2022.4.89

Cardiovascular Toxicity of Oral Antidiabetic Drugs and the Efficacy of Natural Organosulfure Compounds from Aged Garlic Extract (AGE)

Kumkum Sharma, Vibha Rani *

Department of Biotechnology
Jaypee Institute of Information Technology, Noida, Sector- 62, Uttar Pradesh, India
Corresponding Author: : vibharanijiit@gmail.com

Abstract

The cardiovascular toxicity of oral antidiabetic drugs has become a major concern for patient with type-II diabetes, which demands investigation of the potential natural products to reduce the toxicity of these drugs and improve their efficacy. In the present study, we investigated the metabolic and oxidative stress of oral antidiabetic drugs on cardiovascular system; we evaluated the antioxidative and cardioprotective efficacy of aged garlic (AGE) against drug-induced cardiotoxicity. Metabolic stress of selected classes of antidiabetic drug classes including; biguanides (BG), sulfonylureas (SU), glucagon-like peptide-1 (GLP-1) agonists, dipeptidyl peptidase-4 inhibitors (DPP4-I), thiazolidinediones and sodium/glucose cotransporter-2 inhibitors (SGLT-2) was evaluated by MTT cell viability assay on the H9c2 cardiac cell line. Pre-cytotoxic dose, transition dose and cytotoxic dose of each drug were optimized by MTT assay. The results were further validated by morphological analysis at cardiotoxic doses by giemsa staining and trypan blue dye exclusion assay in a six-well plate experiment. Nuclear alterations and oxidative stress excreted by each drug was evaluated by DAPI and DCFH-DA assay respectively. To evaluate the cardioprotective efficacy of AGE, cell viability assay was performed for each drug co-incubated with 30μM AGE for 48h in MTT plates. The study confirms that SU, DPP-IV and TZD exert metabolic toxicity on cardiac cells by elevating the oxidative stress, morphological, nuclear damage. SGL-2 and GLP-1 were found to be moderately cardiotoxic, while biguanide was found to be cardioprotective. Aged garlic, an antioxidative molecule with stable sulfur compounds was found to exert cardioprotective effect for SU and TZD, it was found to suppress cell death and increase the cell viability by significantly reducing the oxidative stress of antidiabetic drugs. We concluded that aged garlic can be supplemented with anti-diabetic drugs to suppress the cardiotoxic effect of antidiabetic drugs in future drug therapeutics.

Keyword: Diabetes, Antidiabetic drugs, Toxicity, Diabetic cardiomyopathy, Phototherapeutics, Aged garlic, Organosulfur compounds.

Introduction

Diabetes is a chronic metabolic disorder characterized by unregulated blood glucose, which over time promotes cardiac hypertrophy, a condition known as diabetic cardiomyopathy (1). The global diabetic prevalence in 2020 is estimated to be 9.3%, rising to 10.2% by 2030 and 10.9% by 2045 (2). The impact of diabetes mellitus on cardiac function is chronic and silent with prevalence rate 19% to 26% (3-6). With diabetes, Antidiabetic drug-induced cardiotoxicity have found to

induce asymptomatic cardiac complications and worsened the clinical outcome allied with heart failure for patients with diabetes than for those without diabetes. Public health guide to manage hyperglycemia uses first line, second line and third line medication to manage glucose concentration; however no permanent cure is available till date (7). Several clinically approved oral antidiabetic drugs of different classes are only available treatment to regulate the glucose level and prescribed directly after the diagnosis. These drugs are consumed for years to prevent the severity of disease but their chronic accumulation and toxicity to heart tissues is also important to be investigated (8). However, limited information is available for the effect of these drugs on cardiovascular system including cardiac metabolic activity, oxidative stress, hypertrophy, ischemic heart disease, and diabetic cardiomyopathy (9-10). With cardiomyopathy, antidiabetic drug inducing cardiotoxicity has become a major problem in patients suffering with diabetes and eventually increases the risk of cardiac complications and becomes an additional threat of heart attack for diabetic patient (11).

The antidiabetic medications prescribed to the patients with type II diabetes mellitus (TIIDM) has revolutionized in recent years. Metformin is considered to be the first-line therapy if dietary and lifestyle modifications are controlled. Other antidiabetic drugs include sulfonylureas (SUs), thiazolidinedione's (TZDs), dipeptidyl peptidase-4 (DPP-4) inhibitors, sodium–glucose cotransporter 2 (SGLT-2) inhibitors, glucagon-like peptide 1 receptor agonists (GLP-1 RAs), and insulin are the second and third line of medication (11). These six classes of antidiabetic drugs are currently approved for the treatment of diabetes and widely prescribed (12). All of these drugs exerts different molecular mechanism to regulate the blood glucose of diabetic patient. Such as; Metformin works by reduction of gluconeogenesis in the liver and increases the insulin sensitivity **(**13). Sulfonylureas are the second class of drugs commonly prescribed with metformin and work by blocking potassium ion channels of beta cells resulting in depolarization and opining of calcium ion channels. The concentration of calcium ions increases intracellularly causing the release of insulin granules outside the cell (14). Thiazolidinediones exert their antidiabetic effect through a mechanism involved in activation of peroxisome proliferator-activated receptor (PPAR-γ), nuclear receptor that reduce insulin resistance in adipose tissue, muscle and liver (15). Dipeptidyl Peptidase-4 (Dpp-4) Inhibitors increase incretin levels, which inhibits glucagon release and increase insulin secretion. **α**-glucosidase inhibitors inhibit **α**-glucosidase and reduce carbohydrate digestion in intestine (16). Additional to these drugs, anticonvulsant drugs are also prescribed to the patient with diabetic nephropathy (17-18). All of these drugs have different mechanism to keep blood glucose level in moderation but their accumulative effect on the cardiovascular system is still not evaluated mechanistically. The toxicity of these drugs can be hidden when the safety testing is only done on healthy hearts but becomes toxic when in a diseased state. These drugs need to be clinically explored for their toxicity on cardiovascular system to prevent other drug induced severity.

Although the cardioprotective efficacy of medicinal plants has been raised over the years. The possible herb-drug synergistic interaction can proved a potential therapeutic effect with lower toxicity to other organs. Garlic (Allium sativum L.) has been consumed in india from ancient time as a medicinal food for preventing disease and promoting heath (19). Though consuming garlic to attain its therapeutic efficacy also has limitation because of the pungent smell and indigestion. Aged Garlic Extract (AGE) is a derivative of garlic prepared by aging the garlic cloves for twenty months (20-21). Aging of garlic converts reactive organosulfur compounds into stable compounds such as S-allyl cysteine (SAC), Diallyl disulfide (DADS), S-allyl mercapto cysteine (SAMC) etc. These newly formed

allyl compound believe to have exceptional therapeutic benefit as of the raw garlic. Our previous studies suggest the antioxidative and cardioprotective efficacy of aged garlic extract (AGE) over raw garlic. The stable organosulfur compounds present in aged garlic were found to have exceptional therapeutic benefits in our previous studies (21). The present study was designed to evaluate the metabolic toxicity of antidiabetic drugs on cardiovascular system and to investigate the protective herb-drug synergy of AGE with antidiabetic drugs to reduce the cardiovascular toxicity and improve antidiabetic therapeutics for future treatment of diabetes.

Materials and Methods

All chemicals used in the present study were obtained from Sigma Aldrich unless or otherwise stated specifically.

H9c2 cell line maintenance

H9c2 cardiomyocytes derived from rat heart were procured from the National Centre for Cell Science (NCCS), Pune. The cells were grown in Dulbecco's Modified Eagle's Medium (DMEM) and supplemented with antibiotics and 10% Fetal Bovine Serum (FBS). The cells were kept in a CO2 humidified incubator (New Brunswick Scientific, USA) containing 5% CO2 and maintained at 37 °C. Cells were subcultured routinely and seeded for experiments or maintained as a running culture with a split ratio of 1:3, up to 10 passages per revived stock.

Sample preparation

Stock and working samples of selected antidiabetic drugs were prepared by dissolving in their respective solvent. Biguanides (50mg/ml), sodium/glucose cotransporter-2 inhibitors (50mg/ml) and dipeptidyl peptidase-4 inhibitors (DPP4-I) (50mg/ml) were solubilized in water. Sulfonylureas (50mg/ml) and glucagon-like peptide-1 (GLP-1) agonists (50mg/ml) were solubilized in ethanol. Thiazolidinediones (50mg/ml) was solubilized in acetone. All the drug samples were sterilized and stored at -2^{0}C before treatment.

Cell cytotoxicity assay

It is a colorimetric assay that quantitate the capacity of reducing 3-(4,5-Dimethylthiazol-2-yl)-2,5-Diphenyltetrazolium Bromide (MTT) dye by living cell mitochondrial reductase enzymes to purple formazan crystals within the cells (23). DMSO is added to solubilize the insoluble formazan crystals into the media and the cell viability is calculated based on the color formation. To measure the cell viability and optimizing doses of the selected antidiabetic drugs along with AGE, cardiomyoblasts were seeded in a 96-welled culture plates at a density of ~ 8000 cells/well. Treatments with increasing concentrations of drugs with and without AGE were given and incubated for 48 h. The induced cells were then stained with 5 mg/ml MTT dye for 3 h after the respective treatment period followed by adding DMSO to solubilize the formazan crystals produced in the cells in the suspension of the culture plate wells. Absorbance of the crystals formed was measured at 570 nm using a microplate reader (BioRad Laboratories, USA). Untreated, control and Treated cell viability was calculated at each dose as (absorbance of treated sample) / (absorbance of control). The results were graphically represented as dose versus percent cellular viability.

Cell viability = Absorbance of sample - Blank / Absorbance of control – Blank

Morphological analysis

H9c2 cardiomyocytes were cultured in a six-well plate for morphological, nuclear, and oxidative stress analysis. ~70% confluent cells was trypsinised and centrifuged at 1500 RPM for 10 minutes. Cell pallet was resuspended uniformly and added in each of the six well and the cells were allowed to adhere for 24 hr. After 24 hr, cells were incubated with different concentrations of aged garlic methanolic extract for 48 hr.

A giemsa staining

Giemsa is a polychromatic stain which stains the nucleus pinkish in colour and the cytoplasm in greyish blue, and used to study the morphology and nuclear integrity of cells. Giemsa has high affinity for the phosphate groups present in DNA and gets attached to the regions of DNA with high adenine–thymine bonding. Cells in different experimental sets were treated followed by rinsing the cells with 1× phosphate buffer saline (PBS) and fixing the cells with 100% cold methanol at - 20°C. 5% giemsa stain (prepared in 1% acetic acid) was then added to each experimental set and kept with gentle shaking 25°C for 15 min. Cells were then observed for morphological alterations at the cellular, cytoplasmic and nuclear level. Images were captured using an inverted microscope at 40× magnification.

B trypan blue dye exclusion assay

Trypan blue stain a diazo dye that specifically stains dead cells blue by binding to the negative charge present on the altered membrane. The stain cannot penetrate the membrane of live cells and hence this technique is named as dye exclusion assay. It is a kind of cell viability assay and in the present study, experimental doses derived from MTT assay were validated using trypan blue dye. Treated cells were trypsinized and resuspended in 1X PBS. 0.4% Trypan blue stain was added in 1:1 ratio and allowed to stand at room temperature for 5 minutes. Total numbers of viable cells were counted and calculated using the formulas mentioned below. The stain was also eluted from the cells using NaOH and quantitated at 595 nm using enzyme-linked immunoassay (ELISA) microplate reader.

Cell viability = Absorbance of sample - Blank / Absorbance of control – Blank

C 4',6-diamidino-2-phenylindoleand or DAPI staining

DAPI is 4',6-diamidino-2-phenylindoleand is a freely permeable blue fluorescent dye. It predominantly stains dsDNA by binding to the A-T rich regions of DNA. This DNA binding results in enhanced florescence in the DAPI filter. Cells grown on coverslips were fixed by methanol fixation and 50 ng/ml DAPI dye was added to the experimental sets. Cells were incubated for 15 minutes at 25°C with gentle shaking in dark. Coverslips were mounted on glass slides and observed under a fluorescent microscope at 100X magnification. The fluorescence intensity was also recorded by spectrofluorometer for the eluted stain from the cells.

Dichloro-dihydro-fluorescein diacetate assay

DCFH stain used to identify and quantify the intracellular H_2O_2 generated upon any stress or oxidative imbalance. This assay is based on the conversion of the nonfluorescent DCFH-DA to 2', 7'- dichlorfluorescein (DCF), a fluorescent compound in presence of excessive peroxides and its increased concentration represents the presence of excessive ROS inside the cells. Cells were fixed with methanol and incubated with 3 µg/ml of DCFH-DA stained in the dark with gentle rocking at room temperature. The stain was eluted and net fluorescence from both detached and adherent cells was measured using a spectrofluorometer at the excitation at 480 nm and an emission wavelength of 530 nm.

Statistical analysis

All experiment were conducted in triplicate and three independent experiments were performed for the quantitative analysis of the data obtained and expressed as mean ± SD. Two-way ANOVA and Student's t-test were done to evaluate the significance of differences in the data obtained. P value less than 0.05 ($p < 0.05$) was considered as statistically significant.

Results and Discussion

In the present study we selected twelve

different drug compounds of six antidiabetic drug classes (Table 1). Cardiotoxic index of these drugs were optimized by incubating the drugs with H9c2 cardiac cell line for 48h in MTT cell viability assay. Morphological and nuclear modulation at optimized doses was then observed. The cell viability and oxidative stress analysis at each doses were observed by DCFH-DA assay.

Table 1. Selected Anti-diabetic Drugs

Class of antidiabetic Drugs	Mechanism of action	Selected Drugs
Biguanide	Inhibition of hepatic glucose production and promotion of skeletal muscle glucose uptake.	Metformin Glucophage
Sulfonylureas (SU)	Depolarization of the beta cell membrane to increase insulin secretion.	Glipizide Glimepiride
Glucagon-like peptide (GLP-1) agonist	Activation of the GLP-1 receptor to augment insulin secretion and inhibit glucagon secretion.	Exenatide Liraglutide
Dipeptidyl peptidase 4 (DPP-IV) inhibitor	Inhibition of endogenous GLP-1 inactivation to augment insulin secretion and inhibit glucagon secretion.	Sitagliptin Vidagliptin
Thiazolidinedione (TZD)	Activation of nuclear receptor peroxisome proliferator activated receptor gamma (PPAR) to increase adiponectin and improve insulin resistance.	Rosiglitazone Pioglitazone
Sodium-glucose-co-transporter inhibitors (SGLT-2)	Inhibition of renal glucose reabsorption.	Canagliflozin Dapagliflozin

a. Biguanides were found to be the least cardiotoxic anti-diabetic drugs.

Biguanide is recommended as the first-line drug for type 2 diabetes mellitus (T2DM) by most international guidelines. The preference for biguanide over other available drugs is based on its efficacy on blood glucose control, tolerability, and safety. Moreover, being derived from the plant *Galega officinalis*, biguanides has a favorable effect on several risk factors on cardiovascular system. In this study, it was observed that biguanides or metformin exerts cardiotoxicity as compared to other classes (24). The cardiovascular outcome of biguanides was found to be safe and did not cause toxic effects on cardiovascular system even at high concentration. Two biguanide compositions namely; Metformin (Met) and Glucophage (Glu) were selected for MTT cell viability assay with concentrations ranging from 5 to 150 µM. The cell viability of cardiomyoblasts treated with increasing concentrations of Met and Glu was derived in comparison to control nontreated cells with 100% cell viability. The IC-50 doses, where cell viability was reduced up to ~50%, were derived for Met and Glu as 100 µM (Fig. 1). No

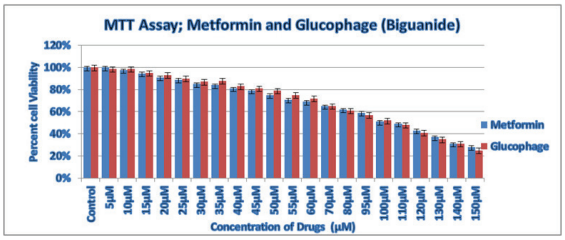

Figure 1. Dose dependent MTT cell viability assay to derive the cardiotoxic doses of Biguanide: a concentrations ranging from 5 µM to 150 µM of metformin and were used and 80 µM was selected as an IC-50 dose. Percent cell viability was compared with respect to Water as a control.

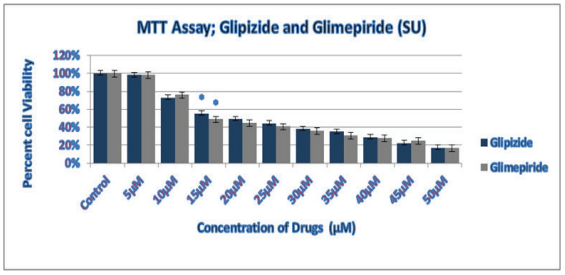

Figure 2. Dose dependent MTT cell viability assay to derive the cardiotoxic doses of Sulfonylurea: a concentrations ranging from 5 μM to 50 μM of glipizide and glimepiride were used and 15 μM was selected as an IC50 dose. Percent cell viability was compared with respect to ethanol as a control.

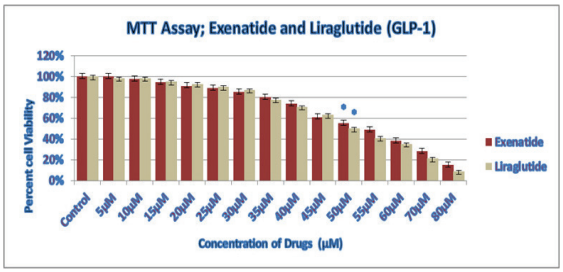

Figure 3. Dose dependent cell viability assay to derive the cardiotoxic doses of GLP-1: concentrations ranging from 5 μM to 80 μM of exenatide and liraglutide were used and 50 μM was selected as an IC50 dose. Percent cell viability was compared with respect to acetone as a control.

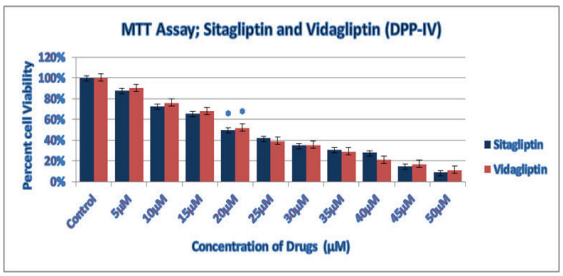

Figure 4. MTT cell viability assay to derive the cardiotoxic doses of DPP-IV: a concentrations ranging from 5 μM to 50 μM of sitagliptin and vidagliptin were used and 20 μM was selected as an IC50 dose. Percent cell viability was compared with respect to water as a control.

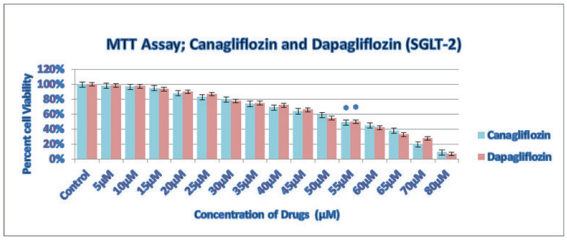

Figure 5. MTT cell viability assay to derive the cardiotoxic doses of SGLT-2: a concentrations ranging from 5 μM to 80 μM of canagliflozin and dapagliflozin were used and 55 μM was selected as an IC50 dose. Percent cell viability was compared with respect to acetone as a control.

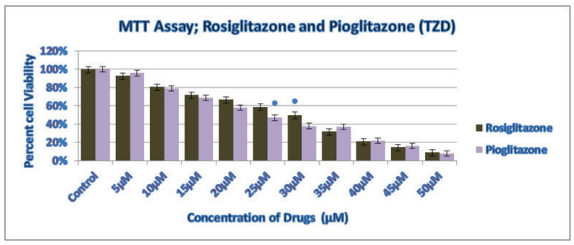

Figure 6. MTT cell viability assay to derive the cardiotoxic doses of TZD: a concentrations ranging from 5 μM to 50 μM of rosiglitazone and pioglitazone were used, 25 μM and 30 μM were selected as IC50 dose respectively. Percent cell viability was compared with respect to acetone as a control.

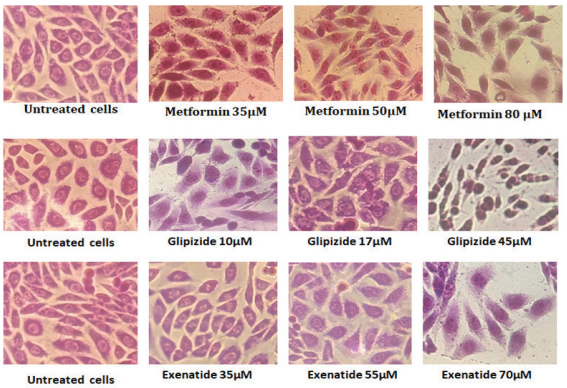

Figure 7. Dose-dependent morphological alteration: Giemsa staining for the cellular integrity of the cells treated with pretoxic, transition and post toxic cardiotoxic doses evaluated by MTT assay.

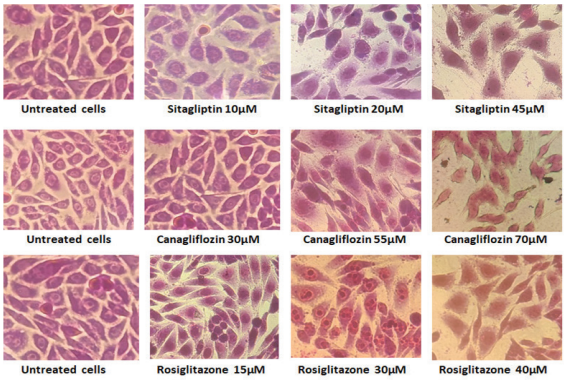

Figure 8. Dose-dependent morphological alteration: Giemsa staining for the cellular integrity of the cells treated with pretoxic, transition and post toxic cardiotoxic doses evaluated by MTT assay.

characteristic stress response was witnessed at pre-cardiotoxic dose (40μM) and transition dose (100μM). A significantly higher number of cell deaths was observed at apoptotic dose (150 μM) (Fig. 12). Approximately ~ 80% cell viability was observed at pre-cardiotoxic dose (40μM), 50% cellular death was observed at transition dose (100μM), and 20% cell viability was found on apoptotic dose (140 μM). These MTT results were further verified by morphological analysis and cell death was observed by trypan blue at these three doses with Giemsa stain. Cellular and nuclear morphology was found to be intact even at the transition dose when compared to control cells (Fig. 7). These evidences suggested that biguanide exerts cardioprotective effect and may improve the cardiovascular safety when supplemented with aged garlic as the viability was improved when MTT assay was conducted with aged garlic at these three doses (Fig.12). The oxidative stress analysis after incubation with antidiabetic drug for 48h was observed by DCFH-DA assay found to be moderately toxic at high concentration (Fig. 10). The synergistic cardioprotective effect of AGE and Met was found to be protective as the cellular viability improved in MTT and trypan blue cell cytotoxicity assays. With these results, it can be concluded that biguanide and aged garlic exert synergistic antidiabetic as well as cardioprotective efficacy (Fig. 9).

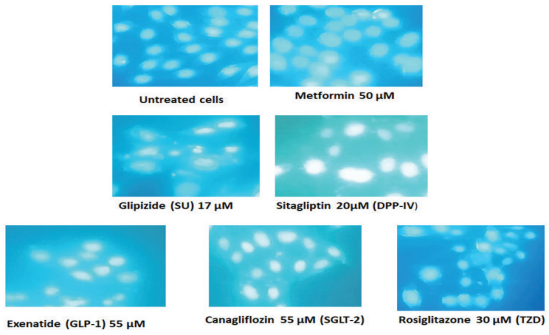

Figure 9. Nuclear alteration: DAPI staining for nuclear integrity of the cells visualized in six well plate treated with cardiotoxic doses of selected anti-diabetic drugs of each classes.

Table 2. Dose Optimization by MTT Assay

Antidiabetic Drugs	Drug Class	IC-50	Pre-cardio-toxic Dose (≤ 80% Viability)	Transition Dose (~ 50% cell viability)	Apoptotic Dose (≥ 80% Viability)
Metformin Melmet	Biguanide	50μM	35μM	50μM	80 μM
Glipizide Glimepiride	SU	17μM	10 μM	17μM	45μM
Exenatide Liraglutide	GLP-1	53μM	35μM	55μM	70μM
Sitagliptin Vidagliptin	DPP-IV	20μM	10μM	20μM	45μM
Canagliflozin Dapagliflozin	SGL-2	55 μM	30 μM	55 μM	70μM
Rosiglitazone Pioglitazone	TZD	27 μM	15μM	30μM	40μM

Table 3. Cardiotoxicity of Anti-diabetic drugs.

Antidiabetic Drugs	Drug Class	Toxicity on Cardiac cell
Metformin Melmet	Biguanide	Least Toxic
Glipizide Glimepiride	SU	Highly Toxic
Exenatide Liraglutide	GLP-1	Moderately Toxic
Sitagliptin Vidagliptin	DPP-IV	Highly Toxic
Canagliflozin Dapagliflozin	SGL-2	Moderately Toxic
Rosiglitazone Pioglitazone	TZD	Highly Toxic

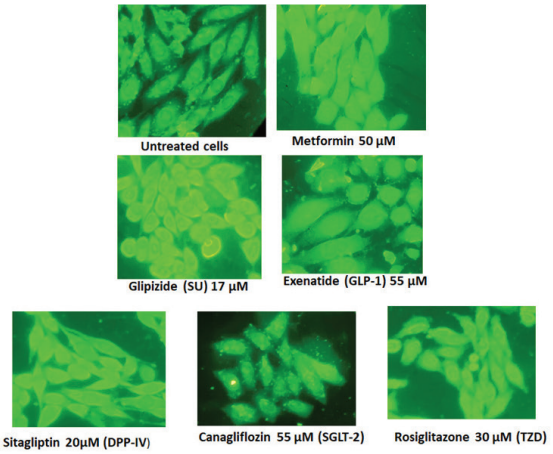

Figure 10. Oxidative stress analysis: DCFH-DA assay for oxidative stress of the cells visualized in six well plate treated with cardiotoxic doses of selected anti-diabetic drugs of each classes.

B. Su, dpp-iv and tzd were found to exert high cardiotoxicity while aged garlic found to have therapeutic potential against su and dpp-iv induced toxicity.

Sulphonylurease (SU) is the second line antidiabetic drugs and prescribed mostly at pre-diabetic and diabetic stage of the patient and therefore its cardiotoxic outcome is essential to evaluate. Glipizide and Glimepiride of SU composition were selected for their cellular cytotoxicity by MTT cell viability assay. The IC-50 doses for both drugs were found to be approximately at ~15 µM concentration (Fig.2). Although a significant cell death was observed even at 10µM concentration. The MTT observations indicated that SU exerted a cardiotoxic effects on cell metabolic activity and viability. These observations were further validated by nuclear and morphological stains by six-well plate experiments (Fig.9). Morphologically, cellular detoriation were observed at 17 µM concentrations, the cell wall and morphological integrity of cardiomyocytes was observed to be scattered as compared to control H9c2 cells, and complete apoptosis was observed at 45 µM concentration (Fig.7). These results indicated the cytotoxic effect of SU on the cardiovascular system. The cardiovascular outcome of sulphonylurease was found to be toxic to the cardiac system even at very low drug concentration. This study suggests that SU significantly reduces the cellular metabolic activity, but the exact mechanism underlying the sulphonylurease toxicity might still not be clear and need to be evaluated on molecular level. However, when the drugs were incubated with aged garlic it significantly improved the cell viability at pre-cardiotoxic transition and apoptotic doses. The cell viability was found to be improved from 70% to 86%, 40% to 72% and 19% to 40% at pre-cardiotoxic, transition and apoptotic dose respectively (Fig.13). Significant improve in cell viability was seen when cells were incubated with aged garlic (30 µM), which provided evidences of the positive effect of stable organosulfure compounds present in AGE to SU induced cardiotoxicity (Fig. 8). In this study we found out the oxidative stress induced by SU drugs supporting the fact that these drugs exert significant cardiotoxicity at low concentration. Supplementing the drug with AGE could improve the cardiovascular safety profile of these drugs. A clear mechanistic understanding of this herb-drug synergy for SU and aged garlic

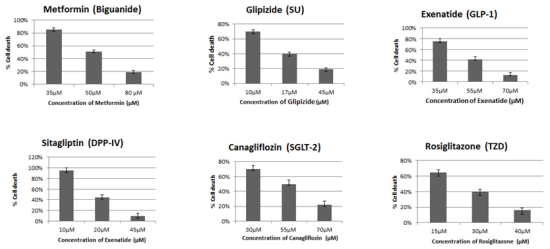

Figure 11. Cell death analysis of selected drug at their precardiotoxic, IC50 and cardiotoxic dose by Trypan blue dye exclusion assay.

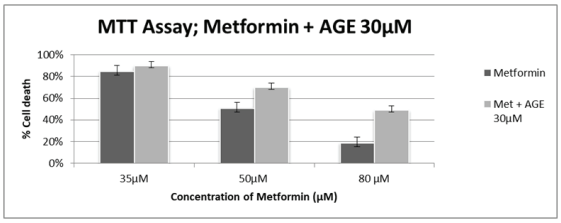

Figure 12. Effect of AGE on percent cell viability in presence of Metformin: MTT assay to investigate the effect of AGE over met induced toxicity was evaluated at different doses.. *p<0.05

may provide the valuable cardiovascular safety outcome in future antidiabetic therapy with antidiabetic and cardioprotective properties.

Dipeptidyl peptidase-4 inhibitors (Sitagliptin and Vidagliptin) medications are either used as single therapy, or in addition to metformin, sulfonylurea, or TZD. These drugs impact postprandial lipid levels. The MTT cell viability IC-50 doses of sitagliptin and vidagliptin were found to be at 20 µM (Fig.4). Although less than 80 % cell death was observed at 10 µM concentration. When cell morphology was observed at Pre cardiotoxic dose (10 µM), transition dose (20 µM) and apoptotic dose (45 µM) (Table 2). Cellular deformities were found to be at transition and cardiotoxic dose. Cellular deformities were observed at 20 µM and 10 µM drug concentration (Fig. 8). Incubation with AGE (30 µM) for 48h was found to improve cellular viability from 95% to 96%, 45% to 63%, and 10% to 35% at pre-cardiotoxic, transition and apoptotic dose respectively (Fig. 15). Aged garlic significantly improved the cell viability at apoptotic dose by approximately three-fold. Synergistic effect of drug with aged garlic extract was found to be protective against cardiovascular drug-induced cardiotoxicity at higher concentration of drug treatment.

Like biguanides, TZDs improve insulin action. Rosiglitazone and pioglitazone were selected for MTT Assay. TZDs are agonists of PPAR and facilitate increased glucose uptake in numerous tissues including adipose, muscle, and liver. Thus, TZDs are not preferred as first-line or even step-up therapy. The IC-50 doses of rosiglitazone and pioglitazone (TZD) were found to be approximately at 27 µM concentration (Fig. 6). Pre-cardiotoxic dose (15 µM), transition dose (30 µM) and apoptotic dose (40 µM) were further selected for the morphological analysis (Fig. 8). Hypertrophy and cell death was observed at 30 µM and 50 µM concentration respectively. Aged garlic incubation was found to improve the cell viability from 65% to 80%, 40% to 75% and 16% to 45% at Pre-cardiotoxic dose (15 µM),

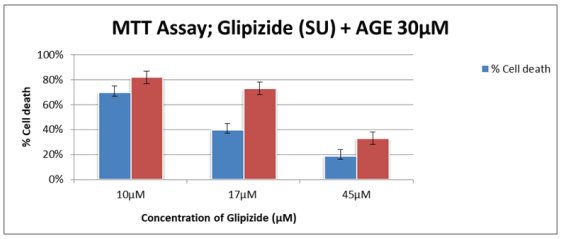

Figure 13. Effect of AGE on percent cell viability in presence of SU: MTT assay to investigate the effect of AGE over SU induced toxicity was evaluated at different doses. *p<0.05

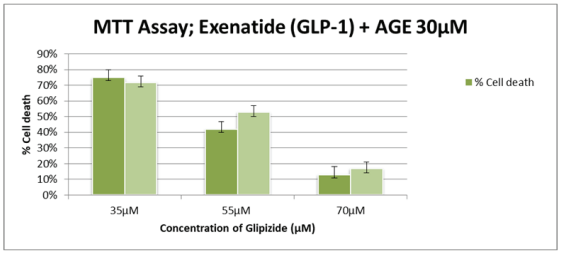

Figure 14. Effect of AGE on percent cell viability in presence of GLP-1: MTT assay to investigate the effect of AGE over GLP-1 induced toxicity was evaluated at different doses.

transition dose (30 µM) and apoptotic dose (40 µM) respectively (14) (Fig. 17). AGE improved the cell viability by approximately two-fold. We concluded that AGE is significantly protective against TZD induced cardiotoxicity.

C. Glp-1 and sgl-2 were found to be moderately cardiotoxic drugs.

Exenatide and Liraglutide were the selected glucagon-like peptide-1 (GLP-1) agonist receptor to investigate the effect on cardiovascular system. These drugs exhibit increased resistance to enzymatic degradation by DPP4. In young patients with recent diagnosis of T2DM, central obesity, and abnormal metabolic profile, treatment with GLP-1 analogs that would have a beneficial effect on weight loss and improve the metabolic dysfunction. The IC-50 doses for both drugs were found to be comparatively greater then SU but not as much as high as metformin. 50 µM doses were found to be the IC-50 dose for both drugs (Fig. 3). Although cell death was increased at higher concentration as only 15 % cell viability was observed at 80 µM concentration. Pre cardiotoxic dose (35 µM), transition dose (55 µM) and apoptotic dose (70 µM) dose of exenatide was selected for morphological analysis in six well plate experiments. No considerable cell death was observed at 35 µM, but significant cell death was observed at 70 µM concentration (Fig. 7). Though GLP-1 agonist was found to be cardiotoxic at high concentration but no significant cell death observed at 50 µM concentration compared to SU. However, when Per cardiotoxic, transition and apoptotic dose of exenatide were incubated with 35 µM AGE for 48h, a slight improvement in cell viability was observed at transition and apoptotic doses but it may not be considered as highly cardioprotective, some of the other studies also indicated the cardiotoxic effect of these drugs on heart (Fig. 11). We concluded that GLP-1 agonist induces moderate cardiotoxicity at low concentration but toxic at high concentration and AGE may not exert cardioprotective effect against GLP-1 induced cardiotoxicity. Further molecular studies are needed to understand the exact mechanism of cardiotoxicity exerted by GLP-1.

Sodium-glucose cotransporter inhibitors are new class of glucosuric agents: canagliflozin, dapagliflozin, were selected to investigate the cellular viability. SGLT-2 inhibitors provide insulin-independent glucose lowering by blocking glucose reabsorption in the proximal renal tubule by inhibiting SGLT2. These drugs provide modest weight loss and blood pressure reduction. The IC-50 doses of

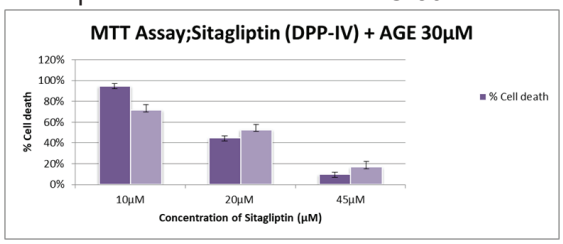

Figure 15. Effect of AGE on percent cell viability in presence of DPP-IV: MTT assay to investigate the effect of AGE over DPP-IV induced toxicity was evaluated at different doses. *p<0.05

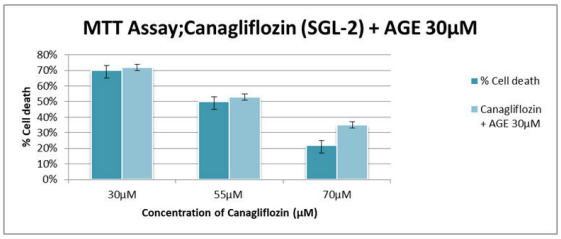

Figure 16. Effect of AGE on percent cell viability in presence of SGL-2: MTT assay to investigate the effect of AGE over SGL-2 induced toxicity was evaluated at different doses. *p<0.05

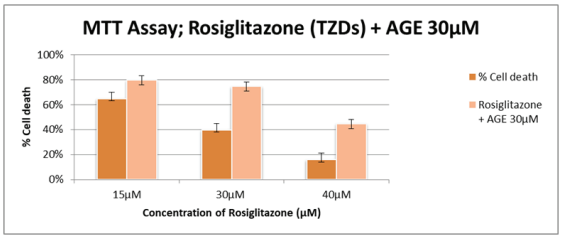

Figure 17. Effect of AGE on percent cell viability in presence of TBA: MTT assay to investigate the effect of AGE over TBA induced toxicity was evaluated at different doses. *p<0.05

canagliflozin and dapagliflozin (SGLT-2) was found to be at 55 µM. Though 80 % of cell death was observed at 30 µM concentration (Fig. 5). Pre-cardiotoxic dose (30 µM), transition dose (55 µM) and apoptotic dose (70 µM) were further selected for morphological analysis. Cellular enlargement or hypertrophy was viewed at transition dose (Fig. 8). Though no significant improvement in cell viability was observed when cells were incubated with aged garlic extract (Fig. 16).

D. Aged garlic extract exert cardioprotective potential through antioxidative activity against drug induced cardiotoxicity.

Aged garlic has been found to have antioxidative and antidiabetic properties. The stable organosulfure compound present in aged garlic has exceptional cardioprotective potential as demonstrated in our previous studies. In this study, we investigated the cardioprotective role of aged garlic against antidiabetic drug-induced cardiotoxicity. In our previous studies, we found that 30 µM is the cardioprotective dose of aged garlic. We incubated the cells for 48h with the pre-cardiotoxic dose, transition dose and apoptotic dose of each drug with 30 µM aged garlic extract. It was found that the cell viability was increased for SU, DPP-IV, and SGT-2 when incubated with aged garlic. Similar results were observed in the morphological and nuclear analysis of H9c2 cell line with six-well plate experiments. Thus, we can conclude that AGE exert a significant cardioprotective effect in diabetes and drug induced cardiotoxicity. Although the exact molecular mechanism is yet to be explored, but stable organosulfure compounds present in AGE may provide dual therapeutic effect on diabetes and cardiovascular system as herb-drug therapy.

Drug-induced toxicity is a major concern for many clinically important drugs. Several antidiabetic compounds were found to cause asymptomatic effects on other organs which led to their post-marketing withdrawal (23). In diabetes, burdening the stress on cardiac tissues (diabetic cardiomyopathy), antidiabetic drugs imposes accumulative stress on the cardiovascular system which ultimately increasing the heart attack ratio among diabetic patients. Currently, assessing cardiovascular safety is a crucial parameter in antidiabetic drug development, and many models have been established to facilitate its prediction to avoid such toxicity. However, cardiotoxicity induced by chronically administered antidiabetic drugs, represents a major problem because cardiovascular stress of these drugs may become evident only after long-term accumulation of the drug or its metabolite (24). Although several natural products have been consumed to reduce hyperglycemia and diabetic complications but limited of those compounds implemented to target specific herb drug therapeutics to improve the bioavailability and efficacy. It has become crucial to investigate the natural products synergistically supplemented with anti-diabetic drugs which do not increase cardiovascular risk but might reduce the risk of chronic heart failure. Therefore, careful selection of herb drug therapy paying particular attention to cardiovascular safety is important in optimizing diabetic therapy. This efficacy and safety of the most commonly prescribed antidiabetic drugs in the context of cardiovascular impacts the future of drug discovery. Our study investigates the cardiotoxicity of conventionally prescribed antidiabetic drugs and the role of aged garlic to reduce cardiotoxicity.

We selected twelve drugs from six antidiabetic drug classes. Biguanide were found to be the least cardiotoxic drug even at high concentration. Being derived from the plant *Galega officinalis*, these drugs exert least cardiac stress. When Biguanide incubated with AGE improved the antidiabetic activity, implying that biguanide has a cardioprotective effect and may improve cardiovascular safety when supplemented with aged garlic (Fig. 12). The oxidative stress analysis after 48 hours of incubation with an anti-diabetic medication was discovered using the DCFH-DA test. In MTT

and trypan blue cell cytotoxicity experiments, the synergistic cardioprotective action of AGE and Met was found to be protective as cellular viability improved with reduced oxidative stress. These observations are also supported by some of the previous data of cardiovascular safety profile for metformin (26). On the other hand SU, DPP-IV and TZD were found exerted a cardiotoxic effects by reducing the cellular metabolic activity. However, when aged garlic were incubated with, SU and TZD significantly improved the cell viability at pre-cardiotoxic transition and apoptotic doses and improved the cellular and nuclear deformities.

SU induced cardiotoxicity was also studied in past research and found to exert left ventricular remodeling (27). AGE improved the cell viability by approximately two-fold. We concluded that AGE is significantly protective against SU and TZD induced Cardiotoxicity (28-29). Synergistic effect of drug with aged garlic extract was found to be protective against cardiovascular drug-induced cardiotoxicity at higher concentration of drug treatment (30). GLP-1 and SGL-2 were found to be cardiotoxic in high concentration (31-33). AGE found to moderately improve the cardiotoxic profile of these drugs.

Natural product have been supplemented with the diet to achieve their therapeutic potential in various disease with less side effects. Though it is also important to keep in mind that diabetes cannot be well-controlled without lifestyle modifications, including proper diet and exercise. Diabetes is a chronic disease that requires a multi-disciplinary approach to optimize blood glucose, blood pressure, and lipid control. Each anti-diabetic drug must be tested for efficacy and therapeutic outcomes before incorporating it into the treatment of diabetic patients. Thus, the toxicity levels of each of the medications were seen and natural plant extracts were used to reduce the cardiotoxic effects. These results suggest that prioritizing drugs on the basis of their cardiovascular protective effects when choosing a treatment for diabetes. Although many antidiabetic drugs have the effect of reducing cardiovascular death and adverse cardiovascular events, it is still unclear which antidiabetic drugs can improve ventricular remodeling and fundamentally delay the process of HF. If drugs can be found to improve ventricular remodeling, it will be of great significance for patients with T2DM with cardiovascular disease (CVD). These results suggest that aged garlic have cardiovascular protective effects should be prioritized when choosing a treatment for diabetes. Herb-drugs synergy can be found to improve cardiac complication, and will be of great significance for patients with T2DM with cardiovascular disease (CVD). The treatment of diabetes mellitus is crucial as the incidence of its occurrence increases. As anti-diabetic medications result in severe cardio toxicity, various remedies need to be formed for better effects. The major anti diabetic drug is considered to be metformin, however combination therapy can also be considered beneficial. Overdoses of these medications may produce major morbidity, with many cases requiring intensive and prolonged medical treatment.

Conclusion

Several antidiabetic drugs have been withdrawn by FDA because of their side effects on other organs, which demand the need of a safer alternative therapeutic. The cardio-protective and antidiabetic role of aged garlic extract has been widely reported, the stable sulfur rich compounds present in AGE were found to be preventive of antidiabetic drug-induced cardiotoxicity. The present study confirms the toxicity of these drugs on cardiomyoblasts. Upon treatment with anti-diabetic drugs, biguanides were found to be safer antidiabetic drugs than sulphonylurease, DPP-IV and TZD. The cardiotoxicity effect was further conformed by altered cellular morphology of H9C2 cardiomyocytes at various concentrations of drugs. SU and DPP-IV were found to be highly toxic drugs among all. The sulfur compounds present in AGE were found

to induce cardio protective potential against antidiabetic drugs and can be supplement with first, second and third line drugs to suppress cardiac stress. The results should be further validated by quantitative assays. These findings suggest the clinical importance of AGE targeting the dual stress responses on the cardiac system of antidiabetic drugs and will not induce any surplus toxicity being a natural and safe compound.

Acknowledgements

The present work was supported by Jaypee Institute of Information Technology, Noida. We acknowledge Department of Biotechnology of JIIT, for providing infrastructural support and funds.

References

1. Bayeva M, Sawicki K, Ardehali H, Taking diabetes to heart deregulation of myocardial lipid metabolism in diabetic cardiomyopathy, *Journal of the American Heart Association*, 2 (2013) 6.

2. Saeedi P, Petersohn I, Salpea P, Malanda B, Karuranga S, Unwin N, Williams R, Global and regional diabetes prevalence estimates for and projections for 2030 and 2045, *Diabetes Research and Clinical Practice*, 157 (2019)107843.

3. Rubler S, Dlugash J, Yuceoglu YZ, Kumral T, Branwood AW, Grishman A,

New type of cardiomyopathy associated with diabetic glomerulosclerosis, *Am J Cardiol*, *30* (1972) 595.

4. Yancy CW, Jessup M, Bozkurt B, American College of Cardiology Foundation; American Heart Association Task Force on Practice Guidelines. 2013 ACCF/AHA guideline for the management of heart failure: a report of the American College of Cardiology Foundation/American Heart Association Task Force on Practice Guidelines.*J Am Coll Cardiol*, 34 (2013) 502.

5. Rydén L, Armstrong PW, Cleland JG, Horowitz JD, Massie BM, Packer M, Efficacy and safety of high-dose lisinopril in chronic heart failure patients at high cardiovascular risk, including those with diabetes mellitus, *Eur Heart J, 12* (2000) 1002.

6. Thrainsdottir IS, Aspelund T, Thorgeirsson G, Gudnason V, Hardarson T, Malmberg K, Sigurdsson G, Rydén L, The association between glucose abnormalities and heart failure in the population-based Reykjavik study, *Diabetes Care, 36 (2015)* 107.

7. Sharma M, Irwin N, Irene P, Trends in incidence, prevalence and prescribing in type 2 diabetes mellitus between 2000 and 2013 in primary care: a retrospective cohort study, *BMJ,* 6 (2013)1.

8. Azimova K, Zinnia S, Debabrata M, Cardiovascular safety profile of currently available diabetic drugs, *The Ochsner Journal*, 14 (2014) 616.

9. Singh S, Jyoti B, Ping H, Cardiovascular effects of anti-diabetic medications in type 2 diabetes mellitus, *Current cardiology reports*, 15 (2013) 327.

10. Ferdinandy P, Baczkó I, Bencsik P, Giricz Z, Görbe A, Definition of hidden drug cardiotoxicity: Paradigm change in cardiac safety testing and its clinical implications. *Eur. Heart J*. 40 (2019)1771.

11. Fenichel RR, Malik M, Antzelevitch C, Sanguinetti M, Independent Academic Task Force. Drug induced to rsadesde pointes and implications for drug development. *J Cardiovasc Electrophysiol,* 15 (2004) 475.

12. Chaudhury Arun, et al, Clinical Review of Antidiabetic Drugs: Implications for Type 2 Diabetes Mellitus Management, *Frontiers*

in endocrinology, 8 (2017) 6.

13. Rena G, Ewan R, Kei Sakamoto, Molecular mechanism of action of metformin: old or new insights, *Diabetologia,* 56 (2013) 1898.

14. Sola D, Luca R, Gian P, Carnevale S, Pamela M, Marcello B, Roberto Mella, Francesca C, Gian P, Sulfonylureas and their use in clinical practice. *Archives of medical science*, 11 (2015) 840.

15. Hauner H, The mode of action of thiazolidinediones. *Diabetes Metab Res Rev*, 2 (2002)10-5.

16. Karagiannis T, Eleni B, Panagiota B, Apostolos T, Cardiovascular risk with DPP-4 inhibitors, *latest evidence and clinical implications*. 19 (2016) 36.

17. Tran KL, Park YI, Pandya S, Muliyil NJ, Jensen BD, Huynh K, Nguyen QT, Overview of Glucagon-Like Peptide-1 Receptor Agonists for the Treatment of Patients with Type 2 Diabetes. *Am Health Drug Benefits*, 10 (2017) 178.

18. Novikov A, Vallon V, Sodium glucose cotransporter 2 inhibition in the diabetic kidney: an update. *Curr Opin Nephrol Hypertens*, 25 (2016) 50.

19. Bradley JM, Organ CL, Lefer DJ, Garlic-derived organic polysulfides and myocardial protection, *J. Nutr*, 102 (2016) 99.

20. Borek C, Antioxidant health effects of aged garlic extract. *J Nutr*, 131(2001) 1010.

21. Banerjee SK, Maulik SK, Effect of garlic on cardiovascular disorders: a review, *Nutr J*, 1 (2002) 4.

22. K Sharma, V Rani, Comparative Phytochemical and Antioxidative Analysis of Raw and Aged Garlic Extract; Indicating the Therapeutic Potential of Stable Organosulfur Compounds *Current Trends in Biotechnology and Pharmacy* 15 (2021) 96.

23. Prabst K, Engelhardt H, Ringgeler S, et al, Basic colorimetric proliferation assays: MTT, WST, and resazurin, *Methods Mol Biol,* 1601(2017)1.

24. Kelleni Mina, Abdelbasset M, Drug Induced Cardiotoxicity: Mechanism, Prevention and Management. *10.5772/intechopen*, (2018) 79611.

25. Bailey C.J, Metformin: historical overview, *Diabetologia,* 60, (2017) 1566.

26. Driver C, Bamitale KDS, Kazi A, Cardioprotective Effects of Metformin, *J Cardiovasc Pharmacol,* 72 (2018) 121.

27. Charles E, Colleen M, Brensinge C, Aquilante, Comparative Safety of Sulfonylureas and the Risk of Sudden Cardiac Arrest and Ventricular Arrhythmia, *Diabetes Care*, 41(2018) 713.

28. Jeon JY, Ha KH, Kim, DJ, Cardiovascular Safety of Sodium Glucose Cotransporter 2 Inhibitors as Add-on to Metformin Monotherapy in Patients with Type 2 Diabetes Mellitus, *Diabetes Metab J*, 45 (2021) 505.

29. Lipscombe LL, Gomes T, Lévesque LE, Hux JE, Juurlink DN, and Alter DA, Thiazolidinediones and Cardiovascular Outcomes in Older Patients With Diabetes, *JAMA,* 298 (2007) 2634.

30. Quinn CE, Hamilton PK, Lockhart CJ, McVeigh GE, Thiazolidinediones: effects on insulin resistance and the cardiovascular system, *Br J Pharmacol*, 153 (2008) 636.

31. Tran K, Park Y, Pandya S, Overview of Glucagon-Like Peptide-1 Receptor Agonists for the Treatment of Patients with Type 2 Diabetes, *Am Health Drug Benefits*, 10 (2017) 178.

32. Sposito A, Berwanger O, de Carvalho, GLP-1RAs in type 2 diabetes: mechanisms that underlie cardiovascular effects and overview of cardiovascular outcome data, *Cardiovasc Diabetol,* 17 (2018)157.

33. Santamarina M, Carlson C, Review of the cardiovascular safety of dipeptidyl peptidase-4 inhibitors and the clinical relevance of the CAROLINA trial, *BMC Cardiovasc Disord*, 19 (2019) 60.

Current Trends in Biotechnology and Pharmacy
Vol. 16 (4) 577 - 602, Oct 2022, ISSN 0973-8916 (Print), 2230-7303 (Online)
10.5530/ctbp.2022.4.90

COVID 19: A New Insight Into Organ Failure and Complications Caused by Novel SARS-CoV-2 Virus and Discussion on the Role of Nanotechnology in Detection, Treatment and Prevention of the Disease

ManneAnupama Ammulu[1], Kanaka Durga Devi Nelluri[2], Praveen Kumar Vemuri[3], Somaiah Chowdary Mallampati[4], Sudhakar Poda[5,*]

[1]Department of Civil Engineering, PVP Siddhartha Institute of Technology, Kanuru, Vijayawda, Andhra Pradesh, 520007, India
[2]Department of Pharmaceutics and Biotechnology, KVSR Siddhartha College of Pharmaceutical Sciences, Vijayawada, Andhra Pradesh, India
[3]Department of Biotechnology, KoneruLakshmaiah University, Vaddeswaram, Andhra Pradesh, India
[4]Department of Mechanical Engineering, PVP Siddhartha Institute of Technology, Andhra Pradesh, India.
[5]*Associate Professor, Department of Biotechnology, AcharyaNagarjuna University, Nagarjuna Nagar, Andhra Pradesh, Guntur, India

*Corresponding author: sudhakarpodha@gmail.com

Abstract

The severe acute respiratory syndrome coronavirus 2 (SARS-CoV-2) virus, which first appeared in Chinese individuals in December 2019, is now causing the COVID-19 pandemic, with 5,79,319 deaths and 13,338,364 confirmed cases as of January 31st, a total of 56.7 lakhs. COVID-19 causes dysregulated immunological responses, metabolic dysfunctions, and negative consequences on a variety of organ functions. Significant risk factors are typically connected with older people who have medical comorbidities including cancer and diabetes. Scientists and doctors have battled to understand the unique virus and its pathogenesis in order to develop suitable treatment drugs and vaccines for COVID-19. The spike protein SARS-CoV-2 has recently been discovered to attach to the enzyme that converts human angiotensin I. The purpose of this study was to examine the involvement of many organs in COVID-19 patients, particularly in severe cases. We also wanted to know what was driving the multiorgan failure caused by SARS-CoV-2. Multi-organ dysfunction manifests itself in a variety of ways, including acute lung failure, acute liver failure, acute kidney damage, cardiovascular disease, a variety of haematological abnormalities, and neurological problems. The most important processes are associated to SARS-direct coV-2's and indirect pathogenic features. Although SARS-CoV2 receptor angiotensin-converting enzyme 2 (ACE-2) was found in the lung, heart, kidney, testis, liver, lymphocytes, and nervous system, the presence of SARS-CoV-2 RNA in these organs was unknown. These epidemics have strained healthcare systems and prompted serious concerns about how to deal with them using traditional drugs and diagnostic tools. In this regard, the application of nanotechnology opens up new avenues for the creation of ground-breaking preventative, diagnostic, and treatment solutions. We examine how nanotechnology can be applied to control the COVID-19 virus by designing nano-based materials such as disinfectants, personal protective equipment, diagnostic systems, and nanocarrier systems for treatments and vaccine development, as well as the challenges and drawbacks that must be overcome.

Keywords: COVID-19, SARS-CoV-2, Multi-organ failure, Nanotechnology

Introduction

The world is currently experiencing a pandemic sickness (COVID-19) caused by SARS-CoV-2, a newly discovered coronavirus [1]. At the time of writing, SARS-CoV-2 had infected almost 12 million people worldwide, resulting in 6,362,614 deaths (WHO, 2022). The disease causes mild to severe respiratory symptoms, with the latter being more common in the elderly and individuals with serious medical diseases such as heart disease, chronic lung disease, cancer, and diabetes [2]. Minor gastrointestinal, cardiovascular, and even neurological issues have been reported in COVID-19 individuals who have been admitted to the hospital [3].

Coronaviruses (CoV) are transmitted by bats and infect humans via an intermediate animal host before overcoming the species barrier. Different bat populations in China have coronaviruses with complex genetics,several of them are the SARS-direct CoV's ancestors. [4], [5]. SARS-CoV in Chinese *Rhinolophus* bats that seemed to adapt to the wild Himalayan palmcivet before spreading to humans [6]. It is most likely that interaction with sick camels caused people to contract the Middle East Respiratory Syndrome Corona Virus (MERS-CoV), which was generated from a *Pipistrellus* bat CoV. [7], [8]. It was confirmed shortly after the initial human SARS-CoV-2 outbreak that this novel virus was connected to a bat-borne coronavirus discovered in the *Rhinolophusaffinis* bat species [9]. The search for antransitional animal host has centred on the pangolin (Manisjavanica), which is thought to be the intermediate host for SARS-CoV-2[10]. The SARS-CoV-2 receptor ACE2 was discovered to be similar to human receptors in bats, pangolins, and a variety of other animals [11].

Over the last two decades, seven coronaviruses that cause more or less severe respiratory disorders have been discovered in humans. SARS-CoV-2, for example, can cause lung damage in patients as well as multi-organ dysfunction, including unfavourable cardiac remodelling, myocardial stress, and congestive heart failure [12]. SARS-CoV-2 has been identified as a human angiotensin I enzyme converting enzyme 2 (ACE2)-tropical virus [13], capable of binding alveolar pneumocytes with ACE2 on their surface [15].

COVID-19 aetiology is complicated, especially in patients with severe disease, due to various organ failures. The angiotensin-converting enzyme 2 (ACE 2) is thought to be a cell entrance receptor for SARS-COV-2 [16]. However, ACE2 mRNAs were found to be expressed in practically all organs in humans, including the brain, heart, kidneys, and testes, indicating that the virus might infect tissues other than the lungs [17,18]. ACE2 is a known peptidase that controls blood pressure by modulating the renin-angiotensin-aldosterone system (RAAS). Pathogenicity of SARS-CoV-2 may be influenced by the host immune system, resulting in tissue damage and, in some cases, death. Lympopenia, reduced lymphocytes, and cytokine storms have all been observed in COVID-19 individuals [19,20-24].

Effects of SARS-CoV-2 on human health

SARS-CoV-2 is distinguished from SARS-CoV by the appearance of an unique spike glycoprotein with a distinct binding affinity to the angiotensin-converting enzyme 2 (ACE2) receptors; it should be noted, however, that SARS-CoV-2 has a 10–20 fold higher binding affinity to ACE2 receptors than SARS-CoV[25,35]. ACE2 can be found in a variety of organs in the human body (figure 1), including the lung, colon, small intestine, testis, kidney, duodenum, oesophagus, gallbladder, and urinary bladder [36,37], making these organs a potential SARS-CoV-2 target [36][37].

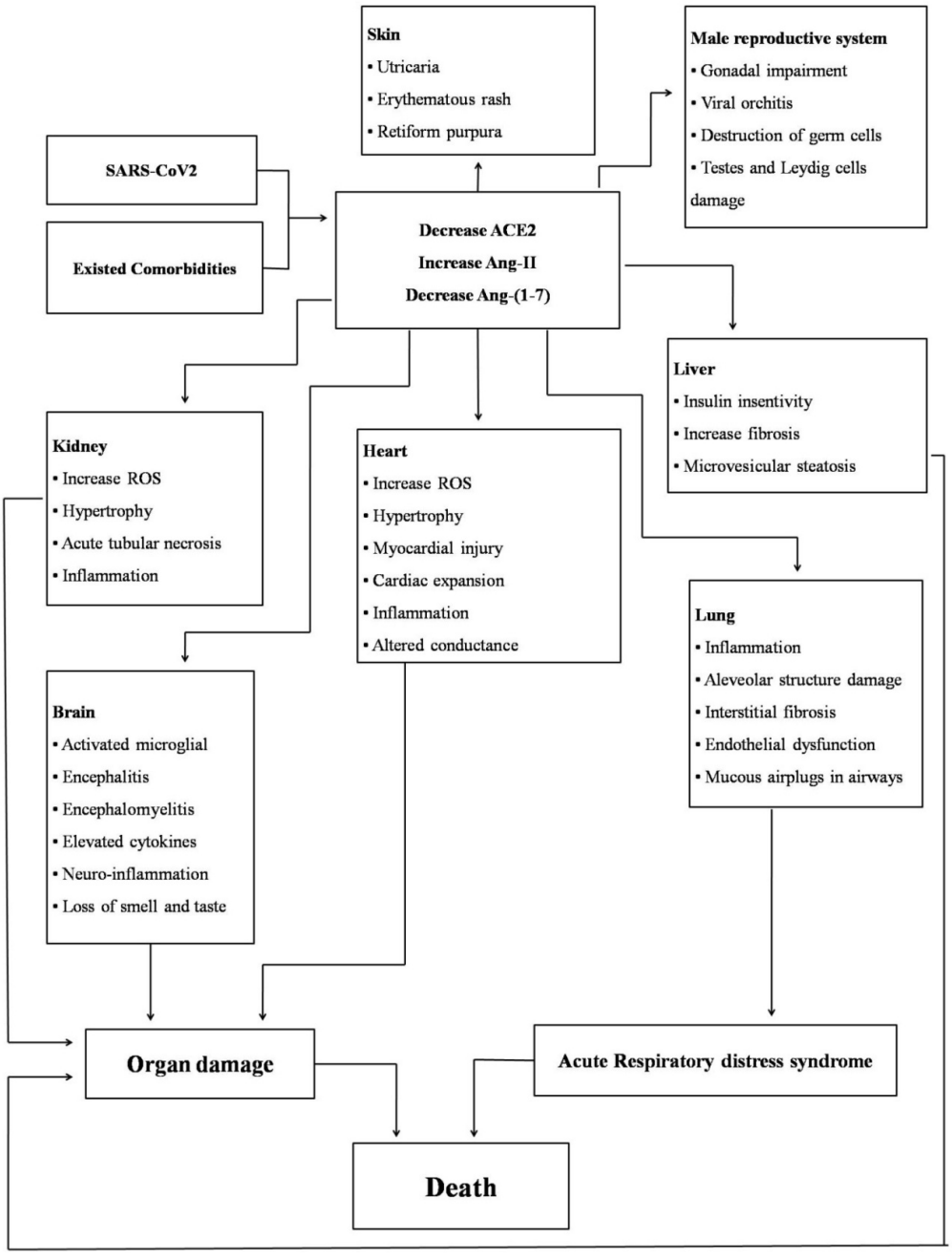

Fig. 1 The impact of SARS-CoV-2 on the human body's various organs.

Covid 19: A new insight into organ failure and complications

Lung damage

Coronaviruses like SARS-CoV-2, MERS-CoV, and SARS-CoV can cause serious morbidity and mortality in those who are infected. Lung infection appears to be the most common location of infection for all three viruses, resulting in acute respiratory distress syndrome and death. SARS-CoV pathogenesis is often initiated by the virus attaching its envelope protein (spikes) to the appropriate receptor, angiotensin-converting enzyme 2 (ACE2). Because ACE2 is widely expressed on the surface of lung and intestinal epithelial cells, these cells are vulnerable to SARSCoV [38]. According to several case studies, the chest imaging and histological observations of the lung caused by SARSCOV2 are similar to those seen in patients with SARSCoV and MERSCoV. A report from Italy [39] and another from China [40] both found significant pathological abnormalities in the lungs caused by new coronavirus pneumonia. Involvement of the lungs is also caused by a strong viral transmission. In respiratory viral infections, interstitial inflammation, disseminated alveolar destruction, and necrotizing bronchitis/ bronchiolitis are common histological findings in the lungs. In both the acute and late (organising) stages of respiratory virus infections, diffuse alveolar damage is the most common. Acute diffuse alveolar injury is characterised by intra-alveolar edoema. The creation of hyaline membranes that line the alveolar walls is followed by the deposition of fibrin. Type II pneumocytes, granulation tissue formation, and collagen deposition characterise the late phases of widespread alveolar injury [40].

Based on the examination of released patients for lung injury, there are widespread concerns. Huang et al. discovered that about three-quarters of COVID-19 patients had pulmonary dysfunction during early convalescence, with the most common symptoms being decreased diffusing ability and a decrease in the FEV1/ FVC ratio (forced expiratory volume in the first, second, and third/forced vital capacity). More than half of COVID-19 cases had abnormal carbon monoxide diffusion capability (DLCO), indicating that intra-alveolar diffusion channels were disrupted [41]. MEO et al. discovered that acute severe respiratory syndrome (SARS) and COVID-19 have the same biochemical and clinical aspects [42]. Previous studies on SARS survivors indicated that impaired DLCO was the most common anomaly, ranging from 15.5 percent to 43.6 percent [3, [43], [44]. The autopsy of COVID-19 patients revealed varying degrees of alveolar structural destruction as well as lung interstitial fibrosis [45]. Few extreme COVID-19 patients had mucous plugs in restricted airways, according to pathological findings [45], which may help to explain the decreasing breathing function. Neuromuscular dysfunction, in addition to acute lung injury, is a common cause of diminished lung capacity. In a few patients with a decreased FEV1 or FEV1 / FVC ratio, it could be due to long-term smoking or significant hyperresponsiveness of the airways [41].

Neurological dysfunctions

It has been proposed that SARS-CoV-2 virus enters the central nervous system via the synapse-connected route found in other coronaviruses like SARS-CoV, which may contribute to a variety of neurological abnormalities such as ataxia, epilepsy, neuralgia, unconsciousness, severe cerebrovascular disorder, and encephalopathy [46]. Mao et al. found neurological symptoms in 36.4 percent of the population, with the severe group being more likely to have significant cerebrovascular dysfunction, reduced cognition, and skeletal muscle injuries [47]. As previously stated, viruses that bind to ACE2 receptors can result in excessively high blood pressure and raise the risk of a brain haemorrhage. However, the virus may be able to cross the blood-brain barrier and enter the central nervous system (CNS) via the vascular system if SARS-spike CoV-2's protein interferes with ACE2 generated in capillary endothelium [48].

Indeed, some people first develop COVID-19 symptoms after experiencing neurological symptoms [47]. Beijing Ditan Hospital has reported a case of viral encephalitis caused by a new CoV that first attacked the CNS. The presence of SARS-CoV-2 in cerebral fluid was confirmed through genome sequencing, strengthening the idea that this modern pneumonia virus can also affect the nervous system [47]. Furthermore, pathogenic germs, such as influenza, are more likely to disrupt the blood-brain barrier in individuals with severe COVID-19 symptoms, resulting in headaches, profuse vomiting, visual loss, and limb convulsions.

SARS-CoV-2 infection causes a variety of neurological symptoms, including cerebrovascular problems, leukoencephalopathy, and other CNS illnesses. While certain types of diffuse white matter injuries (such as post-hypoxic leukoencephalopathy or leukoencephalopathy associated with sepsis) are mimicked by COVID-19-related white matter anomalies, all of these are significant differences that are distributed by neuroanatomic means of the white matter lesions. The pathophysiology of COVID-19 white matter abnormalities is unknown, but it is thought that “silent hypoxia” may play a role in their development. According to Otto Repalino’s cohort study, decreased NAA/Cr ratios were associated with neuronal dysfunction and axonal damage [49].

A significant number of COVID-19 patients have reported a loss of smell or taste. As a result, anosmia and dysgeusia are likely to be observed in COVID-19 patients [50]. Streeck, a German virologist, presented the first report of scent and taste deficiency on March 16th, 2020, identifying this ailment as a significantly more frequent disease (66.7 percent of COVID-19 patients). In February and March of 2020, the first reports of smell and taste abnormalities in COVID-19 patients surfaced. These studies were first anecdotal, but articles soon began to reliably show an increased prevalence of chemosensory impairments [51].

According to numerous case investigations of MERS coronavirus, neurological symptoms such as meningoencephalitis, hyporeflexia, and ataxia have also been reported [52]. Neuronal infection in SARS-CoV-infected hACE2 transgenic mice has been demonstrated to cause mortality [53]. According to accumulating evidence, the virus has been discovered in the cerebrum [54] as well as in the CSF as a result of SARS-CoV infection [55]. Coronaviruses were found in the cerebrum and cerebrospinal fluid of patients with epilepsy, encephalitis, and encephalomyelitis [56]. The average age of meningoencephalitis-related COVID-19 patients was 50.8 (19.09) years, with males being more frequently infected, according to clinical characteristics (70 percent). Chronic seizures, slurred speech, and cognitive impairments, including hearing and motor perseverance, are among the less well-known neurological symptoms [57].

Coagulation disorder

SARS-CoV was found to have similar thrombotic and haematological symptoms to COVID-19 [58]–[60]. Four patients with pulmonary embolism, three patients with deep vein thrombosis, and two patients with significant multi-organ infarctions due to thrombi were detected in a Singapore report involving postmortem investigations of eight known cases of SARS-CoV [61]. In a retrospective study of 157 SARS-CoV-infected patients, thrombocytopenia (55%) was discovered with the lowest platelet count one week after the onset of symptoms, reactive thrombocytosis (49%) was discovered at its peak during the third week (median = 17 days), and extended partial activated thromboplastin time (63%) was discovered throughout the first two weeks [62]. Thrombotic consequences and comparable haematological symptoms of COVID-19 and SARS-CoV illness have also been linked to MERS-CoV. In comparison to COVID-19 and SARS-CoV, there is a scarcity of data. Moderate thrombocytopenia was identified by Kim et al. as a common observation during the first week,

with no distinction made between individuals with mild or severe sickness [63]. MERS-CoV caused disseminated intravascular coagulation (DIC), intracerebral haemorrhage, and multi-organ failure in an apparently healthy patient two weeks after admission, according to Algahtani et al. [64].

Thrombotic issues appear to be a common occurrence in COVID-19 patients. Early research on the COVID-19 pandemic indicated that infected patients typically have thrombocytopenia (36.2 percent) and may have low D-dimer (46.4 percent) [2]. However, these rates are substantially greater in patients with COVID-19 severe illness (57.7% and 59.6%, respectively) [2]. Emerging evidence suggests that patients infected with this new coronavirus may develop DIC [65]. Both thrombocytopenia and increased D-dimer could be explained by an overactive coagulation cascade and platelet activation. Infectious disorders generate a mismatch between the procoagulant and anticoagulant homeostatic mechanisms, resulting in a systemic inflammatory response [66]. In patients infected with the new coronavirus, increased rates of D-dimer and fibrin breakdown, as well as prolonged prothrombin length, were linked to a poor prognosis [65]. In accordance with the diagnostic guidelines of the International Society on Thrombosis and Haemostasis, 15 of the 21 non-survivors (8 percent of the entire cohort) manifested evident DIC (>5 points) [67]. Lippi and colleagues found slightly lower platelet counts in patients with acute disease in a meta-analysis, and thrombocytopenia was connected to a five-fold increased risk of severe disease [65].

Hypokalemia

In the general population, diuretics are primarily employed as pharmacological medicines to treat hypertension and prevent fluid overload. Hypokalemic patients have a considerably higher prevalence of hypertension, cardiovascular illness, and renal impairment than normovolemic patients, which could explain why they require more diuretics. Long-term use of diuretics has been shown to cause hypokalemia and other electrolyte abnormalities [68]. This side effect in the patients could have been the primary cause of several electrolyte imbalances. In comparison to patients with normokalie, hypokalemia was associated with hypocalcemia and a lower plasma magnesium level. While female gender is associated with hypokalemia, early experimental investigations conducted in the 1950s [69] and later confirmed in the 1990s [70] found that women, particularly the elderly, have less exchangeable body potassium than other popular subsets. As a result, women are more likely than males to develop hypokalemia because their potassium deposits have been drained due to differences in body composition, with women having less extracellular water than men.

Hypokalemia was found to be a common electrolyte imbalance among COVID-19 patients, according to Riccardo etalfindings. .'s During hospitalisation, 41 percent of patients with severe symptoms of SARS-CoV-2 infection had hypokalemia. Hypokalemia's incidence and causes are unknown at this time, as it has only been documented as a probable COVID-19 symptom. Hypokalemia, on the other hand, has the potential to cause life-threatening arrhythmia in people infected with SARS-CoV-2 [71]. In this study, for the first time, the clinical features of hypokalemic SARS-CoV-2 patients are presented [71]. They tracked the various causes of hyperkalemia in a sample of hospitalised patients, including diuretic treatment, acid-base dysfunction, and corticosteroid therapy, despite the fact that urine analysis was only available in a small number of patients. Their findings indicate the necessity to frequently measure blood potassium levels in COVID-19 patients, as well as the urine K-to-creatinine ratio or 24-hour potassium excretion, in order to improve patient care. Depending on the severity of the urine loss, potassium should be supplemented, and the electrocardiogram (ECG) should be carefully evaluated, especially if you're using

any potentially arrhythmogenic medications.

In a small percentage of patients, the cause of tubular potassium shortage was unknown (22.2 percent). Hypokalemia was usually minor, unrelated to bad outcomes, and easily treated with potassium supplements. Although hypokalemia was not linked to death in their patient group, it is a potentially fatal illness if left untreated [71].

Kidney damage

SARS-CoV-2 may infiltrate the lungs and cause cytopathic consequences in a variety of organs, including renal tissue [70]. It has been discovered that the kidneys express the SARS-CoV-2 cell-entry receptor ACE2 around 100 times more than the lungs do [33,71]. The pathophysiology of kidney illness in COVID-19 patients is likely multifaceted, involving direct cytotoxic effects on renal tissue, immune complex deposition, and virus-induced cytokines or mediators [72,73]. COVID-19 patients' postmortem data were analysed by Su et al., who discovered proof of COVID-19's severe cytopathic influence on kidney tissue [74]. Hirsch et al. investigated 5449 patients with acute kidney injury (AKI) and proposed COVID-19 ischemic acute tubular necrosis as a significant cause of AKI [75].

They found a significant risk of AKI (29.1%) and a high death rate in patients with AKI (34.6 percent). According to earlier clinical trials, the detection of AKI in COVID-19 patients ranged from 0.5 percent to 36.6 percent [75] [70]. COVID-19 was thought to be unrelated to AKI by Wang et al. [76]. AKI was not documented in that study, even in patients who died in the intensive care unit. AKI was found in 5.1 percent of 701 patients by Cheng et al. [74]. In that study, the among-hospital death rate was 16.1%, but it was estimated that in patients with elevated baseline blood creatinine levels, the rate may reach 33.7 percent. Another Chinese study looked at 1,099 patients and discovered that patients with high creatinine levels (9.6%, n=52) had a greater death or ICU admission rate than patients with normal creatinine levels (1%, n=700) [77].

Acute renal failure appears to be a common complication of COVID-19, since it occurs in one-fifth of SARS-COV-2 pneumonia hospitalised cases. AKI is often recognised in symptomatic elderly people as a severe systemic inflammatory response to the ongoing illness. Size, male sex, and Chronic Kidney Disease (CKD) were all characteristics in our patient sample that contributed to AKI. Because AKI is a standalone risk factor in COVID-19 for all-cause mortality [78], it is critical to determine the etiological mechanism, as well as a technique to prioritise AKI prevention and early detection.

Liver injury

According to recent epidemiological studies, 16–53 percent of COVID-19 patients experienced varying degrees of hepatic injury [78] [79], with some patients developing serious liver injury. The coagulant system anomaly caused by hepatic damage can result in substantial bleeding, especially in patients receiving continuous renal replacement or extracorporeal membrane oxygenation. The deterioration of liver function can lead to hepatic failure and death. In COVID-19 patients, liver damage need immediate care [81]. Existing studies have linked SARS-CoV-2 transmission, hepatotoxic medication treatment, virally mediated cytotoxic T cells, and a dysregulated innate immune response to liver damage in COVID-19 [82]. COVID-19 [83] patients' liver tissue showed moderate microvesicularsteatosis and minor lobular activity. According to preliminary studies, SARS-CoV-2 can bind directly to ACE2-positive cholangiocytes, causing liver function dysregulation.

According to the data, liver damage occurred more frequently and more quickly in very ill COVID-19 patients, advanced more quickly, and healed later than in non-critical patients. In non-critically ill COVID-19 patients, drug characteristics such as lopinavir/ritonavir and arbidol therapy, as well as the number of

concomitant drugs, were predictive predictors of liver damage, which could be attributable to metabolic interactions with the drug. Liver injury was linked to a longer hospital stay and delayed virus eradication in all of the enrolled patients.

SARS-CoV-2 may directly dysregulateliver function by binding to ACE2-positive cholangiocytes [84]. ALT (Alanine aminotransferase) and AST (Aspartate aminotransferase) were found to be the primary markers in COVID-19 patients with serious illness, rather than TBL (Total bilirubin). Immune interactions involving virally mediated cytotoxic T cells and Kupffer cells can cause hepatocyte injury [82]. Researchers speculated that, in addition to the obvious damage caused by SARS-CoV-2, a virus-induced cytokine storm might also play a significant role in critically ill patients with liver damage. Specifically, unlike other studies, Jiang et al. discovered that drug factors, rather than the severity of the disease, may play a larger role in the liver injury of non-critically ill COVID-19 patients [81].

Cardiovascular dysfunction

Patients with chronic cardiovascular disease (CVD) are more likely to develop severe COVID-19 and have a poor prognosis. The most common comorbidities among COVID-19 patients were hypertension (17%), diabetes (8%), and CVD (5%), according to a meta-analysis of 46,248 individuals [85]. CVD and hypertension have grown more prevalent in the extreme patient group than in the non-serious cases [85]. There is also a link between existing CVDs and increased mortality. COVID-19, on the other hand, is well acknowledged to have negative effects on circulatory function, potentially harming or exacerbating the heart. There have been reports of cardiogenic connection in patients who have no history of CVD[86], as well as cases with exclusively cardiac manifestations [86] [87].

Although the exact function of cardiovascular activity in COVID-19 remains unknown, increased cardiac biomarker rates are common. According to Wang et al., 7.2 percent of patients exhibit high troponin levels, as well as electrocardiographic or echocardiographic abnormalities that indicate heart damage [89]. Because ACE2 is highly concentrated in the heart, it raises the risk of a myocardial infection. Both a cytokine storm caused by systemic inflammation and a hypoxic situation caused by ARDS (Acute Respiratory Distress Syndrome) that causes high extracellular calcium rates and contributes to myocyte death are probable harm mechanisms [90]. Increased myocardial demand, as a result of hyperinflammatory reactions or secondary hemophagocyticlymphohistiocytosis, may contribute to atherosclerotic plaque instability and myocardial damage, increasing the risk of acute myocardial infarction [91]. Blood pressure abnormalities are frequently observed as a result of the condition. Arrhythmia-related palpitations were also seen [90] [91]. Arrhythmias can take many different forms, and their causes might range from hypoxic circumstances to ARDS-induced myocarditis. Patients with reduced ejection fraction and cardiac enlargement have been documented by Hu et al. and Zeng et al. [87][92]. As a result, the long-term effects of COVID-19 on cardiovascular function, such as the risk of heart disease, should be observed and investigated further.

Male reproductive system

SARS-CoV-2 is a betacoronavirus with symptoms that are similar to SARS-CoV and MERS-CoV. COVID-19 can cause symptoms that are similar to pneumonia in some persons. Male reproductive systems are similarly susceptible to infection; COVID-19 patients have substantial fluctuations in sex hormones, indicating a gonadal dysfunction [94]. Viruses like HIV, hepatitis B and C, mumps, Epstein-Barr, and papilloma can induce viral orchitis, which can lead to infertility and tumours in the testicles [95]. SARS-CoV can cause orchitis, according to an examination of testis postmortem materials from six patients who died from the virus [95]. In all six specimens, pathological findings included

spermatogenic cell death, germ cell destruction, few or no spermatozoa in the seminiferous epithelium, thicker basement membrane, and leukocyte infiltration. As a result, SARS-CoV-2 may have an effect on the testes. New research on SARS-CoV-2 infection sheds light on impaired male gonadal function [96]. The ratio of testosterone to luteinizing hormone (T to LH) in 81 COVID-19 patients fell considerably when compared to 100 healthy men of the same age (COVID-19 patients: 0.74; healthy men: 1.31, P 0.0001). The serum T/LH ratio (as a measure of male gonadal function) has been suggested as a possible marker of SARS-CoV-2 reproductive dysfunction [97].

SARS-CoV particles have been found in the epithelial cells of testicular seminiferous tubules and Leydig cells, indicating that testicular injury has occurred [97]. ACE2 is highly expressed in the epithelial cells of seminiferous testis ducts, adult Leydig cells, and the prostate gland. The testis cannot be detached from the immune system, despite its special immunological status. Interferons are produced when leukocytes, CD3+ T cells, and CD68+ macrophages infiltrate the interstitial tissue of the testes, inhibiting steroidogenesis and testosterone production [98]. These cells produce inflammatory cytokines that stimulate an autoimmune response and damage the seminiferous epithelium, resulting in autoimmune orchitis [99]. High cytokine levels associated with viral or bacterial infection cause sickness or injury, which can lead to sperm loss and steroidogenesis, both of which have negative impacts on fertility [98]. COVID-19 is not protected by the blood-testis barrier, and inconsistent sex hormone production may be linked to reduced gonadal function. Young adults who want to start a family after recovering from COVID-19 should seek a fertility consultation.

Female reproductive system

To date, no harm to the female reproductive system has been recorded in COVID-19 patients. The involvement of renin–angiotensin (Ang)–aldosterone (RAS) in female reproductive processes like folliculogenesis, steroidogenesis, oocyte maturation, and ovulation has been researched. Reis and colleagues [100] confirmed the presence of an Ang-(1–7)–Mas receptor–ACE2 axis and ACE2 markers at all stages of follicle maturation in the human ovary [101]. However, earlier studies have shown that ACE2 is expressed in granulosa bovine and rat ovarian cells, regulated by gonadotropins, nd involved in folliculogenesis [101] [102].

SARS-CoV-2 could kill endometrial epithelial cells and affect early embryo implant by targeting ovarian tissue and granulosa cells and reducing ovarian function and oocyte production, causing to female infertility or miscarriage. The effect of SARS-CoV-2 on the fallopian tube is currently unknown, however it is something that should be investigated more in the future [104]. During this time, further research is needed to assess the long-term consequences of SARS-CoV-2 infection in men and women on human reproduction, pregnancy outcomes, and offspring growth and development in order to obtain more evidence on the reproductive impacts of associated disorders.

Dermatological manifestations

An old study by Hamming et al. [105] showed the existence of ACE2 in the epidermis basal cell layer extending to the hair follicle basal cell layer, the smooth muscle cells comprising sebaceous glands and eccrine glands.

In the same context, Goren et al. [106] postulated a theory that androgen receptors could play a role in COVID-19 patient's severity. This finding was focused on the increased frequency of extreme COVID-19 in children and adult females relative to adult males. Furthermore, with the reduction of the androgen hormones, the ACE2 activity has shown a decrease. However, this theory is not yet proven.

Patients have been observed to have

cutaneous signs such as Urticaria [107] in addition to the traditional respiratory symptoms, acralischaemia [108], morbilliform [109], livedoreticularis [110], vasiculitis petechial exanthems[111], erythematous rash [112], chilblains-like lesions [113], Pernio-like lesions [114], maculo-papularexanthems [115], croischaemia, retiformpurpura [116], erythema multiforme [117], pityriasisrosea [118], etc. The figure 2 and 3 demonstrates distinct skin signs seen in COVID-19 confirmed patients in a study conducted by Galvan casas et al. [119].

One of the most recent articles released by Recalcati et al., addressing largely to skin reactions connected to COVID-19, finds the existence of various cutaneous illnesses in 18 out of 88 individuals. Of them, 14 (15.9% of the total) patients had an erythematous infection, three (3.4%) had urticarial infection, and one (1.13%) had chickenpox-like symptoms. Young asymptomatic patients with this illness were also observed to have purpuraraynaud's syndrome, chilblain-like, and erythema multiforme-like lesions [116]. According to Henry et al., COVID-19 patients may experience urticarial eruption without any respiratory symptoms. [120].

Because the predominant symptoms were petechiae skin rash and low platelet count, a COVID-19 patient in Thailand was misdiagnosed with dengue [121]. The first retrospective investigation by Galva Casas et al. [119] classified COVID-19 cutaneous symptoms into five separate clinical forms: pseudo-chilblain (19%), vesicular eruptions (9%), urticarial lesions (19%), maculopapular (47%) and livedo or necrosis (19%). (19 percent). 6% of the population. Our goal is to promote awareness of COVID-19 viral infection's cutaneous manifestations and to help dermatologists better understand the skin rash caused by this unique virus. Furthermore, dermatologists should pay extra attention to patients with infectious skin rash in these settings to ensure that COVID-19 cases are not missed.

Fig. 2 All of the patients shown had confirmed COVID -19. (a, b) Acral areas of erythema–oedema with vesicles or pustules (pseudo-chilblain). (c) Monomorphic (i.e. at same stages) disseminated vesicles. (d) Urticarial lesions.

Source: Reproduced from Galvan casas et al. [119]

Fig. 3 All of the patients shown had confirmed COVID -19. (a) Maculopapular eruption. Some of the lesions are perifollicular. (b) Acral

infiltrated papules (pseudovesicular). (c) Acral papules (erythema multiforme like). (d) Livedoid areas.

Source: Reproduced from Galvan casas et al. [119]

Skin damage in healthcare workers managing COVID-19

Many skin problems arise as a result of repeated usage of personal protection equipment [122] due to hyperhydration, rubbing, and allergic contact reactions. Protective equipment caused 97.0 percent of skin injuries among health-care professionals, with lesions on the nasal bridge (83.1 percent), hands, cheeks, and forehead [123]. Hand washing or glove decontamination should be confined to the following times: before handling the patient or performing any aseptic therapy, and after contact with body fluids, touching the patient or some of the patient's objects.They also recommended using ethanol for hand hygiene and, if possible, applying hand cream after each hand hygiene session. Furthermore, a cotton glove should be worn beneath the latex gloves, and topical moisturisers including glucocorticoid cream should be used. A properly fitted mask, goggles, and the application of moisturisers or cream to contact areas are also recommended [122] [124]. When utilising N95 masks.

Role of nanotechnology in detection, treatment and prevention of Covid-19

Nanotechnology has sparked a lot of interest in recent years, and it's now widely employed in fields including health [125], agriculture [126], and bio-labelling [127]. Nanotechnology has been employed in numerous fields of medical research, including gene transfer [128], selective drug delivery [129], artificial implants [130], and public health sensing systems and other biosensors [131]. It can also be utilised for cancer treatment and detection [132] as well as the development of active antiviral, antibacterial, and antifungal medicines. The nanoscale scale of the material, which allows entrance into the cells of living systems, particularly the human body, is the basis for this interest in employing nanotechnology in medicine. Due to the shielding capabilities of some nano-sized materials, nanomaterials may serve a defensive role, preventing degradation of the enclosed product or anti-infection agent [133].

Detection

Diagnostics may play a key role in COVID-19 containment, enabling for the rapid implementation of control measures that limit the spread of the virus by identifying and isolating cases as well as tracking links (i.e. recognising individuals who might have come into touch with an infected patient). COVID-19 is typically diagnosed using reverse transcription polymerase chain reaction (RT-PCR) and screened using CT scans, although each method has drawbacks. Because they can monitor and identify different infections, molecular techniques are more reliable than syndromic testing or CT scans in detecting illnesses [134]. Nanotechnology opens up new possibilities for making low-cost, high-efficiency identification systems, secure personal protection gadgets, and cutting-edge, effective medications. Nanosensors are already a reality, capable of detecting low levels of bacteria and viruses and alerting clinicians when symptoms appear in patients with low viral loads. To diagnose COVID-19, many nano-based methodologies have been developed, which have advantages over molecular procedures. The methods that are currently being tested are listed below.

Reverse transcription loop-mediated isothermal amplification (RT-LAMP) coupled with a nanoparticle-based biosensor (NBS) assay

Covid 19 is now diagnosed by RT-PCR in real-time detection of SARS-CoV-2 nucleic acid [135]. Many types of gene amplification have been employed in comparison to this method, but their main disadvantages are that they are complex, require experienced

personnel, and take a long time. Yang et al. devised an RT-LAMP test for the identification of three genes to diagnose SARS-CoV-2 fast in order to overcome these limitations. In 2003, this method was employed to test for the coronavirus SARS, and it was shown to be quick and simple [136]. Since then, an RT-LAMP NBS assay has been developed to swiftly and accurately detect COVID-19 [137]. This RT-LAMP-NBS test combines LAMP amplification, reverse transcription, and multiplex inspection with nanoparticle-targeted biosensors to diagnose COVID-19 in a single-tube, one-step response. A one-step, one-tube RT-LAMP-NBS assay was designed to identify COVID-19. This technique takes 30 minutes to amplify nucleic acid at a temperature of 60–650 degrees Celsius. The impacts of identification can be seen macroscopically in the form of a colour transformation.

Point-of-care testing

Point-of-care People are diagnosed without having to send samples to national labs, and conclusions are produced without the need for a testing network to classify infected patients. SARS-CoV-2 lateral flow antigen testing is being investigated as a point of care for COVID-19 diagnosis [138]. In commercial lateral flow tests, a paper-like membrane strip is coated with two lines: one that carries antibody conjugates to gold nanoparticles, and the other that collects the antibodies. The membrane collects patient samples (such as blood and urine), and the protein is pushed over the line by capillary action. The antigens bind to the gold nanoparticle-antibody conjugate as the first line goes across the membrane, and the complex flows across the membrane. When the trapped antibodies reach the second side, where the red or blue side is visible, the complex is immobilised. Due to connected plasmon bands, individual gold nanoparticles are red, while the fluid containing clustered gold nanoparticles is blue [139]. The lateral flow test's clinical sensitivity, specificity, and accuracy for IgM were 57 percent, 100 percent, and 69 percent, respectively, and 81 percent, 100 percent, and 86 percent for IgG. A test that detects both IgM and IgG has an 82 percent clinical sensitivity [139].

Optical biosensor nanotechnology

A new device based on optical biosensor nanotechnology could identify the coronavirus directly from patient samples in roughly 30 minutes, removing the need for centralised laboratory testing. The most recent studies will swiftly determine whether a person is afflicted with the coronavirus or influenza virus. The project could be used for purposes other than the present pandemic and human care. The most recent biosensor technology could also be used to investigate various varieties of coronavirus found in reservoir animals like bats, in order to identify and track the virus's potential evolution and avoid future human pandemics. [140].

Nano-based treatment

Experts have been studying the possibility of using nanoparticles to treat bacterial and viral diseases for some years. For example, gold nanoparticles are designed to bind to viruses like Ebola or influenza, and then heat the particles using infrared wavelengths to disrupt the virus's structure. COVID-19 infections have recently been linked to a hyperinflammatory state characterised by a fulminant cytokine storm (hypercytokinemia) prior to the onset of ARDS and death [32]. A better understanding of the biology of acute inflammation can aid in the development of new inflammatory disease treatments [19]. Death may be linked to virally mediated hyperinflammation, according to research on confirmed cases of COVID-19. These unregulated pro-inflammatory systems are typically guided by constant positive feedback loops between pro-inflammatory signalling and oxidative stress, according to evidence and observations. According to the researchers, there is currently no effective way to target counteract this activity.

According to the research of Dormont et al., multidrug nanoparticles could be utilised to monitor and alleviate the effects of uncontrolled inflammation. The nanoparticles of adenosine, an endogenous immunomodulator, were created by conjugating squalene, an endogenous lipid, and encapsulating -tocopherol, a natural antioxidant. This resulted in high drug loading, biocompatible, multidrug nanoparticles, according to the researchers. The researchers discovered that the nanoparticles might deliver therapeutic medicines in a tailored manner by targeting vascular endothelial barrier failure at high-inflammatory sites. In animal models, endotoxemia testing revealed a "significant survival" benefit. As a result, scientists believe that administering adenosine and antioxidants in a targeted manner could be a novel way to treat acute COVID-19 inflammation with few side effects and reliable therapeutic applications. [141].

Vaccination is one of the most important therapy methods for improving the immune response to infectious disorders [142]. Meanwhile, because nanoparticles have been proven to exhibit immunostimulatory properties [143], substantial attention has been focused on developing nano-based medicinal medicines or vaccines against various coronaviruses. In inoculated mice and rabbits, Staroverov et al. evaluated the defensive immunological response elicited by gold nanoparticles (AuNPs) mixed with a type of coronavirus discovered in 2011 as swine transmissible gastroenteritis virus (TGEV) [144]. In vaccinated specimens, TGEV-conjugated colloidal gold was observed to elicit greater IFN- concentrations and neutralising antibody titers. In comparison to the free antigen reaction, vaccination with the antigen-colloidal gold complex increased T-cell proliferation tenfold, and the authors of the study also found that complex administration resulted in reciprocal enhancement of respiratory macrophage function and enhanced protective immunity against TGEV. Gold nanoparticles coupled to a virus could also be considered an antiviral option for vaccine development.

In mice, Sekimukai [145] evaluated the efficacy of two types of adjuvants (AuNPs and Toll-like receptor agonists) in combination with recombinant S protein against SARS-CoV infection. In contrast to a Toll-like receptor agonist-adjuvanted vaccine, vaccination with AuNP-adjuvanted protein elicited a high IgG response but did not develop protective antibodies or reduce eosinophilic infiltration. Gold nanoparticles, spike protein nanoparticles, and hollow polymeric nanoparticles have all been shown in animal models to have great potential to trigger an immune response against coronavirus [146]–[148]. For SARS-COV-2, a messenger RNA (mRNA) lipid nanoparticle vaccination is being explored. It is based on previous SARS-CoV and MERS reports [149].

Prevention

SARS-CoV-2 is disseminated mostly through minute droplets of virus particles that enter the body through the eyes, mouth, or nose as a result of breathing, speaking, sneezing, or coughing. Preliminary research also suggests that these germs can survive for days when stuck to countertops, handrails, and other hard surfaces. Nanoparticles will destroy certain diseases long before they enter the body, according to Webster, because they cling to numerous things and structures. His lab has developed nanoparticle-forming materials that may be sprayed on goods to combat viruses. He claimed that the virus was inactive even if it was on a table, a countertop, or an iPhone [150].

Many modern masks fail to maintain their air filtration function, and their electrostatic activity vanishes when exposed to water. As a result, their filtering capability is greatly reduced, making re-use almost impossible. Professor Kim's nanofilter mask, on the other hand, is made by crossing and aligning thin nanofibers to generate small air holes that keep viruses out while allowing people to breathe easily. That is, unlike traditional masks, the filter produces

a physical barrier rather than relying on static electricity. The material has been demonstrated to retain more than 94 percent of its filtration ability after 20 regular washings with soap and is safe to use for up to a month. In fact, it showed no deformations in its nano-fibre framework after three hours of soaking in ethanol and resisted 4,000 mechanical crumples and strains [151].

Antiviral nature of nanoparticles

Nanoparticles could be an interesting treatment option. Against the alphacoronavirus porcine epidemic diarrhoea virus (PEDV), Du et al. first revealed a new treatment method based on silver nanoparticles in 2018 [152]. They discovered that Ag2S nanoclusters (NCs) can stop PEDV from multiplying in treated Vero cells. Treatment with Ag2S NCs decreased viral budding and viral negative-strand RNA synthesis, which could explain why. Furthermore, the Ag2S NCs have been demonstrated to favourably control the proliferation of IFN-activating genes and the generation of pro-inflammatory cytokines, resulting in resistance to PEDV infection, making them a viable therapeutic candidate for further research.

To combat human coronavirus NL63, Ciejka et al. created a biopolymeric material for the creation of nano/microspheres (NS/MS) with a high potential for adsorbing coronaviruses [153]. When N-(2-hydroxypropyl)-3-trimethyl chitosan (H-HTCC)-NS/MS was added to viral suspensions, the number of copies of viral RNA dropped, and this was found to have a strong link with the amount of H-HTCC-NS/ MS employed. According to their findings, 2.5 mg/500 l H-HTCC-NS/ MS could reduce the amount of H-HTCC-NS/ MS by 99.60 percent. The decrease was 99.92 percent when 10 mg/500 l of HHTCC-NS/MS was introduced.

In a patent discovered in 2014 by Cho et al., a mixture of silver colloid, titanium dioxide (TiO2) nanoparticles, a dispersion stabiliser, binder, and water displayed antibacterial, antifungal, and antiviral properties (US 8,673,331 B2) [154]. At a 100-fold dilution of the formulation concentration, antiviral efficacy against PEDV and TGEV was demonstrated at a rate of 99.99 percent or greater, according to antiviral research findings. When the formulation concentration was diluted 1000 times, the viruses' development was reduced at a rate of 99.9% for PEDV and 93.0% for TGEV, respectively. As a result, Cho et alproposed .'snanomaterials' antiviral activity was dependent on the composition's concentration, implying that dose should be changed to achieve optimal inhibition [133].

Antiviral activity of zinc

Antiviral activity of zinc against rhinoviruses, common cold virus infections, and influenza viruses is excellent. Zinc can also be utilised to treat COVID-19 infections and reduce the risk and severity of infection [140]. In vitro, zinc nanoparticles inhibit influenza virus multiplication, and zinc oxide nanoparticles appear to be effective against H1N1 influenza virus infections. SARS coronavirus replication is also inhibited by zinc [155]. The virus's respiratory syncytial replication is inhibited by zinc salts, and viral replication of hepatitis C is reduced. Zinc supplementation has significantly reduced the prevalence of pneumonia in children in underdeveloped nations. Although the antiviral activity of zinc is unknown, it may hinder the virus from adhering to the mucosa and multiplying later. Zinc has been shown to have antiviral activity in vitro by promoting the production of antiviral interferon-alpha or gamma and reducing inflammatory reactions [156]. Zinc also affects immune cell function and aids in the activation of enzymes involved in a variety of cellular processes [157].

Zinc deficiency has been linked to an increased vulnerability to bacterial and viral illnesses, according to new research. Zinc deficiency has been demonstrated to impact B-cell development in vivo, resulting in insufficient antibody production and macrophages with low phagocytic activity against parasites [158]. Zinc may have antiviral effects by either limiting virus

replication or increasing the immune response, according to research. Consuming roughly 50 mg of zinc per day strengthens the host immune system, reduces the host's sensitivity to viral infection, and provides additional defence against infection with COVID-19 to lower disease risk [159], [160]. The usage of ionic zinc oxide nanoparticles in a mask covering has antiviral and antibacterial properties. Zinc oxide nanoparticles can be included into these materials to stabilise them and kill microorganisms on contact [140].

As a result, the nanomaterials may have antiviral properties against a wide range of coronaviruses. Antiviral nanomedicines against SARS-CoV, MERS-CoV, and SARS-CoV-2 should be studied even more urgently.

Conclusion

There is a global health concern that is affecting people all over the world. COVID-19 has surpassed the infection-to-mortality ratio's upper limit, separating it from other viral illnesses. To build a firm foundation for averting prospective pandemics, doctors and scientists must collaborate to eliminate the SAR-CoV-2 menace. Science and technology development and implementation are our primary weapons in the fight against COVID-19. The involvement of comorbidities and impairment of extrapulmonary organs have the greatest impact on disease progression. ARDS, cardiac arrest, renal failure, trauma, and multi-organ failure are all causes of death. When enforcing prevention and protective measures, thorough awareness of the comorbidities and potential organ damage is crucial. Recognizing this may make it easier to prioritise individual patient care and reduce the danger of decompensation. Apart from the rapid publication of study findings, this report seeks to provide medical information about COVID-19. Clinical symptoms induced by SARS-CoV-2 infection should be closely monitored to determine whether the virus has impacted internal organs and, if so, how effective treatment can be administered. For the formulation of an effective treatment approach, an individual's demographic records and previous medical history are required. In this review, we focused on the impact of COVID-19-induced human body impairments in order to provide researchers with a more detailed explanation of COVID-19's clinical implications. The role of nanotechnology approaches in managing, detecting, and preventing COVID-19 spread was also discussed. Nanotechnology offers a unique combination of capabilities that will dramatically advance our understanding of viral illnesses and the development of critical diagnostic and therapeutic technologies. It has been suggested that nanoparticle-based vaccines have a higher potential for eliciting a stronger defensive immune response than standard antigen-based immunizations. Furthermore, results demonstrated that nano-assays have the potential to give improved sensitivity and specificity when used for early phase quick detection of viral infection when compared to current approaches.

Abbreviations

SARS-CoV-2: **S**evere Acute Respiratory Syndrome Coronavirus 2; **ACE-2**: angiotensin-converting enzyme 2; **MERS-CoV**: Middle east respiratory syndrome-related Corona virus; **DPP4:**dipeptidyl peptidase 4; **ECG:** Electrocardiogram; **DIC**: Disseminated Intravascular Coagulation; **AKI:** Acute Kidney Injury; **CKD:** Chronic Kidney Disease; **CVD:** Cardio Vascular Disease; **ARDS**: Acute Respiratory Distress Syndrome; **TGEV**: swine transmissible gastroenteritis virus; **PEDV**: porcine epidemic diarrhea virus

References

[1] Y. Wu et al., "Nervous system involvement after infection with COVID-19 and other coronaviruses," Brain. Behav. Immun., vol. 87, no. March, pp. 18–22, 2020, doi: 10.1016/j.bbi.2020.03.031.

[2] W. Guan et al., "Clinical characteristics of coronavirus disease 2019 in China,"

N. Engl. J. Med., vol. 382, no. 18, pp. 1708–1720, 2020, doi: 10.1056/NEJMoa2002032.

[3] M. Su, Y. Hsieh, Y. Wang, and A. Lin, "Exercise Capacity and Pulmonary Function in Hospital Workers Recovered from Severe Acute Respiratory Syndrome," Respiration, vol. 74, pp. 511–516, 2007, doi: 10.1159/000095673.

[4] B. Hu, X. Ge, L. Wang, and Z. Shi, "Bat origin of human coronaviruses," Virol. J., vol. 12, no. July 2003, pp. 1–10, 2015, doi: 10.1186/s12985-015-0422-1.

[5] D. Forni, R. Cagliani, M. Clerici, and M. Sironi, "Molecular Evolution of Human Coronavirus Genomes," Trends Microbiol., vol. 25, no. 1, pp. 35–48, 2017, doi: 10.1016/j.tim.2016.09.001.

[6] H. Song, C. Tu, G. Zhang, S. Wang, K. Zheng, and L. Lei, "Cross-host evolution of severe acute respiratory syndrome coronavirus in palm civet and human," Proc Natl Acad Sci USA, vol. 102, no. 7, pp. 2430–5, 2005.

[7] Q. Wang et al., "Article Bat Origins of MERS-CoV Supported by Bat Coronavirus HKU4 Usage of Human Receptor CD26," Cell Host Microbe, vol. 16, no. 3, pp. 328–337, 2014, doi: 10.1016/j.chom.2014.08.009.

[8] J. S. M. Sabir et al., "Co-circulation of three camel coronavirus species and recombination of MERS-CoVs in Saudi Arabia," Science (80-.)., vol. 351, no. 6268, pp. 81–85, 2016.

[9] P. Zhou et al., "A pneumonia outbreak associated with a new coronavirus of probable bat origin," Nature, vol. 579, no. March, 2020, doi: 10.1038/s41586-020-2012-7.

[10] V. Metagenomics and R. Sendai, "Viral Metagenomics Revealed Sendai Virus and Coronavirus Infection of Malayan Pangolins," Viruses, vol. 11, no. 11, p. 979, 2019.

[11] J. Luan, Y. Lu, X. Jin, and L. Zhang, "Spike protein recognition of mammalian ACE2 predicts the host range and an optimized ACE2 for SARS-CoV-2 infection," Biochem. Biophys. Res. Commun., vol. 526, no. 1, pp. 165–169, 2020, doi: 10.1016/j.bbrc.2020.03.047.

[12] C. A. Devaux, J. M. Rolain, and D. Raoult, "ACE2 receptor polymorphism: Susceptibility to SARS-CoV-2, hypertension, multi-organ failure, and COVID-19 disease outcome," J. Microbiol. Immunol. Infect., vol. 53, no. 3, pp. 425–435, 2020, doi: 10.1016/j.jmii.2020.04.015.

[13] C. Wu et al., "Structural basis for the recognition of SARS-CoV-2 by full-length human ACE2," Science (80-.)., vol. 3, no. 3, pp. 1–8, 2020, doi: 10.20944/preprints202003.0226.v1.

[14] Y. Qiu et al., "Predicting the angiotensin converting enzyme 2 (ACE2) utilizing capability as the receptor of SARS-CoV-2," Microbes Infect., vol. 22, no. 4–5, pp. 221–225, 2020, doi: 10.1016/j.micinf.2020.03.003.

[15] P. Wang and Y. Cheng, "Increasing host cellular receptor angiotensin converting enzyme 2 (ACE2) expression by coronavirus may facilitate 2019-nCoV infection," bioRxiv, vol. 2, pp. 1–22, 2020, [Online]. Available: https://doi.org/10.1101/2020.02.24.963348.

[16] Y. Y. Zheng, Y. T. Ma, J. Y. Zhang, and X. Xie, "COVID-19 and the cardiovascular system," Nat. Rev. Cardiol., vol. 17, no. 5, pp. 259–260, 2020, doi: 10.1038/s41569-

020-0360-5.

[17] M. Donoghue et al., "UltraRapid Communication A Novel Angiotensin-Converting Enzyme – Related to Angiotensin 1-9," Circ Res, vol. 87, pp. e1–e9, 2000.

[18] S. R. Tipnis, N. M. Hooper, R. Hyde, E. Karran, G. Christie, and A. J. Turner, "A human homolog of angiotensin-converting enzyme: Cloning and functional expression as a captopril-insensitive carboxypeptidase," J. Biol. Chem., vol. 275, no. 43, pp. 33238–33243, 2000, doi: 10.1074/jbc.M002615200.

[19] Y.-M. Chen et al., "COVID-19 severity is associated with immunopathology and multi-organ damage," medRxiv, p. 2020.06.19.20134379, 2020, doi: 10.1101/2020.06.19.20134379.

[20] A. Ramaiah and V. Arumugaswami, "Insights into Cross-species Evolution of Novel Human Coronavirus 2019-nCoV and Defining Immune Determinants for Vaccine Development .," bioRxiv, no. Jan 30, 2020.

[21] J. F. Chan et al., "Genomic characterization of the 2019 novel human-pathogenic coronavirus isolated from a patient with atypical pneumonia after visiting Wuhan," Emerg. Microbes Infect., vol. 9, no. 1, pp. 221–236, 2020, doi: 10.1080/22221751.2020.1719902.

[22] A. Wu et al., "Composition and Divergence of the Novel Coronavirus (2019-nCoV) Originating in China," Cell Host Microbe, vol. 27, no. 3, pp. 325–328, 2020, doi: 10.1016/j.chom.2020.02.001.

[23] Y. Yuan et al., "Cryo-EM structures of MERS-CoV and SARS-CoV spike glycoproteins reveal the dynamic receptor binding domains," Nat. Commun., vol. 8, p. 15092, 2017, doi: 10.1038/ncomms15092.

[24] H. Li, S. Liu, X. Yu, S. Tang, and C. Tang, "Coronavirus disease 2019 (COVID-19): current status and future perspectives," Int. J. Antimicrob. Agents, vol. 55, p. 105951, 2020.

[25] D. Wrapp et al., "Cryo-EM structure of the 2019-nCoV spike in the prefusion conformation," Science (80-.)., vol. 367, no. March, pp. 1260–1263, 2020.

[26] F. Li, "Structure , Function , and Evolution of Coronavirus Spike Proteins," Annu Rev Virol, vol. 3, pp. 237–264, 2016, doi: 10.1146/annurev-virology-110615-042301.

[27] F. A. Paules. CL, Marston. HD, "Coronavirus infections-more than just a common cold," JAMA - J. Am. Med. Assoc., no. January, 2020, doi: 10.1007/82.

[28] V. S. Raj et al., "Dipeptidyl peptidase 4 is a functional receptor for the emerging human coronavirus-EMC," Nature, vol. 495, no. 7440, pp. 251–254, 2013, doi: 10.1038/nature12005.

[29] K. Kuba et al., "A crucial role of angiotensin converting enzyme 2 (ACE2) in SARS coronavirus-induced lung injury," Nat. Med., vol. 11, no. 8, pp. 875–879, 2005, doi: 10.1038/nm1267.

[30] D. S. Hui et al., "The continuing 2019-nCoV epidemic threat of novel coronaviruses to global health — The latest 2019 novel coronavirus outbreak in Wuhan, China," Int. J. Infect. Dis., vol. 91, pp. 264–266, 2020, doi: 10.1016/j.ijid.2020.01.009.

[31] J. Villar, H. Zhang, and A. S. Slutsky, "Lung Repair and Regeneration in ARDS: Role of PECAM1 and Wnt Signaling," Chest, vol. 155, no. 3, pp. 587–594, 2019, doi:

10.1016/j.chest.2018.10.022.

[32] H. Wang and S. Ma, "The cytokine storm and factors determining the sequence and severity of organ dysfunction in multiple organ dysfunction syndrome," Am. J. Emerg. Med., vol. 26, no. 6, pp. 711–715, 2008, doi: 10.1016/j.ajem.2007.10.031.

[33] N. Chen et al., "Epidemiological and clinical characteristics of 99 cases of 2019 novel coronavirus pneumonia in Wuhan, China: a descriptive study," Lancet, vol. 395, no. 10223, pp. 507–513, 2020, doi: 10.1016/S0140-6736(20)30211-7.

[34] B. Diao et al., "Reduction and Functional Exhaustion of T Cells in Patients With Coronavirus Disease 2019 (COVID-19)," Front. Immunol., vol. 11, pp. 1–14, 2020, doi: 10.3389/fimmu.2020.00827.

[35] Y. Chen, Y. Guo, Y. Pan, and Z. Joe, "Structure analysis of the receptor binding of 2019-nCoV," Biochem. Biophys. Res. Commun., vol. 525, no. 1, pp. 135–140, 2020, doi: 10.1016/j.bbrc.2020.02.071.

[36] X. Zou, K. Chen, J. Zou, P. Han, and J. Hao, "Single-cell RNA-seq data analysis on the receptor ACE2 expression reveals the potential risk of different human organs vulnerable to 2019-nCoV infection," Front. Immunol., vol. 14, no. 2, pp. 185–192, 2020.

[37] P. Pramanik and P. Pramanik, "Diabetes mellitus augments the complications of patients with COVID-19: a review," Int. J. Res. Med. Sci., vol. 8, no. 7, p. 2716, 2020, doi: 10.18203/2320-6012.ijrms20202925.

[38] C.-L. E. Cells et al., "Apical Entry and Release of Severe Acute Respiratory Syndrome-Associated Coronavirus in Polarized," J. Virol., vol. 79, no. 15, pp. 9470–9479, 2005, doi: 10.1128/JVI.79.15.9470.

[39] F. Albarello et al., "2019-novel Coronavirus severe adult respiratory distress syndrome in two cases in Italy : An uncommon radiological presentation," Int. J. Infect. Dis., vol. 93, pp. 192–197, 2020, doi: 10.1016/j.ijid.2020.02.043.

[40] Jain A, "COVID - 19 and lung pathology," Indian J Pathol Microbiol, vol. 63, pp. 171–2, 2020, doi: 10.4103/IJPM.IJPM.

[41] Y. Huang et al., "Impact of coronavirus disease 2019 on pulmonary function in early convalescence phase," Respir. Res., vol. 21, no. 163, pp. 1–10, 2020.

[42] S. A. Meo, A. M. Alhowikan, I. M. Meo, and D. M. Halepoto, "Novel coronavirus 2019-nCoV : prevalence , biological and clinical characteristics comparison with SARS-CoV and MERS-CoV," Eur. Rev. Med. Pharmacol. Sci., vol. 24, pp. 2012–2019, 2020.

[43] D. S. Hui et al., "The 1-Year Impact of Severe Acute Respiratory Syndrome on Pulmonary Function , Exercise Capacity , and Quality of Life in a Cohort of Survivors *," Chest, vol. 128, no. 4, pp. 2247–2261, 2005, doi: 10.1378/chest.128.4.2247.

[44] K. Ong et al., "Pulmonary function and exercise capacity in survivors of severe acute respiratory syndrome," Eur Respir J, vol. 24, pp. 436–442, 2004, doi: 10.1183/09031936.04.00007104.

[45] Z. Xu et al., "Case Report Pathological findings of COVID-19 associated with acute respiratory distress syndrome," Lancet Respir., vol. 8, no. 4, pp. 420–422, 2020, doi: 10.1016/S2213-2600(20)30076-X.

[46] T. H. Li, Yan Chao, Wan Ju Bhai, "The neuroinvasive potential of SARS - CoV2

may play a role in the respiratory failure of COVID - 19 patients," J. Med. Virol., no. February, pp. 24–27, 2020, doi: 10.1002/jmv.25728.

[47] L. Mao, M. Wang, S. Chen, Q. He, and J. Chang, "Neurological Manifestations of Hospitalized Patients with COVID-19 in Wuhan , China : a retrospective case series study," medRxiv, 2020.

[48] A. M. Baig, A. Khaleeq, U. Ali, and H. Syeda, "Evidence of the COVID-19 Virus Targeting the CNS: Tissue Distribution, Host-Virus Interaction, and Proposed Neurotropic Mechanisms," ACS Chem. Neurosci., vol. 11, no. 7, pp. 995–998, 2020, doi: 10.1021/acschemneuro.0c00122.

[49] Otto Repalino et al., "Brain MR Spectroscopic findings in three consecutive COVID-19 Patients: Preliminary Observations," medRxiv, vol. 21, no. 1, pp. 1–9, 2020.

[50] Giacomelli A et al., "Self-reported Olfactory and Taste Disorders in Patients With Severe Acute Respiratory Coronavirus 2 Infection: A Cross-sectional Study," Clin. Infect. Dis., 2020, doi: 10.1093/cid/ciaa330.

[51] C. S. von Bartheld, M. M. Hagen, and R. Butowt, "Prevalence of Chemosensory Dysfunction in COVID-19 Patients: A Systematic Review and Meta-analysis Reveals Significant Ethnic Differences," medRxiv, vol. 0352, p. 2020.06.15.20132134, 2020, doi: 10.1101/2020.06.15.20132134.

[52] J. Kim, "Neurological Complications during Treatment of Middle East Respiratory Syndrome," J Clinil Neurol, vol. 13, no. 3, pp. 227–233, 2017.

[53] J. Netland, D. K. Meyerholz, S. Moore, M. Cassell, and S. Perlman, "Severe Acute Respiratory Syndrome Coronavirus Infection Causes Neuronal Death in the Absence of Encephalitis in Mice Transgenic for Human ACE2 ," J. Virol., vol. 82, no. 15, pp. 7264–7275, 2008, doi: 10.1128/JVI.00737-08.

[54] Y. Ding et al., "Organ distribution of severe acute respiratory syndrome (SARS) associated coronavirus (SARS-CoV) in SARS patients : implications for pathogenesis and virus transmission pathways," J. Pathol., vol. 203, pp. 622–630, 2004, doi: 10.1002/path.1560.

[55] K. Lau, W. Yu, C. Chu, S. Lau, and B. Sheng, "Possible central nervous system infection by SARS coronavirus," Emerg Infect Dis, vol. 10, no. 2, pp. 342–344, 2004.

[56] K. Bohmwald, N. M. S. Gálvez, M. Ríos, and A. M. Kalergis, "Neurologic Alterations Due to Respiratory Virus Infections," Front. Med., vol. 12, no. October, pp. 1–15, 2018, doi: 10.3389/fncel.2018.00386.

[57] R. Mondal, U. Ganguly, S. Deb, G. Shome, and S. Pramanik, "Meningoencephalitis associated with COVID-19 : A systematic review," medRxiv, no. June 26, 2020.

[58] K. H. Ng et al., "Pulmonary artery thrombosis in a patient with severe acute respiratory syndrome.," Postgrad. Med. J., vol. 81, no. 956, pp. 1–3, 2005, doi: 10.1136/pgmj.2004.030049.

[59] T. Umapathi et al., "Large artery ischaemic stroke in severe acute respiratory syndrome (SARS)," J. Neurol., vol. 251, no. 10, pp. 1227–1231, 2004, doi: 10.1007/s00415-004-0519-8.

[60] M. Yang et al., "Hematological findings in SARS patients and possible mechanisms

(review).," Int. J. Mol. Med., vol. 14, no. 2, pp. 311–315, 2004, doi: 10.3892/ijmm.14.2.311.

[61] P. Y. Chong et al., "Analysis of Deaths during the Severe Acute Respiratory Syndrome (SARS) Epidemic in Singapore: Challenges in Determining a SARS Diagnosis," Arch. Pathol. Lab. Med., vol. 128, no. 2, pp. 195–204, 2004, doi:10.1043/1543-2165(2004)128<195:AODDTS>2.0.CO;2.

[62] R. S. M. Wong et al., "Haematological manifestations in patients with severe acute respiratory syndrome: Retrospective analysis," Br. Med. J., vol. 326, no. 7403, pp. 1358–1362, 2003, doi: 10.1136/bmj.326.7403.1358.

[63] E. S. Kim et al., "Clinical progression and cytokine profiles of middle east respiratory syndrome coronavirus infection," J. Korean Med. Sci., vol. 31, no. 11, pp. 1717–1725, 2016, doi: 10.3346/jkms.2016.31.11.1717.

[64] H. Algahtani, S. Ahmad, and S. Bader, "Neurological Complications of Middle East Respiratory Syndrome Coronavirus: A Report of Two Cases and Review of the Literature," Case Rep. Neurol. Med., vol. 2016, pp. 1–6, 2016, doi: 10.1155/2016/3502683.

[65] G. Lippi, M. Plebani, and B. M. Henry, "Thrombocytopenia is associated with severe coronavirus disease 2019 (COVID-19) infections: A meta-analysis," Clin. Chim. Acta, vol. 506, no. March, pp. 145–148, 2020, doi: 10.1016/j.cca.2020.03.022.

[66] D. Giannis, I. A. Ziogas, and P. Gianni, "Coagulation disorders in coronavirus infected patients: COVID-19, SARS-CoV-1, MERS-CoV and lessons from the past," J. Clin. Virol., vol. 127, no. March, p. 104362, 2020, doi: 10.1016/j.jcv.2020.104362.

[67] N. Tang, D. Li, X. Wang, and Z. Sun, "Abnormal coagulation parameters are associated with poor prognosis in patients with novel coronavirus pneumonia," J. Thromb. Haemost., vol. 18, no. 4, pp. 844–847, 2020, doi: 10.1111/jth.14768.

[68] S. Arampatzis et al., "Impact of diuretic therapy-associated electrolyte disorders present on admission to the emergency department : a cross-sectional analysis," BMC Med., vol. 11, no. 83, 2013.

[69] Sagild U, "TOTAL EXCHANGEABLE POTASSIUM I N NORMAL SUBJECTS," J. Clin. Lab. Investig., vol. 8, pp. 44–50, 1956.

[70] H. Su et al., "Renal histopathological analysis of 26 postmortem findings of patients with COVID-19 in China," Kidney Int., vol. 98, no. 1, pp. 219–227, 2020, doi: 10.1016/j.kint.2020.04.003.

[71] M. Riccardo et al., "Hypokalemia in Patients with COVID-19," medRxiv, no. June 18, 2020, [Online]. Available: https://doi.org/10.1101/2020.06.14.20131169.

[72] Z. Li et al., "Caution on Kidney Dysfunctions of COVID-19 Patients," SSRN Electron. J., pp. 1–25, 2020, doi: 10.2139/ssrn.3559601.

[73] C. Huang et al., "Clinical features of patients infected with 2019 novel coronavirus in Wuhan, China," Lancet, vol. 395, no. 10223, pp. 497–506, 2020, doi: 10.1016/S0140-6736(20)30183-5.

[74] Y. Cheng et al., "Kidney disease is associated with in-hospital death of patients with COVID-19," Kidney Int., vol. 97, no. 5, pp. 829–838, 2020, doi: 10.1016/j.kint.2020.03.005.

[75] A. D. Hazzan, S. Fishbane, and K. D.

Jhaveri, “Acute kidney injury in patients hospitalized with COVID-19,” Clin. Investig. (Lond)., no. May, pp. 209–218, 2020, doi: 10.1016/j.kint.2020.05.006.

[76] L. Wang et al., “Nephrology Coronavirus Disease 19 Infection Does Not Result in Acute Kidney Injury : An Analysis of 116 Hospitalized Patients from Wuhan , China,” Am. J. Nephrol., vol. 51, pp. 343–348, 2020, doi: 10.1159/000507471.

[77] T. et al Sinan, “Kidney function on admission predicts in-hospital mortality in COVID-19,” in medRxiv, 2020.

[78] A. Gaetano et al., “Incidence , Risk Factors and Mortality Outcome in Patients with Acute Kidney Injury in COVID-19 : A Single-Center Observational Study,” medRxiv, 2020.

[79] X. Xu et al., “Clinical findings in a group of patients infected with the 2019 novel coronavirus (SARS-Cov-2) outside of Wuhan , China : retrospective case series,” BMJ, vol. 2019, no. January, pp. 1–7, 2020, doi: 10.1136/bmj.m606.

[80] W. F. Zhang C, Shi L, “Liver injury in COVID-19 : management and challenges,” Lancet Gastroenterol Hepatol., vol. 5, no. January, pp. 428–30, 2020.

[81] S. Jiang, R. Wang, L. Li, D. Hong, and R. Ru, “Liver Injury in Critically Ill and Non-critically Ill COVID-19 Patients : A Multicenter , Retrospective , Observational Study,” Front. Med., vol. 7, no. June, pp. 1–10, 2020, doi: 10.3389/fmed.2020.00347.

[82] Y. Xiao, H. Pan, Q. She, F. Wang, and M. Chen, “COVID-19 and the liver : little cause for concern,” Lancet Gastroenterol. Hepatol., vol. 5, no. 6, pp. 529–530, 2020, doi: 10.1016/S2468-1253(20)30084-4.

[83] Z. Xu et al., “Since January 2020 Elsevier has created a COVID-19 resource centre with free information in English and Mandarin on the novel coronavirus COVID- research that is available on the COVID-19 resource centre - including this for unrestricted research re-use a,” Lancet Respir. Med., vol. 8, no. January, pp. 420–2, 2020.

[84] X. Chai, L. Hu, Y. Zhang, W. Han, Z. Lu, and A. Ke, “Specific ACE2 Expression in Cholangiocytes May Cause Liver Damage After 2019-nCoV Infection,” bioRxiv, 2020.

[85] J. Yang, Y. Zheng, X. Gou, K. Pu, Z. Chen, and Q. Guo, “Prevalence of comorbidities and its effects in patients infected with SARS-CoV-2 : a systematic review and meta-analysis,” Int. J. Infect. Dis., vol. 94, pp. 91–95, 2020, doi: 10.1016/j.ijid.2020.03.017.

[86] H. A. Khan IH, Zahra SA, Zaim S, “At the heart of COVID - 19,” J. Card. Suregry, pp. 1–8, 2020, doi: 10.1111/jocs.14596.

[87] Fried JA et al., “The Variety of Cardiovascular Presentations of Covid-19,” Circulation, pp. 1930–1936, 2020, doi: 10.1161/CIRCULATIONAHA.120.047164.

[88] F. Y. Hu H, Ma F, Wei X, “Coronavirus fulminant myocarditis treated with glucocorticoid and human immunoglobulin,” Eur Hear. J, no. March 16, p. 1307800, 2020, doi: 10.1093/eurheartj/ehaa190.

[89] et al. Wang D, Hu B, Hu C, “Clinical Characteristics of 138 Hospitalized Patients With 2019 Novel Coronavirus–Infected Pneumonia in Wuhan, China,” JAMA, vol. 323, no. 11, pp. 1061–1069, 2020, doi: 10.1001/jama.2020.1585.

[90] Z. et al Sevim, “Covid-19 and Multiorgan Response,” Curr Probl Cardiol, vol. 00, no.

100618, 2020, [Online]. Available: https://doi.org/10.1016/j.cpcardiol.2020.100618.

[91] H. A. Khashkhusha TR, Chan JSK, "ACE inhibitors and COVID - 19 : We don ' t know yet," J. Card. Suregry, pp. 1172–1173, 2020, doi: 10.1111/jocs.14582.

[92] K. Liu et al., "Clinical characteristics of novel coronavirus cases in tertiary hospitals in Hubei Province," Chin. Med. J. (Engl)., vol. 0, no. 9, pp. 1025–1031, 2020, doi: 10.1097/CM9.0000000000000744.

[93] J. Hui et al., "First case of COVID - 19 complicated with fulminant myocarditis : a case report and insights," Infection, no. 0123456789, 2020, doi: 10.1007/s15010-020-01424-5.

[94] Ma L et al., "Effect of SARS- CoV-2 infection upon male gonadal function: a single center- based study," medRxiv, 2020, [Online]. Available: https://doi.org/10.1101/2020.03.21.20037267.

[95] J. Xu et al., "Orchitis : A Complication of Severe Acute Respiratory Syndrome (SARS) 1," Biol. Reprod., vol. 74, pp. 410–416, 2006, doi: 10.1095/biolreprod.105.044776.

[96] Ling Ma et al., "Effect of SARS-CoV-2 infection upon male gonadal function: A single centerbased study," medRxiv, 2020, [Online]. Available: https://doi.org/10.1101/2020.03.21.20037267.

[97] Wang S et al., "The need for urogenital tract monitoring in COVID-19," Nat. Rev. Urol., vol. 17, no. June, pp. 314–315, 2020, doi: 10.1038/s41585-020-0319-7.

[98] M. P. Hedger and A. Meinhardt, "Cytokines and the immune-testicular axis," J. Reprod. Immunol., vol. 58, pp. 1–26, 2003.

[99] J. Xu et al., "Orchitis: A Complication of Severe Acute Respiratory Syndrome (SARS)1," Biol. Reprod., vol. 74, no. 2, pp. 410–416, 2006, doi: 10.1095/biolreprod.105.044776.

[100] F. M. Reis, D. Ph, D. R. Bouissou, V. M. Pereira, and D. Ph, "Angiotensin- (1-7), its receptor Mas , and the angiotensin-converting enzyme type 2 are expressed in the human ovary," Fertil. Steril., vol. 95, no. 1, pp. 176–181, 2011, doi: 10.1016/j.fertnstert.2010.06.060.

[101] Vaz-Silva J et al., "The Vasoactive Peptide Angiotensin-(1–7), Its Receptor Mas and the Angiotensin-converting Enzyme Type 2 are Expressed in the Human Endometrium," Reprod. Sci., vol. 16, pp. 247–256, 2009, doi: 10.1177/1933719108327593.

[102] M. H. Barreta et al., "The components of the angiotensin- (1-7) system are differentially expressed during follicular wave in cattle," J. Renin-AngiotensinAldosterone Syst., vol. 0, no. 0, pp. 1–9, 2013, doi: 10.1177/1470320313491996.

[103] M. Pereira et al., "Gonadotropin Stimulation Increases the Expression of Angiotensin-(1 – 7) and Mas Receptor in the Rat Ovary," Reprod. Sci., vol. 16, no. 12, pp. 1165–1174, 2009.

[104] Rong Li et al., "Potential risks of SARS-CoV-2 infection on reproductive health," RBMO, vol. 41, no. 1, 2020.

[105] I. Hamming, W. Timens, M. L. C. Bulthuis, A. T. Lely, G. J. Navis, and H. van Goor, "Tissue distribution of ACE2 protein, the functional receptor for SARS coronavirus. A first step in understanding SARS pathogenesis," J. Pathol., vol. 203, no. 2, pp. 631–637, 2004, doi: 10.1002/path.1570.

[106] Andy Goren et al., "What does androgenetic alopecia have to do with COVID-19 ? An insight into a potential new therapy," Dermatol. Ther., no. March, pp. 2–3, 2020, doi: 10.1111/dth.13365.

[107] Najafzadeh M et al., "Urticaria (angioedema) and COVID-19 infection," JEADV, vol. 1, pp. 1–2, 2020, doi: 10.1111/jdv.16721.

[108] J. Calv, O. Id, A. N. A. Brinca, O. Id, C. Cardoso, and O. Id, "Acro-ischemia and COVID-19 infection: clinical and histopathological features," J. Eur. Acad. Dermatology Venereol., pp. 0–2, 2020, doi: 10.1111/jdv.16687.

[109] M. Hunt and C. Koziatek, "A Case of COVID-19 Pneumonia in a Young Male with Full Body Rash as a Presenting Symptom," Clin. Pract. Cases Emerg. Med., vol. 4, no. 2, pp. 219–221, 2020, doi: 10.5811/cpcem.2020.3.47349.

[110] C. J. et al Manalo IF, Smith MK, "A dermatologic manifestation of COVID-19: transient livedo reticularis," J Am Acad Dermatol, no. 20, pp. 30558–2, 2020, [Online]. Available: https://doi.org/10.1016/j.jaad.2020.04.018.

[111] L. Castelnovo, F. Capelli, A. Tamburello, P. M. Faggioli, and A. Mazzone, "Symmetric cutaneous vasculitis in COVID-19 pneumonia," J. Eur. Acad. Dermatology Venereol., 2020, doi: 10.1111/jdv.16589.

[112] G. Neely, R. Cabrera, and L. Hojman, "Parvovirus B19: Un virus ADN asociado a múltiples manifestaciones cutáneas," Rev. Chil. infectología, vol. 35, no. 5, pp. 518–530, 2018, doi: 10.4067/s0716-10182018000500518.

[113] A. Rodríguez-Villa Lario et al., "Histological findings in chilblain-lupus like COVID lesions: in search of an answer to understand their etiology," J. Eur. Acad. Dermatology Venereol., pp. 0–3, 2020, doi: 10.1111/jdv.16733.

[114] C. Guarneri, E. Venanzi Rullo, R. Gallizzi, M. Ceccarelli, S. P. Cannavò, and G. Nunnari, "Diversity of clinical appearance of cutaneous manifestations in the course of COVID-19," J. Eur. Acad. Dermatology Venereol., pp. 1–2, 2020, doi: 10.1111/jdv.16669.

[115] C. A. Rubio-Muniz et al., "The broad spectrum of dermatological manifestations in COVID-19. Clinical and histopathological features learned from a series of 34 cases," J. Eur. Acad. Dermatology Venereol., vol. 20, no. 59, pp. 17–19, 2020, doi: 10.1111/jdv.16734.

[116] X. Bosch-Amate et al., "Retiform purpura as a dermatological sign of coronavirus disease 2019 (COVID-19) coagulopathy," J. Eur. Acad. Dermatology Venereol., vol. 2019, no. c, pp. 2019–2020, 2020, doi: 10.1111/jdv.16689.

[117] H. Janah, A. Zinebi, and J. Elbenaye, "Atypical erythema multiforme palmar plaques lesions due to Sars-Cov-2," J. Eur. Acad. Dermatology Venereol., 2020, doi: 10.1111/jdv.16623.

[118] A. H. Ehsani, M. Nasimi, and Z. Bigdelo, "Pityriasis rosea as a cutaneous manifestation of COVID-19 infection," J. Eur. Acad. Dermatology Venereol., no. c, pp. 1–2, 2020, doi: 10.1111/jdv.16579.

[119] D. Casas, A. Catal, and D. Fern, "Classification of the cutaneous manifestations of COVID-19 : a rapid prospective nationwide consensus study in Spain with 375 cases," Br. J. Dermatol., pp. 71–77, 2020, doi: 10.1111/bjd.19163.

[120] D. Henry, M. Ackerman, E. Sancelme, A.

Finon, and E. Esteve, “Urticarial eruption in COVID-19 infection,” J Eur Acad Dermatol Venereol, vol. 2019, pp. 2019–2020, 2020, doi: 10.1111/jdv.16472.

[121]W. V. Joob B, “COVID-19 can present with a rash and be mistaken for Dengue,” J Am Acad Dermatol, vol. 82, no. January, 2020.

[122]D.H. Fahmy et al, “COVID-19 and dermatology : a comprehensive guide for dermatologists,” JEADV, 2020, doi: 10.1111/jdv.16545.

[123]Lan J et al., “Skin damage among healthcare workers managing coronavirus disease-2019,” Am Acad Dermatol., vol. 82, no. January, pp. 1215–1216, 2020, [Online]. Available: https://doi.org/10.1016/j.jaad.2020.03.014.

[124]Yin Z, “Covid-19: countermeasure for N95 mask-induced pressure sore,” J Eur Acad Dermatology Venereol, vol. 16490, no. c, p. 16490, 2020, doi: 10.1111/jdv.16490.

[125]D. F. Emerich and C. G. Thanos, “Nanotechnology and medicine,” Expert Opin. Biol. Ther, vol. 3, no. 4, pp. 655–663, 2003.

[126]R. Prasad, A. Bhattacharyya, and Q. D. Nguyen, “Nanotechnology in Sustainable Agriculture : Recent Developments , Challenges , and Perspectives,” Front. Microbiol., vol. 8, no. June, pp. 1–13, 2017, doi: 10.3389/fmicb.2017.01014.

[127]H. S. Mansur, A. A. P. Mansur, E. Curti, and M. V De, “Journal of Materials Chemistry B,” J. Mater. Chem. B, vol. 1, no. 12, pp. 1696–1711, 2013, doi: 10.1039/c3tb00498h.

[128]Michael K. Riley II and Wilfred Vermerris, “Recent Advances in Nanomaterials for Gene Delivery — A Review,” Nanomaterials, vol. 7(5), no. 94, pp. 1–19, 2017, doi: 10.3390/nano7050094.

[129]J. K. Patra et al., “Nano based drug delivery systems: Recent developments and future prospects,” J. Nanobiotechnology, vol. 16, no. 1, pp. 1–33, 2018, doi: 10.1186/s12951-018-0392-8.

[130]M. Schmidt and S. Fiorito, “Nanosurfaces and nanostructures for artificial orthopedic implants,” Nanomedicine, vol. 2, pp. 861–874, 2007.

[131]J. E. Kim, J. H. Choi, M. Colas, H. Kim, and H. Lee, “Gold-based hybrid nanomaterials for biosensing and molecular diagnostic applications,” Biosens. Bioelectron., vol. 80, pp. 543–559, 2016, doi: 10.1016/j.bios.2016.02.015.

[132]R. Misra, S. Acharya, and S. K. Sahoo, “Cancer nanotechnology : application of nanotechnology in cancer therapy,” Drug Discov. Today, vol. 15, no. 19–20, pp. 842–850, 2010, doi: 10.1016/j.drudis.2010.08.006.

[133]G. Nikaeen, S. Abbaszadeh, and S. Yousefinejad, “Application of nanomaterials in treatment , anti-infection and detection of coronaviruses,” Nanomedicine, vol. 15, pp. 1501–1512, 2020.

[134]Weihua Yang et al., “Rapid Detection of SARS-CoV-2 Using Reverse transcription RT-LAMP method,” medRxiv, 2020.

[135]S. Law, A. W. Leung, and C. Xu, “Severe acute respiratory syndrome (SARS) and coronavirus disease-2019 (COVID-19): From causes to preventions in Hong Kong,” Int. J. Infect. Dis., vol. 94, pp. 156–163, 2020, doi: 10.1016/j.ijid.2020.03.059.

[136]Weihua Yang et al., “Rapid Detection of SARS-CoV-2 Using Reverse transcription

RT-LAMP method," medRxiv, 2020, doi: 10.7143/jhep.47.248.

[137]Xiong Zhu et al., "Reverse transcription loop-mediated isothermal amplification combined with nanoparticles-based biosensor for diagnosis of COVID-19," medRxiv, 2020.

[138]J. Xiang et al., "Evaluation of Enzyme-Linked Immunoassay and Colloidal Gold- Immunochromatographic Assay Kit for Detection of Novel Coronavirus (SARS-Cov-2) Causing an Outbreak of Pneumonia (COVID-19)," medRxiv, 2020, doi: 10.1101/2020.02.27.20028787.

[139]B. Udugama et al., "Diagnosing COVID-19: The Disease and Tools for Detection," ACS Nano, vol. 14, no. 4, pp. 3822–3835, 2020, doi: 10.1021/acsnano.0c02624.

[140]W. Abdul, A. Muhammad, K. Atta Ullah, A. Asmat, and B. Abdul, "Role of nanotechnology in diagnosing and treating COVID-19 during the Pandemi," Int. J. Clin. Virol., vol. 4, no. 1, pp. 065–070, 2020, doi: 10.29328/journal.ijcv.1001017.

[141]F. Dormont et al., "Squalene-based multidrug nanoparticles for improved mitigation of uncontrolled inflammation in rodents," Sci. Adv., vol. 6, no. 23, pp. 1–12, 2020, doi: 10.1126/sciadv.aaz5466.

[142]R. Hewson, "Emerging viruses and current strategies for vaccine intervention," Clin. Exp. Immunol., vol. 196, no. 2, pp. 157–166, 2019, doi: 10.1111/cei.13295.

[143]Zaman M et al., "Nanovaccines and their mode of action," METHODS, vol. 60, no. 3, pp. 226–231, 2013, doi: 10.1016/j.ymeth.2013.04.014.

[144]S. A. Staroverov, I. V Vidyasheva, K. P. Gabalov, O. A. Vasilenko, V. N. Laskavyi, and L. A. Dykman, "Immunostimulatory Effect of Gold Nanoparticles Conjugated with Transmissible Gastroenteritis Virus," Bull. Exp. Biol. Med., vol. 151, no. 4, pp. 436–439, 2011.

[145]H. Sekimukai et al., "Gold nanoparticle-adjuvanted S protein induces a strong antigen-specific IgG response against severe acute respiratory syndrome-related coronavirus infection, but fails to induce protective antibodies and limit eosinophilic infiltration in lungs," Microbiol. Immunol., vol. 64, no. 1, pp. 33–51, 2020, doi: 10.1111/1348-0421.12754.

[146]Y. S. Kim et al., "Chaperna-mediated assembly of ferritin-based middle East respiratory syndrome-coronavirus nanoparticles," Front. Immunol., vol. 9, no. MAY, pp. 1–20, 2018, doi: 10.3389/fimmu.2018.01093.

[147]S. Jung, K. Won, E. Lee, D. Seo, H. Kim, and H. Kim, "Heterologous prime – boost vaccination with adenoviral vector and protein nanoparticles induces both Th1 and Th2 responses against Middle East respiratory syndrome coronavirus," Vaccine, vol. 36, no. January, pp. 3468–3476, 2020.

[148]L. C. W. Lin et al., "Viromimetic STING Agonist-Loaded Hollow Polymeric Nanoparticles for Safe and Effective Vaccination against Middle East Respiratory Syndrome Coronavirus," Adv. Funct. Mater., vol. 29, no. 28, pp. 1–15, 2019, doi: 10.1002/adfm.201807616.

[149]C. W. C. Warren, "Nano Research for COVID-19," ACS Nano, vol. 14, pp. 3719–3720, 2020, doi: 10.1021/acsnano.0c02540.

[150]Roberto Molar Candanosa, "Here's how Nanoparticles could help us get

closer to a treatment for COVID-19," News@northeastern, 2020. https://news.northeastern.edu/2020/03/04/heres-how-nanoparticles-could-help-us-get-closer-to-a-treatment-for-covid-19/.

[151]A. Dikhayeva, "Reusable Face Mask Material Developed in KAIST," 2020. [Online]. Available: http://herald.kaist.ac.kr/news/articleView.html?idxno=10184.

[152]T. Du et al., "Glutathione-Capped Ag2S Nanoclusters Inhibit Coronavirus Proliferation through Blockage of Viral RNA Synthesis and Budding," ACS Appl. Mater. Interfaces, vol. 10, no. 5, pp. 4369–4378, 2018, doi: 10.1021/acsami.7b13811.

[153]Y. N. Chen, Y. H. Hsueh, C. Te Hsieh, D. Y. Tzou, and P. L. Chang, "Antiviral activity of graphene–silver nanocomposites against non-enveloped and enveloped viruses," Int. J. Environ. Res. Public Health, vol. 13, no. 4, pp. 4–6, 2016, doi: 10.3390/ijerph13040430.

[154]Y. Y. Cho IH, Lee DG, "Composition with sterilizing activity against bacteria, fungus and viruses, application thereof and method for preparation thereof. US8673331," 2014.

[155]S. A. Read, S. Obeid, C. Ahlenstiel, and G. Ahlenstiel, "The Role of Zinc in Antiviral Immunity," Adv. Nutr., vol. 10, no. 4, pp. 696–710, 2019, doi: 10.1093/advances/nmz013.

[156]L. Dong, S. Hu, and J. Gao, "Discovering drugs to treat coronavirus disease 2019 (COVID-19)," Drug Discov. Ther., vol. 14, no. 1, pp. 58–60, 2020, doi: 10.5582/ddt.2020.01012.

[157]G. A. Eby, "Zinc lozenges as cure for the common cold - A review and hypothesis," Med. Hypotheses, vol. 74, no. 3, pp. 482–492, 2010, doi: 10.1016/j.mehy.2009.10.017.

[158]C. J. Field, I. R. Johnson, and P. D. Schley, "Nutrients and their role in host resistance to infection.," J. Leukoc. Biol., vol. 71, no. 1, pp. 16–32, 2002, doi: 10.1189/jlb.71.1.16.

[159]A. S. Prasad, "Zinc: Mechanisms of host defense," J. Nutr., vol. 137, no. 5, pp. 1345–1349, 2007, doi: 10.1093/jn/137.5.1345.

[160]S. Overbeck, P. Uciechowski, M. L. Ackland, D. Ford, and L. Rink, "Intracellular zinc homeostasis in leukocyte subsets is regulated by different expression of zinc exporters ZnT-1 to ZnT-9," J. Leukoc. Biol., vol. 83, no. 2, pp. 368–380, 2008, doi: 10.1189/jlb.0307148.10.1043/1543-2165(2004)128<195:AODDTS>2.0.CO;2.